Report Number 96-28

Research

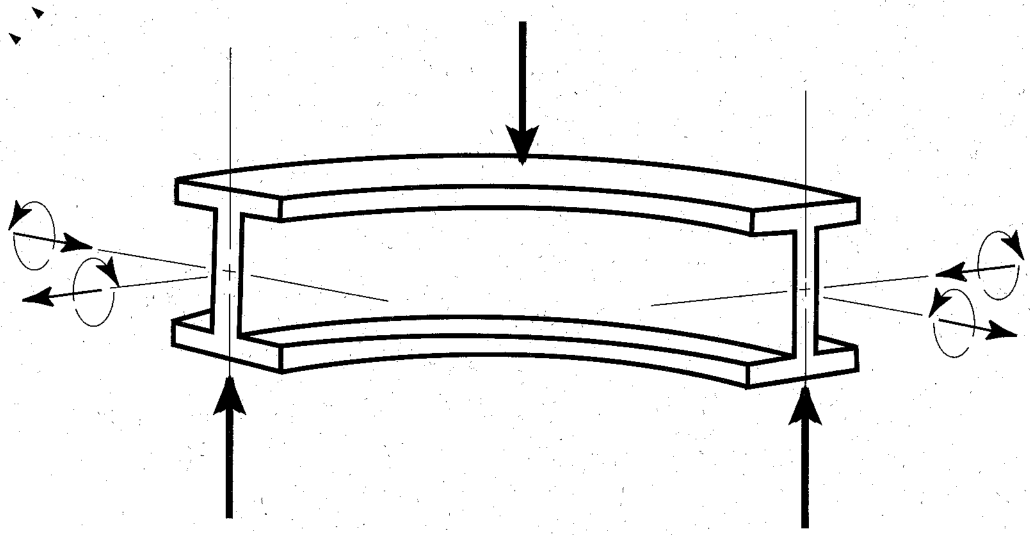

Stresses in Steel Girder Bridges

UNIVERSITY OF MINNESOTA
CENTER FOR
TRANSPORTATION
STUDIES

Technical Report Documentation Page

1. Report No.	2.	3. Recipient's Accession No.
MN/RC - 96/28		

4. Title and Subtitle	5. Report Date
STRESSES IN STEEL CURVED GIRDER BRIDGES	August 1996
	6.
7. Author(s) Theodore V. Galambos, Jerome F. Hajjar, Roberto T. Leon, Wen-Hsen Huang, Brian E. Pulver, and Brian J. Rudie	8. Performing Organization Report No.
9. Performing Organization Name and Address Department of Civil Engineering Institute of Technology University of Minnesota Minneapolis, Minnesota 55455-0220	10. Project/Task/Work Unit No. 11. Contract (C) or Grant (G) No. (C) 72443 TOC #155
12. Sponsoring Organization Name and Address Minnesota Department of Transportation 395 John Ireland Boulevard Mail Stop 330 St. Paul, Minnesota 55155	13. Type of Report and Period Covered Final Report 1994-1996 14. Sponsoring Agency Code

15. Supplementary Notes

16. Abstract (Limit: 200 words)

Steel curved I-girder bridge systems may be more susceptible to instability during construction than bridges constructed of straight I-girders. The primary goal of this project is to study the behavior of the steel superstructure of curved steel I-girder bridge systems during all phases of construction, and to ascertain whether the linear elastic analysis software used by Mn/DOT during the design process represents well the actual stresses in the bridge. Sixty vibrating wire strain gages were applied to a two-span, four-girder bridge, and the resulting stresses and deflections were compared to computational results for the full construction sequence of the bridge. The computational results from the Mn/DOT analysis software were first shown to compare well with results from a program developed specifically for this project (called the "UM program"), since the latter permits more detailed specification of actual loading conditions on the bridge during construction. The UM program, in turn, correlated well with the field measurements, especially for the primary flexural stresses. Warping stresses induced in the girders, and the stresses in the crossframes, were more erratic, but showed reasonable correlation. It is concluded that Mn/DOT's analysis software captures the behavior well for these types of curved girder bridge systems, and that the stresses in these bridges may be relatively low if their design is controlled largely by stiffness.

17. Document Analysis/Descriptors		18. Availability Statement
Bridges	Lateral-torsional Buckling	No restrictions. Document available from:
Curved Steel I-girder	Warping	National Technical Information Services,
Diaphragm	Structural Stability	Springfield, Virginia 22161
Crossframe	Construction Sequence	
Composite Deck	Field Measurement	
Torsion	Vibrating Wire Strain Gage	

19. Security Class (this report)	20. Security Class (this page)	21. No. of Pages	22. Price
Unclassified	Unclassified	345	

Stresses in Steel Curved Girder Bridges

Final Report

Prepared by

Theodore V. Galambos

Department of Civil Engineering
University of Minnesota
Minneapolis, Minnesota 55455

Jerome F. Hajjar

Department of Civil Engineering
University of Minnesota
Minneapolis, Minnesota 55455

Roberto T. Leon

Sch. of Civil and Environ. Eng.
Georgia Institute of Technology
Atlanta, Georgia 30332

Wen-Hsen Huang

Virginia Dept. of Transportation
Div. of Structures and Bridges
Richmond, Virginia

Brian E. Pulver

Wiss, Janney, Elstner Associates
330 Pfingsten Road
Northbrook, Illinois 60062

Brian J. Rudie

Minn. Dept. of Transportation
Office of Bridges and Structures
Roseville, Minnesota 55113

August 1996

Published by

Minnesota Department of Transportation
Office of Research Administration
Transportation Building
395 John Ireland Boulevard
St. Paul, Minnesota 55155-1899

ACKNOWLEDGMENTS

The authors would like to express their sincere appreciation to the Offices of Bridges and Structures, Materials, and Research Administration at the Minnesota Department of Transportation for support of this research on steel curved girder bridges. The authors would also like to give special thanks to the PDM Bridge Company, fabricators of the curved girder bridge; the Lunda Construction Company, the general contractors on the bridge construction; and High Five Erectors, the erectors of the steel superstructure of the bridge. Without their extensive cooperation, this research would not have been possible. In particular, the authors would like to thank the following individuals for their substantial contributions to this project:

Minnesota Department of Transportation:
Offices of Bridges and Structures, Materials, and Research Administration
D. Flemming, G. Peterson, P. Rowekamp, S. Ellis, K. Anderson, T. Nieman, J. Southward

Minnesota Department of Transportation: Field Office
D. Reinsch, L. Lillie, P. Koff, J. Michaels

The PDM Bridge Company, Eau Claire, Wisconsin
J. Bates, R. Cisco

Lunda Construction Company, Rosemount, Minnesota
D. Davick

High Five Erectors, Shakopee, Minnesota
B. Theis

University of Minnesota
J. Millman, A. Staples, P. Bergson

TABLE OF CONTENTS

List of Tables

List of Figures

EXECUTIVE SUMMARY

Composite, I-shaped, steel curved girder bridges are relatively stiff and strong when the structure is completely erected and subjected to service loading resulting from daily traffic. However, the structure may be quite flexible and potentially susceptible to stability problems during construction, prior to its stabilization after hardening of the concrete deck. When designing these types of bridges, linear elastic analysis software is typically used to determine the stresses and deflections in the steel members due to wet weight of the concrete, and after hardening of the concrete deck. In order to insure safe design, it is vital that the stresses and deflections resulting from such analyses be representative of the stress state in the actual bridge structure. In addition, it is important to know whether the stress state in this type of bridge at other points in the construction process may be represented computationally, to insure that no unusual stress states occur which are possibly being neglected in current design practice. Curved girder bridge systems exhibit special behavior as compared to bridge systems with straight girders. Such unique behavior includes, for example, the effect of warping restraint on the behavior of the I-girders, the behavior of crossframes in a curved girder system, and the potential susceptibility of these bridges to lateral-torsional buckling during construction, due to the initial curvature of the girders. These added considerations require special care to be taken regarding the accuracy of the computational simulations used to obtain forces for design. In spite of this, to date there have been few measurements of actual stresses in these girders recorded during construction. Consequently, this project seeks to determine the range of stresses exhibited in a typical steel curved girder bridge during all stages of construction, and to compare these stresses with results obtained using linear elastic analysis software commonly used for design.

The Minnesota Department of Transportation (MN/DOT) uses an analysis program, DESCUS-I, to determine the stresses for the design of steel curved I-girder bridge systems. The primary objective of this research involves instrumenting and monitoring the strains and stresses in the steel superstructure of a two-span curved I-girder bridge (MN/DOT Bridge No. 27998) during its entire construction process, and comparing these field measurements with results obtained from two analysis programs: MN/DOT's DESCUS-I, and the University of Minnesota Steel Curved

Girder Bridge System Analysis Program (referred to herein as the UM program), which was developed specifically for this project and which permits more detailed specification of loading and assessment of stress states. These two software programs are first compared to insure they yield the same results for similar bridge topology, properties, and loading. Subsequently, results from the UM software are compared to the field measurements to determine the capability of these types of programs to simulate actual stress distributions measured during construction. Conclusions drawn from this study include: 1) This bridge was shored in the early stages of construction of the steel superstructure, and the bridge design was controlled by stiffness, not strength. Therefore, stresses well below the yield stress occurred throughout construction. 2) Computational results consistently matched well qualitatively and often quantitatively with measured results, both for stresses and deflections. The bridge behavior was predictable at all stages. 3) The primary difference between measured and computed results was due mainly to the erratic effects in the field of warping restraint and weak axis bending on the measured results. 4) Fit-up stresses were measured in the crossframes, but they dissipated as construction progressed, and they remained below 6 ksi. 5) The MN/DOT curved girder program, DESCUS-I, compares well to the UM program, which in turn compares well to the field measurements. Consequently, it may be concluded that the DESCUS-I program represents construction and final live load stresses and deflections well, both for the bare steel and the composite bridge system. It should be emphasized that while the ability to make direct comparisons between DESCUS-I and the field measurements is somewhat limited (due to constraints of specifying actual loading, etc. in DESCUS-I), it may be concluded that stresses obtained from DESCUS-I are representative of what is seen in the field for the type of studied in this project. 6) It is recommended that a minimum of 20 to 30 psf live loading for construction be included in analyses to capture maximum stresses. Future research in this area should include further tests with increased live loading. Two trucks placed on this structure induced only approximately 2 ksi in the measured members. If additional trucks are placed on the structure, more substantial and reliable strain readings may be made, which will provide firmer evidence of the service load behavior of these types of structures. In addition, it may be possible to ascertain whether composite behavior diminishes over time.

CHAPTER 1

INTRODUCTION

Composite, I-shaped, steel curved girder bridges are relatively stiff and strong when the structure is completely erected and subjected to service loading resulting from daily traffic. However, the structure may be quite flexible and potentially susceptible to stability problems during construction, prior to its stabilization after hardening of the concrete deck. When designing these types of bridges, linear elastic analysis software is typically used to determine the stresses and deflections in the steel members at two points during the construction process and useful life of the bridge: 1) due to dead load just after the pouring of the concrete deck, but prior to the deck hardening; and 2) due to live load on the finished bridge structure. In order to insure safe design according to the American Association of State Highway and Transportation Officials (AASHTO) provisions [1], it is vital that the stresses and deflections resulting from such analyses be representative of the service-level stress state in the actual bridge structure; this insures that appropriate stress distributions are used for member design according to either Working Stress or Load and Resistance Factor Design methodologies, and that serviceability limit states are evaluated accurately. In addition, it is important to know whether the stress state in this type of bridge at other points in the construction process may be represented computationally, to insure that no unusual stress states occur which are possibly being neglected in current design practice. Curved girder bridge systems exhibit special behavior as compared to bridge systems with straight girders [2]. Such unique behavior includes, for example, the effect of warping restraint on the behavior of the I-girders, the behavior of crossframes in a curved girder system, and the potential susceptibility of these bridges to lateral-torsional buckling during construction, due to the initial curvature of the girders. These added considerations require special care to be taken regarding the accuracy of the computational simulations used to obtain forces for design. In spite of this, to date there have been few measurements of actual stresses in these girders recorded during construction. Consequently, this project seeks to determine the range of stresses exhibited in a typical steel curved girder bridge system during all stages of construction, and to compare these stresses with computational results obtained using linear elastic analysis software commonly used for design.

1.1 OBJECTIVE

The Minnesota Department of Transportation (MN/DOT) uses an analysis program, DESCUS-I [3], to determine the stresses for the design of steel curved I-girder bridge systems. As is the case with all analysis programs, assumptions must be made regarding the idealization of these structures. In addition, these programs do not account explicitly for the stresses and deflections induced by fabrication and construction practices. The primary objective of this research involves instrumenting and monitoring the strains and stresses in the steel superstructure of a two-span curved I-girder bridge during its entire construction process [4], and comparing these field measurements with results obtained from two analysis programs: MN/DOT's DESCUS-I, and the University of Minnesota Steel Curved Girder Bridge System Analysis Program (referred to herein as the UM program), which was developed specifically for this project and which permits more detailed specification of loading and assessment of stress states [5]. For this project, MN/DOT Bridge No. 27998 was selected for the research. Specific objectives of this project include:

1. Measure the strains in the steel superstructure of this curved I-girder bridge system, beginning at the fabrication yard, and track of these strains through the transportation of the girders and crossframes to the site, erection of the steel structure, casting of the deck, and application of live load to the completed bridge.

2. Conduct detailed analyses of the bridge to determine the stresses (derived from the strain readings) and deflections during the different phases of construction, as well as due to live loading on the completed structure. These analyzes use both MN/DOT's DESCUS-I analysis program and the UM software. These two software programs are first compared to insure

they yield similar results for similar bridge topology, properties, and loading. Subsequently, results from the UM software are compared to the field measurements to determine the capability of these types of programs to simulate actual stress distributions measured during construction. Once these comparisons are made, conclusions are drawn regarding the suitability of DESCUS-I to determine stresses for design.

1.2 BACKGROUND ON CURVED GIRDER ANALYSIS APPROACHES

There are many commercial, proprietary, and in-house computer programs available for the analysis of curved girder bridges. Stegmann and Galambos [6] and Zureick et al. [7] summarize common methods of analysis for curved steel girder bridges. In addition, three texts present the theory for the development of these analytical and computational approaches, including Dabrowski [8], Heins [9], and Nakai and Yoo [10]. These references range in time from 1975 to 1993, and they reflect the work performed predominantly in the late 1960-s and the early 1970-s under the sponsorship of the Federal Highway Administration by the *Consortium of University Research Teams* (CURT).

This section provides a brief background on analysis methods for steel curved girder bridge systems. The reader is referred to Appendix G for further detail, and to Zureick et al. [7].

Zureick et al. [7] indicate that there are two basic types of computational approaches for analyzing curved bridge girder systems: approximate methods and refined methods. The approximate methods include: a) the plane grid method; b) the space frame method; and c) the V-load method. Refined techniques include: a) direct analytical solution of the differential equation governing the behavior of the curved girders (for analyzing isolated girders); b) the finite difference method; c) the finite strip method; d) the slope-deflection method; and e) the finite element method. The approximate methods are suitable for design, while the refined methods are best used for a detailed evaluation of the behavior of a final design or of an existing structure.

In addition, Stegmann and Galambos [6] classify these analysis methods as: Level I methods (most sophisticated research tools); Level II methods (for final design and investigation of existing bridges); and Level III methods (for preliminary design). The program DESCUS-I may be classified as a Level II, refined approach utilizing the finite element method. This software effectively takes into account both the flexural and warping normal stresses in the curved girders, which are the main stresses governing the design of steel curved girder bridges. The UM program is of essentially the same degree of sophistication, although it has several additional features, including nonlinear analysis capabilities [5], not discussed in this report. Chapter 5 provides further details of these two software programs.

1.3 SCOPE

Because of the substantial coordination required to measure strains in an actual bridge system from fabrication through opening of the bridge, only one curved I-girder bridge was included in this project. The conclusions resulting from this project must therefore be interpreted within the context of the specific type of bridge selected. MN/DOT Bridge No. 27998 is an off-ramp from an interstate highway, and it has a general layout that is similar to that used throughout the country for these types of bridges. A main distinguishing feature of the bridge is that it includes four concentric I-girders, each of differing depth ranging from 50 to 70 inches. Each beam differs in depth in order to maximize the webs depths while maintaining the superelevation and while minimizing the vertical clearance over the interstate highway below. The bridge girders are divided into three segments over two spans, with one central support (see Chapter 2). The spans range from 139 to 155 feet each, and the girders are continuous over the center support. The in-plane radius of curvature of the bridge is relatively small, varying from approximately 270 feet to 300 feet. In addition, two of the three supports have substantial skews relative to the tangential axis of the bridge at the point of support. Thus, the complex behavior typical of these types of common curved bridge systems is well represented by this bridge. In addition, its design was controlled mainly by insuring adequately small live load deflection (*L/800*), which is common in these types of bridges. The construction process went relatively smoothly, as did the field measurements (i.e., there were no substantial anomalies which biased the results), and for these reasons it is felt that the scope of this project is justifiably broad, such that the conclusions are relevant for the type and scale of curved I-girder bridge system studied in this work. Nevertheless, it is important to recognize that the conclusions drawn in this report are based upon the results of studying only a single bridge.

1.4 OUTLINE OF THE REPORT

Chapter 2 begins with a description of the curved girder bridge. It then outlines in detail the instrumentation strategy of the bridge. Chapter 3 follows with a detailed summary of the strains recorded on the bridge. These include strains recorded at key points in time during construction, as well as strains recorded on a nearly continuous basis during the pouring of the concrete deck. Chapter 4 summarizes the strains recorded due to controlled live loading on the bridge: two trucks of known weight were placed at various positions on the bridge, which was otherwise closed to traffic. Chapter 5 outlines the details of the finite element models used to compare to the field measurements, and it compares the DESCUS-I software of MN/DOT with the UM software to show that they yield essentially identical results for similar structural models. Chapter 6 compares the UM software analysis results to the field measurements, and also reports the two sets of deflection measurements made in the field. Conclusions are drawn in Chapter 7. Appendices A through C contain the complete set of strain data measured during the entire project. Appendix D outlines in detail the construction sequence of the steel superstructure. Appendix E details the calculations made to determine the dead loads applied to the bridge in the analyses. Appendix F outlines the manner in which gravity loads were assigned as point loads to the four I-girders in the analysis programs. Appendix G provides more detailed background on techniques for analyzing steel curved girder bridge systems. Appendix H presents the specification of the gage used for strain measurements on this project.

CHAPTER 2

INSTRUMENTATION OF THE GIRDERS

2.1 BRIDGE LAYOUT AND GAGE PLACEMENT

This chapter outlines the instrumentation strategy for measuring the strains in the curved girder bridge system. Figures 2.1 and 2.2 show plan and elevation views, respectively, of MN/DOT Bridge No. 27998 [11]. Relevant dimensional information is included in these figures. The location of the crossframes, end diaphragms, and supports, including the orientation of their skew, is clear in Figure 2.1. Figures 2.2 and 2.3, in turn, show the girder and deck dimensions (including the differing depths of the four I-girders -- Figure 2.2), as well as the topology of a typical crossframe (Figure 2.3). Also, as seen in Figure 2.2, stiff I-shaped end diaphragms are used in lieu of crossframes at the two ends of the bridge.

2.1.1 GAGE PLACEMENT DESIGN

Sixty gages were attached to the steel superstructure of the bridge. This number was felt to be optimal given the budget and time constraints present for this project. Figures 2.4 and 2.5 (and, equivalently, Figures A.1 and A.2) show the position of these gages. Twenty-four gages were placed along a section at the midspan of span 1 (i.e., the southern span) in order to determine the stresses occurring in the positive moment region of span one. Span one was selected since it was to be erected first. In the positive moment region, the stresses are expected to be negative (compressive) in the top flanges and positive (tensile) in the bottom flanges. This section was labeled as Gage Line A and the gages were numbered as 1A, 2A,...24A starting with the outside facia girder and progressing to the inside facia girder (see Figure 2.5)[3]. Six gages, three on the top and three on the bottom, were attached to each of the four girders to determine the stresses in

[3] Note that girder 1 is labeled as the outside facia girder in Figure 2.5 and in all strain measurements reported herein, while the MN/DOT drawing (Figure 2.1) labeled the outside facia girder as "beam 4".

the top and bottom flanges. The three gages on a given flange and neighboring web determine the changes in stress occurring across the width of the flanges so as to determine the effects of warping. For each girder, four gages were placed, two on the bottom of the top flange and two on the top of the bottom flange, as close to the edges of the flanges as possible. The last two gages were affixed to the web approximately 1.5 inches away from the flange since it was not possible to affix the gages directly to the center of the flanges. These web gages are most appropriate for tracking the predominant strong axis flexural forces in the girders. Twenty-four gages were also placed along a section over the middle pier in order to determine the stresses occurring in the negative moment region. In the negative moment region, the stresses are expected to be positive in the top flanges and negative in the bottom flanges. This section was labeled as Gage Line B and the gages were numbered from 1B to 24B in the same manner as described for Gage Line A. The location of the gages for Gage Line B was the same as Gage Line A (Figure 2.5). The final twelve gages were located at a section where diagonal crossframes were present. The crossframes consist of four angle sections, two horizontal and two diagonal, welded to gusset plates that are bolted to the curved girders. A gage was attached to each angle section to monitor the axial stress present in each of the members. This section was labeled Gage Line C, and the gages were numbered 1C to 12C, starting with the top horizontal member connected to the outside facia girder and the next inside girder and proceeding down and towards the inside facia girder. Note that the gages and wires were purposely located in areas of the girders which would not interfere with the construction or erection of the girders. These locations were based on information received during a series of planning meetings held with the erector and construction crews. The following section details the data acquisition system developed to collect the information desired.

2.2 DATA ACQUISITION SYSTEM

The data acquisition system consists of the *Geokon VK-4100* Vibrating Wire Strain Gage, *Belden 8730* Wire, *AMP* Five Pin Soft Shelled Connectors, the *Geokon GK-403* Vibrating Wire Readout Box, and a fabricated termination box. The following sections outline each of the components of the data acquisition system.

2.2.1 *Geokon VK-4100* Vibrating Wire Strain Gage

The strains of the curved girders were measured using vibrating wire strain gages. Vibrating wire strain gages have a known length of wire within the gage. This wire is tensioned between the two ends of the gage. These two ends are then affixed to the surface of the girder, the wire is plucked by an electromagnetic coil present in the gage cover, and the resonant frequency of vibration of the wire is measured. This initial reading is the zero reading for that gage. As load is applied to the structure, deformations occur in the members of the structure. This causes the affixed ends to move relative to one another and this changes the tension in the wire. The wire is plucked once again, and the change in frequency is measured, thus indicating directly the new strain reflective of the deformations present. Using the zero readings, a strain due to a given loading can be calculated and converted to stress using Young's modulus of elasticity (if linear elastic behavior is assumed, which is appropriate for this project, as will be discussed when the field measurements are reported in Chapters 3 and 4). Vibrating wire gages have an advantage over standard foil gages because once the gage is attached, the zero reading is not lost if the power supply is removed. This is important for this project since the gages were attached prior to transport of the girders to the construction site. In addition, these gages providing accurate strain readings over a long period of time with little to no drift, which is another key advantage these particular gages.

The type of vibrating wire strain gage used was the *Geokon VK-4100 Vibrating Wire Strain Gage* [12] (see Appendix H for the gage specifications). These gages are designed primarily for measuring strains in steel bridges and other types of steel members. The range of strain that can be measured is 2500 microstrain with a sensitivity of one microstrain. The gage length is 2.5 inches while a total length of the gage coil housing is 3 inches. The total height of the gage is 1/2 inches, and its width is 7/8 inches. The operational temperature range of the gage is -40 °C to +250 °C. The thermal coefficient of expansion is 12 ppm/ °C, which is the same as that of steel. This is important because the girders will expand/contract due to the heating/cooling of the structure. If the gages did not respond at an equivalent rate, erroneous strain readings would result since the strain registered could reflect the change in temperature, the change in the loading condition, or a combination of both. The temperature differential between the girders and the gages would have to be known to determine the amount of strain induced by the temperature change. This residual strain would then have to be subtracted from the total reading to indicate the strain due to that particular loading stage. While the temperature was registered during each of the gage readings, the above correction was not deemed to be necessary in this work because of the similar thermal properties of the gage and the steel members.

Included with the gage is an electromagnetic plucking coil, which resides in the coil housing, which is the reading device for the gage. The coil housing has a ten foot "pigtail" of wire included. At the end of the "pigtail" is a female *AMP* connector.

2.2.2 *Belden 8730* Wire

The *Belden 8730* wire is a shielded, four condition wire. It consists of four separate coated wires and an uncoated ground wire. The wire coatings are colored white green, black, and red. The colors of the wire represent, respectively, the negative thermistor lead, the positive thermistor lead, the negative vibrating wire lead, and the positive vibrating wire lead. At one end of the wire is a male *AMP* connector that attaches to the "pigtail", while the other end is attached to a female *AMP* connector, which is located in the termination box (see below).

2.2.3 *AMP* Five Pin Soft Shelled Connector

The *AMP* five pin soft shelled connectors are constructed by stripping the wire coating from the *Belden 8730* wire and crimping the appropriate individual male or female contact pin to the end of each of the five wires. The contact pins are then inserted into the connector shells to complete the construction of the connectors. These connectors allow for quick and easy connection of the wires to the "pigtails" and termination box in the field because the male and female connectors snap together securely.

2.2.4 *Geokon GK-403* Vibrating Wire Readout Box

The *GK-403 Readout Box* may be used with all of the models of vibrating wire strain gages that *Geokon* produces (see Appendix H for the specifications of the readout box). There are six different settings, A-F, that allow the different strain gages to be read. The *VK-4100* gage is read using channel E. The readout box, when attached to the wires leading from a gages, automatically causes the electromagnetic coil to "pluck" the wire of the gage, making it vibrate. The frequency of the wire is then measured. This frequency is transmitted to the readout box, and it is converted within the readout box to microstrain. The calculation used for channel E is:

$$\mu\varepsilon = (F^2 * 10^{-3}) * 0.39102 \qquad (2.1)$$

with F equaling the frequency in Hertz. Up to 256 readings may be stored in a storage array in the readout box, which can later be downloaded as an ASCII file to a personal computer using the communications program, Procomm, which is included by *Geokon* with the readout box.

2.2.5 Termination Box

The termination box, designed and fabricated at the University of Minnesota, is a waterproof box constructed using sheet metal and aluminum. The box has an access hole to the back of a panel which holds sixty connectors labeled for each gage. This box consolidates the wires from the sixty gages on the bridge, and makes it possible to read all sixty gages at one convenient location. With this box, all sixty gages could be read and recorded in approximately five minutes. The termination box is located on top of the southern abutment, just under the bridge deck at that ocation. It is kept covered with plastic, and is accessed with a 16 foot extension ladder.

2.3 FIELD INSTRUMENTATION OF GIRDERS

2.3.1 Gage Attachment Procedure

The steel superstructure was fabricated at the PDM Bridge Company (PDM) in Eau Claire, Wisconsin. After its fabrication, the structure were shipped in pieces by truck to the job site for erection. To insure an accurate zero reading, with as close to zero stress in the girders as possible, the strain gages were attached on site at PDM, and the zero readings were taken at PDM. The areas on the girders where the strain gages were to be attached were masked off to prevent painting in those areas. Once the priming and painting of the girders was completed, they were moved out to a storage yard where the attachment of the gages occurred. In some cases, the surface of the steel where the gages were to be attached had paint, rust, or dirt present. In those cases the surface was ground smooth to the bare steel, and a fine grit sand paper was used to further smooth the surface. The surface was then cleaned and degreased. The location of each gage was measured and marked with a straight edge and pencil to insure the alignment of the gage. Each gage was then held in place, and the gage was welded to the member using a capacitance spot welder. The welder was a *Micromeasurements Model 700 Portable Strain Gage Welding and Soldering Unit.* Approximately 34 spots were welded per gage to hold the gage in place. Approximately 40 watt-seconds of energy per weld was used to properly weld each gage to the steel.

After the welding process was completed, the tabs of the gage were waterproofed. A drop of cyanoacrylate glue was applied to the tabs of the gage. The glue wicks underneath the tab to protect against corrosion. *Micromeasurements M-Coat F*, an acrylic waterproofing compound, was then applied to the top of the tabs to waterproof the welds. After the waterproofing was dry, the plucking coil was welded into place over the gage. Two straps hold the plucking coil in place with ten welds per strap. Before the coil was put into place, *Dow Corning RTV-3145* silicone rubber was placed on the underside of the coil to add another layer of waterproofing protection against corrosion. The same waterproofing techniques were used to protect the welds on the straps that hold the coil housing in place over the gage. Additional silicone was placed around the coil housing for added protection.

For gage line B and C, the *AMP* female connectors at the "pigtail" ends were wrapped in plastic and left in place for transport. For gage line A, the "pigtail" was connected at PDM to the *AMP* male end connector, which in turn was attached to the *Belden* wire, which was coiled for transport. When the girders were erected, the coiled wire at the end of the girders was run to the termination box, as is described in the next section.

2.3.2 Wire Placement

The frequency values that represent the strain measurements are transferred to the readout box via *Belden 8730* wire. After discussions with MN/DOT and Lunda Construction, it was agreed that it would be most efficient to attach the wires for the gages to the girders before their transportation to the construction site. The wire layout was tailored to insure that the wires would be safe and unobtrusive during transportation and construction. In particular, at PDM, the ends of the wires for Gage Lines A, B, and C were coiled and attached to adhesive bases with locking tie wraps, and the adhesive bases were affixed to the girders in unobtrusive locations. The wires for Gage Line A were routed from the gages directly to the bottom flange, where they were collected, bundled with tie wraps, and routed back along the web-flange intersection to the end of the girder to be placed at the southern abutment. For additional protection, where it was possible the wires were passed through the notch in the stiffeners where the flange and web meet. Since there is a splice present in span one, the wires for Gage Line B could not be attached directly to their girders (over the middle pier) until after transportation occurred. Instead, the wires for Gage Line B were put in their proper place on the girders which contain Gage Line A, since all wires of Gage Line B must pass by Gage Line A on their way to the termination box. The length of wire needed to reach the gages over the middle pier was coiled and attached to the girder at a location near the splice. The wires were then routed to the gages and connected to the Gage Line B "pigtails" after the erection of the girders. The wires for Gage Line C were similarly bundled with the other wires of Gage Lines A and B, and connected to the crossframe gages after their erection process.

2.3.3 Zero Readings

Readings were taken after the gages were attached at PDM. The support conditions of the girders, including wood blocking, were noted for these readings. Once the girders were delivered to the construction site, a second set of zero readings was taken. Table 2.1 provides a comparison of the zero readings taken at PDM, and the readings taken after the girders were delivered to the job site while they were sitting on the ground. When the readings were taken at PDM, not all of the temperatures were recorded. Therefore a comparison was made to determine the effect this might have on the readings. The largest discrepancy occurred with the zero readings for girder 312D2 which were taken inside the paint shop at PDM Bridge, but out in the sun at the construction site. The greatest percent difference was 5.32% on this girder. Most of the other readings did not vary by more than 2 to 3 percent. The zero readings for the other girders were taken in the sun both at PDM and the construction site. The effects of the sun could thus be a reason for some of the larger discrepancies (i.e., 4 to 5 percent) found in some of the gages. However, the difference between the two readings is generally small, and the PDM readings were used as the zero for this project.

2.3.4 Gage Damage and Replacement

Two gages were damaged during the erection and construction of the bridge. These problems resulted from miscommunication between the University of Minnesota researchers and the different construction crews, or within the construction crews. During the erection of the girders, the gage labeled 11B was damaged by a "come along". A "come along" is a device used to keep the curved girder vertical when it is lifted from the ground. The attachment of the "come along" to the top flange of the girder at its midspan crushed gage 11B. The other top flange gages were spared by chance. The use of the "come along" was not discussed during the planning meetings, and should be accounted for in future projects of this nature. The second gage, gage 1A, was damaged when the cantilever supports for the formwork were put into place. This formwork consists of a 4 x 4 board wedged between the girder's top flange and the cantilever supports, and then 3/4" plywood is placed on top of the supports. It was the wedging of the board between the flange and the support that damaged the gage. The construction crew placing the formwork was not informed about the location of the gages, and the gages were not visible from above the girders. This lead to the damaging of the gage. Both of these gages were replaced. It should be noted that on the whole, the cooperation of MN/DOT personnel, the erectors, and the construction crews was exceptional, which was directly related to the success of this field instrumentation study.

Table 2.1. Difference Between the Zero Readings at PDM and on the Construction Site

Initial Strain Readings At PDM on 7/13/95 Temperature 35 C			7/17/95 & 7/18/95 on Construction Site on the Ground		Zero Strain		
Member	Gage Number	Strain ($*10^{-6}$)	Strain ($*10^{-6}$)	Temperature (C)	Difference	% Diff	% Diff
308D1	1A	2173.6	2231.1	35.5	57.5	2.65	2.58
	2A	1991.5	2010.0	35.7	18.5	0.93	0.92
	3A	1957.5	1946.2	35.6	-11.3	0.58	0.58
	4A	1991.6	2027.9	32.8	36.3	1.82	1.79
	5A	2379.4	2389.7	34.3	10.3	0.43	0.43
	6A	1938.7	1921.1	31.2	-17.6	0.91	0.92
307C1	7A	2193.5	2255.7	36.4	62.2	2.84	2.76
	8A	2488.3	2537.9	36.4	49.6	1.99	1.95
	9A	1722.8	1757.7	44.2	34.9	2.03	1.99
	10A	2172.2	2223.3	44.5	51.1	2.35	2.30
	11A	2431.2	2485.9	36.2	54.7	2.25	2.20
	12A	2281.2	2298.3	33.7	17.1	0.75	0.74
306B1	13A	2355.8	2352.3	32.0	-3.5	0.15	0.15
	14A	2200.6	2213.7	31.1	13.1	0.60	0.59
	15A	2239.9	2230.0	37.9	-9.9	0.44	0.44
	16A	1657.5	1648.0	37.4	-9.5	0.57	0.58
	17A	2192.5	2222.0	32.5	29.5	1.35	1.33
	18A	1832.1	1850.8	29.5	18.7	1.02	1.01
305A1	19A	2426.5	2430.2	32.6	3.7	0.15	0.15
	20A	2105.4	2155.2	32.2	49.8	2.37	2.31
	21A	2163.0	2130.0	-	-33.0	1.53	1.55
	22A	1567.5	1545.7	31.5	-21.8	1.39	1.41
	23A	2476.4	2485.9	32.3	9.5	0.38	0.38
	24A	1802.8	1796.3	29.3	-6.5	0.36	0.36
312D2	1B	1228.5	1280.0	34.7	51.5	**4.19**	**4.02**
	2B	1895.1	1960.5	34.3	65.4	**3.45**	**3.34**
	3B	2144.8	2169.0	33.7	24.2	1.13	1.12
	4B	1691.7	1781.7	32.2	90.0	**5.32**	**5.05**
	5B	1670.3	1681.9	34.9	11.6	0.69	0.69
	6B	2592.3	2663.4	36.3	71.1	2.74	2.67
311D2	7B	1440.3	1459.2	34.7	18.9	1.31	1.30
	8B	2179.9	2194.0	34.1	14.1	0.65	0.64
	9B	2376.0	2413.2	33.6	37.2	1.57	1.54
	10B	2188.4	2208.6	31.7	20.2	0.92	0.91
	11B	1910.6	1928.3	35.1	17.7	0.93	0.92
	12B	1785.3	1861.8	36.9	76.5	**4.28**	**4.11**
310B2	13B	2191.4	2209.8	32.3	18.4	0.84	0.83
	14B	2327.7	2345.7	32.0	18.0	0.77	0.77
	15B	2605.2	2647.3	31.7	42.1	1.62	1.59
	16B	2224.9	2257.6	29.9	32.7	1.47	1.45
	17B	1601.8	1524.9	32.0	-76.9	**4.80**	**5.04**
	18B	2589.6	2647.5	36.9	57.9	2.24	2.19
309A2	19B	1658.0	1668.0	32.1	10.0	0.60	0.60
	20B	2059.6	2075.8	32.0	16.2	0.79	0.78
	21B	2192.3	2217.3	31.2	25.0	1.14	1.13
	22B	2599.0	2641.5	29.5	42.5	1.64	1.61
	23B	1643.3	1659.8	31.7	16.5	1.00	0.99
	24B	2262.9	2326.1	35.5	63.2	2.79	2.72

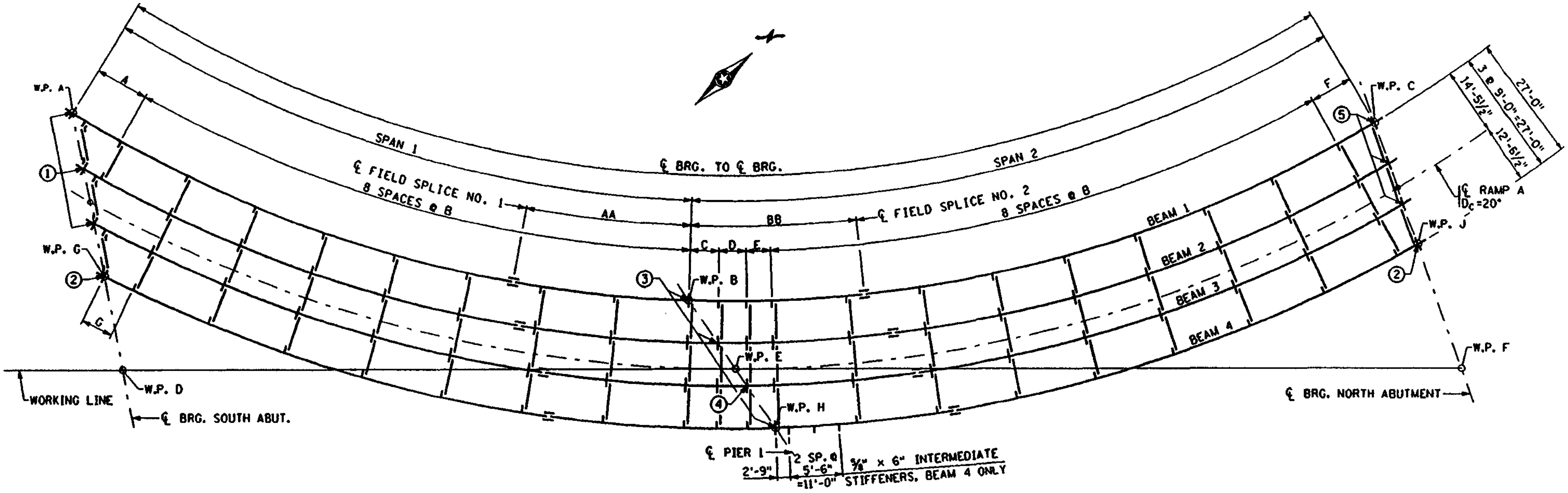

FRAMING PLAN

DIAPHRAGM SPACING	A	B	C	D	E	F	G
℄ BEAM 1	11'-11"	16'-0"	6'-5⅝"	5'-11⅝"	5'-6⅜"	9'-5¼"	---
℄ BEAM 2	4'-1⅝"	16'-6⅜"	6'-8⅛"	6'-2"	5'-8½"	8'-0"	---
℄ BEAM 3	---	17'-0¾"	6'-10¾"	6'-4⅜"	5'-10¾"	6'-6¾"	13'-7¼"
℄ BEAM 4	---	17'-7"	7'-1¼"	6'-6¾"	6'-0⅞"	5'-1⅝"	6'-8½"

FIELD SPLICE LOCATIONS	AA	BB
℄ BEAM 1	38'-0"	38'-0"
℄ BEAM 2	43'-0"	38'-0"
℄ BEAM 3	44'-0"	37'-0"
℄ BEAM 4	49'-0"	39'-0"

SPAN LENGTHS	RADIUS	SPAN 1	SPAN 2
℄ BEAM 1	272'-0¼"	139'-10⅞"	155'-4¾"
℄ BEAM 2	281'-0¼"	143'-0⅝"	152'-1⅜"
℄ BEAM 3	290'-0¼"	146'-3⅜"	148'-11⅛"
℄ BEAM 4	299'-0¼"	149'-6⅞"	145'-10⅛"

1. VULCANIZED EXPANSION CURVED PLATE BEARING ASSEMBLY, TYPE 1
2. VULCANIZED EXPANSION CURVED PLATE BEARING ASSEMBLY, TYPE 2
3. FIXED CURVED PLATE BEARING ASSEMBLY, TYPE 1
4. FIXED CURVED PLATE BEARING ASSEMBLY, TYPE 2
5. VULCANIZED EXPANSION CURVED PLATE BEARING ASSEMBLY, TYPE 3.

Figure 2.1. Framing Plan

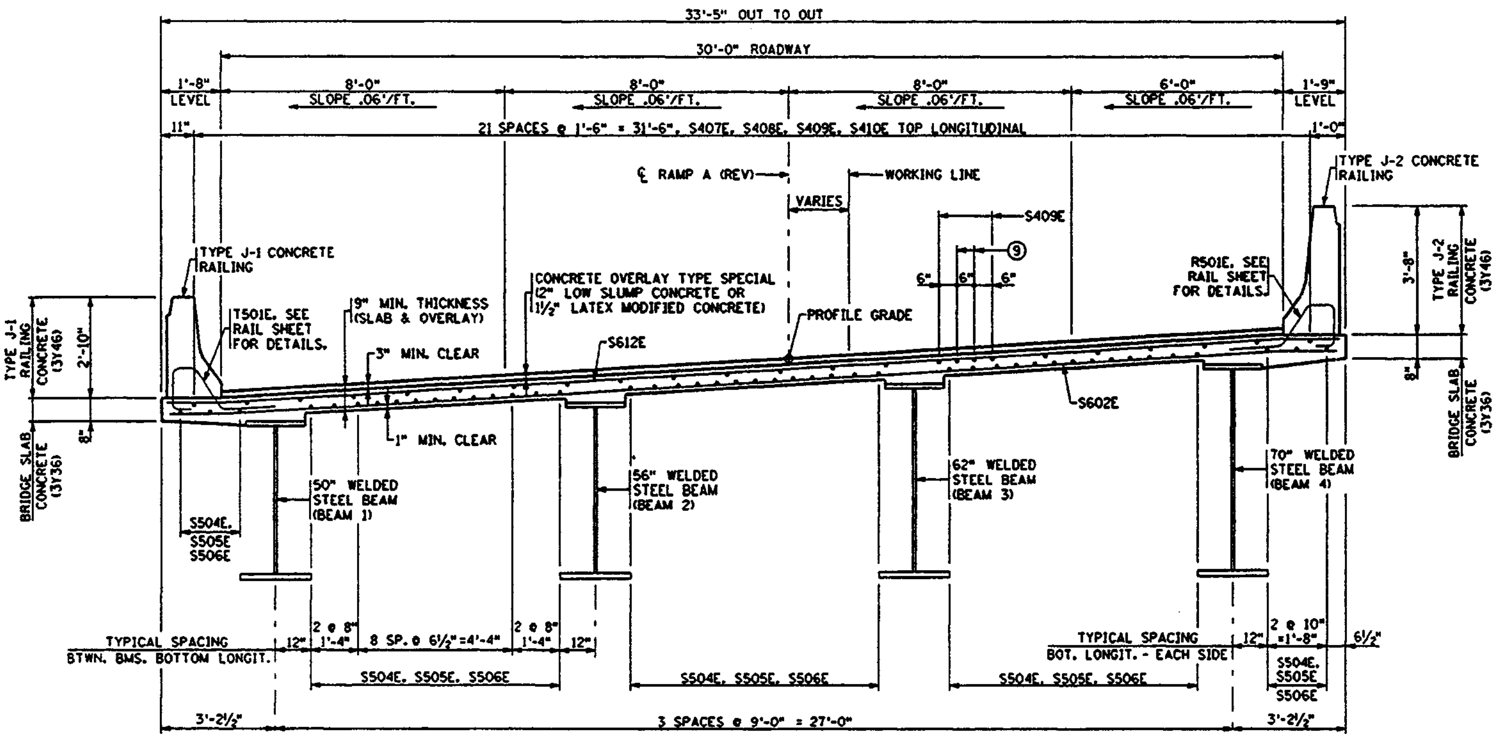

TRANSVERSE SECTION

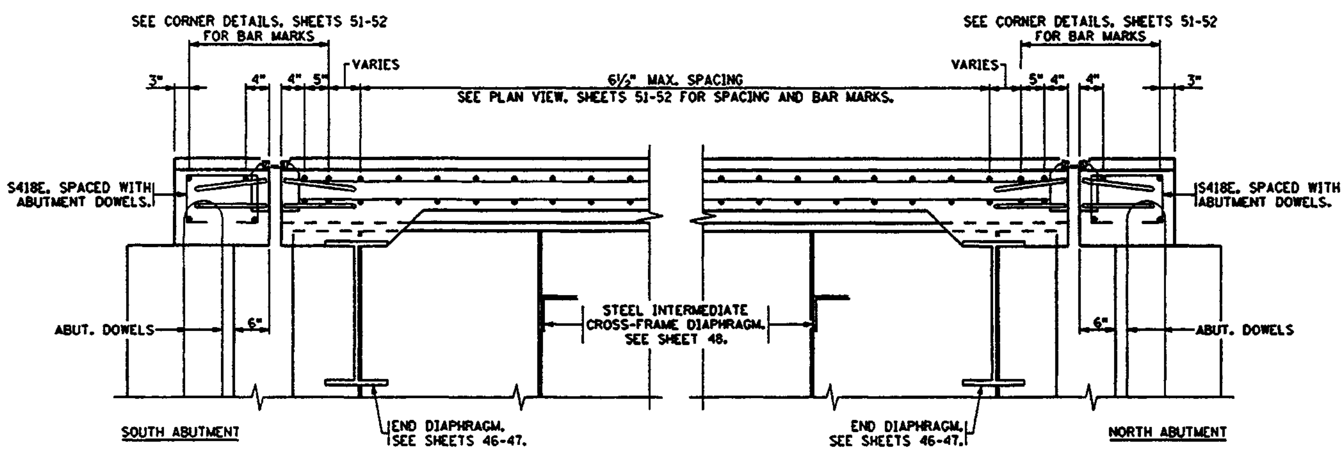

PART LONGITUDINAL SECTION

Figure 2.2. Superstructure profiles.

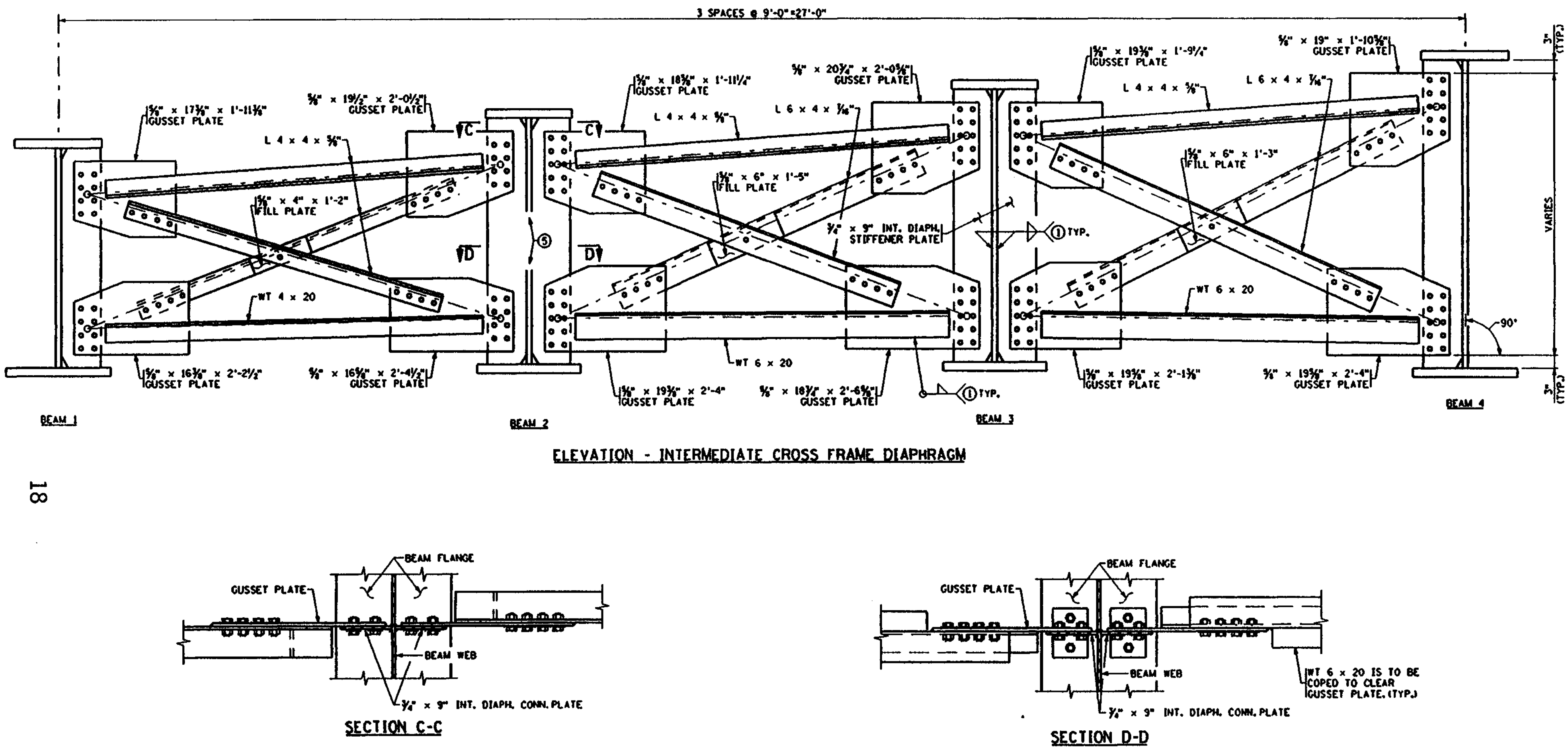

NOTES:

ALL STEEL SHALL CONFORM TO SPEC. 3309.

① SEE SPEC. 2471.3J4b1 FOR MINIMUM SIZE OF FILLET WELD. WELD SIZE NEED NOT EXCEED ⅜" FOR INTERMEDIATE DIAPHRAGM STIFFENERS.

② BOLT HOLES IN GUSSET PLATE MAY BE FIELD DRILLED.

Figure 2.3. Elevation of intermediate cross frame diaphragms

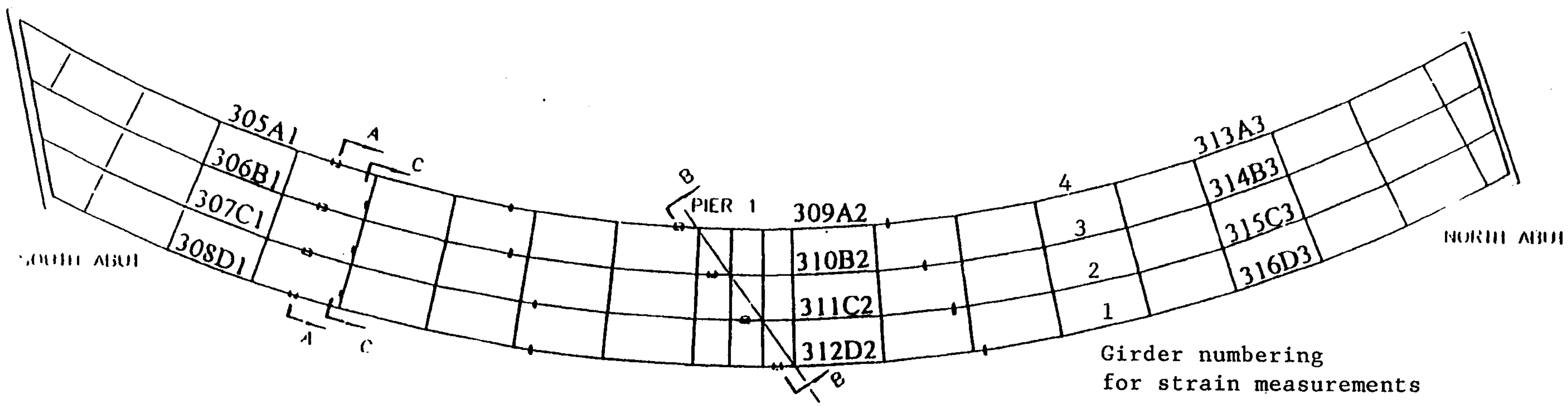

Figure 2.4. Plan view of the girders displaying the girder nomenclature

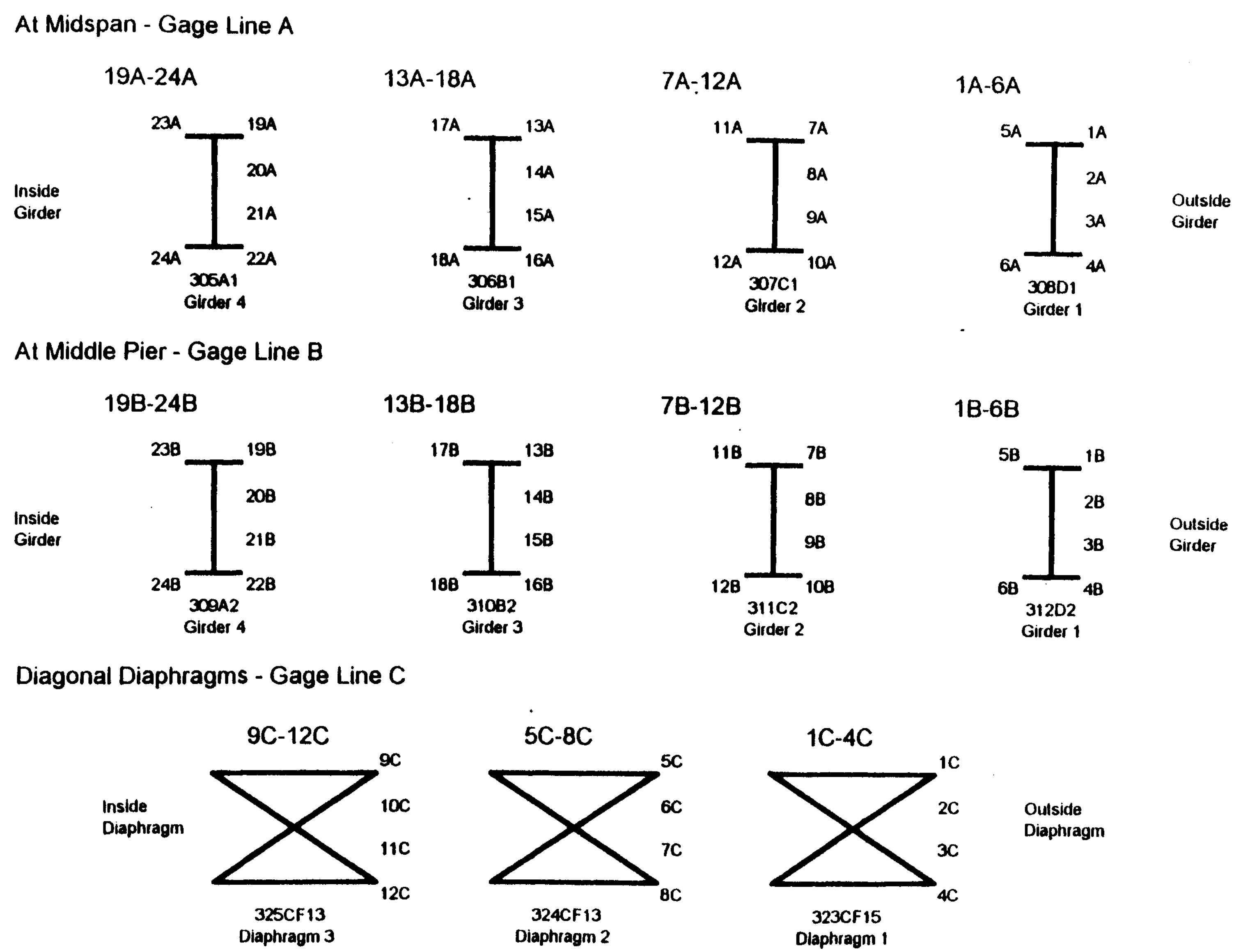

Figure 2.5. Nomenclature used to describe gage locations, girders, and diaphragms.

CHAPTER 3
FIELD MEASUREMENTS DURING CONSTRUCTION OF THE BRIDGE

3.1 INTRODUCTION

This section contains a description of the stresses resulting from the construction and erection of the bridge. Figures 2.1 through 2.5 display a plan of the bridge and the girder nomenclature. The construction sequence is divided into different loading stages designed to examine the stresses present during what was determined to be the critical stages of the construction of the bridge. This allowed for the observation of the stresses the structure experienced during the construction of the bridge. The following list details the loading stages after which readings were taken:

1. The erection of span 1
2. Half of span 2 was erected
3. All girders and crossframes erected (bolts loose on all crossframes)
4. All girders and crossframes erected (all bolts "rattled up" into their tightened position)
5. All deck formwork in place
6. All deck formwork and reinforcement in place
7. During the pouring of the reinforced concrete deck
8. Parapet walls poured
9. During truck live loading

The readings from these stages are arranged into two sections to make the results easier to analyze. The two sections are classified as: *Stresses due to Construction,* and *Stresses During* *the Pouring of the Reinforced Concrete Deck.* The *Stresses During the Truck Live Loading* will be discussed in Chapter 4.

At each of the loading stages detailed above, strain readings were taken, and the data was stored in the readout box. Zero readings, recorded at PDM on July 13, 1995, were used as a base line of "zero" stress to which the remaining readings were compared (see Chapter 2).

3.2 ERECTION AND CONSTRUCTION PROCEDURE AND SEQUENCING

The following is a description of the erection and construction procedure. This section provides a general overview of how the structure was constructed, and how this procedure affected the stresses in the structure. A detailed construction sequence of the bridge is included in Appendix D.

3.2.1 Erection of the Curved Girders and Crossframes

The erection of the bridge began on July 17, 1995 in span 1 (i.e., the southern span) with the innermost girders. Girders 305A1, 309A2, 306B1, and 310B2 (see Figure 2.4) were delivered to the construction site in the morning by PDM. They were placed on the ground until the evening when the erection began. The erection of the girders occurred from 11:00 p.m. to 7:00 a.m. to reduce traffic congestion. Two 100 ton crawler cranes and one 50 ton 4-wheel crane were used to lift the girders and crossframes into place. Girder 305A1 was hoisted by a 100 ton crane, using a 20 foot spreader bar (which allowed for two lifting points), and the 50 ton crane, using a single lifting point, and the southern end of the girder was placed on the southern abutment. (There were some fit-up problems that occurred resulting from an improperly sized hole in the girder bearing plate. This problem was fixed after the erection was completed.) The other 100 ton crane then hoisted girder 309A2 using a "come-along" and a 30 foot spreader, and aligned it , with the help of the some workers, with girder 305A1. The "come-along" is a device shown in Figure 3.1. The "come-along" prevents the girder from tilting out of the vertical plane, and this helps the fit up of the two girders. With the two girders being in alignment, the bolts for the splice were put into place and the nuts were tightened using an air pump driver. While this was being done, a shoring tower was placed approximately at the midspan of span 1 to support the bottom flange and increase the stability of the girders. The shoring tower helps to control the vertical geometry of the structure so that it acts as a unit until all girders are connected by crossframes, and it also improves the alignment of the total structure, which helps during the attachment of the crossframes. A shoring tower was used for each girder during the erection of both spans 1 and 2. Note that while MN/DOT did anticipate the possible use of shoring towers, and thus provided shoring tower locations, this structure was actually designed presuming no shoring towers were to be used -- it was the steel erector that opted to use them.

After the splice was tightened, the 100 ton and 50 ton crane holding girder 305A1 were released, and the two cranes lifted girder 306B1 into place while the second 100 ton crane continued to support girder 309A2. After the girder was placed on the southern abutment, the 50 ton crane was released, and it began to lift crossframes which were connected between girders 305A1 and 306B1. A crossframe was placed at approximately the quarter point of the span and at the southern end of the span. These two crossframes were held in place with four bolts (one per gusset plate). The second 100 ton crane released girder 309A2 and hoisted girder 310B2, once again using the "come-along". This girder was then aligned with 306B1, and the splice connecting the two girders was tightened. The remaining crossframes for that span were placed and secured. The following night, girders 307C1, 311C2, 308D1, and 312D2 were erected in a similar manner. This is the point at which the first set of strain readings were taken. During July 24 and July 25, 1995, the four girders in span 2 (northern span) were erected. The erection began with the outermost girder and proceeded towards the innermost girder. The 100 ton and the 50 ton crane were employed to hoist the girders and crossframes into place. Note that the four shoring towers were moved from span 1 to span 2 during the day of July 25 (after two of the four girders of span 2 were erected). Following each night's erection, all of the bolts were placed for all of the crossframes. In some cases the bolts were pounded into place with a sledge hammer which could have induced stresses in the structure. After the entire steel structure was erected, the entire structure was "rattled up". The "rattling up" procedure involved the final tightening of all bolts, connecting the crossframes to the girders, along with the removal of all the shoring towers. This was the final state of the structure before the formwork was constructed.

3.2.2 Construction of the Formwork and Placement of Reinforcement

After the erection of the girders and crossframes, the placement of the formwork began. The formwork consists of whalers, 2" x 10" boards with end clamps attached to the top flange of the girders, supporting 3/4" plywood decking spanning between the girders. Outside the two outermost girders, right triangle bar supports were spaced approximately every five feet, and 2" x 6" boards supported the formwork for the concrete to be poured outside of the girders. These supports are cantilevers wedged against the underside of the top flange with a 4"x 4" board in order to force the tip of the triangle against the web to create a reaction against the weight of the forms. Figure 3.2 shows a such a support, with the dark lines being the girder and triangular support, and the gray being the board and formwork.

Other loading resulted from the weight of the workers and their equipment. In general there were five to ten workers and two air compressors weighing 2,784 lb. each on the bridge during the construction. After the formwork was finished, the shear connectors were welded to the top flanges of the girders. These shear connectors allow the steel girders and the reinforced concrete to act compositely to resist the forces in the positive moment regions. The final preparation of the structure before the pouring of the concrete deck involved the placement of the reinforcement. The bottom layer of steel was in the longitudinal direction. Next the transverse steel was placed followed by the top layer of longitudinal reinforcement. The concrete deck was poured on August 11, 1995. After the deck was allowed to properly cure, the reinforcement cage for the parapet walls (i.e., the concrete traffic bariers) was fabricated. Once this task was completed, a slip former was used to form the parapet walls. The slip former was the shape of the parapet walls. The concrete was pumped directly into the slip former, and this allowed the walls to be fabricated as the slip former progressed along the bridge. The final step in the construction of the bridge was the pouring of the two inch low slump concrete overlay. Once all of this construction was completed, the bridge was opened to traffic.

3.3 CONSTRUCTION STRESSES

This section contains observations of the data acquired during the various construction stages. When describing a particular stress, the given location of the stress may be classified in different ways depending on how specific a reference is required. The convention used to reference these locations is as follows. Starting with the outside facia girder and proceeding towards the inside facia girder, the girders are labeled as girder 1, girder 2, girder 3, and girder 4. If an individual girder is referenced, then the designations from the structural plans are used, i.e., girders 308D1, 312D2, and 316D3 are spliced together to form girder 1. If a more exact is location needed, then the gage line can be specified. Finally, the actual gage number can furnish an exact location. The same notation is used when describing the crossframes, except that crossframe 323CF15 is called crossframe 1, crossframe 324CF13 is called crossframe 2, and crossframe 325CF13 is called crossframe 3. Figures 2.4 and 2.5 illustrate all of these designations described above. When describing a stress value, a negative value indicates compression and a positive value indicates tension. Units of kilo-pounds (kips) per square inch, ksi, will be used throughout this report to display the values of stress observed.

The strains obtained from the field measurements are longitudinal (i.e., they are oriented along the primary axis of the member), and are linearly related to longitudinal stress by Young's modulus of elasticity, which for the steel in this project is taken as 29,000 ksi. This calculation of stress from strain, based upon linear elastic behavior, presupposes there is no yielding or significant geometric nonlinearity in any member during construction. For this structure, the nominal yield stress of the steel members is 50 ksi.

3.3.1 Stresses During Construction of the Steel Superstructure

This section summarizes the stresses observed at each of the loading stages detailed above. At each stage of construction a complete set of strain readings was taken, and the data was reduced to observe the stresses relating to that stage. In Appendices A, B, and C, the cross-sectional stresses for all sixty gages are displayed on one sheet per one set of readings. A cover sheet detailing the loading condition, reading objective, and general observations accompanies each data sheet. The change in stress between each loading stage was also examined. This allowed the correlation of the resulting stresses to the additional loading for that stage. Another cover sheet accompanied the data sheet that detailed the changes in stress. An overview follows that discusses the general behavior observed during the erection and construction of the bridge. Refer to Appendices A, B, and C for the detailed results.

There was little obvious correlation of stresses to loading in the first two loading stages. These readings were taken during the erection of the steel girders and crossframes (see Appendix A). There was not enough dead load to induced significant stress in the girders. The largest stress, 5.88 ksi, was observed in a member of the crossframes. This stress probably resulted from the placement of the bolts. As described earlier, the alignment between the girders and the crossframes was not exact. The day following the erection of the girders, the remaining bolts were placed. In many cases, the bolts were hammered into place to allow proper fit up. This fit up process could have induced these stresses. The largest stresses otherwise were -3.77 ksi in compression and 3.27 ksi in tension. All of the observed values are minimal compared to the total allowable stress of the members. In the July 24 readings, girder 312D2 does exhibit clear strong axis bending behavior, plus the effects of warping, which is to be expected since this is the sole girder at the time contributing to the negative moment across the full span. On July 24, stresses could also have been induced by the crane when hoisting the girders into place, which could be another possible explanation for these erratic stresses.

Clearer stress distributions resulted on July 26, after erection of the full steel skeleton, loosely bolted. Once all of the girders were in place with all of the bolts still loose, the general trend of the behavior of the girders, except for girder 1 at the middle pier, was as expected. At this loading stage, the maximum and minimum stresses were -4.34 and 6.5 ksi, which are fairly minimal.

Once all of the bolts were in place, the whole structure was "rattled up" which involved the final aligning of the structure through the tightening of all of the bolts. The change in stress observed for this loading stage ranged from -0.87 ksi to 1.15 ksi. As can be observed, the "rattling up" of the structure did not significantly increase the stresses. This illustrates that the majority of the erection induced stresses (as opposed to stresses due to self weight) resulted from the alignment corrections that allowed the placement of the crossframe bolts. Aside from four gages (i.e., girders 2 and 3 at the midspan), the behavior of the girders is as expected. The range of stresses present in the structure resulting from the erection of the steel members were:

midspan: -3.78 ksi to 2.87 ksi
middle pier: -4.75 ksi to 6.74 ksi
crossframes: -3.04 ksi to 4.41 ksi

After the formwork was placed, the largest stress increase ranged from -1.75 to 1.27 ksi. There was one isolated increase that was not within this range, in which girder 309A2 had a change in stress of 3.08 ksi. The reason for this isolated increase is not explainable, although it may relate to an odd eccentricity present in the construction live load in that area.

The next reading was taken after the reinforcement was placed. The stresses did not increase much, with the changes ranging from -0.66 to 0.65 ksi. The largest values of stress present before the pouring of the concrete deck were:

midspan: -4.36 ksi to 3.18 ksi
middle pier: -4.78 ksi to 7.75 ksi
crossframes: -3.68 ksi to 5.60 ksi

The girders behaved as expected at the midspan (i.e., for girders in a positive moment region) and the middle pier (i.e., for girders in a negative moment region) due to the loading of the reinforced concrete deck. The loads were finally sufficient to yield consistent behavior of the stresses; any anomolies due to fitup and small load eccentricities were overwhelmed by the increase in deadweight on the bridge. The change in stress due to the pouring of the concrete deck ranged from -7.87 to 6.00 ksi. The greatest magnitude of stresses present at this stage were:

midspan: -9.65 ksi to 5.95 ksi
middle pier: -11.72 ksi to 11.79 ksi
crossframes: -9.13 ksi to 10.75 ksi

The pouring of the concrete parapet walls (August 25) induced stresses whose magnitudes were consistent with the expected behavior at the midspan and middle pier. However, several of the midspan top flange gages picked up a tiny amount of tension during the parapet wall pour. This could be due to the stresses redistributing across the cross section of the bridge due to the additional loading along the outer edges of the deck, or the composite action of the bridge at the midspan. In general, once the deck hardened, the top flange gages at the midspan showed much less change in stress than the bottom flange, and these results from the parapet wall pour show that the neutral axis of the girders due to strong axis bending was probably near or in the top of the girder top flanges. The stress envelope for this load stage is:

midspan: -7.99 ksi to 6.88 ksi
middle pier: -13.79 ksi to 13.26 ksi
crossframes: -9.17 ksi to 9.77 ksi

The final construction stress reading was taken after the 2 inch concrete overlay was poured. This was the final state of the bridge before it was opened to traffic. The behavior of the girder flanges was as predicted at the midspan and middle pier, although the crossframe behavior was less predictable, as was customary throughout the construction process. The final state of stresses for the bridge before being put into service were:

midspan: -11.10 ksi to 7.73 ksi

middle pier: -14.68 ksi to 13.27 ksi

crossframes: -12.36 ksi to 9.87 ksi

These values are well within the allowable stresses of the structure, and they are comparable to the computer predicted values, as will be shown in Chapter 6. For the final three loading stages at the middle pier, the largest compressive stress occurred at the top inside flange tip of the inside facia girder, and the largest tensile stress occurred at the bottom inside flange tip of the same girder. In the crossframes, the largest tensile stress occurred in the top horizontal of crossframe 1 while the largest compressive stress occurred in the bottom horizontal of crossframe 1. The largest stresses at the midspan varied with each loading stage.

3.3.2 Stresses During the Pouring of the Reinforced Concrete Deck

The following section contains the data taken during the pouring of the concrete bridge deck. Each loading stage occurred at thirty minute intervals, and at every loading stage a complete reading of all sixty gages was recorded. In an attempt to record as readings continuously as possible, sixteen gages (1A, 4A, 5A, 6A, 13A, 16A, 17A, 18A, 1B, 4B, 5B, 6B, 13B, 16B, 17B, and 18B) were read approximately every ten minutes. The pouring of the bridge deck began at 4:15 a.m. at the north abutment. Concrete locations are referenced from the north abutment for the loading condition for each loading stage. There were ten to fourteen workers at a given time working the concrete. These workers' various duties included directing the wet concrete with the concrete pump, spreading the concrete, vibrating the concrete, hand finishing the concrete, and running the finishing machine. A break was taken by the workers from 6:10 a.m. to 6:40 a.m. The following defines the time of each loading stage:

Stage 0: 4:15 a.m. - The girders with the formwork and reinforcement in place
Stage 1: 4:45 a.m. - The concrete deck located at the first quarter point of span two
Stage 2: 5:15 a.m. - The concrete deck located at the midspan of span two
Stage 3: 5:45 a.m. - The concrete deck located at the middle pier
Stage 4: 6:15 a.m. - The concrete deck located at the first quarter point of span one
Stage 5: 7:00 a.m. - The concrete deck located at the midspan of span one
Stage 6: 7:30 a.m. - The concrete deck located at the third quarter point of span one
Stage 7: 7:50 a.m. - The entire concrete was finished
Stage 8: 8:15 a.m. - Reading taken to determine the stress change after thirty minutes

Figure 3.3 (and, equivalently, Figure B.1) details the location of each loading stage on a plan view of the bridge. The following section summarizes the data recorded for each of the loading stages during the pouring of the concrete deck. Appendix B contains these stresses. For each loading stage, there is a cover sheet describing the loading condition, reading objective, and general observations, followed by two sheets: one displaying the change in stress between each stage and the other the actual stress present. The observations on the cover sheets describe the changes in the stresses from load stage to load stage. This approach permits the observation of the behavior of the girders as the pour progressed along the bridge, regardless of the in-situ stresses at the time of the reading. In addition, Appendix B contains graphs showing the total stress and the change in stress in each gage as a function of time.

Stages 1, 2, & 3: In a two span bridge when the loading is in one span, a negative moment region is created in the other span. Except for girder 4, the girder stresses at the midspan of span 1 exhibited behavior expected in a negative moment region, which is tension in the top flange and compression in the bottom flange. Girder 4 experienced compression in the top flange and tension in the bottom flange. This is due to an apparent moment or differential deflection acting across the width of the girders. Beginning at the outside facia girder, the stresses are the largest. At each respective gage location, the stress decreases, and ultimately reverses sign as the inside facia girder is approached. Figure 3.4 illustrates this point. The girders at the middle pier are also experiencing stresses indicative of a negative moment region, which is expected.

As the pour continued to the midspan of span 2 the girders, with the exception of girder 4, continued to respond with the stress pattern observed in the previous loading stage. The differential behavior across the width of the deck continued to be observed. The stress changes at the midspan increased, in most cases, by 2 to 2.5 times that of the increase observed in load stage 1. At the middle pier, the largest increase in stress was 2.8 times that of the stress changes in load stage 1. The change in stress in the crossframes was approximately of the same magnitude as that of the girders, and the diagonals in the crossframes continued to display compression in the top members, except for gage 10C, and tension in the bottom members.

At stage 3 the pour had reached the middle pier. The change in stress continued with the same expected pattern. The range of the stress change from stage 2 to 3 at the midspan was 0.07 to 0.65 ksi (tension) and -0.06 to -0.19 ksi (compression), and the range of stress change from stage 2 to 3 at the middle pier was 0.14 to 1.01 ksi (tension) and -0.19 to -0.78 ksi (compression). The change in the stresses in the crossframes was 0.02 to 0.67 ksi and -0.07 to -0.49 ksi. The envelope of the magnitude of stresses present after the pouring of the second span (from the beginning of the pour) was:

midspan: -4.50 ksi to 2.42 ksi
middle pier: -1.54 ksi to 9.71 ksi
crossframes: -1.32 ksi to 2.03 ksi

Stages 4,5,6, & 7: The next four loading stages observed the behavior of the girders when the concrete was poured in the first span. There was a thirty minute break between the completion of the pour in span 2 and the start of the span 1 pour. When the concrete had reached the first quarter point there-was not much change in the stresses. Except for a few gage locations, the beginning of a stress reversal at the midspan was observed, which is expected since the midspan will be a positive moment region. The middle pier stresses continued to respond as gages in a negative moment region. A stress reversal was also observed in the diagonals of the crossframes. The top two members displayed a change in tensile stress with the bottom two members exhibiting a change in compressive stress. The range of stress changes for the cross sections were -0.98 ksi to 76 ksi for the crossframes and -0.59 ksi to 0.39 ksi for the girders.

When the concrete reached the midspan of span 1 a definite increase in stress was observed. At the midspan, the top flanges displayed an increase in compressive stress and the bottom flanges an increase in tensile stress. The opposite behavior was occurring at the middle pier, and the previously described behavior in the crossframes continued. The stress change envelope at the midspan was -3.12 ksi to 1.31 ksi. The stress change envelope at the middle pier was -1.47 ksi to

1.65 ksi. The stress change envelope in the crossframes was -2.94 ksi to 3.21 ksi (there was a value of greater magnitude, but it was extrapolated from nearby data, since a crossframe gage temporarily did not read, and therefore this value is not used here as the largest tensile stress).

The trend in the stresses continued when the pour reached the third quarter point. The stress changes ranged -6.05 ksi to 2.80 ksi at the midspan, -1.30 ksi to 1.28 ksi at the middle pier, and -3.73 ksi to 2.12 ksi in the crossframes.

The stresses did not change significantly when the concrete pour was finished and had reached the southern abutment. Twenty-five minutes after the pour was finished, another set of readings was taken to observe any changes in stress that might occur due to composite action beginning to form. There was no significant change in stress to confirm the onset of composite action. The final state of stress of the bridge with wet concrete and no composite action was:

midspan: -9.29 ksi to 6.25 ksi
middle pier: -8.89 ksi to 10.83 ksi
crossframes: -8.84 ksi to 11.65 ksi

In addition to these "snapshots" of the stresses, plots were prepared displaying the stresses as the pour progressed. Plots displaying both the magnitude of stress and the change in stress observed during the pouring of the concrete deck are located in Appendix B. These plots were developed to display the bridge stresses versus the time line of the pouring of the deck. Each plot displays the cross section for a single member at a given location, i.e., the first plot is of girder 1 at the midspan of span 1 (gages 1A-6A). As stated above, two plots were constructed for each of these cross sections: one displaying the change in stress versus time, and the other displaying the actual stress versus time. The abscissa displays the actual time of day, and the ordinate displays the stress in units of kips per square inch (ksi). The pouring of the concrete deck began at 4:15 a.m. at the northern abutment, progressed through span 2 to span 1, and was completed at the southern abutment at 7:50 a.m. When examining these plots, the left end of the abscissa represents the north abutment and the right end the south abutment. Icons displaying the progression of the pour are included on Figure B-18 to mark each loading stage on the time line. Once the pouring of the deck began, a full set of readings was taken every thirty minutes. These readings are represented by a solid line. The continuous readings taken for sixteen of the gages (see the gage numbers listed previously) are represented by a dashed line.

As documented above, the top flanges for the midspan gages generally experienced tensile stress while the bottom flanges experienced compressive stresses when the concrete was being placed in span 2. This was due to the negative moment created at this location in span 1. At 7:00 a.m., when the pour had progressed to the midspan of span 1, a reversal of stress occurred due to the positive moment created by the load of the wet concrete. The top flanges then experienced compressive stress while the bottom flanges experienced tensile stress. Throughout the entire pour, a negative moment region was located at the middle pier, so the top flanges experienced tension and the bottom flanges experienced compression. These stresses increased as the concrete pouring progressed to the southern abutment. The bottom two members in the crossframes experienced tension when the wet concrete was in span 2, and underwent a reversal of stress to compression once the concrete entered span 1. The top two members displayed the opposite behavior. When the concrete was in span 2, the stress experienced was compressive which increased in tension once the concrete entered span 1. There are interruptions in the lines in the plots of the crossframe stresses. This occurred because there were times when a gage did not read, so that data point was omitted

The behavior of the girders and crossframe observed during the pouring of the concrete deck was as expected. The range of the stresses were also of the magnitude that was expected before the pouring of the deck began. None of the stresses observed were extraordinary, and they were well within the capacity of stress that the bridge could support. This is significant since this is a critical portion of the construction of the bridge. The steel girders must support this large load without the benefit of composite action that the cured concrete deck will provide once the bridge is placed in service.

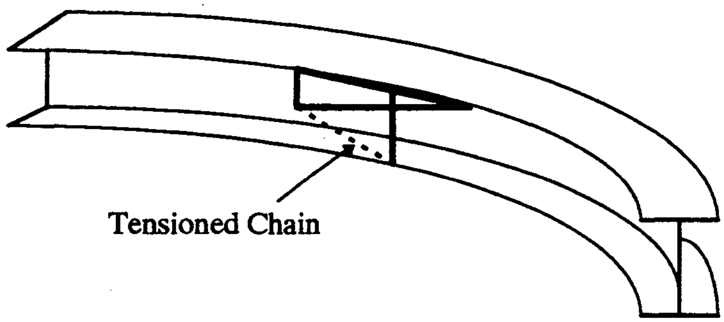

Figure 3.1. Come-along device

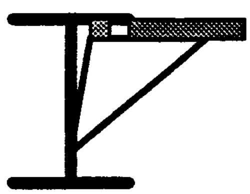

Figure 3.2. Right triangular bar support with plywood formwork

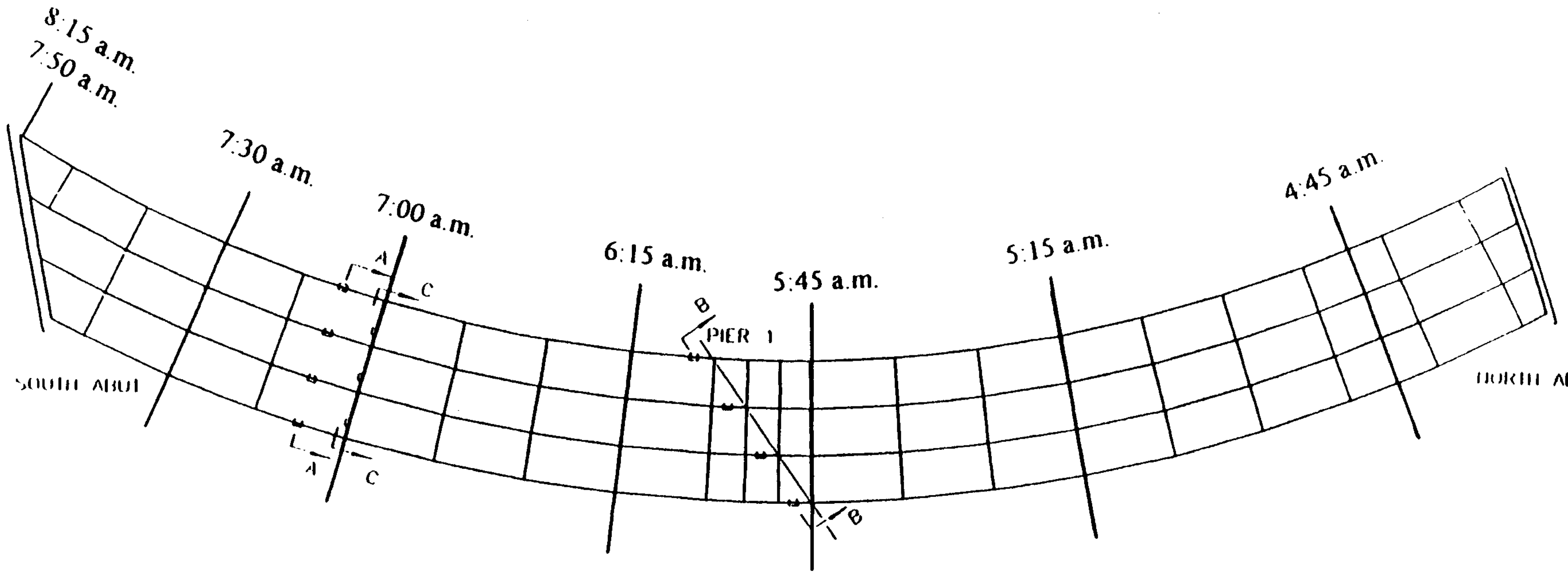

Figure 3.3. Plan view of the bridge displaying the progression of the pouring of the concrete deck

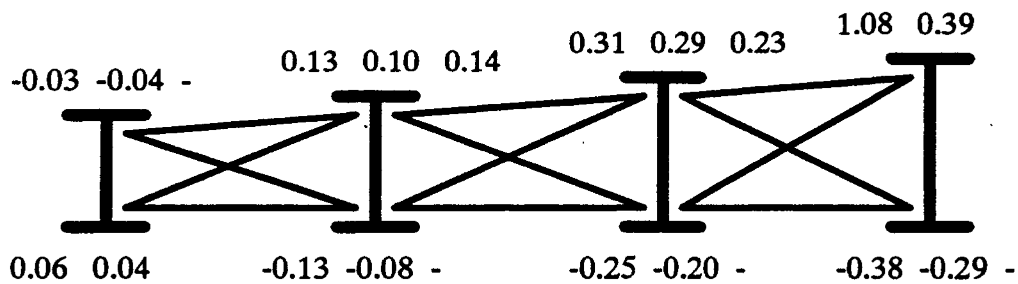

Figure 3.4. Example of girder stresses varying across the width of the bridge's cross section

CHAPTER 4

FIELD MEASUREMENTS DURING LIVE LOADING OF THE BRIDGE

4.1 INTRODUCTION

The final stage of this project was observing the behavior of the bridge under live load. The method for applying live load involved using two dump trucks weighing approximately 50 kips each. The beds of the trucks were loaded with sand, and their actual weights were measured with truck scales. Four basic loading configurations were selected including:

- Two Trucks Side by Side at the Quarter Points of the Bridge
- One Truck at the Quarter Points of the Bridge
- Two Trucks End to End at the Midspan of Each Span
- One Truck at the Midspan of Each Span Simultaneously

In all of the above cases, the trucks were centered along the width of the bridge. The quarter points, including the midspan, were measured and marked on the deck of the bridge. The trucks were guided to these areas, and the front tires of the trucks were located so that their center of gravity were as close to the quarter points as possible.

At each loading position a complete set of readings was taken, and they are displayed in Appendix C. Again, a cover sheet is included to describe the stresses observed. In addition to these separate readings, plots were made for the first two loading configurations, i.e., the trucks being located at the quarter points for each span. These plots display the member stresses for a given truck location, and allow the observation of how the stresses change as a vehicle travels along the bridge. In all of the stress readings taken, the change in stress was monitored. Before the trucks were placed on the bridge, a set of readings was taken to document the final unloaded stress state of the bridge. These readings were used as the baseline for comparing the stresses induced from the trucks. This was done to observe the behavior of the bridge without the stresses from construction affecting the readings. The locations where the trucks were placed were labeled from 1 to 6, and actually corresponded to specific crossframe positions at the approximate quarter points of the bridge (see Figure 4.1). The placement of the trucks started from the southern abutment and continued towards the northern abutment. Figure C-1 shows the exact locations of all fifteen cases of truck loading measured. Cases 1 through 6 correspond to two trucks placed side by side at the six locations, and cases 10 through 15 correspond to one truck placed at the six locations. Case 7 placed one truck on each span. Cases 8 and 9 had two trucks placed end to end on each span. In the following four sections the results from the truck live loading are discussed.

4.2 TWO TRUCKS SIDE BY SIDE AT THE QUARTER POINTS OF THE BRIDGE

For this loading condition the two trucks were placed side by side on the bridge deck at each of the bridge's quarter points. In general, the behavior of the girders was as expected. When the trucks were located in span 1, a positive moment region was created at the midspan, and a negative moment region was created at the middle pier support. Except for gage 19A, the inside tip of the top flange of the inside facia girder, the top flanges experienced compressive stress, and the bottom flanges experienced tensile stress. The maximum stresses for both flanges were observed when the two trucks were placed at truck location 2 which was directly over the gages at the midspan of span 1. As the placement of the trucks continued away from truck location 2, these stresses decreased until a reversal in the stresses occurred at truck location 4. At this location the trucks were in span 2, so a negative moment region was created at the midspan of span 1. This produced tension in the top flanges and compression in the bottom flanges. When compared to the stresses observed when the trucks were in span 1, these stresses were fairly minimal. The stresses observed for the top flanges were minimal throughout this loading stage because of the composite action present in the midspans of the bridge. In these regions, the steel girders had the assistance of the concrete deck, through the shear connectors, in resisting the truck live loading. These stresses ranged between approximately 0.10 ksi and approximately -0.30 ksi. The bottom flange stresses ranged between approximately 1.50 ksi and approximately -0.30 ksi. The largest stress observed during this loading stage was 1.48 ksi at gage location 12A. At the middle pier gage line, the top flanges experienced tensile stress and the bottom flanges experienced compressive stress at all of the truck loading locations. This behavior was expected because this line of gages is located at the middle pier, and loading in either of the spans would cause this area of the bridge to be a negative moment region. The stresses in both the bottom and top flanges increased and reached a maximum as truck location 3 was approached. The stresses decreased at truck location 4. This was probably a result of the loading being directly resisted by the middle pier and not transferring the load to gage line B. The stresses increased and approached the previously observed magnitudes at truck location 3 when the trucks were at location 5. The top flange stresses were once again minimal when compared with the values of stress in the bottom flanges. It appears that some composite action is occurring with the top flange and concrete deck even though no shear connectors are present in this area. This could be a result of bond between the concrete and steel. The stress for the top flanges was not greater than approximately 0.15 ksi, and the stress for the bottom flanges was not greater than approximately -0.75 ksi. The largest stress observed at the middle pier was -0.72 ksi. The stresses observed in the crossframes ranged from approximately -1.75 ksi to 1.00 ksi. The largest stress observed during the loading occurred at truck location 3 and had a value of -1.76 ksi. The diagonal members of the crossframes experienced the largest tensile and compressive stress with the horizontal members experiencing values in between. For these small loadings, there was not always an observable pattern or explanation for the individual behavior of the members of the crossframes.

4.3 ONE TRUCK AT THE QUARTER POINTS OF THE BRIDGE

The next loading condition involved the placement of one 50 kip truck at each quarter point of the two spans. The truck was centered along the width of the bridge. Equivalent behavior was generally observed as described for the two trucks placed side by side. In some cases though, the load from one truck was insufficient to induce the expected behavior in a negative or positive moment region. The same basic trends in the stresses were observed (i.e., maximum stresses occurred at truck location 3, with a stress reversal at truck location 4), but sometimes a stress that was expected to be compressive was observed to be a tensile stress. This behavior was observed more for the inside girders 3 and 4. It appears that the stiffer two girders 1 and 2 were resisting a greater portion of the stress, which caused the inside girders to experience a warping stress which caused some of the top flanges to experience tension instead of compression. The same behavior was also observed at the middle pier gages. The maximum stresses observed ranged from approximately -0.15 ksi to approximately 0.80 ksi at the midspan and approximately -0.45 ksi to approximately 0.10 ksi. Once again there was not an explainable pattern to the behavior of the crossframes. The range of stress experienced was approximately -1.00 ksi to approximately 0.30 ksi. These results show that greater loading is required if a definitive bridge behavior is to emerge from truck live loading.

4.4 TWO TRUCKS END TO END AT THE MIDSPAN OF EACH SPAN

In this loading stage, the two 50 kip trucks were placed end to end and centered at the midspan of each span. The trucks were also centered along the width of the bridge. This loading stage had an equivalent effect to that of the two trucks side by side at truck locations 2 and 5. Positive moment action was generated at the midspan of span 1 when the two trucks were located in span 1, and negative moment action was generated at the midspan of span 1 when the two trucks were located in span 2. A negative moment region was present at the middle pier gage line for both truck loading locations. The largest tensile stress was observed at the midspan of span 1 with the trucks in span 1 and equaled 1.37 ksi. The largest compressive stress located at the middle pier with the two trucks in span one equaled -0.68 ksi. The largest stresses in the crossframes were -1.81 ksi and 0.82 ksi. These stresses occurred with the two trucks in span 1.

4.5 ONE TRUCK AT THE MIDSPAN OF EACH SPAN SIMULTANEOUSLY

This loading stage involved placing one 50 kip truck at the midspan of each span at the same time. The stresses observed were not as significant as those in the previous loading stage. Again a positive moment region was observed at gage line A and a negative moment region was at gage line B. The largest tensile stress in the bottom flanges at the midspan was 0.66 ksi, and the largest compressive stress observed in the bottom flanges at the middle pier was -0.75 ksi. The range of stresses observed in the crossframes was -0.79 ksi to 0.38 ksi.

Notes:

The centerline of front wheels of each truck coincides with the line of crossframe; e.g., Case 2 on line 5.

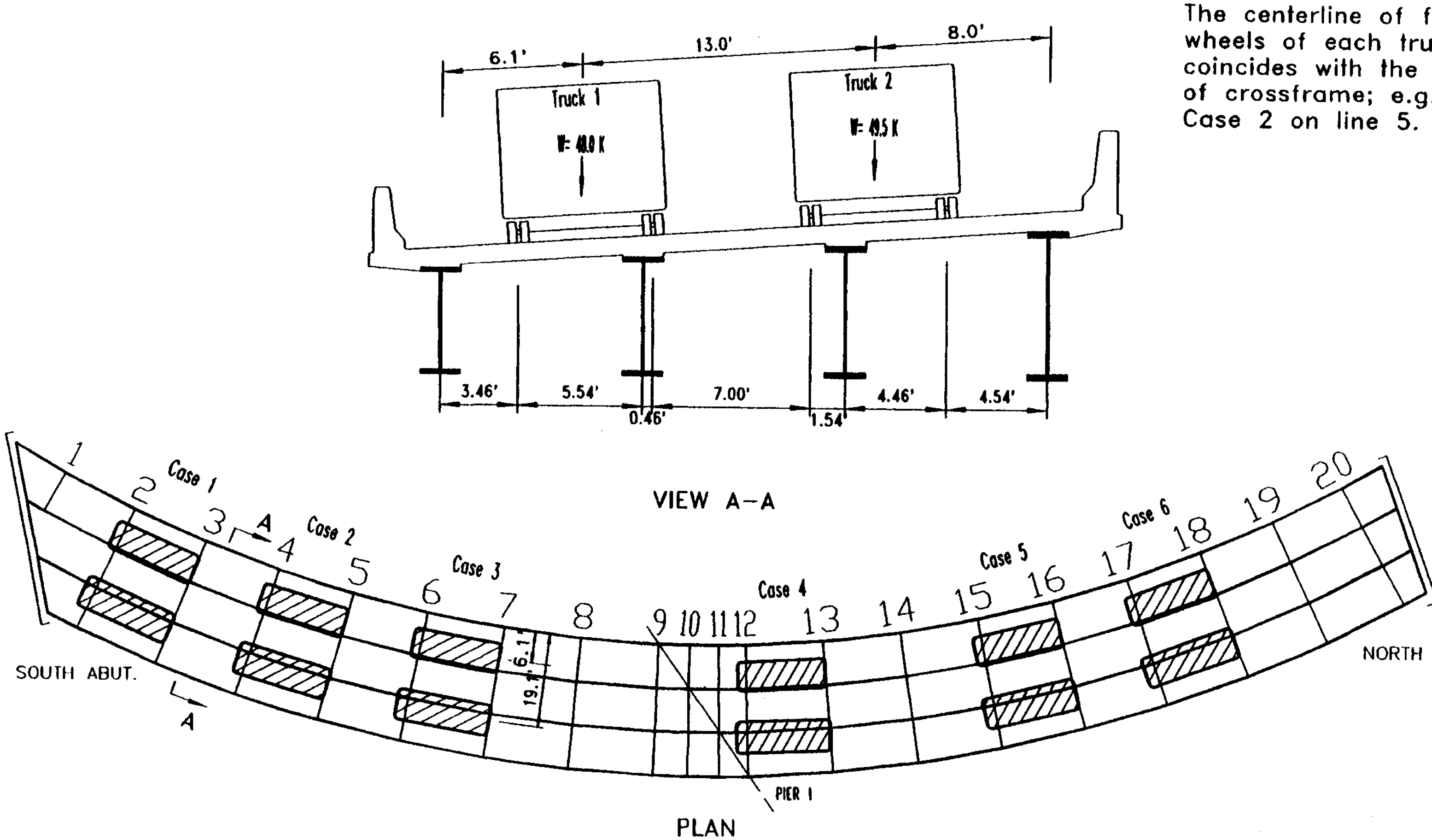

Figure 4.1. Plan of field tests for cases 1 to 6

CHAPTER 5
FINITE ELEMENT MODEL

5.1 INTRODUCTION

This chapter outlines the finite element models used to obtain computational results to compare to the field measurements. To permit detailed modeling of the specific topology and loading of this bridge during all phases of construction, the research team developed the University of Minnesota Steel Curved Girder Bridge System Analysis Program (i.e., the UM program). Before using this program to compare analysis results to the field measurements, the results from the program are compared to those obtained using DESCUS-I. In this way, conclusions may be drawn about the level of stresses seen in the subject bridge during construction, and about the ability of the software programs to reproduce these stresses accurately.

5.2 THE GRILLAGE METHOD

Among all the methods available for analyzing curved girder bridge systems, the Grillage Method, based on using a planar grid model, is most appropriate for practical use. This is the basic type of analysis used by the UM program, and is similar in its essentials to the type of analysis used in DESCUS-I. The basic idea of the Grillage Method is to use a two-dimensional finite element model to simulate the three-dimensional effects of bridge superstructures. Figure 5.1a illustrates the grillage model of this research, which uses four types of structural members, including longitudinal curved I-girders, crossframes, abutment beams, and transverse grids, for the curved steel I-girder bridge system. Figure 5.1b shows a cross section view of this bridge system. A primary difference between the Grillage Method and the Grid Method (which is commonly used for straight girder bridge systems) is that the Grillage Method includes a warping degree-of-freedom in the analysis.

The Grillage Method is a stiffness-based finite element procedure which first assembles the system stiffness matrix by adding all element stiffnesses directly from the referenced nodal degrees-of-freedom. Once the global stiffness matrix is formed, an equation solver, based on the Cholesky decomposition algorithm, is used to solve the simultaneous equations for the displacements. Warping effects of open sections are taken into consideration, similar to the way proposed by Mondkar and Powell [13]. This section describes the basic assumptions and element library of the Grillage Method followed by a discussion of the modeling and boundary conditions of the MN/DOT bridge.

5.2.1 Basic Assumptions

The basic assumptions in the Grillage Method are as follows:

1. All members have a monosymmetric cross section.

2. The structure behaves like a grillage: any force or displacement vector acting at a node has four components, or degrees-of-freedom, including one translational component normal to the plane of grillage, two rotational components about axes in the plane of grillage, and one additional component, referred to as the twisting rate, to account for the warping effect.

3. The interaction behavior among all grillage members is obtained with respect to the average plane, which is referred to as the grillage plane, defined by the principal centroidal axes of the curved girders. However, members other than the curved girders which have their centroidal axes at a different level from the grillage plane are permitted in this method by accounting for their offsets from this plane, so that the analysis can be practical and flexible, yet mathematically consistent.

4. Shear deformation is neglected.

5. Nonuniform torsion (warping) is included.

6. Support conditions are idealized as either fixed or pinned.

7. Straight members such as crossframes, abutment beams, and supports may be either radially positioned or skewed.

8. Girder spacing and member section may be varied.

9. Composite construction is considered.

10. Loading applied to the girder can include any number of concentrated and/or uniformly distributed loads.

5.2.2 Element Library

This section briefly describes the different finite element models included in the grillage method.

5.2.2.1 Curved I-Girder

The curved I-girders are represented by a three-dimensional two-node curved beam element with seven degrees-of-freedom at each node. In a curved steel I-girder bridge, the in-plane (in the plane of curvature) displacements, including the two translational displacements in the plane of the bridge, and one rotational displacement about the axis perpendicular to the plane of the bridge, are small compared to the out-of-plane displacements, and may be neglected. This is the principal idea behind the Grillage Method, which generally assumes four degrees-of-freedom at each node as shown in Figure 5.2a. The girder members may vary in depth, width, or other cross section dimensions along their length. The composite action with the concrete deck on top of the girder is only considered in the positive moment region or in the regions with shear studs. The program output gives stress resultants, including vertical shear force, torsion, bending moments, and bimoments corresponding to each degree-of-freedom, respectively. The computer program also provides information suitable for computing the normal (longitudinal) stresses in the girders.

5.2.2.2 Crossframes

In Figure 5.2b, crossframes of the X-bracing type are shown to be modeled as of truss frames made up of four pinned-end truss elements, for which only axial force is assumed. Noncomposite construction is considered in each crossframe since there are no shear studs connecting the crossframe members to the concrete slab. The axial force and its associated stress are calculated for each truss member of the crossframe in this method.

5.2.2.3. End Abutment Beams and/or Transverse Grids

End abutment beam and transverse grid elements are assumed to use the same type of straight beam finite element formulations in this analysis. End abutment beams are assumed not to be integral with the concrete slab since the spacing between longitudinal girders is in general not large. Therefore, the abutment beam is predominantly subject to negative moments which are not able to develop the composite behavior. Transverse grid elements, used to simulate the transverse behavior of the concrete deck, are assumed as straight beams with an effective width of concrete, and they are assumed to be attached on the top of the crossframes, spanning from girder to girder. Although the transverse grid and the crossframe share the same nodes in the analysis model, they are assumed to deform independently, except for the nodal continuity at their ends. Accordingly, noncomposite construction is considered for the transverse grids. Figure 5.2c shows the reduced degrees-of-freedom of the straight beam element. Output for this element includes the nodal displacements corresponding to the nodal degrees-of-freedom, and the stress resultants (member forces) at the beam ends. Bending normal stresses at top and bottom edges of the beam are also provided.

5.2.3 Modeling and Joint Conditions of The Project Bridge

This section describes the finite element model used in the analyses for this project.

5.2.3.1 Modeling

The structural analyses were performed by modeling the two-span curved I-girder system as a grid, shown in Figure 5.3. The south span, span 1, and the north span, span 2, are identified in the figure. There are 104 nodes, 100 curved girder elements, 58 crossframes, and 6 end crossframes for the mesh of the bare steel structure in this figure. An extra non-structural node number 105 is required for the reference center of curvature. The curved girder elements may also have composite properties if composite behavior is active, and in such cases the additional transverse reinforced concrete beam members are also considered as part of the crossframes acting on the top of crossframes. The nodes are located at points of crossframes, splices, supports and changes of cross section. Figure 5.3 also shows all the geometry required for the mesh modeling, such as the radius of curvature and arc length for each girder.

5.2.3.2 Joint Conditions

As described in Section 5.2.1, four degrees-of-freedom at each joint are appropriate for the analysis of curved I-girder bridges. However, a fifth and sixth degree-of-freedom are incorporated into these analyses for the following reasons. First, for consideration of thermal expansion, the use of vulcanized expansion bearings is necessary. The girders are allowed to displace in their longitudinal direction, and the skew end crossframes at both abutments thus induce axial forces when reacting against the curved girders. To better track the structural response of the project bridge, the axial degree-of-freedom is included at each joint in all analyses conducted with the UM program. The five degrees-of-freedom (d1 to d5) include: two translational components, where d1 is oriented along the axial direction of girders and d2 is oriented normal to the plane of the grillage; two rotational components about axes in the plane of the grillage, where d3 is oriented about the axial direction and d4 is oriented about the axis normal to the plane generated by d1 and d2; and one component referred to as the twisting rate to account for the warping effect, referred to as d5. For convenience, the boundary conditions at all supports for the subsequent structural analyses are assumed to be fixed for degrees-of-freedom d2 and d3, which means that the vertical deflection and the axial twist are restrained. Degree-of-freedom d1, representing the axial translation, is also fixed at the interior pier, since the fixed bearings are designed here. The joint conditions at all modeling nodes are tabulated in Table 5.1.

Second, the restraint of lateral (transverse) displacements provides artificial support at the nodal joints, thus affecting the analysis results in the crossframes. To investigate the stresses in the crossframes, a sixth degree-of freedom was often included in the UM program analyses (i.e., a degree-of-freedom in the transverse direction of the bridge at each node). These analyses are identified accordingly in Chapter 6.

In order to model pin connections, end force release codes may be employed on the straight beam elements in accordance with the connection types or other physical considerations between these elements and the girder elements. In the following analyses, all the straight beam elements, including the end crossframes and the transverse grid members, are considered not to transfer bending moments about the minor axes of their cross sections. In addition, the skew end diaphragms at both abutments are further considered not to transfer bending moments about the major axes.

5.3 COMPARISON BETWEEN DESCUS-I AND THE UM PROGRAM

In order to compare to field measurements during construction, it is necessary to be able to model detailed topological and loading conditions of the bridge, so as to match conditions in the field. The UM program provides much more control over these issues than DESCUS-I, and it is for this reason that it is used to compare to the field measurements. In order to be able to draw conclusions about the quality of the DESCUS-I program, the results from both of these programs are compared in this section. The differences between the two programs are compared first, followed by sample results from the comparison.

5.3.1 Differences in Formulation Between DESCUS-I and the UM Program

The methodology behind these two computer programs have differences described as follows:

1. Polynomial functions are chosen as the displacement shape functions in DESCUS-I while displacement solutions which are a combination of hyperbolic and trigonometric functions are used in the UM program.

2. The spacing of crossframes is defined as the width of the concrete grid elements in DESCUS-I, while only three tenths of this spacing is selected in the UM program to account for the shear lag, as described in Hambly [14].

3. The warping normal stresses are computed by interpolating between the fixed and the pinned end conditions in each girder element in DESCUS-I, while they are calculated from the bimoments in the UM program, since an additional degree-of-freedom for warping is considered in the grillage method of the UM program.

In addition, in the DESCUS-I analyses, the torsional rigidity of the girders was neglected, and the top chord of each crossframe was considered to have zero cross-sectional area. This was consistent with the modeling used for this bridge's design. These quantities were all calculated in the UM program.

5.3.2 Comparison of Computational Results

Two types of structural behavior are compared between the two programs. Noncomposite behavior is applied initially until the concrete hardens. This is followed by composite behavior, once the concrete strength is developed. The example of the noncomposite analysis being discussed is the bare steel structure subjected to the self weight of the steel and the wet concrete slab. Figure 5.4 depicts the vertical deflection of Beam 3 (the second to the outermost girder) along its length. Figure 5.5 shows a typical bending moment diagram of Beam 4, which is the outermost girder. The difference between the results obtained from DESCUS-I and the UM program is quite small. The percentage differences for the vertical deflections and the bending moments between these two programs are tabulated in Table 5.2. The maximum difference is found to be 9.43% in Beam 4 for vertical deflections and 5.23% in Beam 1 for bending moments, but most results are much closer.

The composite analysis models the composite structure with the ratio of the steel modulus to the concrete modulus, N, equal to 24 to account for long-term loading under superimposed dead loads (SDL) of 0.3775 k/ft uniformly distributed on each girder. This SDL includes the parapet, a two inch overlay, and the wearing surface. Results of the vertical deflection of Beam 2 and the bending moment of Beam 4 are shown in Figures 5.6 and 5.7, respectively. The percentage difference for this case is tabulated in Table 5.3, and the maximum difference is found to be 9.76% in Beam 4 for vertical deflections and 5.97% in Beam 1 for bending moments, although most errors are much smaller. The major differences occur at the innermost girder for bending moment and at the outermost girder for vertical deflections. The deflection differences are caused primarily by difference #3 (as listed in Section 5.3.1) of the methodology behind these two programs outlined earlier. The difference is found to be very minimal on the two interior girders where the torsional effects are relatively insignificant.

Because the two programs compare well for the two primary phases of construction typically analyzed during the design process, the UM program is utilized in this research to compare to field measurements. Subsequently, conclusions may then be drawn regarding the ability of DESCUS-I to provide a reasonable representation of the stresses in curved girder bridge systems.

Table 5.1 Nodal degrees-of-freedom

Conditions	Node No.	d_1	d_2	d_3	d_4	d_5	Notes
Abutments	1-4, 101-104	1	0	0	1	1	0- fixed, 1-free
Pier	48, 52, 56, 60	0	0	0	1	1	0- fixed, 1-free
Fixed point	105	0	0	0	0	0	0- fixed, 1-free
Free nodes	others	1	1	1	1	1	0- fixed, 1-free

Notes: The degrees-of-freedom d1 to d5 are defined as

d1- the linear component along the axial direction

d2- the linear component normal to the plane of the grid

d3- the rotational component about the axial direction

d4- the rotational component about the other axis normal to the plane entailing d1 and d2.

d5- the component regarding warping degree-of-freedom

Table 5.2 Percentage difference between MN/DOT DESCUS-I and UM programs due to bare steel subjected to steel weight and wet concrete

Span No.		Beam 1	Beam 2	Beam 3	Beam 4	Average
1	D	0.0	-1.97	-3.81	-3.13	-3.0~ 0.0
	M	-2.78	-0.52	-3.85	-4.44	-2.9
2	D	-3.34	-1.07	2.31	9.43	-2.2~ 5.9
	M	-5.23	-3.02	-3.05	-0.27	-2.9

Notes: Percentage Difference = (MN/DOT - UM) / UM * 100%

D- Deflection; M- Bending Moment

Table 5.3 Percentage difference between MN/DOT DESCUS-I and UM programs due to composite structure (N=24) subjected to superimposed dead loads

Span No.		Beam 1	Beam 2	Beam 3	Beam 4	Average
1	D	-2.33	0.0	2.5	9.76	-2.3~ 6.1
	M	-3.17	-0.98	1.28	0.86	-2.1~ 1.1
2	D	3.57	0.0	-1.89	1.89	-1.9~ 2.7
	M	5.97	-0.79	4.78	-0.57	-0.7~ 5.4

Notes: $N = E_s/E_c$

Percentage Difference = (MN/DOT - UM) / UM * 100%

D- Deflection; M- Bending Moment

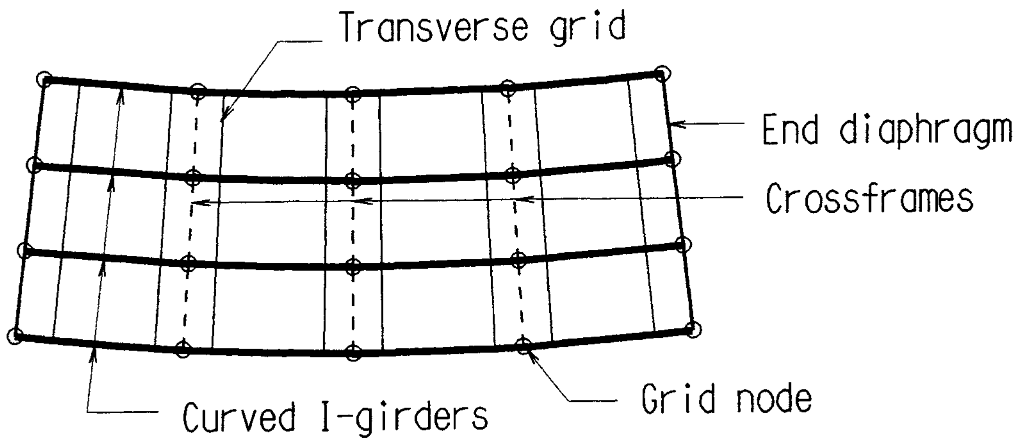

(a) Typical grillage model

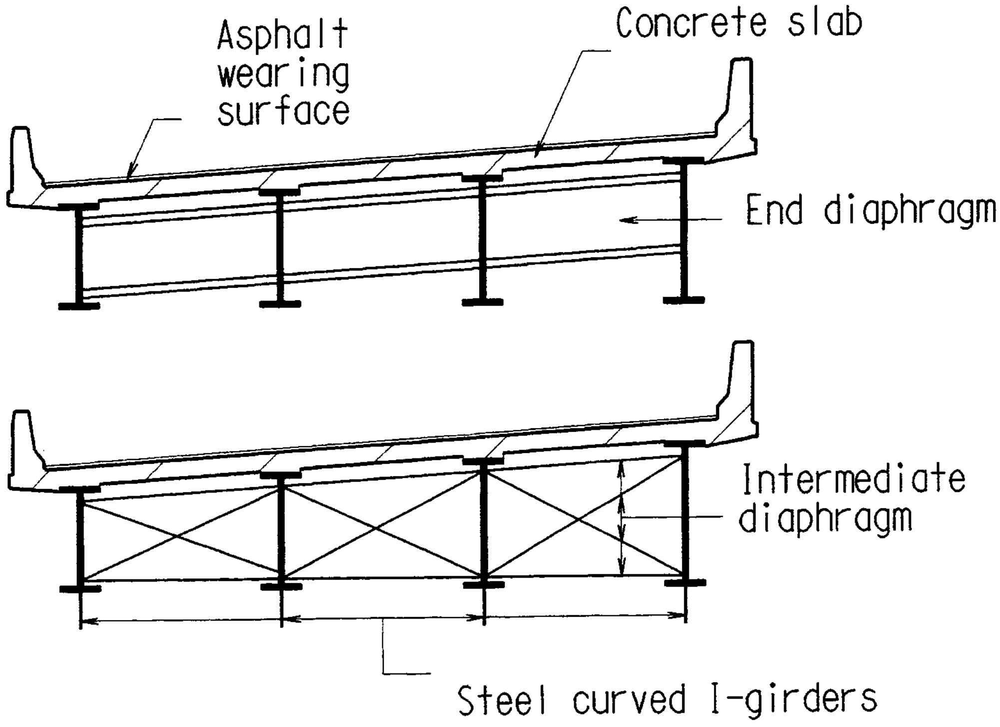

(b) Profiles of diaphragms

Figure 5.1. Grillage model and bridge profiles

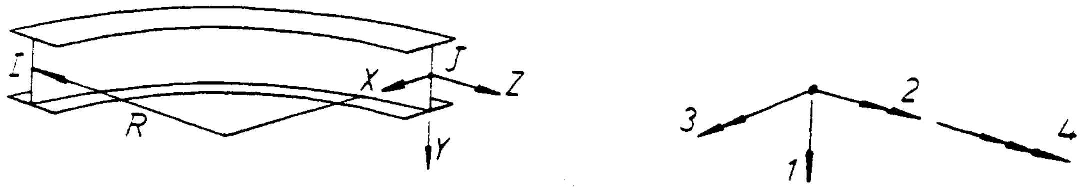

Two nodes per element

Reduced nodal degrees of freedom

(a) Curved I-girders

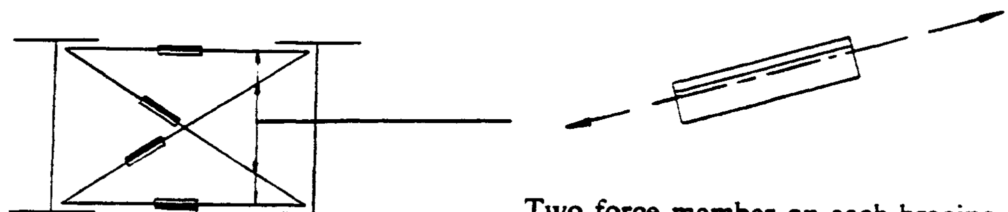

Two-force member on each bracing

Four bracing members per frame

(b) Crossframes

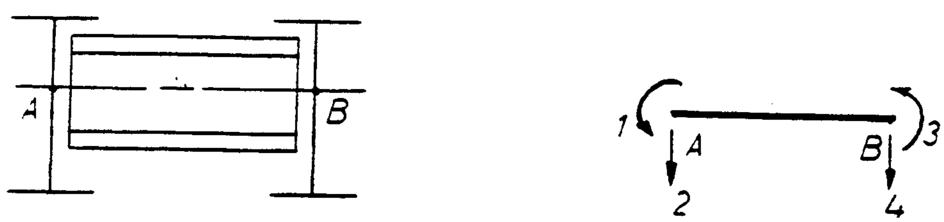

Two nodes per element

Reduced element degrees of freedom

(c) Abutment end diaphragms and/or transverse grids

Figure 5.2. Elements in the Grillage Method

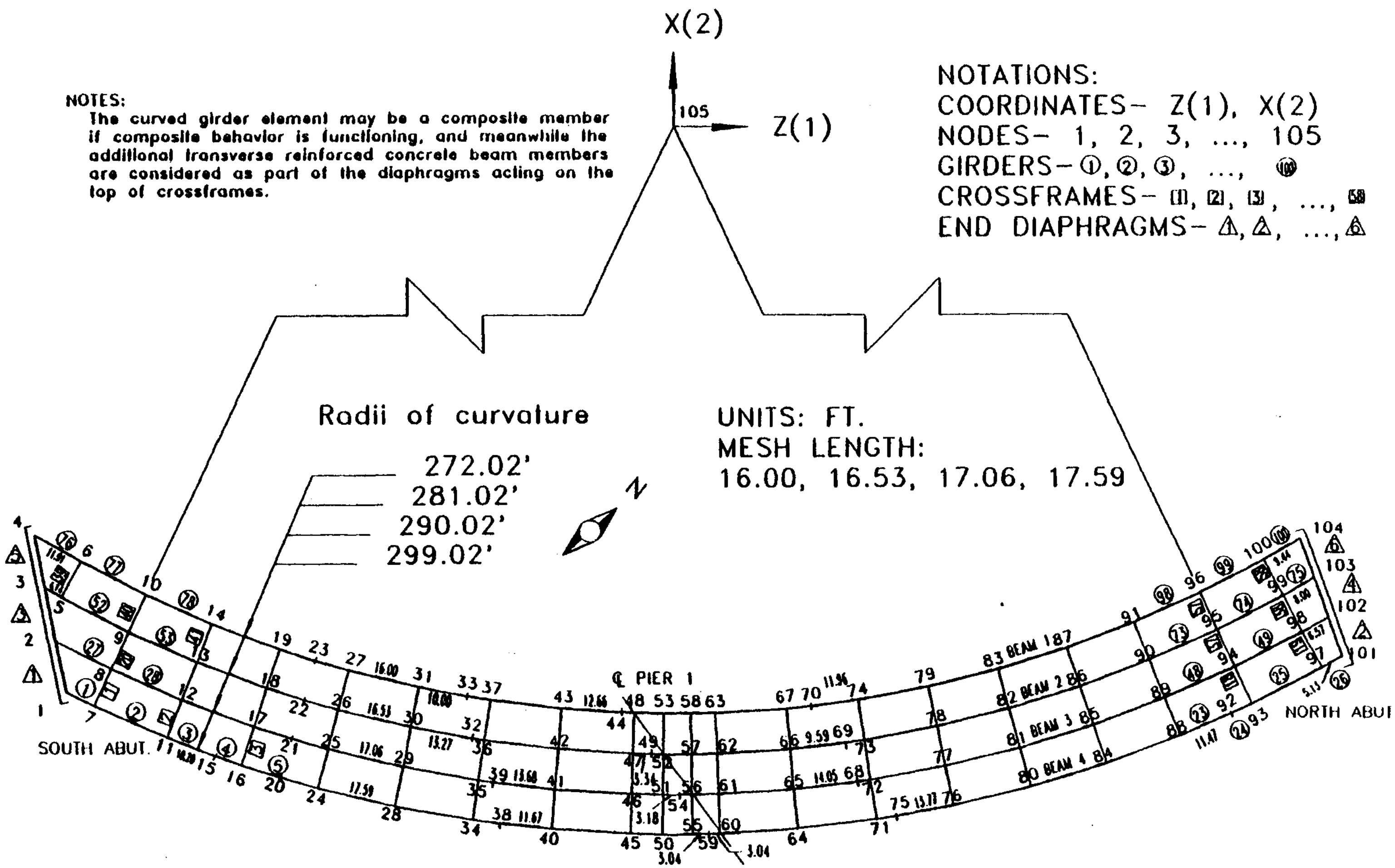

Figure 5.3. Modeling of the grid system

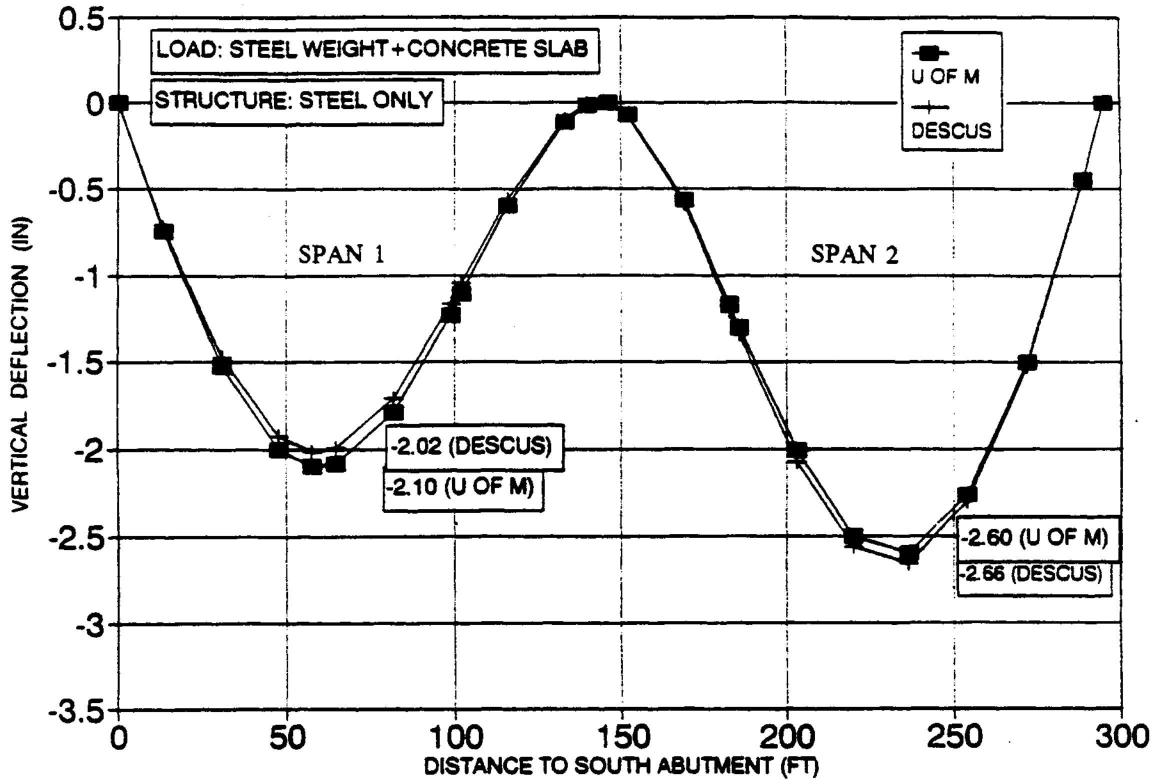

Figure 5.4. Comparison of vertical deflections between DESCUS and UM programs for non-composite analysis (Beam 3)

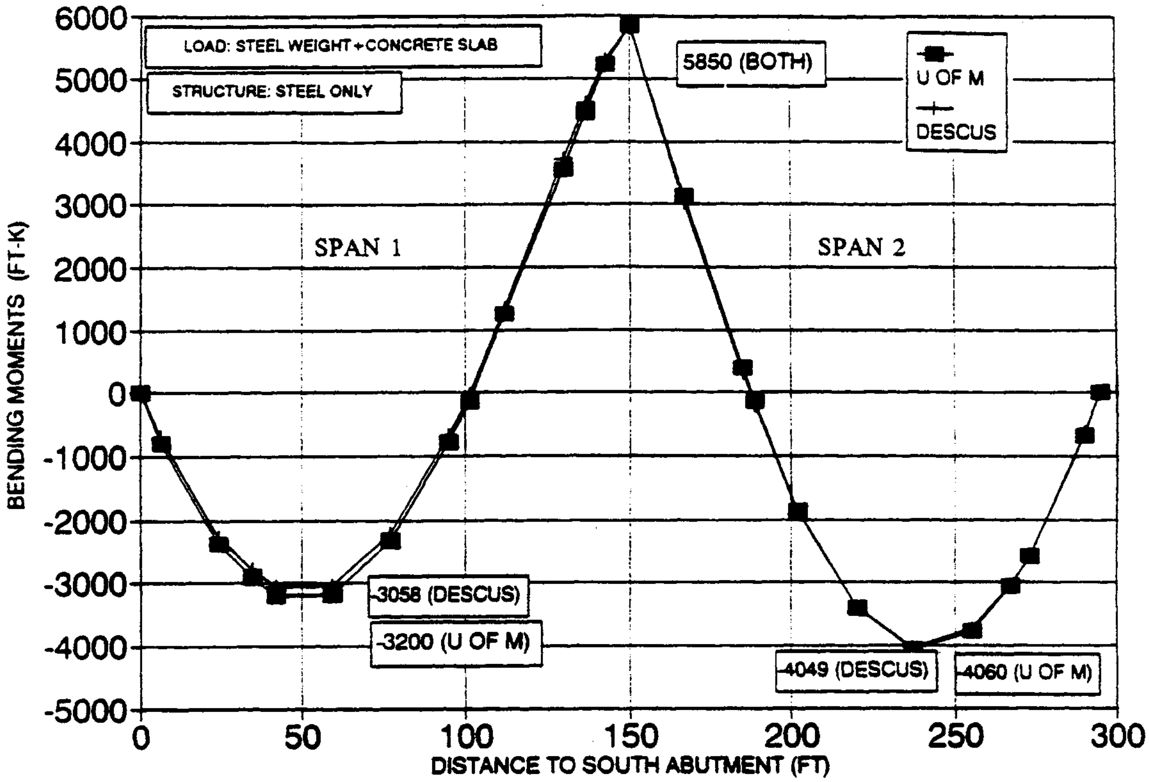

Figure 5.5. Comparison of bending moment diagrams between DESCUS and UM programs for non-composite analysis (Beam 4)

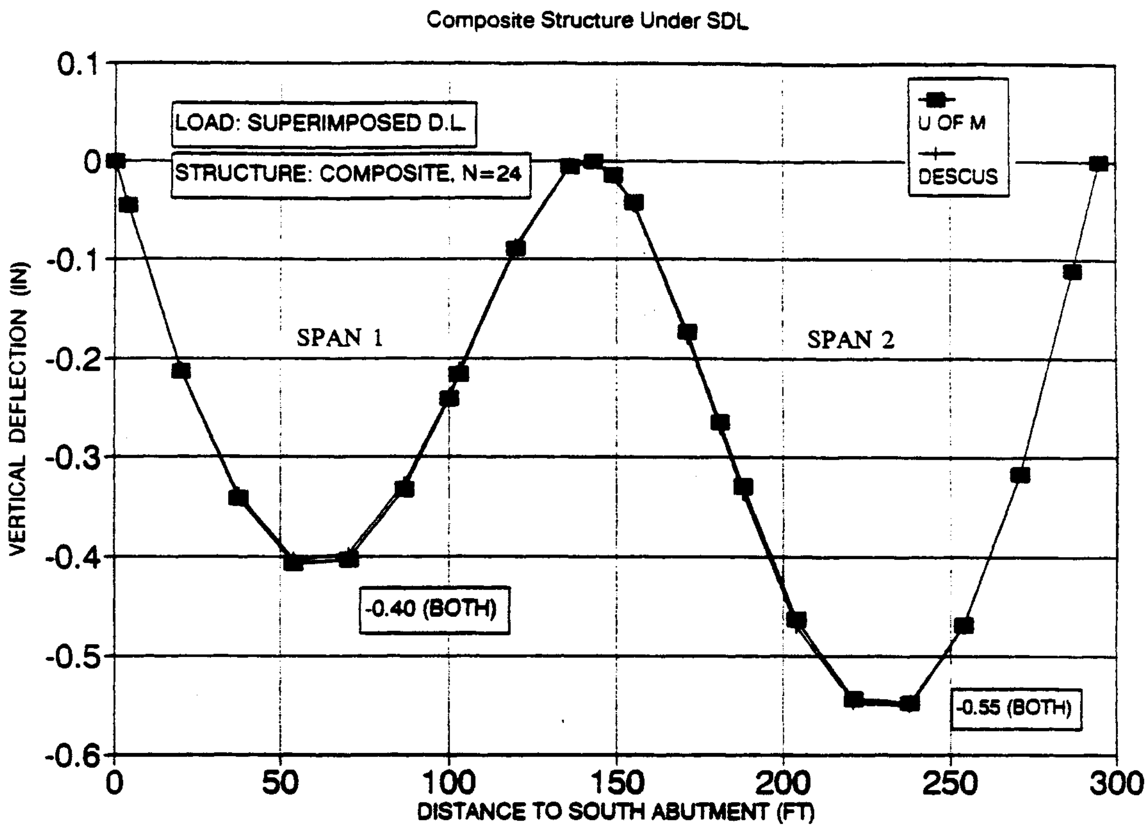

Figure 5.6. Comparison of vertical deflections between DESCUS and UM programs for composite analysis (N=24, Beam 2)

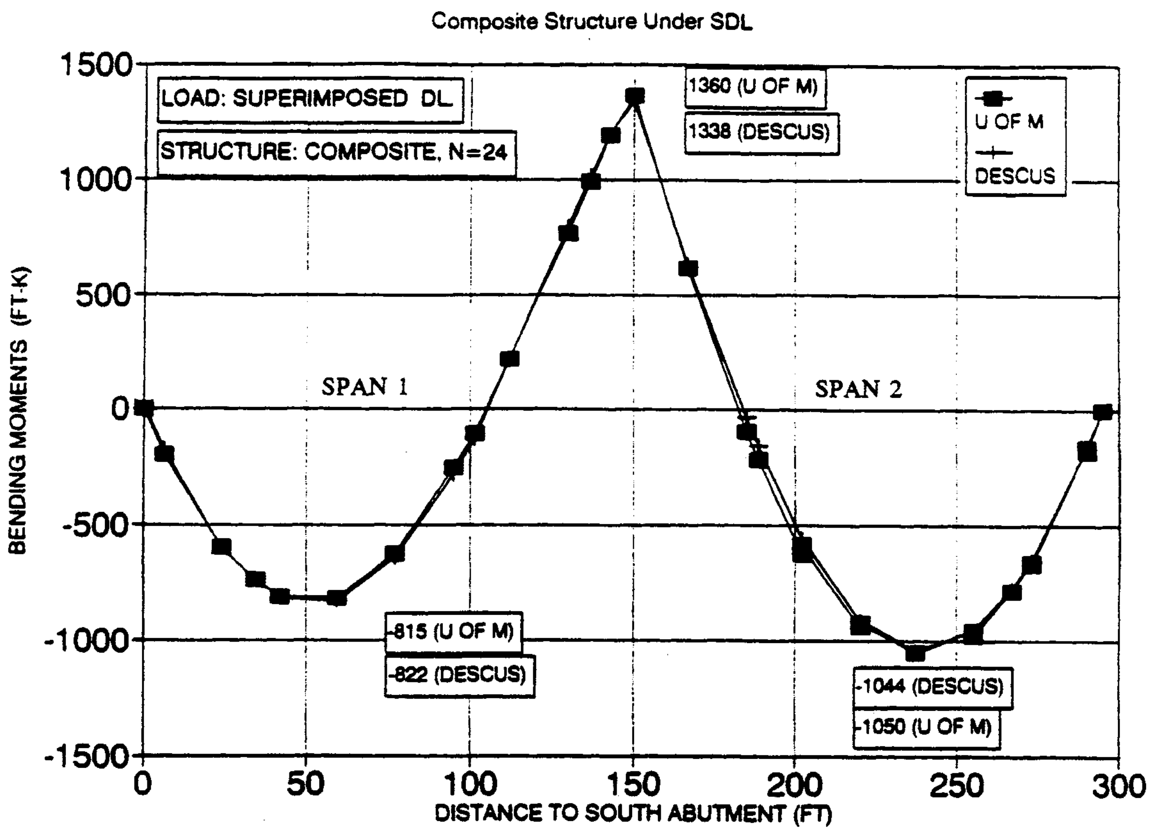

Figure 5.7. Comparison of bending moment diagrams between DESCUS and UM programs for composite analysis (N=24, Beam 4)

CHAPTER 6

COMPARISON BETWEEN THE COMPUTATIONAL ANALYSIS AND THE FIELD MEASUREMENTS

This chapter compares the results of analyses using the UM program with stresses obtained from field measurements of strain conducted on MN/DOT Bridge No. 27998. Prior to comparing results, the loading applied within the different analyses is detailed first.

6.1 STRUCTURAL LOADING

For comparisons of computed and field stresses, the finite element model and loading of the bridge structure are modified at each critical stage of construction to track the changes in the bridge. Table 6.1 tabulates the model used in each structural analysis, along with the corresponding loads considered for each construction-phase. There are five construction steps listed in this table, including the final live loading test.

For simplicity, the applied loads due to formwork, concrete pouring, and equipment loads are defined in terms of uniformly distributed floor loads. These are computed in Appendix E. In the grillage method, the applied loads can be either concentrated loads input at nodal points, or uniformly distributed linear loads input on the girder elements, as mentioned previously in assumption (10) of Section 5.2.1. Accordingly, an appropriate lateral transfer of uniform floor load to each girder of the bridge system must be considered before the structural analysis. Simple distribution factors based on tributary area may be satisfactory if the girders are uniform in their cross sections. However, more rigorous distribution factors are required for a curved I-girder system, since the depth of the I-girder varies from the innermost girder to the outermost girder to provide an adequate superelevation for the curved roadway alignment. The distribution factors obtained using both approaches are listed in Table

6.2, and the derivation of these factors is outlined in Appendix F, including the distribution factors for floor loads, parapets, and test trucks. The rigorous distribution factors consider the behavior of the bridge cross section as a whole, considering are used for the analyses below.

The self-weight of the girders and the crossframes can be either implicitly generated by a special input key, or considered as applied loads and explicitly input for each girder element. The self-weight of the end diaphragms transmitted directly to the abutment bearings is not considered in the structural analysis unless the support reactions and/or the maximum stresses in the end diaphragms need to be determined. An additional 20% of the crossframe self-weight is added to the girder self-weight to account for the stiffeners connecting crossframes on the webs of the girders.

6.2 COMPARISON OF FIELD MEASUREMENTS AND FINITE ELEMENT ANALYSES

Chapter 2 describes the instrumentation strategy and measurements taken in the field as part of this research. Details of the gage locations are repeated for convenience in Figure 6.1. Gage locations are designated in Figure 6.2. Deflection measurements, including vertical displacements and flexural rotations of the girders, were also made. The displacement measurements were obtained by taking the elevation with a surveying rod and level with an accuracy of plus or minus 1/16". The rotation angles were obtained during erection by measuring the relative lateral displacements with a carpenter level, which proved to be too inaccurate for the magnitude of rotation seen in this work. The rotations during loading from the two trucks were obtained by taking voltage readings from an inclinometer, which has a more appropriate sensitivity of plus or minus 0.0001 degree (1.75 microradian) or better. Locations of the measuring points for deflection and rotation are shown in Figure 6.3.

To be consistent with the construction sequence, four steps are classified in the following. From step 1 to step 3, the structure being analyzed is a bare steel frame. The loading includes the self-weight of the steel structure, the falsework, the wet weight of the concrete, and the equipment plus workers, depending on the progress of the construction. In step 4, the superimposed dead loads, including parapets and the concrete overlay, are applied to the composite structure, which consists of the steel frame and the concrete slab (note that the stiffness of the overlay itself is neglected in all composite models in this work, since its stiffness is low; only the weight of the overlay is included in the models). Finally, two test trucks, weighing between 48 and 50 kips each, were used to simulate the service load on the composite structure. Figures 6.4 and 6.5 describe the weight and axle distance for these trucks.

6.2.1 Stresses During Steel Assembly

Three sets of reading taken during steel erection are investigated here. Self-weight from all steel members is considered as the applied load in this phase. For the designations of the gages, Figure 6.2 should be referred to.

<u>Step 1-1:</u> The first reading was taken on July 19, 1995, when the girders for span 1 were in place. The crossframes were in place but held with only three to four bolts. The end diaphragms at the south end abutment were not erected yet. At approximately midspan were four shoring towers, which were used during the erection and left in place until the remaining girders were placed. Figure 6.6 illustrates the stresses predicted by the UM program as well as the field measurements, on the three gage lines. Gage 11B, designated in Figure 6.2, was broken during the erection, so no reading came from this gage.

No direct correlations can be drawn between the computed and the measured stresses in this step. For example, in gage line A, the computed stresses differs from the measured stresses even for the web gages, which relate directly to the primary major axis bending moment of the girders. Reasons for this are twofold: (1) The shoring towers were modeled as supports in the analysis. The rigid model for the shoring towers in the grillage analysis does not simulate the actually elastic supports. (2) The lateral bending and the warping behavior may not agree with the linear analysis model since the connection bolts between the crossframes and girders are not fully tightened -- in other words, the loading on the girders are so small, that local eccentricities and minor fitup stresses dominate the results. In gage line B, the bending normal stresses on the webs are correlated better than the warping stresses on the flanges; however, the flange tip stresses, which are more affected by warping, do not consistently correlate. In gage line C, high stresses obtained from strain readings show that some initial strain exists in the crossframes, e.g., 5.88 ksi in gage 1C, probably due to fitup. The significant finding from this reading is that, when shoring towers are used, the stresses in the bridge are minor, as would be expected (note that the nominal yield stress of the steel is 50 ksi)

Step 1-2: The second reading was taken at 4 a.m. on July 25 during the erection of the second girder from the outermost girder of span 2, when the girder was being held by the crane and the splice was being tightened. The end diaphragms on the south abutment were in place. All of the bolts for the crossframes of span 1 had been put into place, but they were not fully tightened. Stress results and the structure to be analyzed are shown in Figure 6.7.

At the outermost girder near the middle pier, gages 1B through 6B, stress increases due to the newly added girders are noticeable in this figure. As can be seen in this girder, the correlations between the computed and the measured stresses are improved when the stresses are increased. The computed stresses are less well correlated in gages 7B to 12B, however, with the measured stresses not increasing as much as the computed. This is not unexpected, as this girder was still being held by the crane during erection at the time of the reading -- this added support could not be modeled well in the analysis. Although the measured stresses are somewhat random at this stage, the magnitude of the stresses are on the same order as the computed stresses (i.e., not more than 3 ksi).

Step 1-3: The third reading was taken at 11 p.m. on July 28 when all the girders were erected in place and all the crossframes were fully tightened (rattled up). All the shoring towers were removed and the steel frame became a self-supported structure. In many cases, the bolts of the crossframes were hammered into place. This may affect the gages on the crossframes but is not considered herein explicitly in the analysis. Stress results for Step 1-3 are shown in Figure 6.8.

Better correlations may be found in Step 1-3, because the structure skeleton is completed and its behavior becomes more regulated or predictable. In both gage lines A and B, the primary flexural bending behavior is consistently correlated between the structural analyses and the field measurements except for gage 15A, in which the values are 1.36 ksi and -0.67 ksi for the computation and the field measurement respectively. The warping stresses obtained from analysis on the flanges indicate the direction of twist for each girder is in the same direction, i.e., clockwise looking north. However, this prediction of warping stresses differs from the measurements. In gage line A, the measured stresses indicate lateral (weak axis) bending on Beam 1 through Beam 3, in which Beam 1 bends in one direction while Beams 2 and 3 bend in the other direction. In gage line B, Beams 1 and 2 are warping in the opposite direction from the prediction; warping in Beam 3 is not clear from the measurements since gage 11B was not functioning at this time. Correlation for warping can be seen in Beam 4 for both A and B gage lines, which are warped in the same fashion as the prediction from analysis. The stresses in the crossframes correlate better in the diagonal members than in the top and bottom chords. Note, however, that the level of stress is still so small that small eccentricities in the field can explain these variations. The maximum stress increases during the erection of the steel backbones are 6.74 ksi (measured) versus 4.53 ksi (computed) in gage 1B for girders, and 4.41 ksi (measured) in gage 1C versus 1.93 ksi (computed) in gage 2C for the crossframes. The linear model for structural analysis predicts the behavior relatively well in this stage.

6.2.2 Stresses During Placing of the Formwork and the Reinforcing Steel

The completed steel frame is used as the base structure for the analysis including formwork and reinforcing bar. The estimate of the uniform floor loads in this phase is 5 psf for formwork and 10 psf for reinforcing as determined in Appendix E. Three sets of readings are selected to compare with the prediction from structural analyses.

<u>Step 2-1:</u> This reading was taken at 6 a.m. on August 1. The loading includes the formwork, two generators, and five to ten workers. The formwork was in place from the south abutment to approximately midspan of span 1, while the joists to support the plywood forms had been placed in span 1 up to the middle pier. For purpose of analysis, a uniform load of 5 psf was distributed on half span of span 1 to model the formwork. Comparisons between computed and measured stresses are shown in Figure 6.9. Gage 1A was found broken by the jamming of the 4"x4" plywood joist.

The computed stresses are all increased by approximately 1.2 ksi. The measured stresses, on the other hand, showed little change, and did not uniformly increase due to the small amount of extra formwork applied to the bridge. Reasons for this could be that the supporting whalers and the joists redistribute some of the stress and further accentuate local irregularities in the stress distribution.

<u>Step 2-2:</u> The reading was taken at 6:30 a.m. on August 7 when the formwork was completed, the shear studs were in place, and all equipment had been removed from the structure. A uniformly distributed floor load of 5 psf was assigned to both spans to model the formwork in the structural analysis. Stress results are compared in Figure 6.10.

Two gages, designated as 1A and 11B, which were damaged during the erection of steelwork and the placement of formwork, respectively, were replaced on August 2. Accordingly, it was required to initialize these two strains and their corresponding datum stresses. The first strain readings after replacement, Step 2-1, were picked to serve the purpose. As a result, the stress shown on gage 1A and 11B should read as the stress increase after reattachment, rather than the total stress from the unstressed state.

In Figure 6.10, bending stresses from both sources were increased in gage line B near the middle pier but were decreased in gage line A as compared to Step 2-1. This is logical, since the primary difference in loading between Steps 2-1 and 2-2 is the addition of plywood on span 2. Also note that the measured stress in crossframe gage 1C continued to increase.

<u>Steps 2-3a and 2-3b:</u> Readings were taken on August 10 when all reinforcing steel was in place. Loading assigned to the bridge is the sum of formwork and the reinforcing, i.e., 15 psf. Figure 6.11 shows the comparison of the computed stress and the measured stress.

Better correlation between the computations and the measurements can be found in this step. The difference of the maximum stress between the analysis and the field measurements for the girders has changed from 2.21 ksi (6.74-4.53) in Step 1-3 to 0.76 ksi (6.4-5.64) in Step 2-3a. However, the primary bending behavior of the girders, as seen in the web gages, continues to correlate better than the warping, seen in the flange gages. Nevertheless, most of the beam flanges show clear correlation with respect to warping behavior. Stresses in the crossframes are still somewhat more random.

To investigate effects of local stresses during this stage of construction, an additional 30 psf uniform surcharge is considered in case 2-3b to simulate higher point loads and to investigate better correlation with some higher measured stresses. Stress results for this case using a 45 psf floor load plus steel self-weight are shown in Figure 6.12. Almost all the computed stresses in the girders are far beyond the measured stresses, except for the gages 19A and 23B, where the computed stresses are -3.31 and 5.79 ksi respectively and the measured stresses are -4.73 and 7.58 ksi. However, the maximum stress is computed as 7.80 ksi in gage 1B (on the outermost girder) and is measured as 7.58 ksi in gage 23B (on the innermost girder). Therefore, the additional 30 psf is adequate for computing the maximum stress. It is thus suggested that at least 20 to 30 psf of uniform surcharge (construction load) is required in design and analysis of curved I-girder systems subjected to formwork and reinforcing bar loading.

6.2.3 Results During Pouring of The Concrete Deck

During the pouring of the concrete deck on August 11, complete readings were taken once every 30 minutes from 4:15 a.m. to 8:15 a.m. Three typical sets of data are discussed in the following to compare with the analysis. The distributed floor loads range from 95 psf to 125 psf with the inclusion of a 0 psf to 30 psf of the surcharge to account for the construction and/or equipment loads. The base structure throughout this phase is assumed to be bare steel, i.e., non-composite behavior, even though the composite behavior is developing during the concrete pour as the concrete hardens.

Step 3-1: The first set of readings chosen to compare with the analysis results were taken at 5:45 a.m. when span 2 (north span) concreting was about to be completed. In addition to the self-weight of the base structure, the distributed floor load consists of 5 psf for the formwork, 10 psf for the reinforcement, 80 psf for the concrete, and 15 psf for the construction load. Accordingly, the distributed floor load is 15 psf on span 1 and 110 psf on span 2, where the wet concrete is in place. The stress comparison is shown in Figure 6.13.

In this step, stresses are increased about 2 to 3 ksi. Since only one span is loaded by the concrete weight, it may be seen that gage line B picks up stress, while gage line A tends to show some unloading behavior. The correlation of stresses is showing a clear improvement, as the effects of local fitup stresses are starting to dissipate under the more substantial loading.

Step 3-2: Readings were taken at 7 a.m when the concrete pouring was approximately up to the midspan of span 1. Loading for the zone with no concrete was still assigned as 15 psf. For the zone where the wet concrete was in place, there are two loading types: In the whole of span 2 and one panel of the crossframe over the middle pier, the floor pressure is estimated as 95 psf. For the rest of the bridge, the floor is assumed to weigh 110 psf since the activity of pouring concrete is taking place in this region. The stress comparison is recorded in Figure 6.14.

Correlation continues to improve as loading increase. Excellent correlation (less than 15% difference) can be found in the following gages: (1) 20A, 2B, 9B, 15B, 20B, and 21B for the girder webs, (2) 10A, 17A, 23A, 1B, 11B, 17B, and 24B for the girder flanges, and (3) 7C and 10C for the crossframe bracings. Difference of stresses obtained from two sources are attributed to the variations of the estimated loading magnitude, the construction loads, and the ever-changing location of the placed concrete.

Step 3-3a, 3-3b, 3-3c: Readings were taken at 7:50 a.m. when the concrete was all in place. Three levels of floor loads, including 95, 110, and 125 psf, are assigned to cases 3-3a, 3-3b, and 3-3c respectively, these loads spanning from the south abutment to the midspan of span 1 to investigate the loading due to the construction equipment and the workers. The 95 psf uniform floor loading is assigned to the other three quarters of the bridge floor. Stress correlations for these three cases are shown in Figure 6.15 to 6.17. respectively.

Note that in order to investigate stresses in gage line C, the nodal degree-of-freedom for lateral displacement was released for this step and all subsequent steps, as mentioned in section 2.3.2. Releasing these degrees-of-freedom substantially increased the crossframe stresses and brought them more into line with the measured results, although it appears that initially higher stresses in the field are retained in the crossframes up to this point in the loading.

Overall, better correlations in an average sense are found in Step 3-3a, which has the 95 psf floor load everywhere. In this loading condition, gages with differences less than 15% of the measured stresses from the computed stresses may be found in the gages 5A, 17A, 19A, 1B, 11B, 17B, and 24B for the flanges, 3A, 8A, 20A, 2B, 9B, 15B, 20B and 21B for the webs, and 7C, 9C, and 10C for crossframes. Both the primary bending behavior and the warping plus minor bending behavior (exhibited in the girder flanges) generally correlate well in this case. The maximum normal stress is 11.01 ksi measured in gage 23B in this step. With the 15 psf surcharge in the construction area (case 3-3b), the stress in gage 23B is computed to be 9.37 ksi as shown in Figure 6.16, while with the 30 psf surcharge around the same region (case 3-3c), the stress in gage 23B is computed 9.70 ksi. Therefore the best correlation for determining the maximum stress in the girders is found in loading case 3-3c. As a result, at least 20 to 30 psf of surcharge is again suggested to account for construction loading during the concrete casting.

<u>Comparison of Deflections #1:</u> The first set of deflections were correlated at this loading stage. The initial elevation was surveyed when the steel backbone had just been rattled up. After the concrete deck was in place, another leveling was performed to get the vertical deflection and the axial rotation angles at the midspan of each span. Loading to be assigned in this case is a 110 psf uniform floor load, including live load. The bare steel model was used for the analysis. Results are tabulated in Table 6.3, in which the deflections are correlated much better than the rotations. Since rotations are so small, attention is focused on the displacements. As the concrete pouring proceeds into span 1, composite behavior is developing in span 2, especially during the thirty minute intermission right after the passing of the middle pier. Ignoring the composite behavior may result in the overestimate of the deflections on span 1 as compared with field data. However, it was also found that a temperature difference of ten to fifteen degrees Centigrade caused a change in deflection on the order of 0.02 feet in the girders. Thus, temperature alone could explain the difference between the computational and field results. The average percentage differences of the surveyed deflections from computed deflections are 4% below

for span 1 (south) and 19% above for span 2 (north). It is noted that the deflections measured on span 2 were taken five days later than those measured on span 1. Although the hardening of concrete improves the bridge stiffness, deformation may continue to grow as the concrete hardens, which may explain the larger measured deflection readings in span 2., although, again, a temperature difference alone (as compared to the intial deflection measurements when the steel was rattled up) could cause much of these differences.

6.2.4 Stresses From Parapets and The Overlay

For modeling the parapets, the estimated vertical loads were computed to be 443 plf for the inner parapet and 578 plf for the outer parapet, respectively. The vertical distribution to each girder is listed in Table 6.2. The reading was taken with little construction loading on the bridge. Composite behavior is considered here. A nominal strength of the concrete designed to be 5,000 psi for the deck was considered to be satisfactory (cylinder strengths from the slab were 5,625, 6,057, and 6,197 psi). Also, only a 2% of difference was found between using a modulus ratio of steel to concrete of N= 24 as compared to that of N= 8. Figure 6.18 shows the comparison between analysis results and field measurements using N equal to 8 (Step 4-1). Incremental stresses due to parapet loads, applied on the composite structure, are computed first. Then the total stresses to date in this figure are accumulated from step 3-3a in Figure 6.15.

Due to adding the parapets, an approximately 2.0 ksi stress increase can be found in the girders. Stress redistribution can also be seen in Figure 6.18: the outermost crossframe used to be the most highly stressed, but now the other two crossframes have picked up more stress. Again, correlation in most of the web gages is quite good. Correlation in the flange gages also exhibit good correlation, but not as consistently as the web gages, again showing that the primary bending behavior is more predictable from analysis than the warping plus minor bending behavior. Excellent correlation between analysis and experiment (less than 20% error) may be found as follows: (1) In the flanges of the girders, gages 10A, 16A, 17A, 1B, 4B, 5B, and 11B, (2) in the webs, gages 3A, 8A, 20A, 2B, 3B, 9B, and 20B, and (3) in the crossframes, 7C, 9C, 10C and 11C.

Loading of the 2 inch overlay is estimated as a floor pressure of 24 psf over all the bridge, and the results are collected in Figure 6.19 (Step 4-2). The structural system remains the same, except the parapet member has developed its strength and is included in the computation of effective width of the concrete slab for the edge girders. With the addition of overlay on the bridge, in average, the stresses increased less than 1.0 ksi in the girders.

6.2.5 Truck Loading

After the bridge was opened for traffic, the bridge was closed for a night, and two snow plow trucks weighing 48.1 kips, denoted as truck 1, and 49.4 kips, denoted as truck 2, were provided by MN/DOT to permit live load measurements. The axle loads and wheel spacings are shown in Figs. 6.4 and 6.5. Composite behavior is considered throughout the analysis. A total of fifteen loading cases, including six cases of two-trucks side by side, three cases of two-trucks in line, and six cases of a single truck (truck 2) were conducted on the night of October 7, 1995. Five cases are discussed herein. The plan of the truck loading is shown in Figures 6.20 to 6.22.

It is assumed that the truck weight is transferred to the nodal points surrounding the center of gravity of the truck. The methodology for distribution of the truck weight is discussed in Section F.3 of Appendix F. It is also noted that most of the plywood forms underneath the bridge had been removed before this service loading test. Hence, unloading due to the removal of the forms was considered by taking a set of readings when the bridge had no vehicles on it. Only the differential stresses from this reading are reported for the truck loads. To get total values of the current stress state, results of the previous stress state in Figure 6.19 should be added to the truck load results.

Figure 6.23 shows the differential stresses of case 2, in which two trucks are side by side near the midspan of span 1. The stresses at the bottom flanges are consistently correlated in gage lines A and B, while stresses at the top flanges differ between the analysis and the measured results. Reasons for this could be twofold. First, the deck greatly relieves the stress at the top flange, due both to redistribution of stress through the slab, and because the top flange is close to the neutral axis of the section in positive bending. Second, if the stresses in the deck are low and the shear stress to be transferred between the concrete slab and the steel girder's top flange in the negative moment region is smaller than the friction resistance, the behavior may approach that of a fully composite member. Thus, an analysis in which the negative moment region is modeled as bare steel, may not be able to precisely describe the stress distribution in the concrete slab. In order not to lose generality and to be consistent with the actual service condition that these trucks may place on the bridge, the results will be reported first for a model in which the negative moment region near the middle pier is governed by non-composite behavior.

The discussion of the stress correlation focuses on the bottom portion of the girders, since the measured stress on the top portion is negligibly small for this small loading. Good correlation was found at the bottom three gages of each girder, and in the crossframes. Since case 2 is a midspan loading of span 1, better correlation occurs in gage line A. Excellent results, with less than 20% difference between the computed and measured stresses for this loading condition, are indicated in gages 9A, 21A, 3B, 15B, and 21B for the webs, 4A, 10A, 12A, 16A, 18B, and 22B for the flanges of the girders, and 3C and 12C for crossframes.

The results of test cases 3, 7, 8, and 13 are presented in the following figures denoted from Figures 6.24 to 6.27. In Figure 6.24, again better correlations are found at gage line A, such as gages 3A, 4A, 6A, 9A, 10A, 15A, 16A, 21A, and 24A, since this loading condition is more related to the midspan loading of case 2. However, excellent correlation can still be found in gage lines B and C.

In investigating the possibility that composite action was active over the center support, fully composite behavior across the entire bridge was used to generate Figures 6.25 to 6.27. Figure 6.25 shows the condition of both spans loaded. This results in good correlation in gage lines A and B, such as 4A, 9A, 10A, 12A, 15A, and 16A in gage line A and 3B, 6B, 12B, 15B, 21B, and 24B in gage line B. Also, stresses on the top portion of the girders show better correlation from the analysis of a fully composite model than that of a non-composite model in the negative moment region. Stresses in the crossframes are fairly well correlated, except for gages 1C, 5C, and 8C, which exhibit reverse signs of stress state. Similarly, case 8, the span 1 loaded condition, and case 13, the span 2 loaded condition, yield good correlations in gage lines A and B, respectively. Similarly, excellent correlations are found in gages 4A, 6A, 9A, 10A, 12A, 15A, 16A, 3B, 15B, and 21B for case 8 (most on line A) and 3A, 24A, 4B, 12B, 15B, 21B, and 24B for case 13 (most on line B) are shown in Figures 6.26 and 6.27, respectively.

Comparison of deflections #2: Deflections and rotations due to the trucks are discussed in this section. Two sets of zero surveying readings were taken before and after the field tests separately and were averaged to get the zero deflections and rotations for the following tests. An inclinometer was used for measuring the rotation angle at the intersection of outermost girder, Beam 4, and the fourth crossframe from the north abutment in span 2, as shown in Figure 6.3. The structure under consideration is fully composite.

Results are tabulated in Table 6.4 for deflections and Table 6.5 for rotation angles respectively. As far as the structural behavior is concerned, correlations of the deflections and the rotations from both sources are excellent even though the values are small. For the comparison of rotation angles, better correlations are found by using the inclinometer rather than the method of the carpenter level, used in the previous comparison of rotations.

6.3 STRESSES IN THE CROSSFRAMES NEAR THE SKEW SUPPORTS

To investigate the possibility that skew supports greatly affect the stress distribution in the crossframes near the support, the analysis results of two sets of crossframes were studied due to the truck loading. Figures 6.28 through 6.37 show the total axial stress in each crossframe element due to the 15 cases of truck loading for crossframes 39, 1, 20, and 40 (near the south abutment, which experience high shear and low moment), and crossframes 8, 27, 47, and 9, 28, and 48 (near the center support, which experience both high moment and high shear). These crossframe designations are shown in Figure 5.3 (the crossframes near the center pier are not labeled explicitly in the figure, but the crossframe numbering scheme is apparent). First, studying crossframes 1, 20, and 40, one can see that crossframe 1 has almost three times the stress, primarily due to the dead load (it is apparent that the variation in stress due to the truck live loading is minimal). In addition, crossframe 39, which is just next to the support, between the inner two girders, also has stresses comparable to crossframe 1. However, if one looks at Figures 6.32 to 6.37, it is apparent that crossframes 8 and 9, next to the outside girder, have larger stresses than the other crossframes at their section, even though they are further away from the skewed support. Thus, it must be concluded for this bridge that, with the exception of a lone crossframe such as 39, the crossframes in the stiffer region of the bridge, e.g., next to the outer facia girder for this bridge, attract more force, regardless of their position relative to the skew support.

However, it is interesting to note that the chords are less stressed than the diagonals, potentially indicating high shearing action. (The computational results of the instrumented crossframe show similar results, although the measured results themselves were inconsistent in terms of determining which crossframe members, chords or diagonals, were most stressed -- this may be due to the instrumented crossframes being susceptible to local irregularities due to their low stress levels.) These figures also reveal a predictable variation in stress as the trucks move across the bridge, as was discussed in Section 6.2.5.

In general, however, it should be noted that the stress distribution in crossframes can be complex and may include flexural as well as axial stress components. The conclusions drawn above from these analyses regarding the effects of skew on crossframe stresses and the potential dominance of shearing action cannot be assured to apply to other similar curved girder bridges.

Table 6.1 Loading condition and the corresponding structures

Sequence	Loading	Structure	Construction
Step 1	Steel Weight	Steel	Assembling of the steel
Step 2	Steel+Formwork+Rebar +Equipment	Steel	Formwork and reinforcing
Step 3	Steel+Formwork+Concrete+Equipment	Steel	Pouring of the concrete
Step 4	Parapets+Overlay	Steel+Slab (Composite)	Placing parapets and overlay
Field Test	Truck weight	Steel+Slab (Composite)	Complete

Table 6.2 Vertical loading distribution factors

Loading (plf)		Beam 1	Beam 2	Beam 3	Beam 4	Multiplier
Floor Loads (plf)	RD	0.92	0.92	1.021	0.883	qd*
	SD	0.87	1.0	1.0	0.87	
Parapet (plf)		0.185	0.209	0.279	0.327	P_1+P_2**
Truck[a] (lbs)	panel front	0.064	0.071	0.091	0.103	W***
	panel rear	0.130	0.144	0.186	0.211	

Notes:

a- A typical example for truck 2 at location x_l= 14.56 ft.

* q- uniform floor pressure (psf)

d- spacing between two girders (ft)

** P_1- uniform weight of the inner parapet, 443 plf

P_2- uniform weight of the outer parapet, 578 plf

*** W- truck unit weight in pounds

RD- Rigorous Distribution (used for the analyses in this research)

SD- Simple Distribution by Tributary Areas

Table 6.3 **Deflection comparison after pouring of the concrete deck**

Locations	Deflections		Beam 1	Beam 2	Beam 3	Beam 4
Span 1 (South)	Displacements (FT.)	LA	-.108	-.108	-.108	-.116
		M	-.109	-.109	-.103	-.104
	Rotations (DEG.)	LA	.017	.036	0.054	.078
		M	NA	0	0	.2
Span 2 (North)	Displacements (FT.)	LA	-.161	-.144	-.125	-.108
		M	-.183	-.168	-.146	-.140
	Rotations (DEG.)	LA	-.070	-.096	-.094	-.068
		M	0	-.3	-.3	-.2

Notes:

1. Bare steel structure is subjected to the loading of concrete and formwork
2. Notations: FT.- Displacement units, Foot; and DEG.- Rotation units, Degree; LA - Linear Analysis; and M - Measurement
3. The net floor loading is 110 psf.

Table 6.4 Deflection comparison during truck loading

Deflections (FT.) on Span 1 (South), computed/measured				
Loading	Beam 1	Beam 2	Beam 3	Beam 4
2	-.021/-.012	-.023/-.012	-.026/-.022	-.027/-.020
5	.005/.008	.007/.018	.012/.013	.015/.010
7	-.007/-.007	-.007/-.007	-.007/-.002	-.007/-.005
8	-.015/-.017	-.019/-.012	-.027/-.027	-.031/-.030
11	-.009/-.007	-.011/-.007	-.013/-.012	-.015/-.015
Deflections (FT.) on Span 2 (North), computed/measured				
Loading	Beam 1	Beam 2	Beam 3	Beam 4
2	.005/.005	.007/.005	.010/.020	.012/.007
4	-.007/-.000	-.006/-.000	-.005/-.000	-.005/-.008
5	-.028/-.020	-.029/-.025	-.029/-.020	-.030/-.023
7	-.011/-.010	-.011/-.015	-.011/-.005	-.011/-.018
9	-.016/-.010	-.017/-.015	-.018/-.010	-.019/-.018
14	-.014/-.010	-.014/-.015	-.015/-.010	-.018/-.008

Note: Downward deflections are negative.

Table 6.5 Comparison of axial rotation angles obtained from field tests at Beam 4 on the midspan of the north span

Loading Case	Computed Rotations (DEG.)	Measured Rotations (DEG.)
2	-.016	-.009
3	-.018	-.012
4	-.002	.002
5	.013	.006
6	.014	.005
7	.002	.004
8	-.022	-.013
9	.010	.009
10	-.003	-.001
11	-.009	-.005
12	-.010	-.005
13	-.001	.002
14	.009	.006
15	.010	.004

Note: Positive rotation is clockwise looking north.

Notes:

Line A- located at midspan between crossframes 4 and 5, 24 gages in total
Line B- located 3 feet (approx.) from PIER I in south span, 24 gages in total.
Line C- located on three crossframes at frame line 5, 12 gages in total.

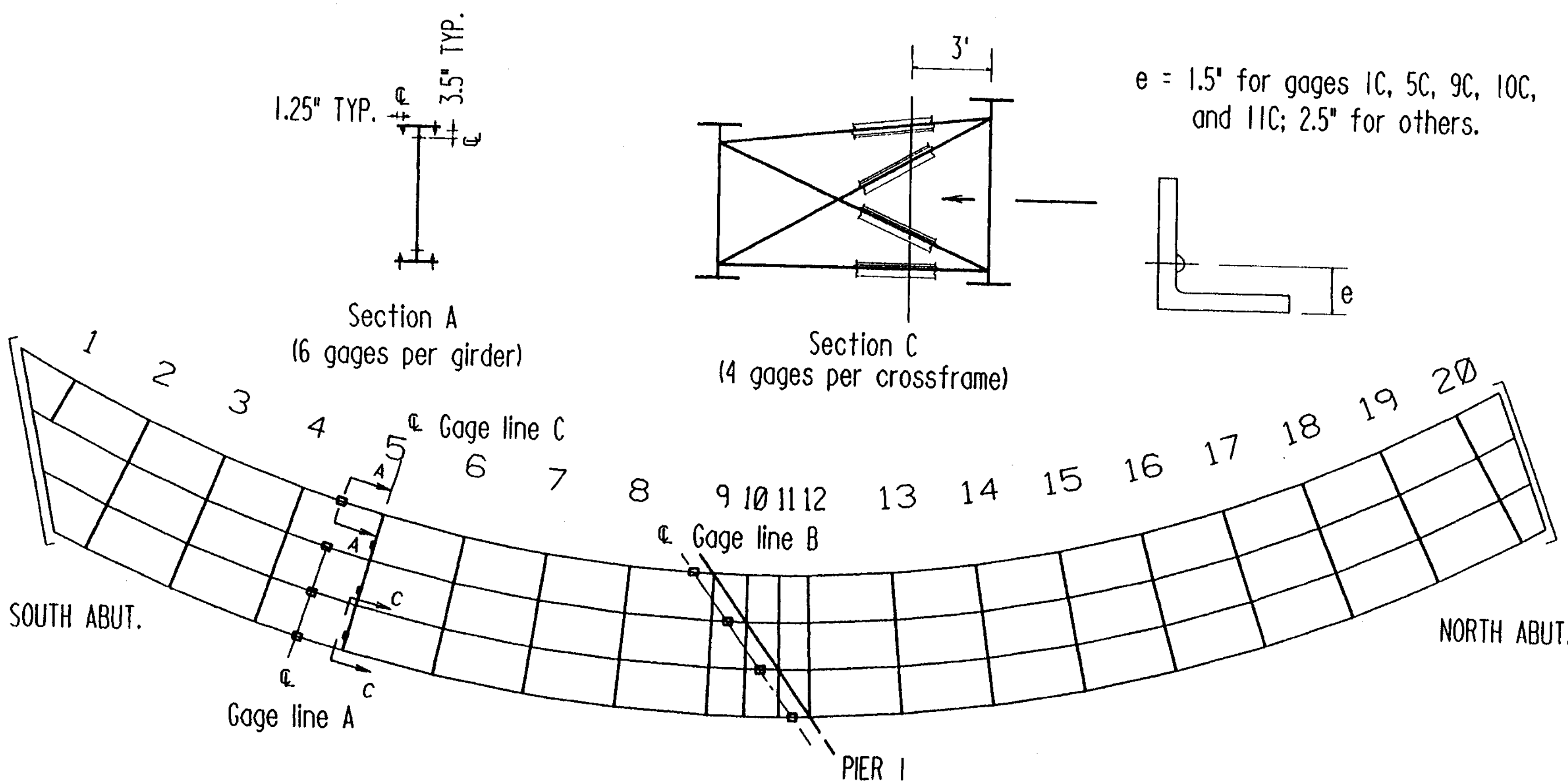

Figure 6.1. Instrumentation of strain gages

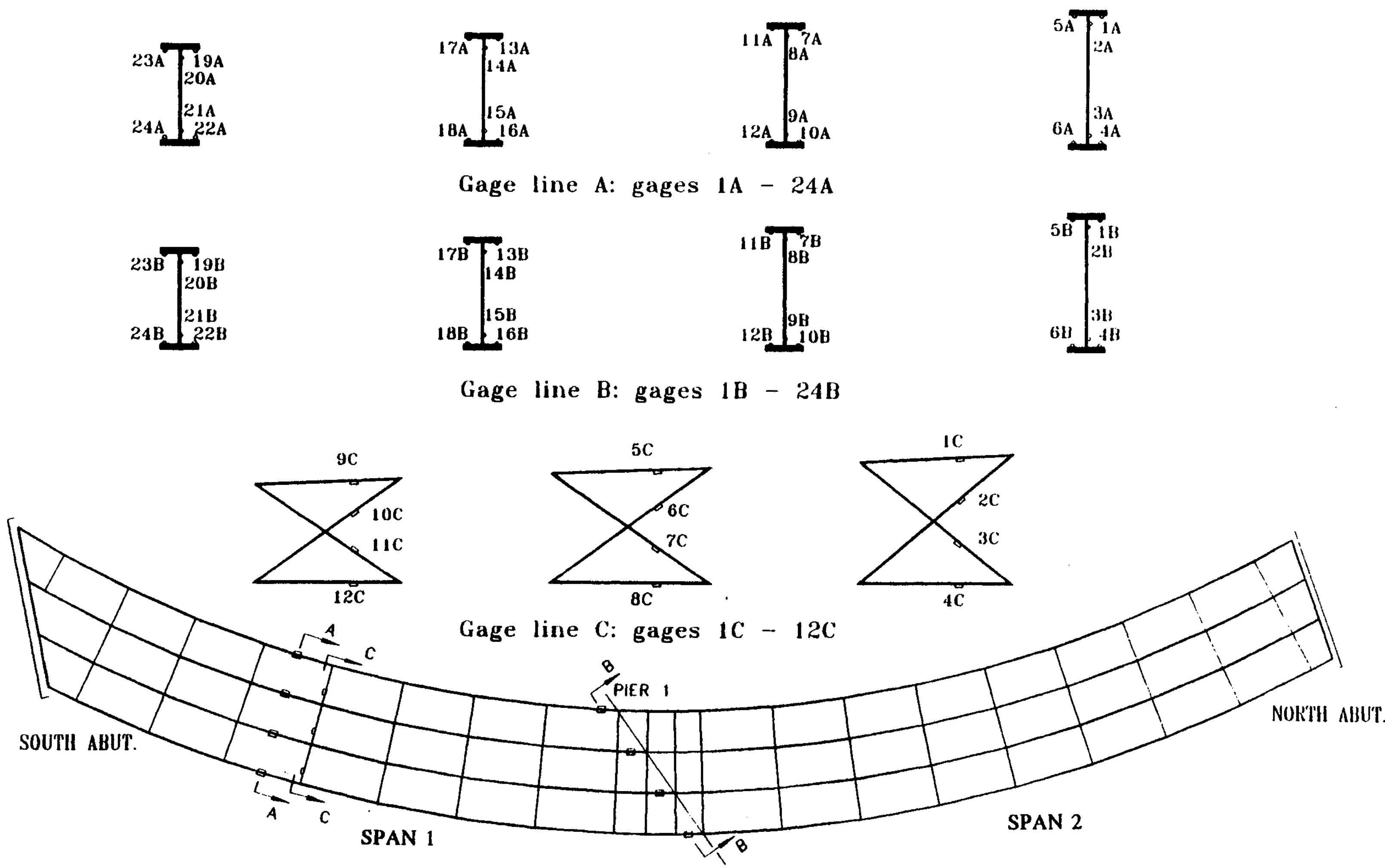

Figure 6.2. The designation of strain gages

Notes:

1. The surveying points are underneath the centerline of the girder's web
2. Traffic condition on TH94 affects the surveying points of the south span

X- The proposed surveying points

O- The actual surveying points

T- The tiltmeter measuring point

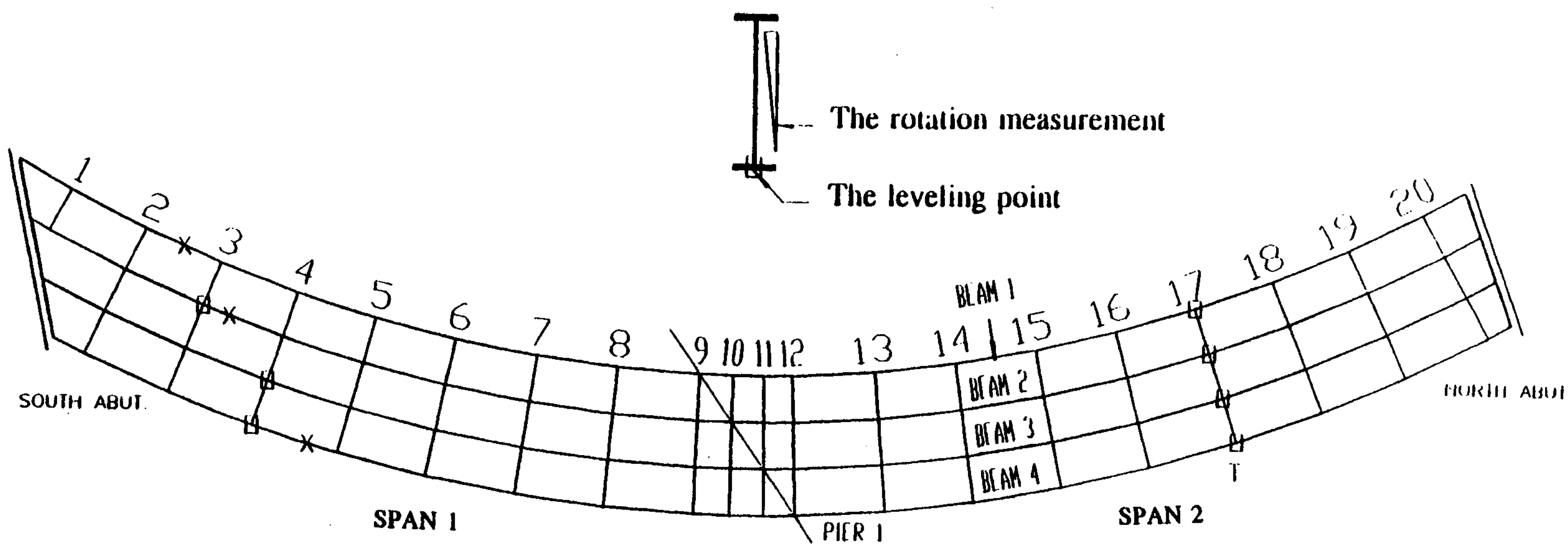

Figure 6.3. Locations of deflection and rotation measuring

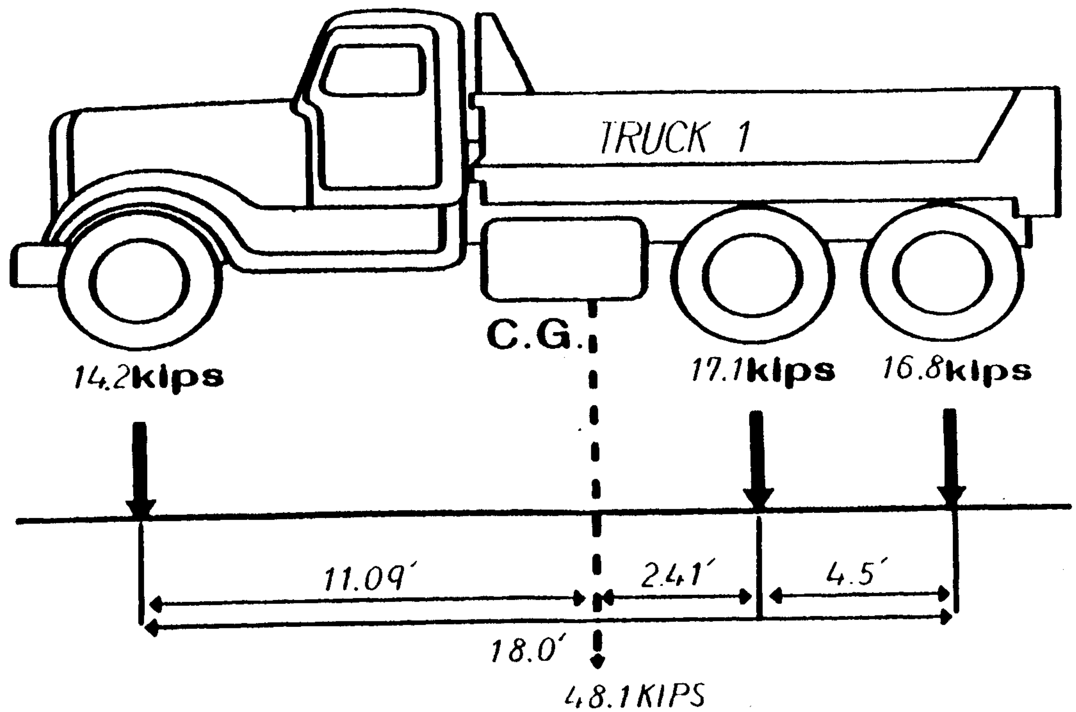

Figure 6.4. MN/DOT snow plowing truck 1, unit weight= 48.1 kips

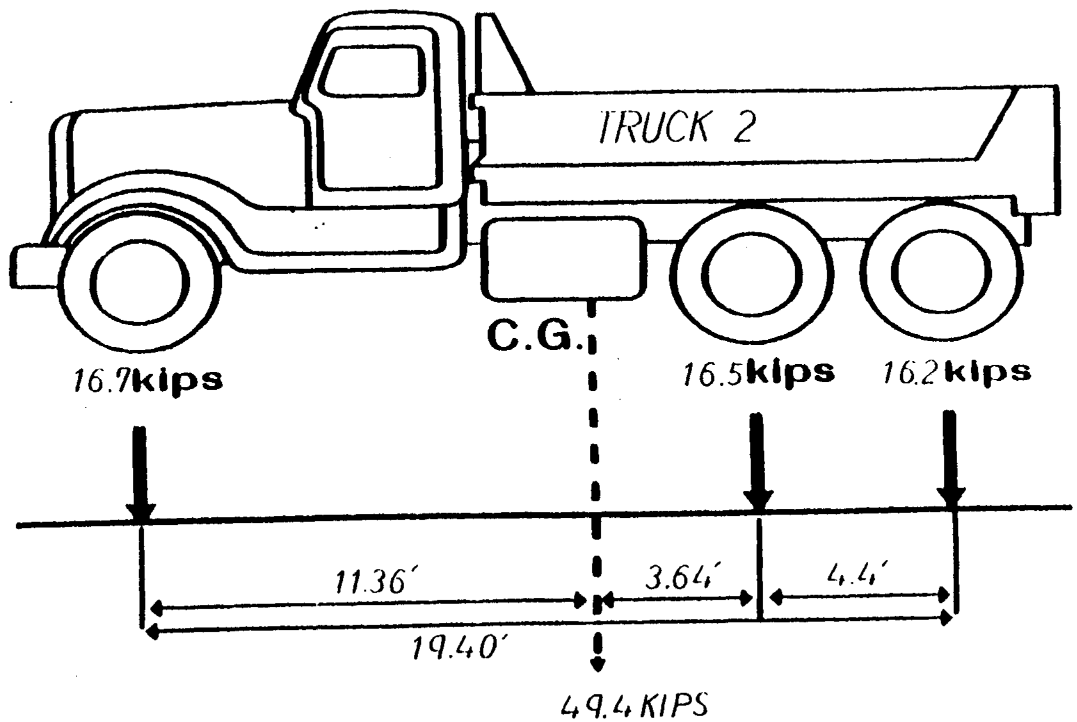

Figure 6.5. MN/DOT snow plowing truck 2, unit weight = 49.4 kips

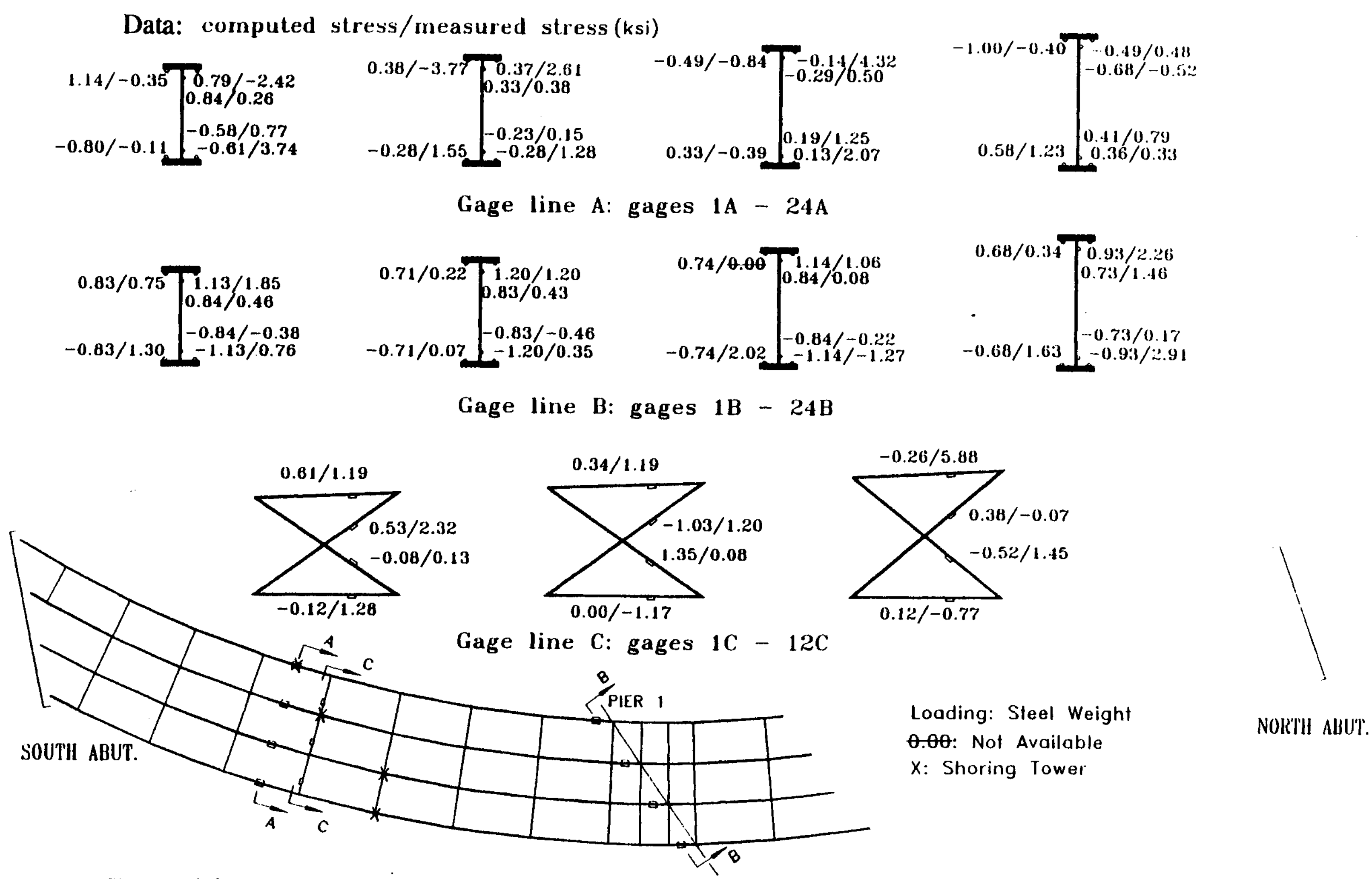

Figure 6.6. Stress comparison at three gage lines for Step 1-1

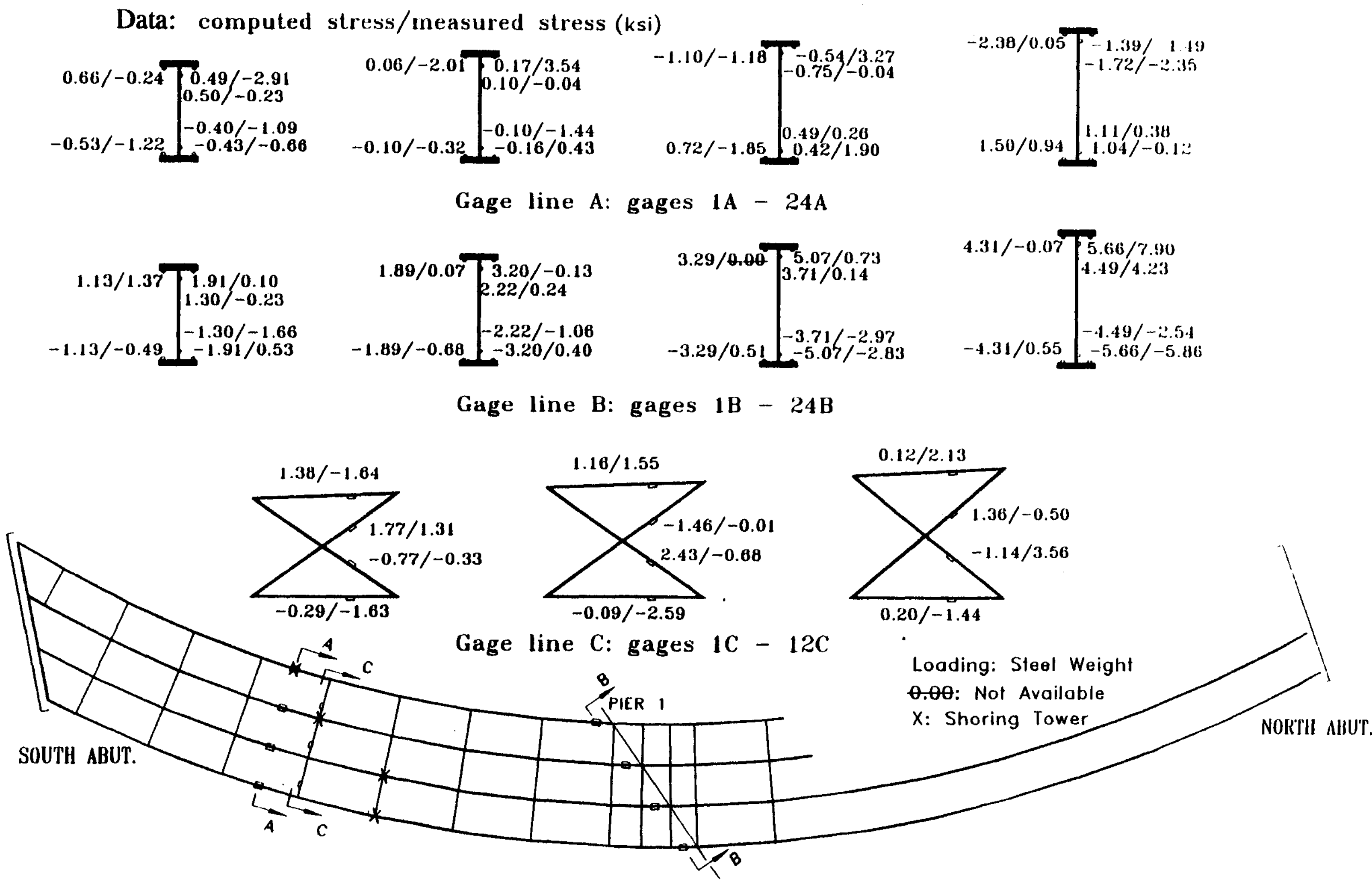

Figure 6.7. Stress comparison at three gage lines for Step 1-2

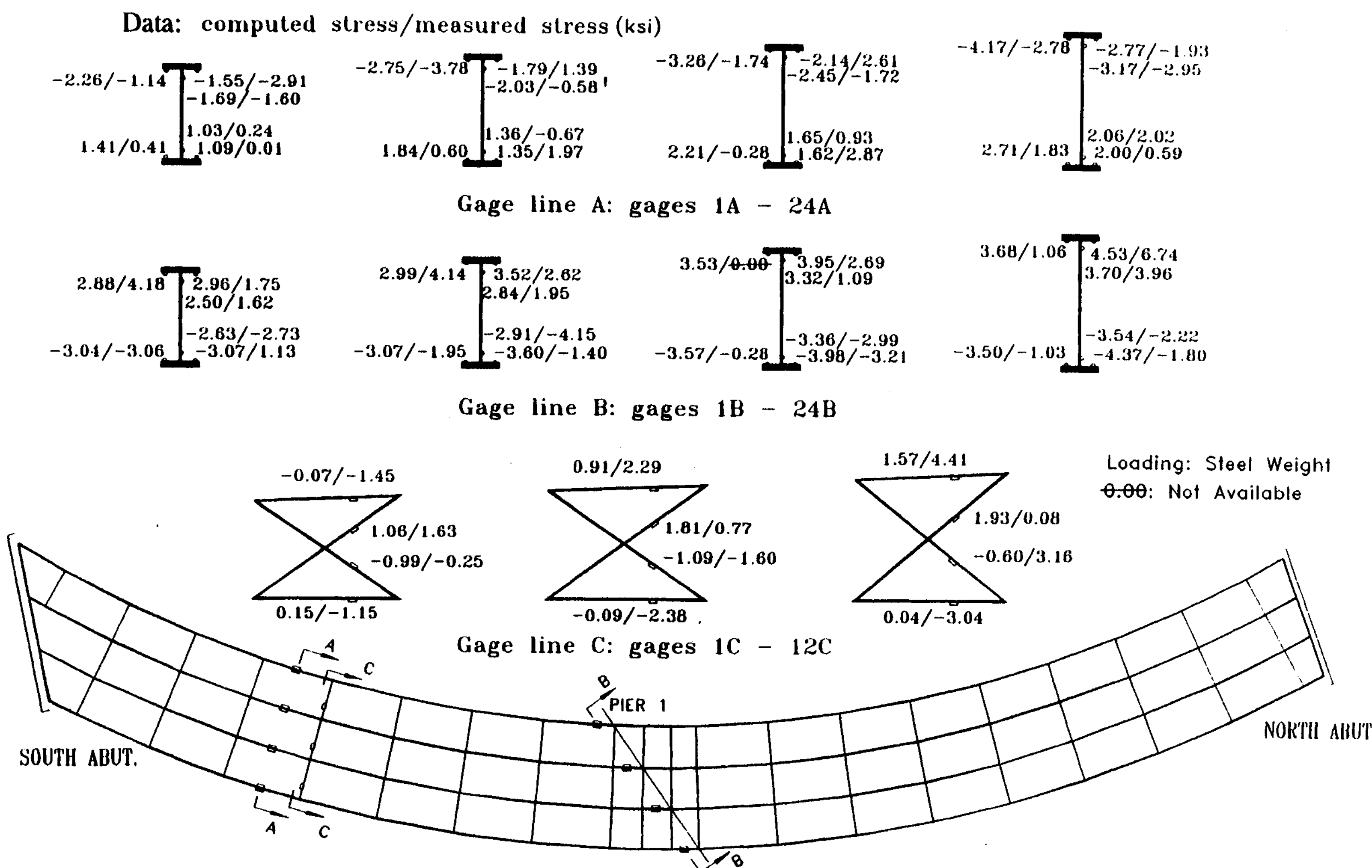

Figure 6.8. Stress comparison at three gage lines for Step 1-3

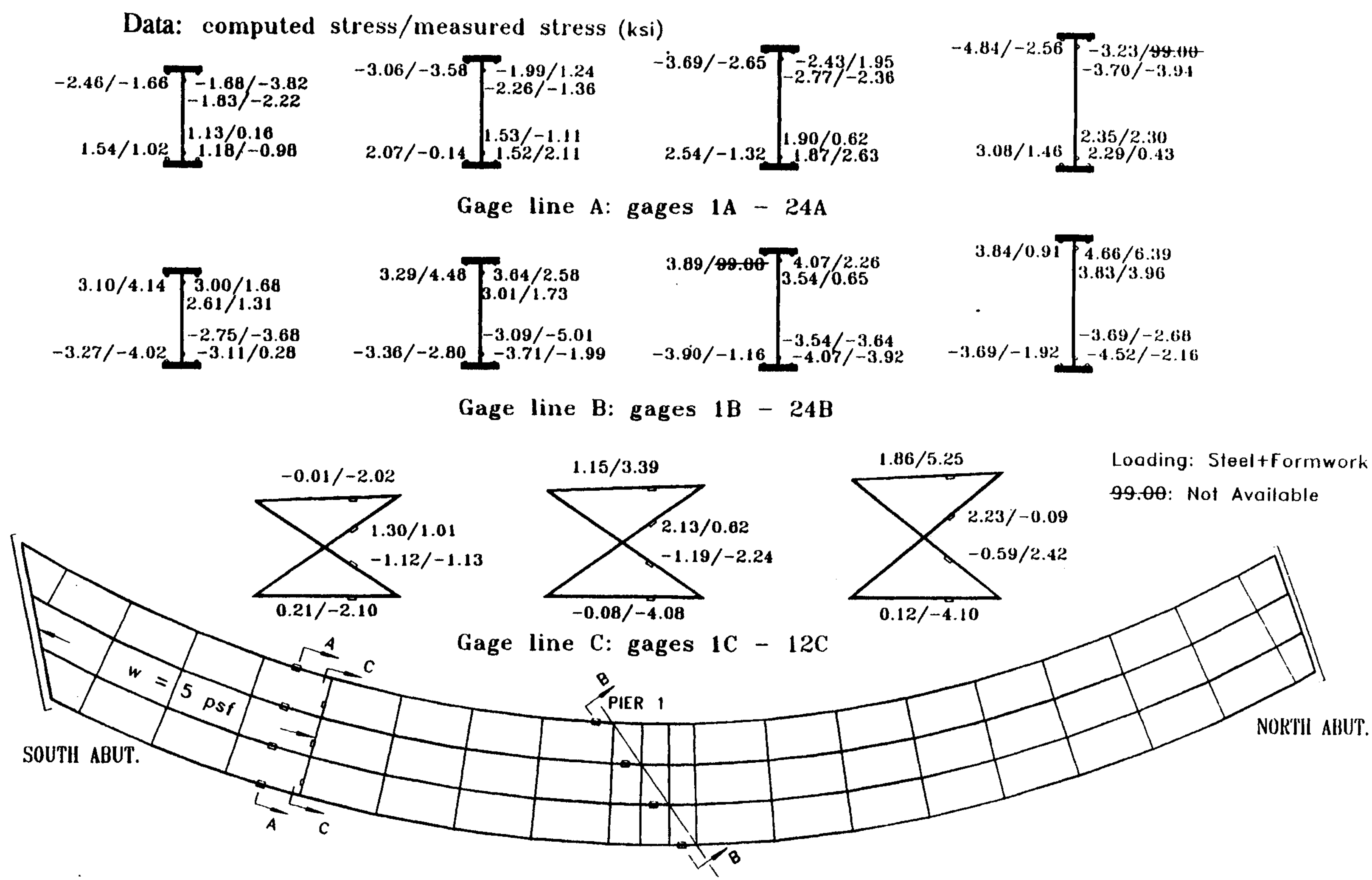

Figure 6.9. Stress comparison at three gage lines for Step 2-1

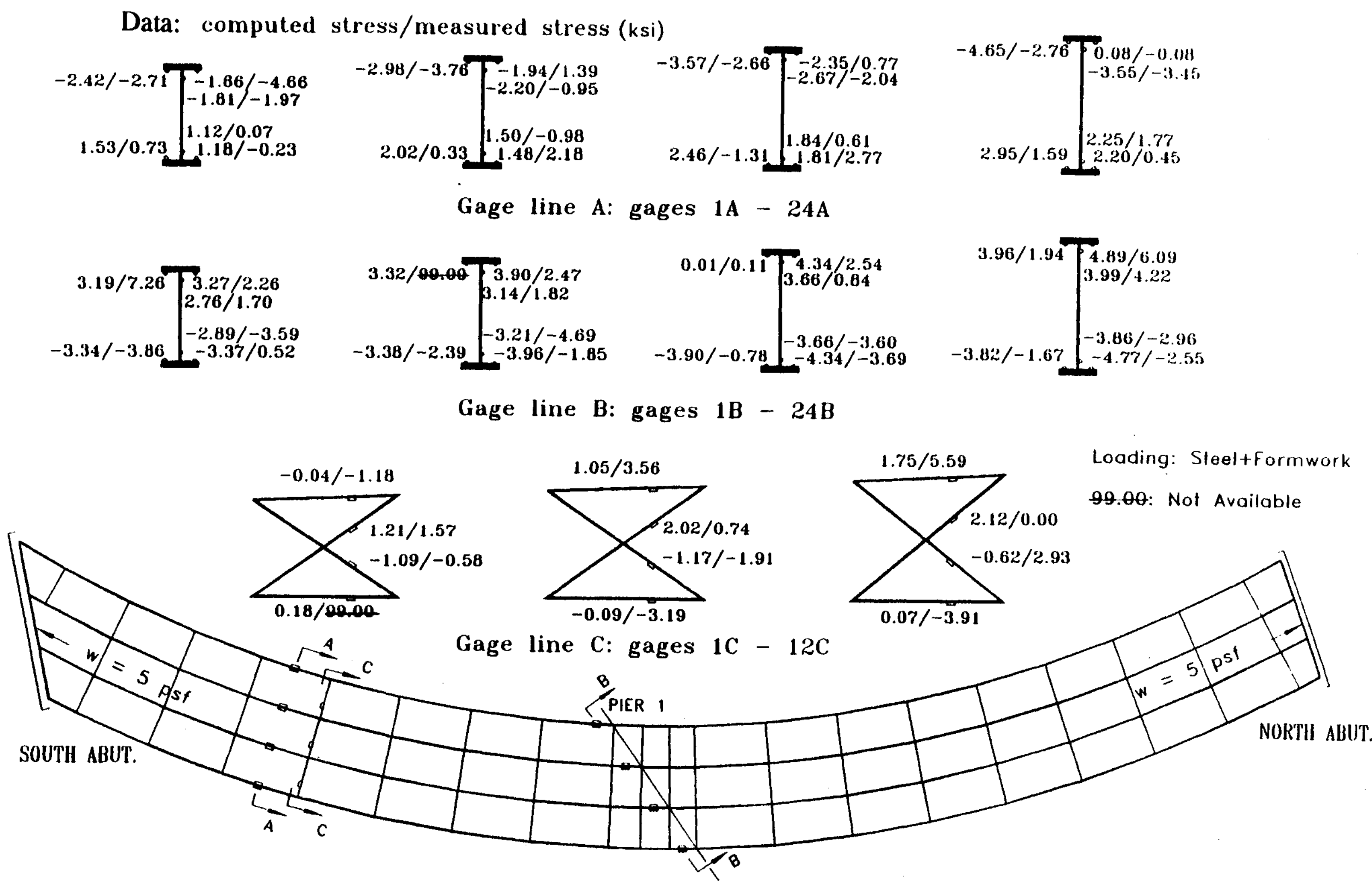

Figure 6.10. Stress comparison at three gage lines for Step 2-2

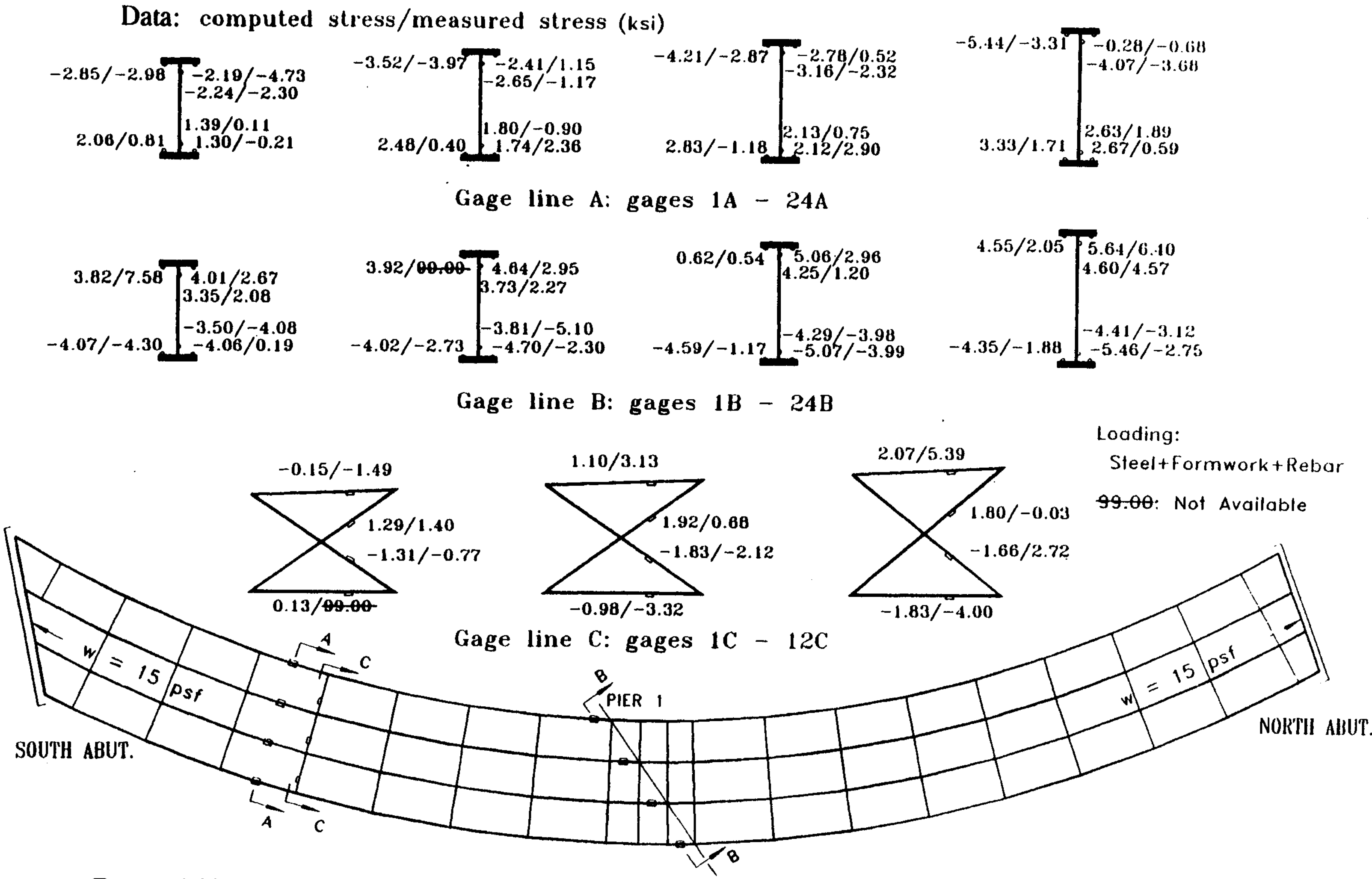

Figure 6.11. Stress comparison at three gage lines for Step 2-3a

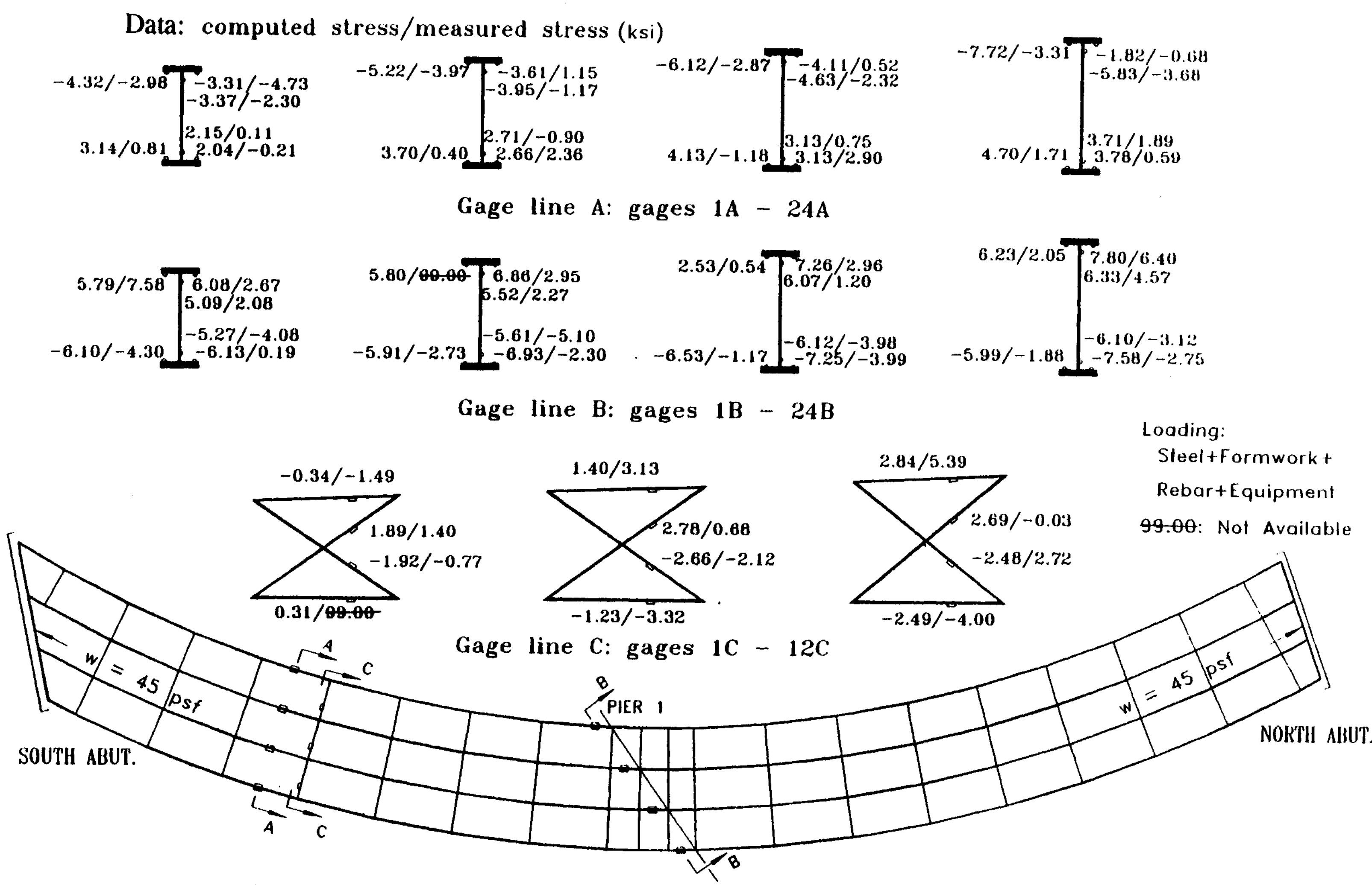

Figure 6.12. Stress comparison at three gage lines for Step 2-3b

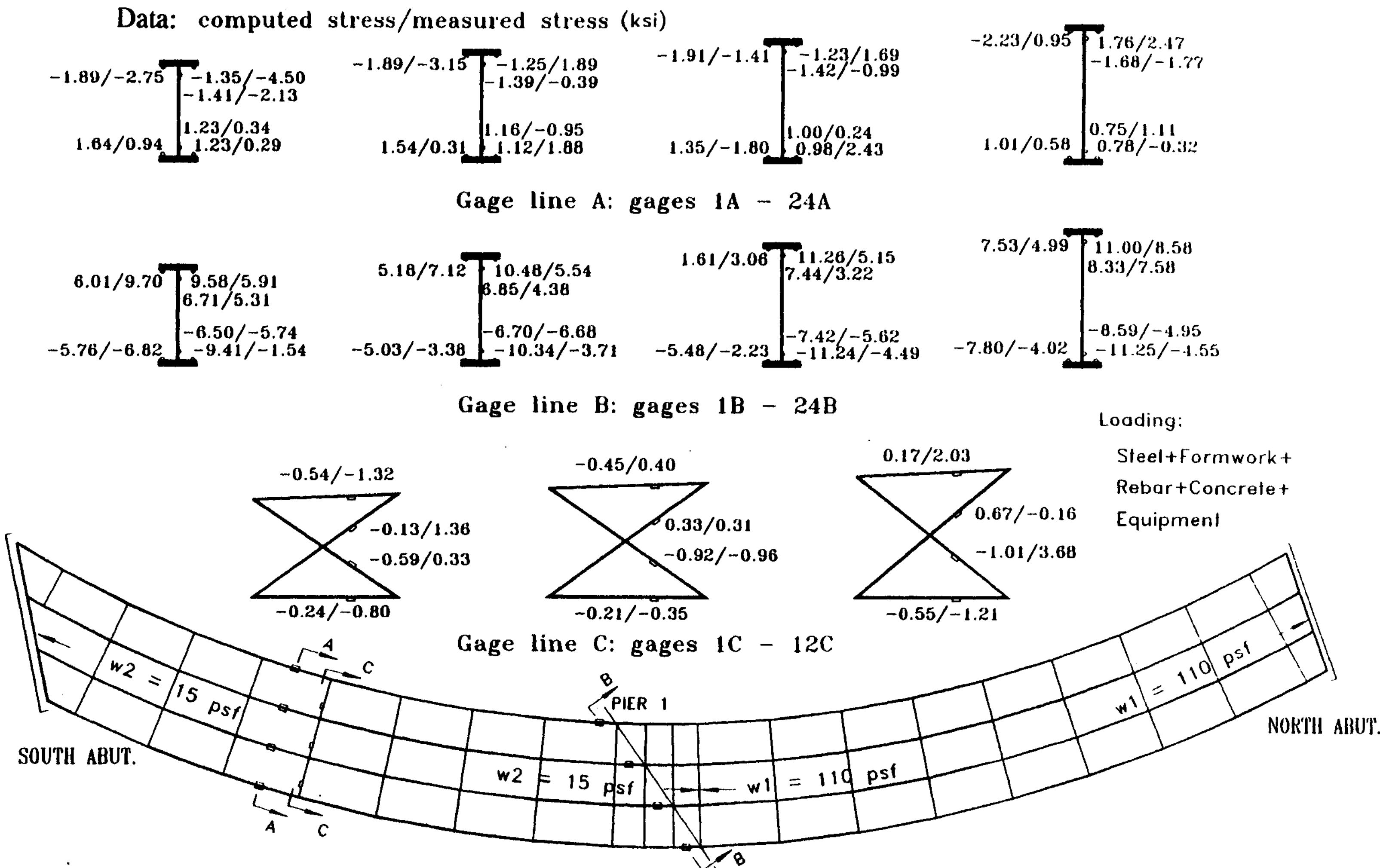

Figure 6.13. Stress comparison at three gage lines for Step 3-1

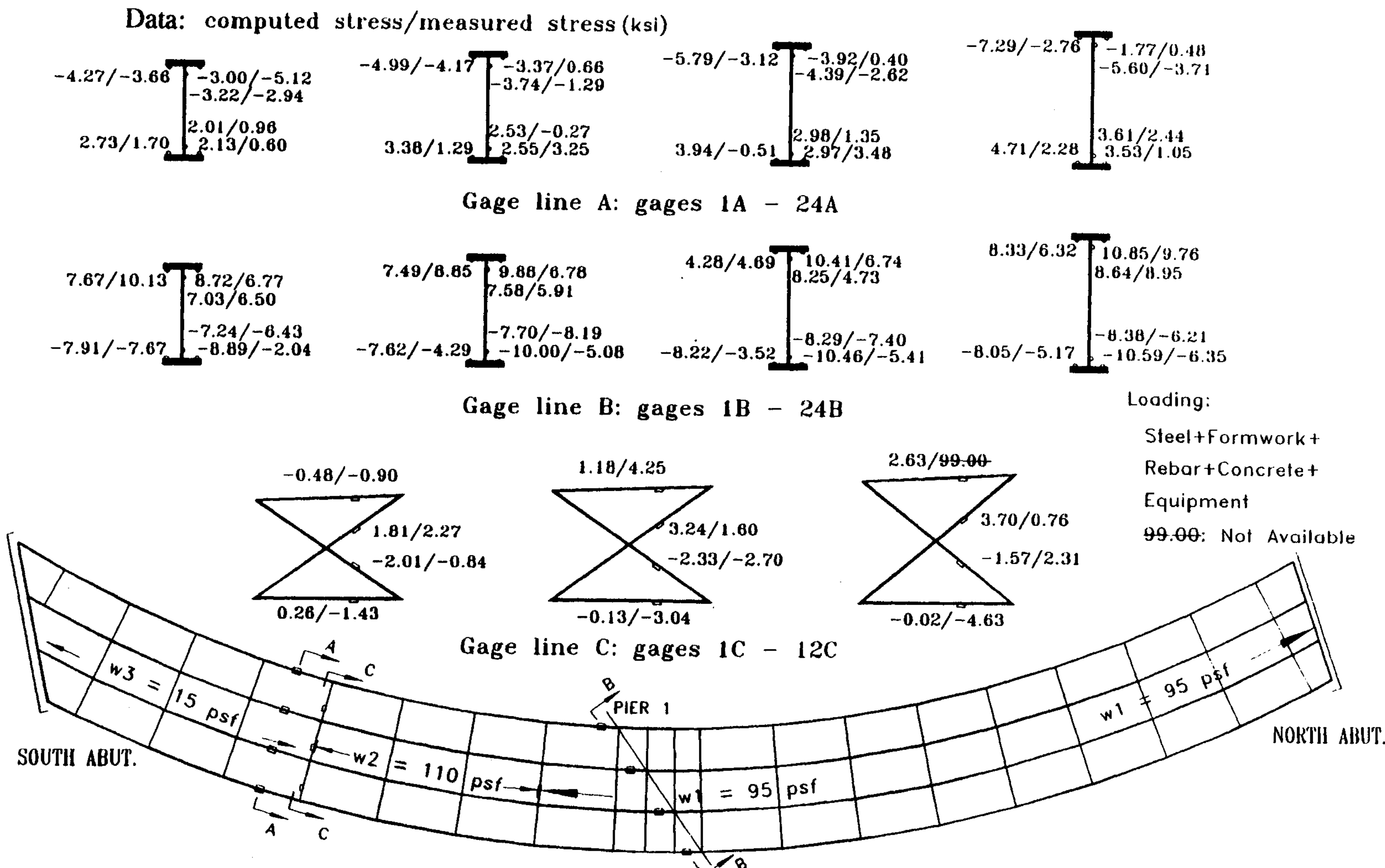

Figure 6.14. Stress comparison at three gage lines for Step 3-2

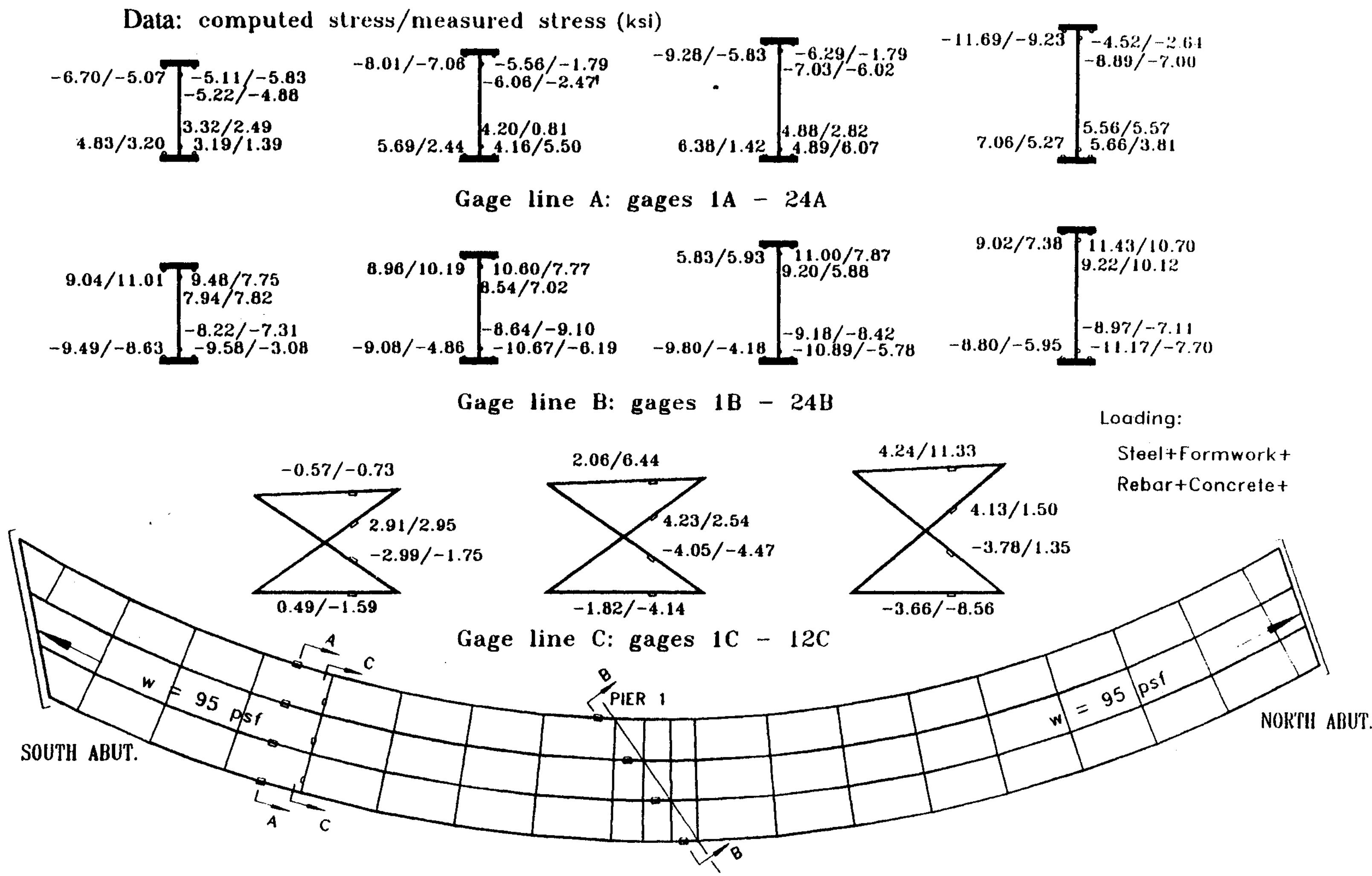

Figure 6.15. Stress comparison at three gage lines for Step 3-3a

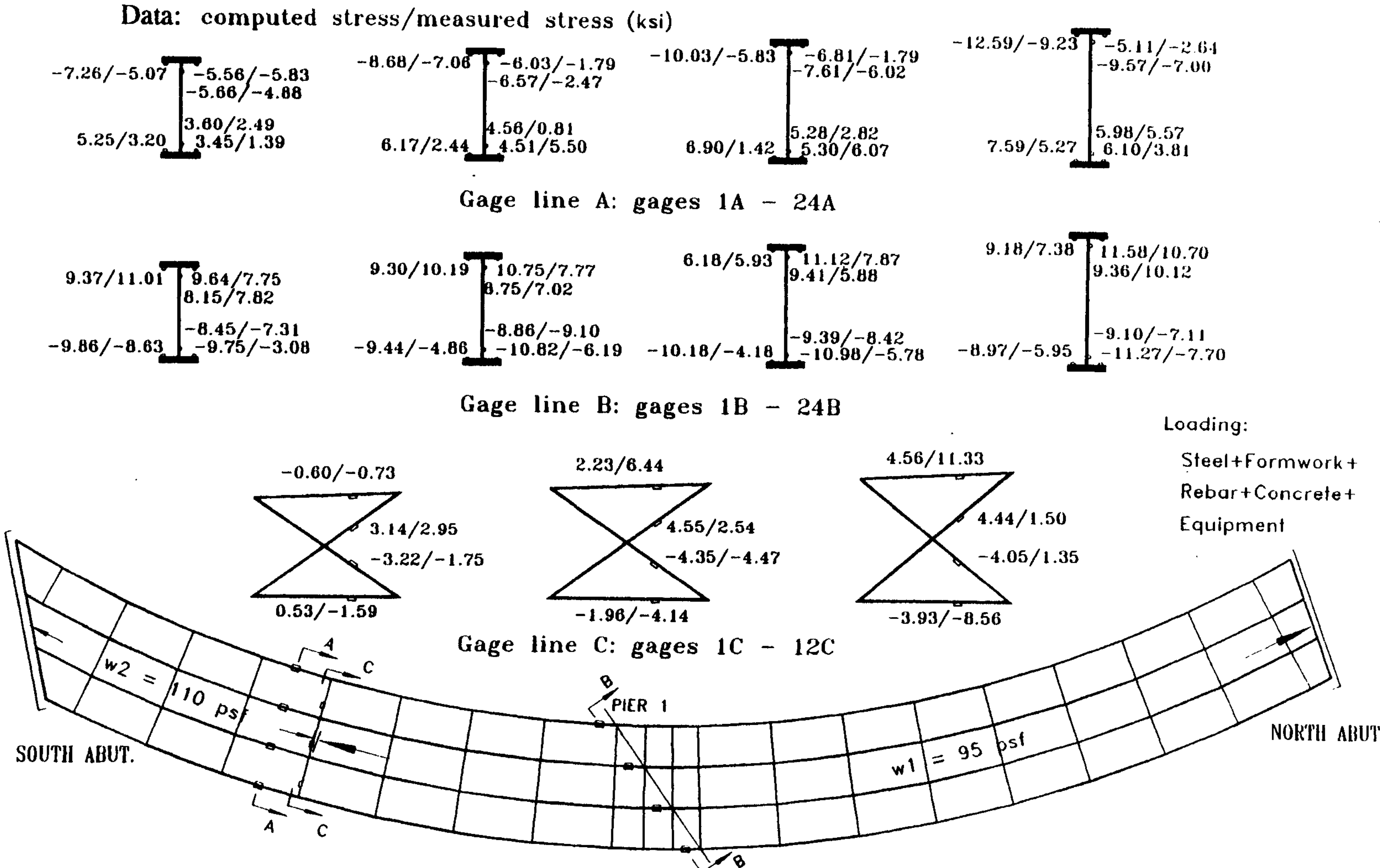

Figure 6.16. Stress comparison at three gage lines for Step 3-3b

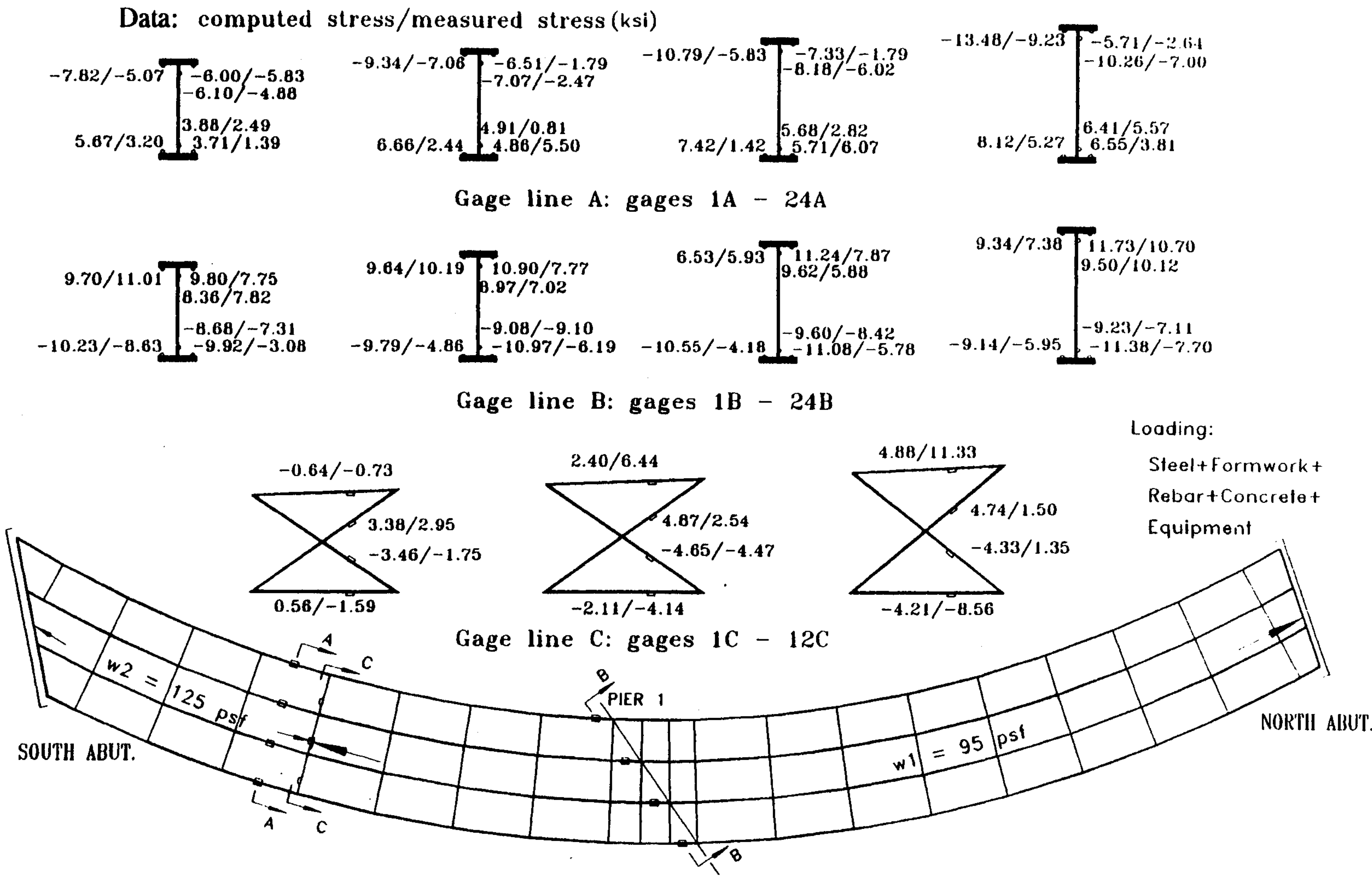

Figure 6.17. Stress comparison at three gage lines for Step 3-3c

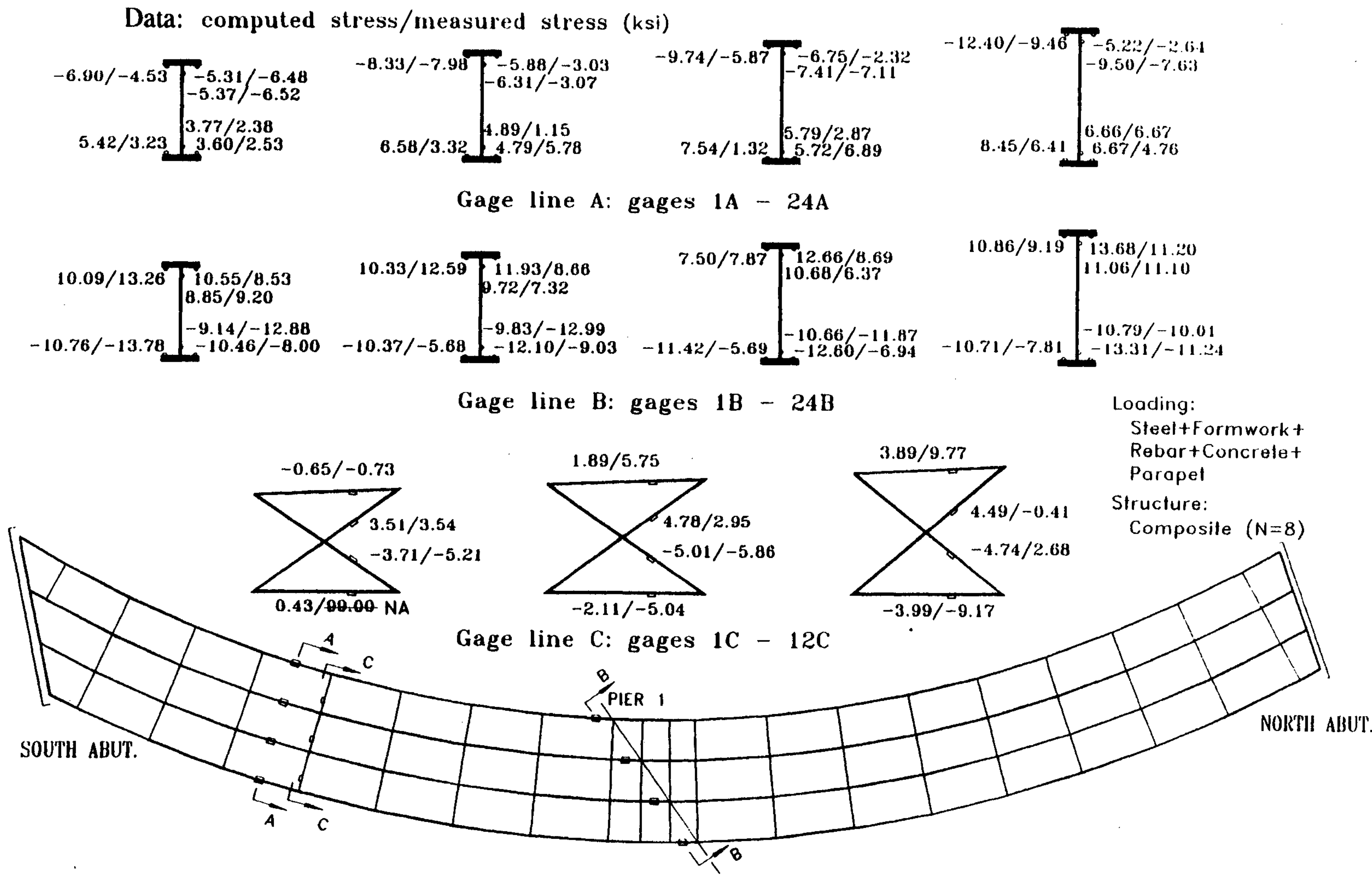

Figure 6.18. Stress comparison at three gage lines for Step 4-1 (N=8)

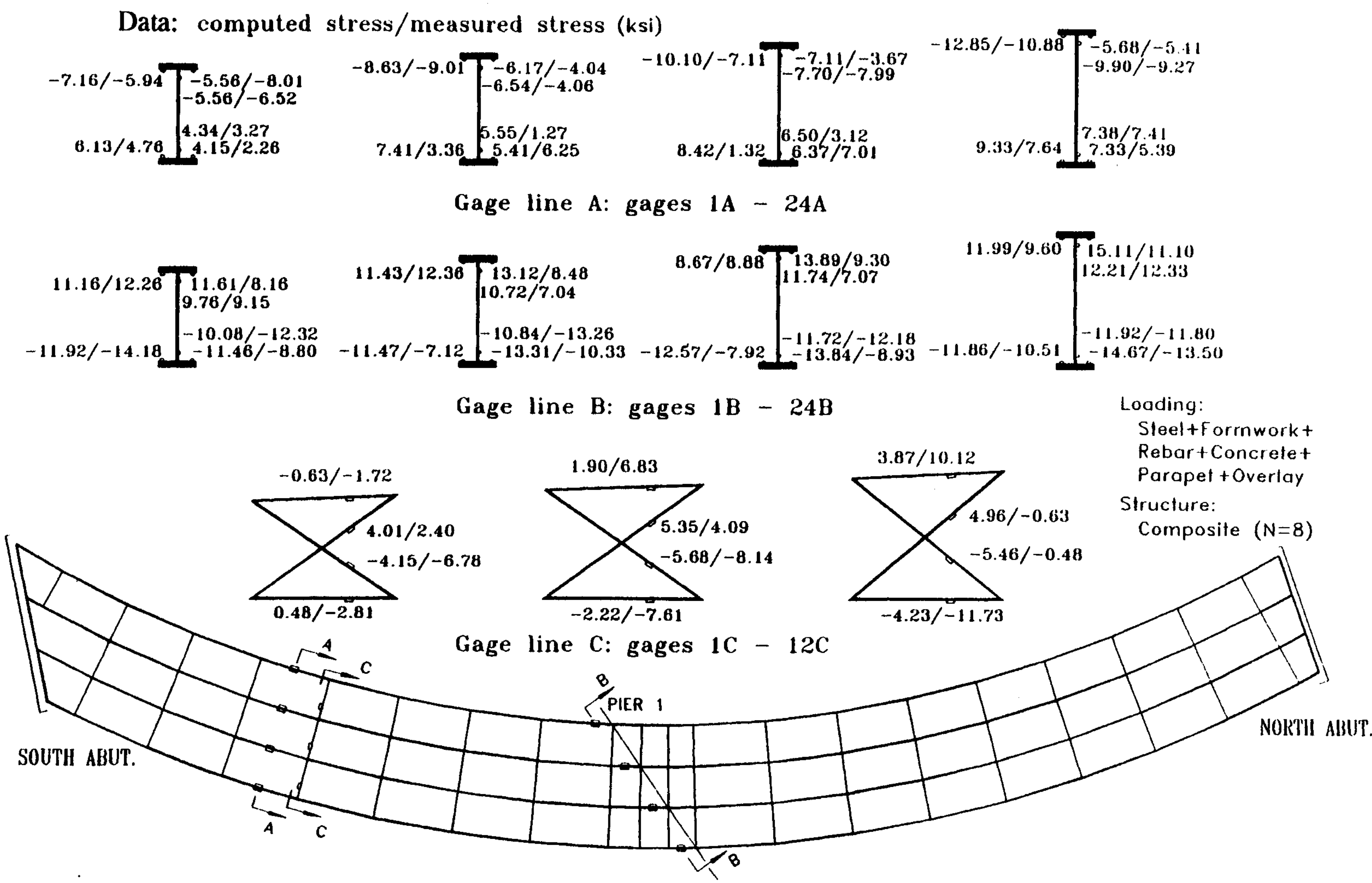

Figure 6.19. Stress comparison at three gage lines for Step 4-2 (N=8)

Notes:

The centerline of front wheels of each truck coincides with the line of crossframe; e.g., Case 2 on line 5.

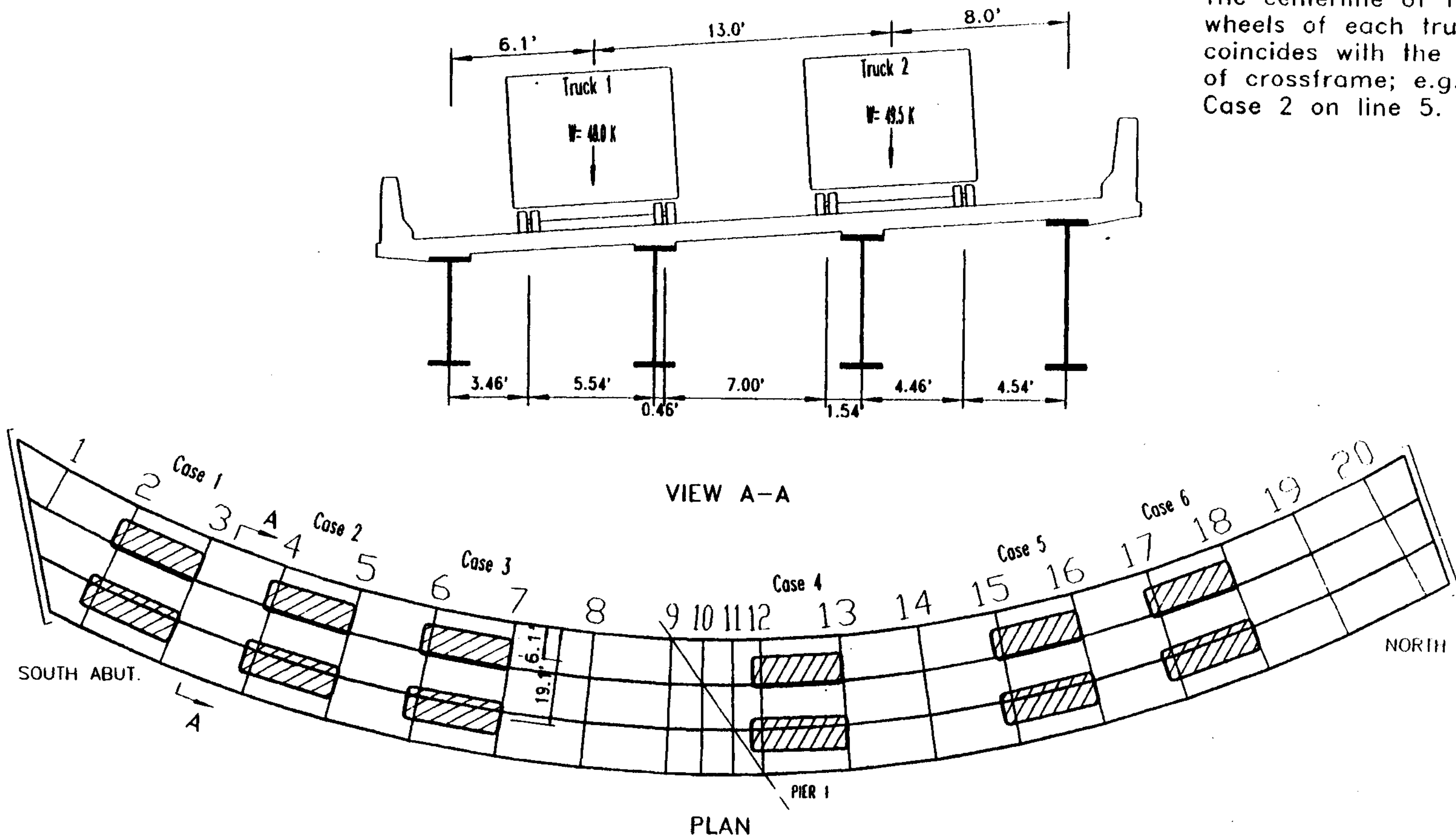

Figure 6.20. Plan of field tests for cases 1 to 6

Notes:

The centerline of front wheels of each truck coincides with the line of crossframe; e.g., Case 8 on lines 5 & 7 for trucks 1 and 2 respectively

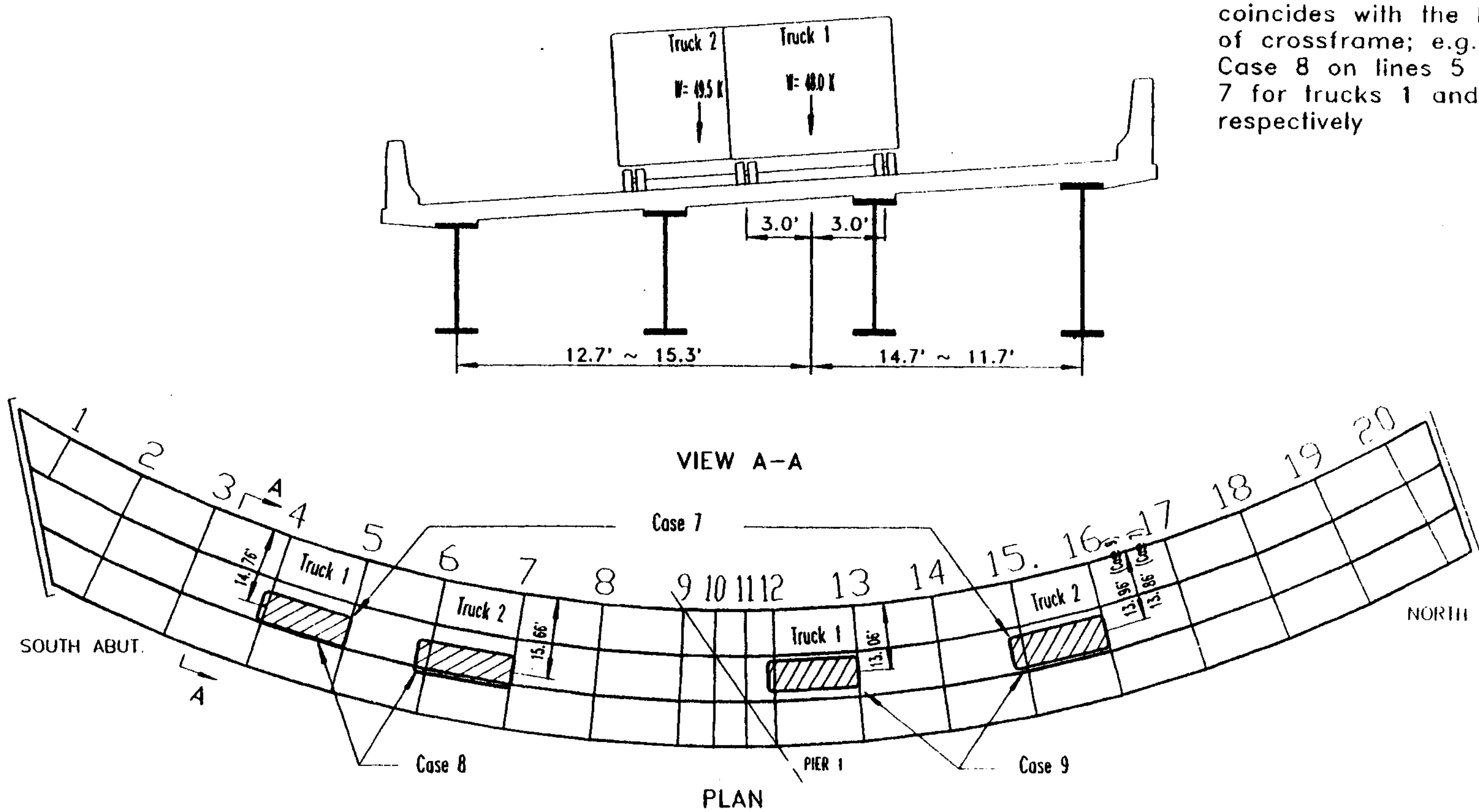

Figure 6.21. Plan of field tests for cases 7 to 9

Notes:

The centerline of front wheels of each truck coincides with the line of crossframe; e.g., Case 11 on line 5.

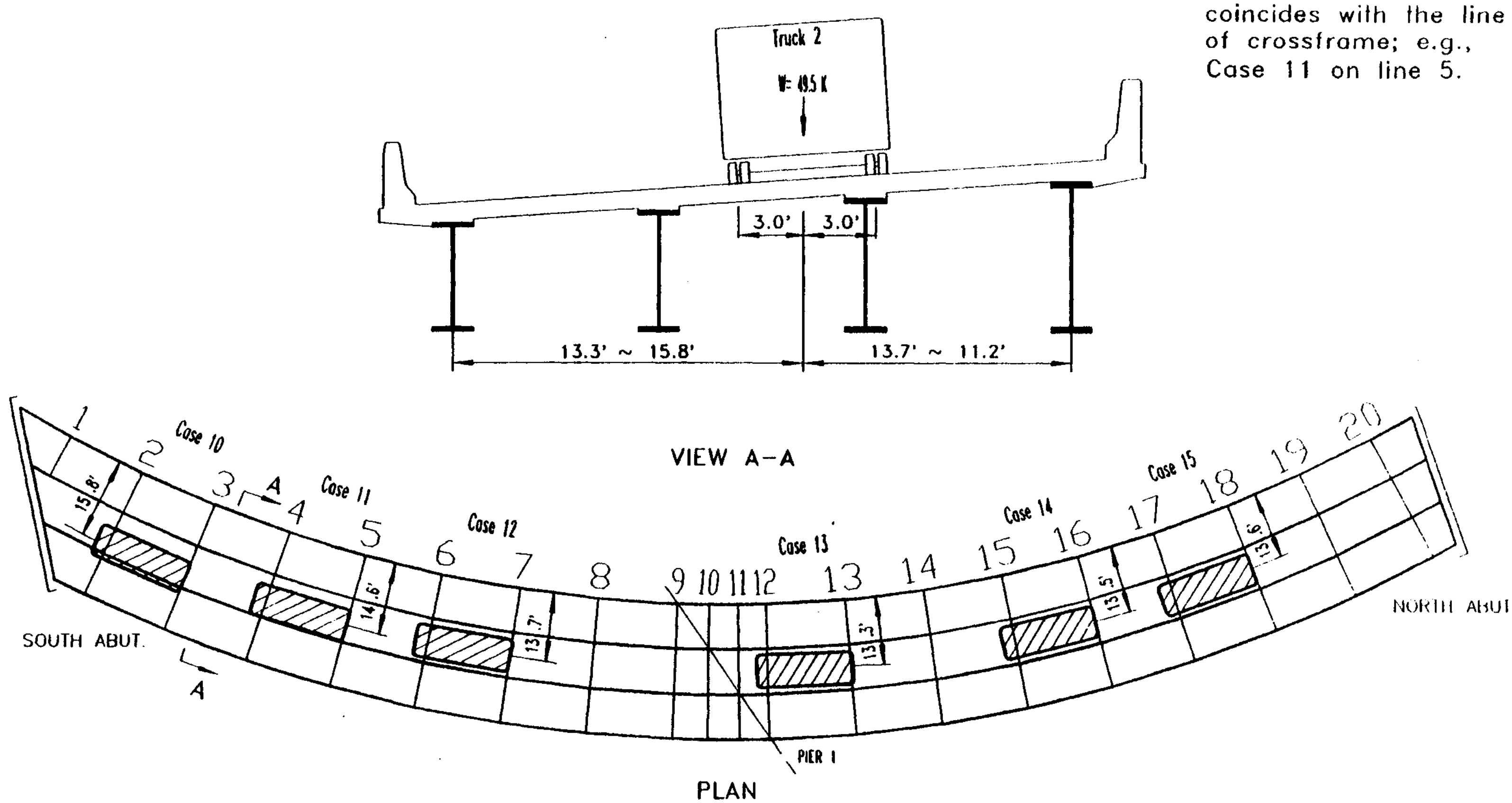

Figure 6.22. Plan of field tests for cases 10 to 15

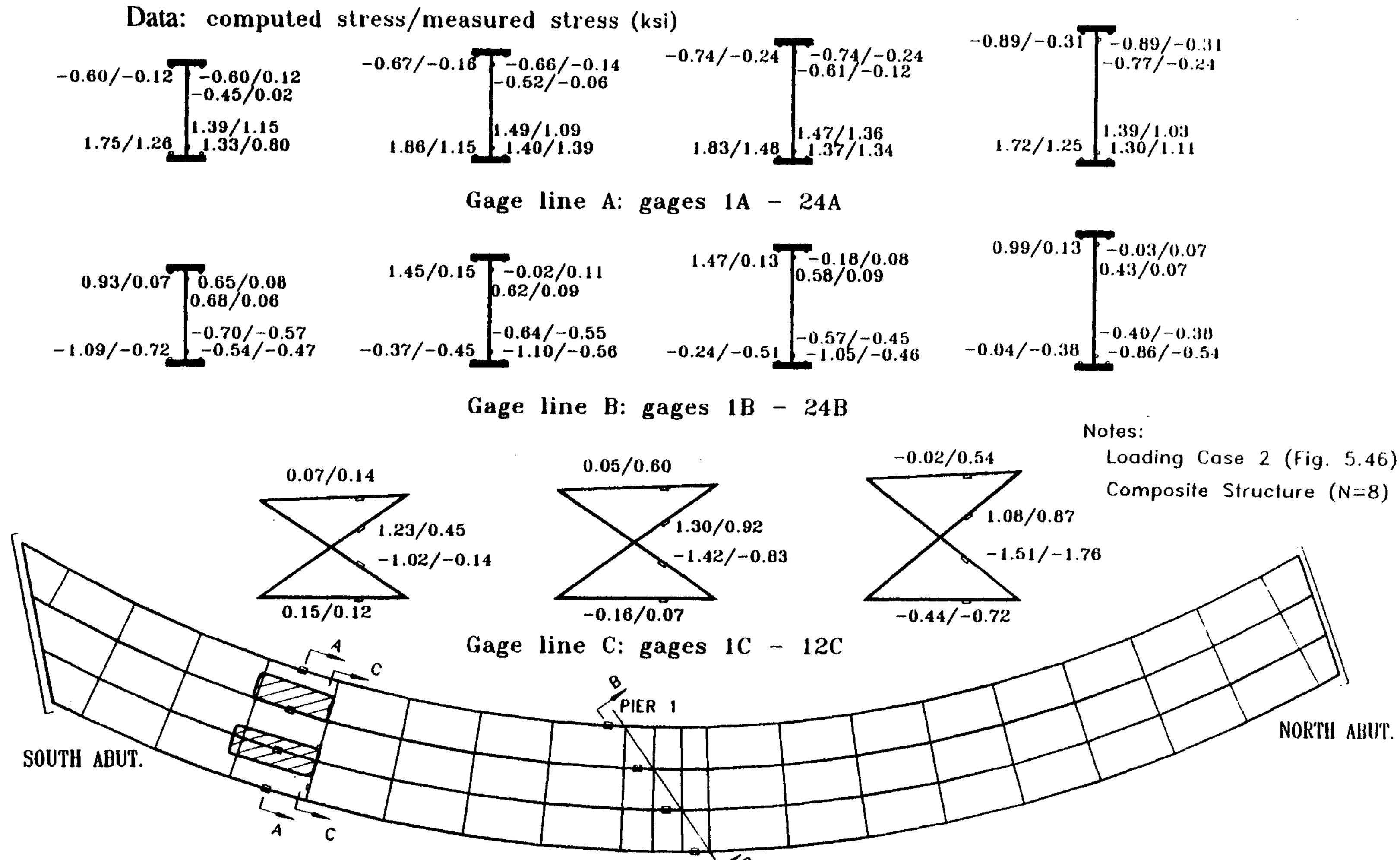

Figure 6.23. Stress comparison at three gage lines for truck load Case 2

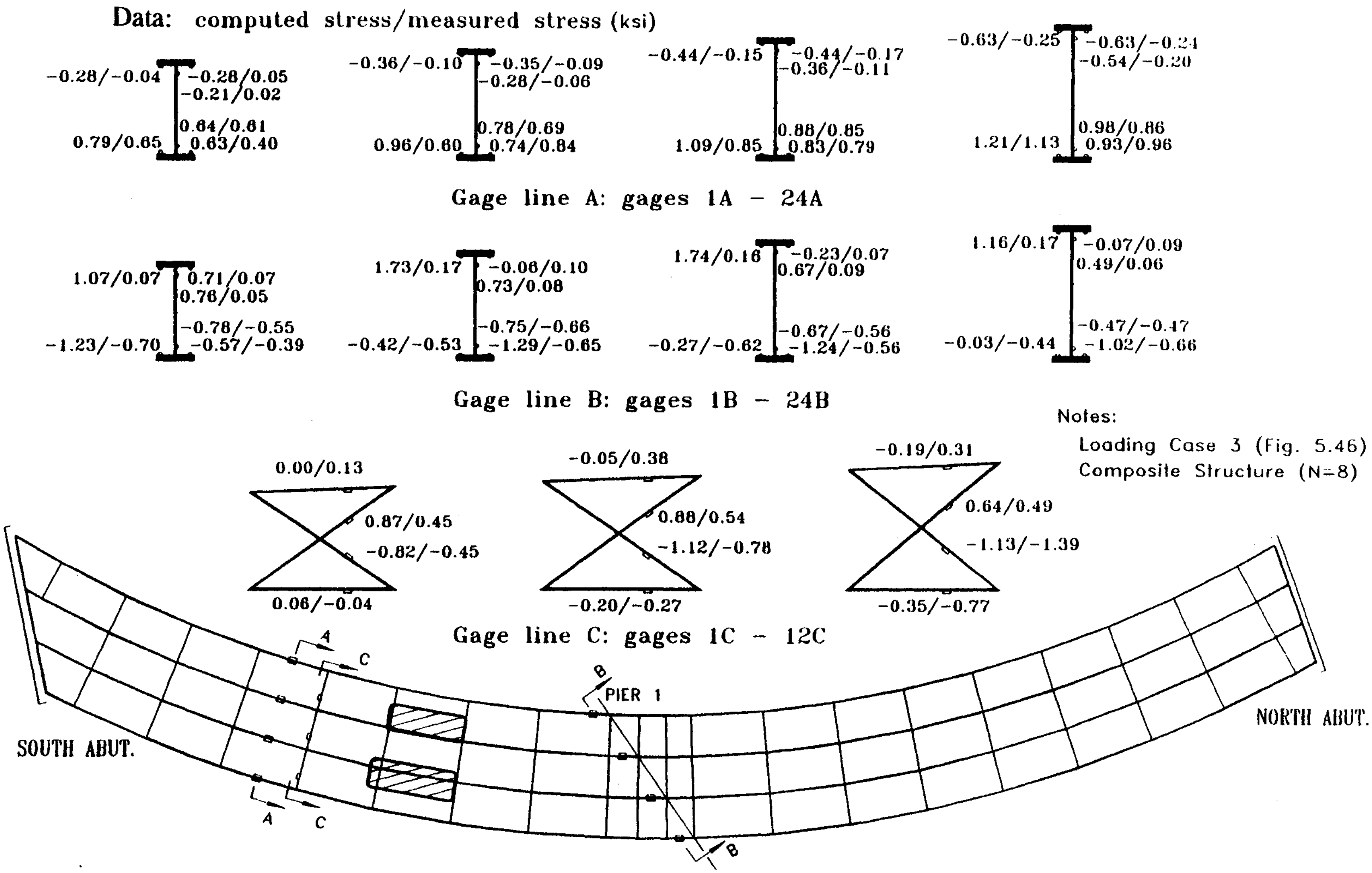

Figure 6.24. Stress comparison at three gage lines for truck load Case 3

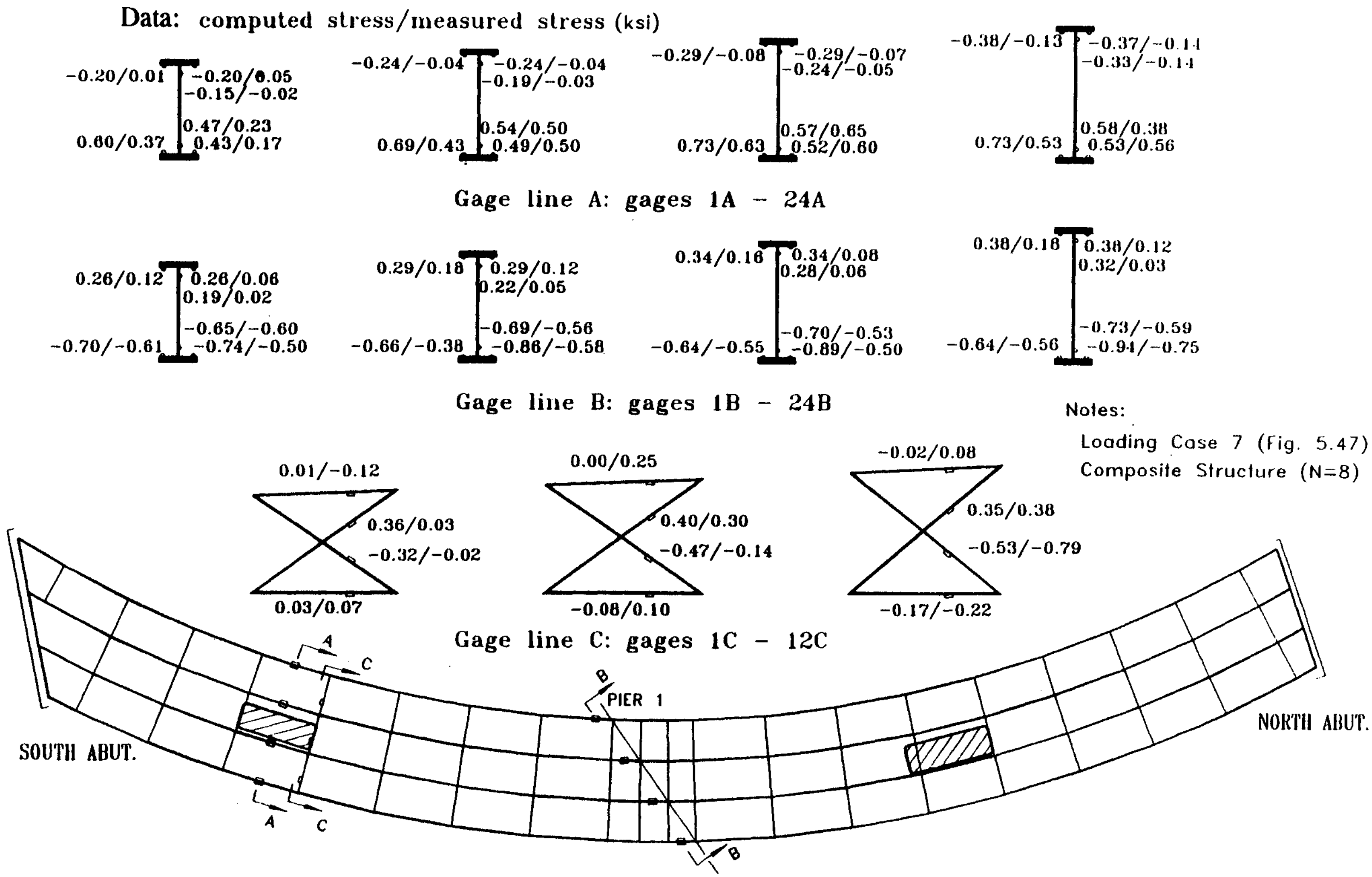

Figure 6.25. Stress comparison at three gage lines for truck load Case 7

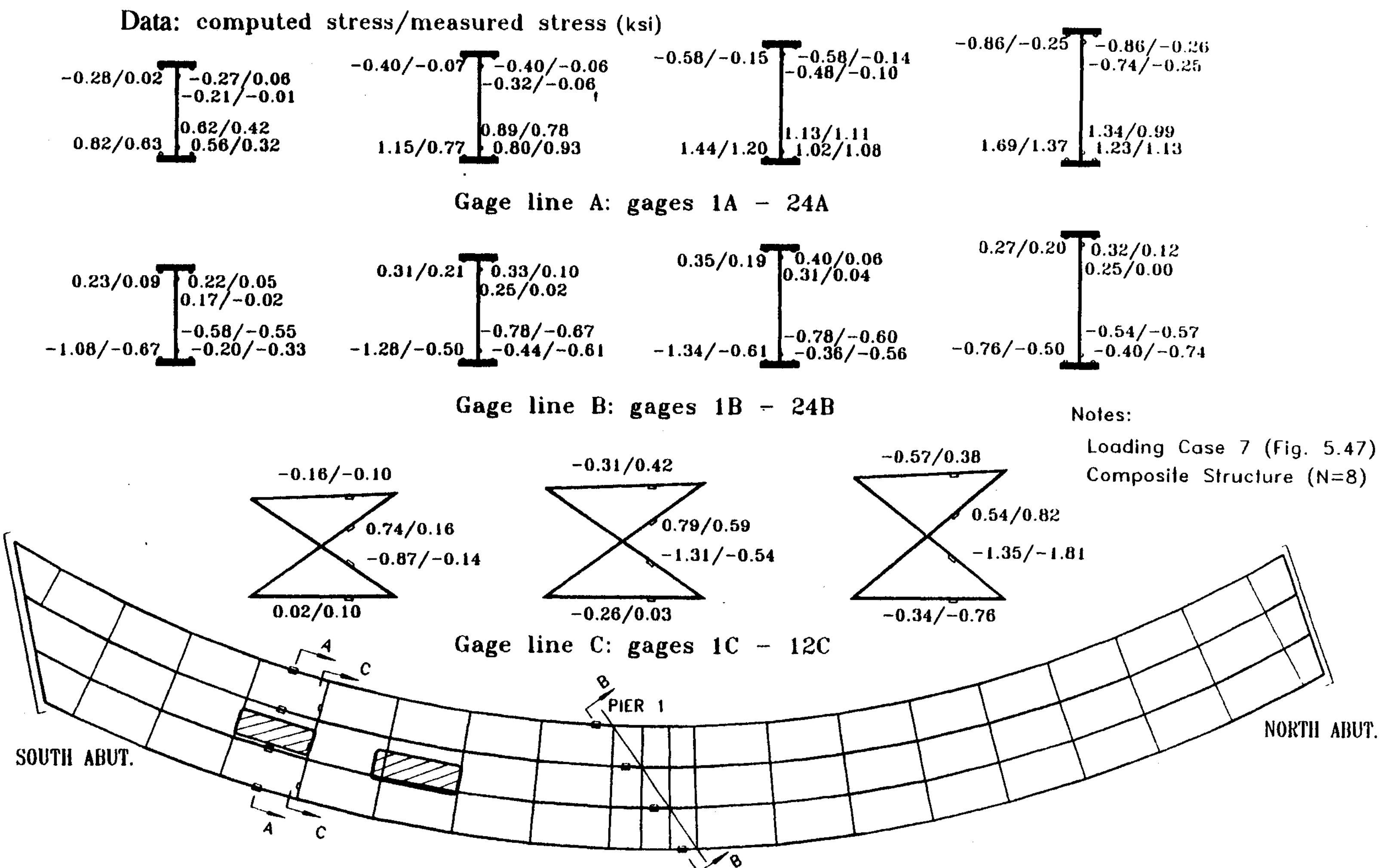

Figure 6.26. Stress comparison at three gage lines for truck load Case 8

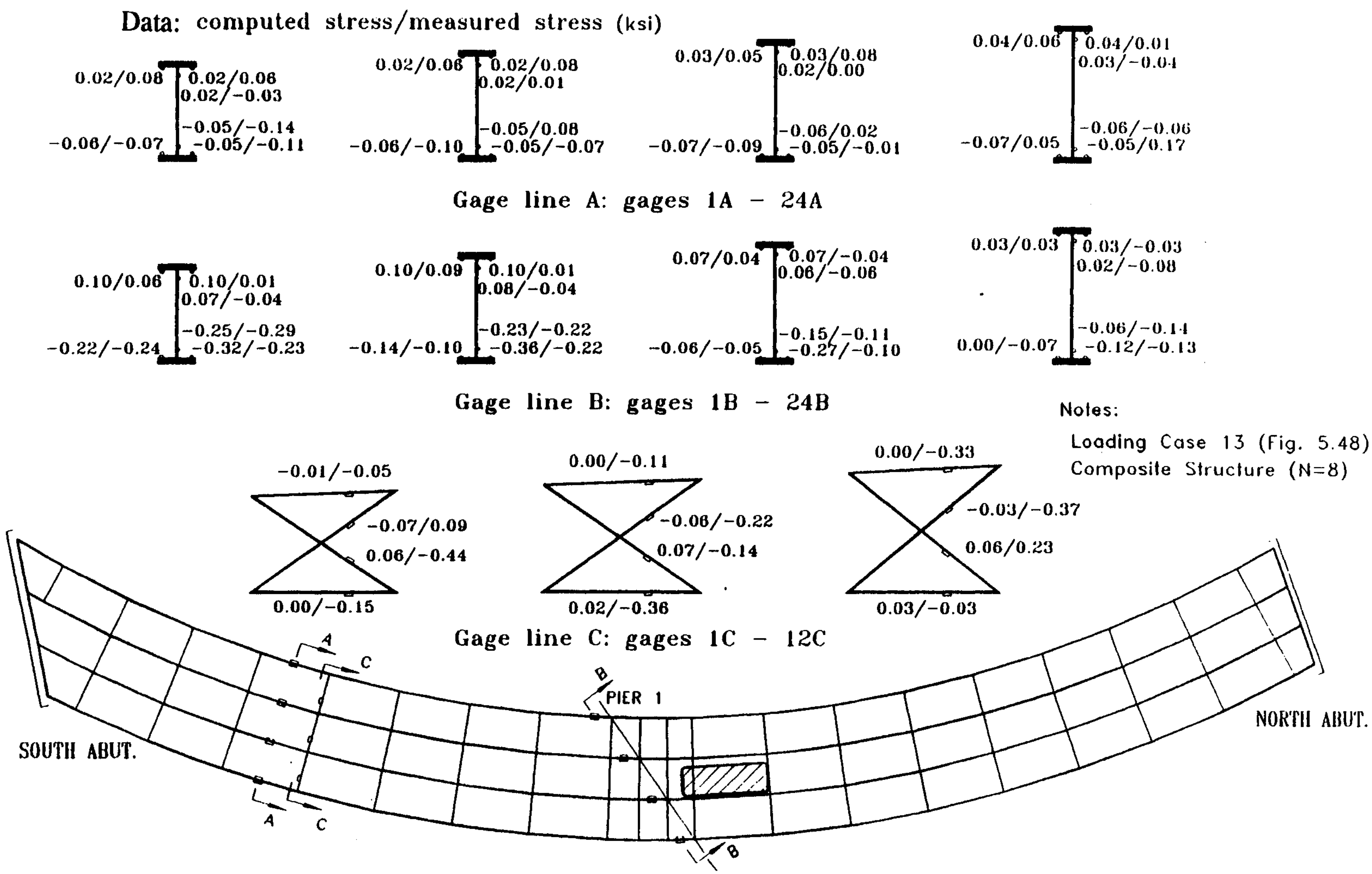

Figure 6.27. Stress comparison at three gage lines for truck load Case 13

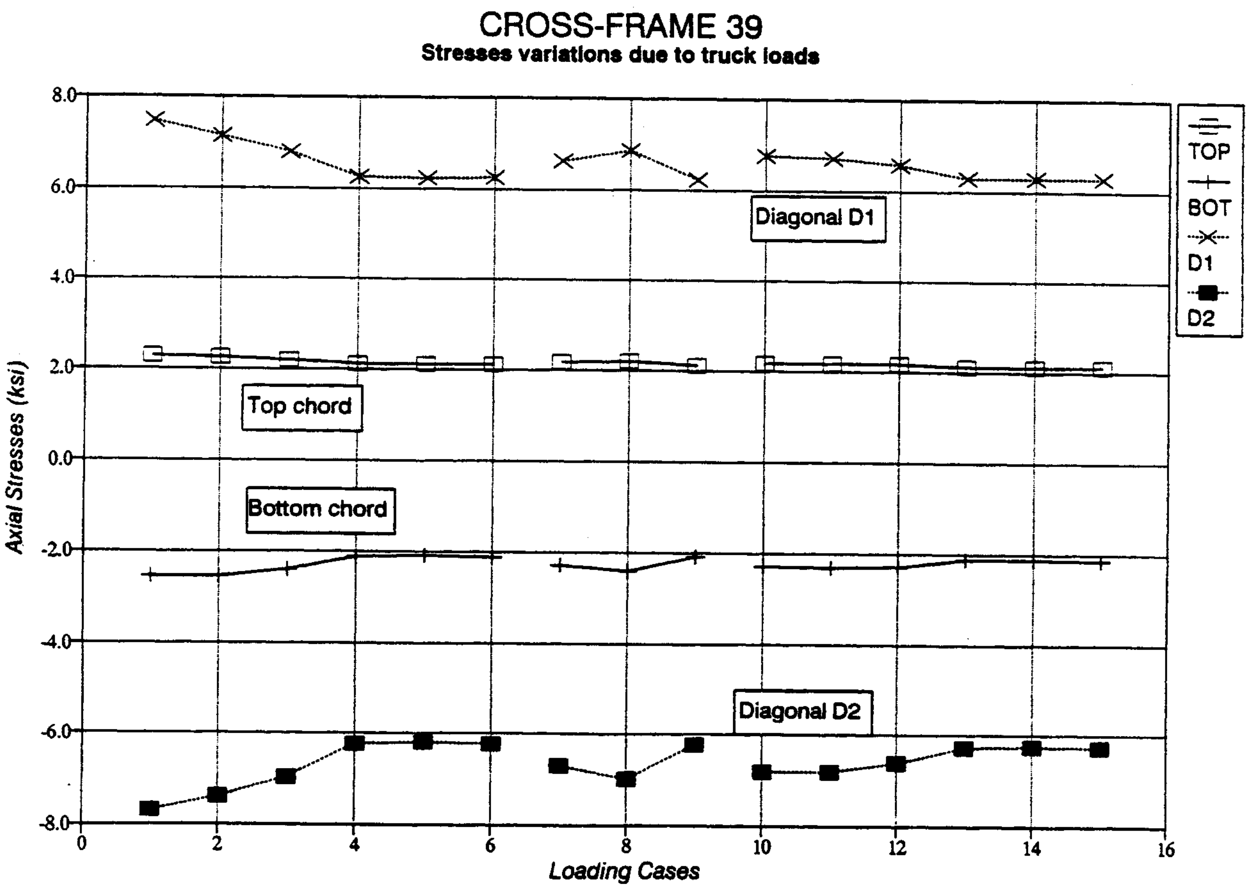

Figure 6.28. Stress variations due to truck loads in crossframe 39

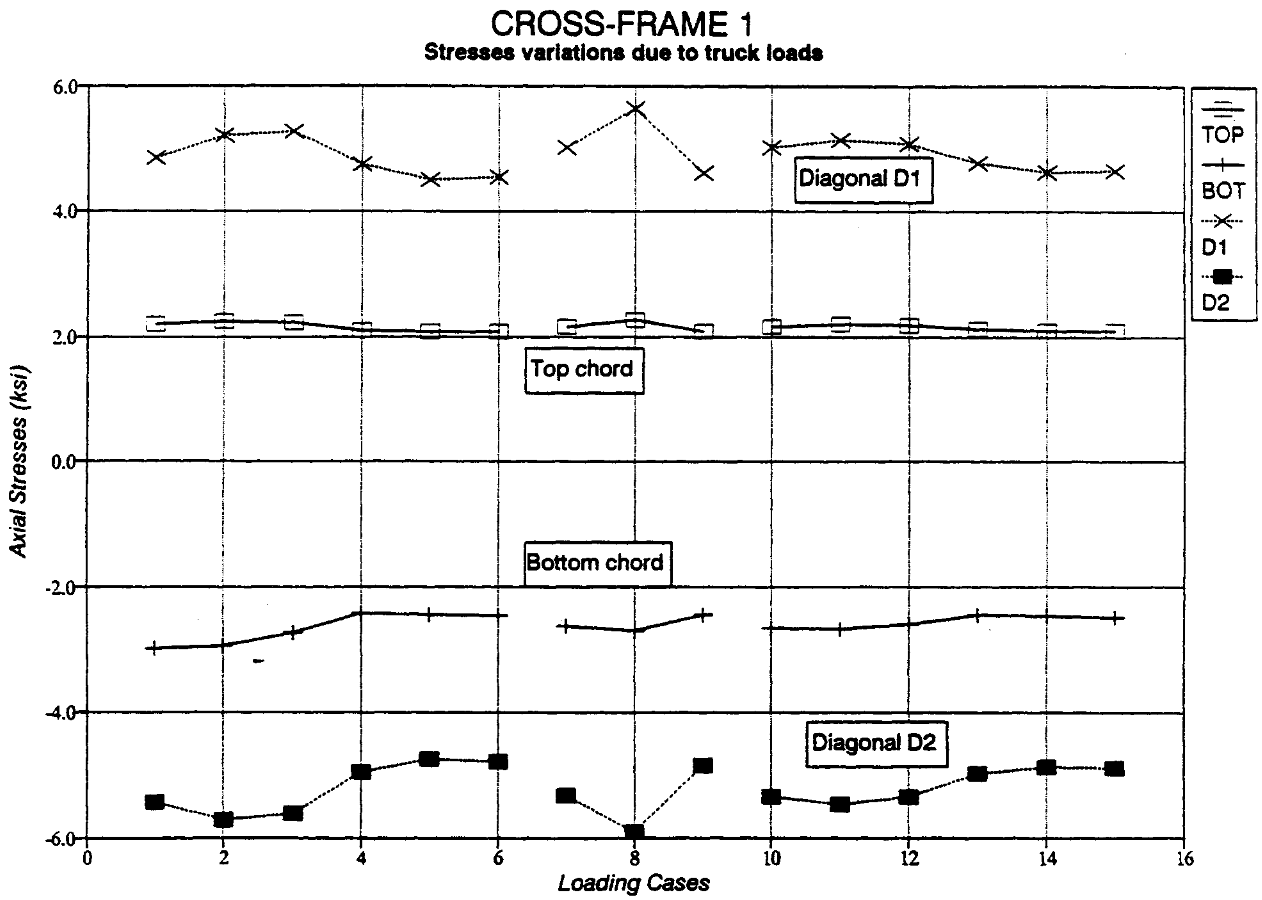

Figure 6.29. Stress variations due to truck loads in crossframe 1

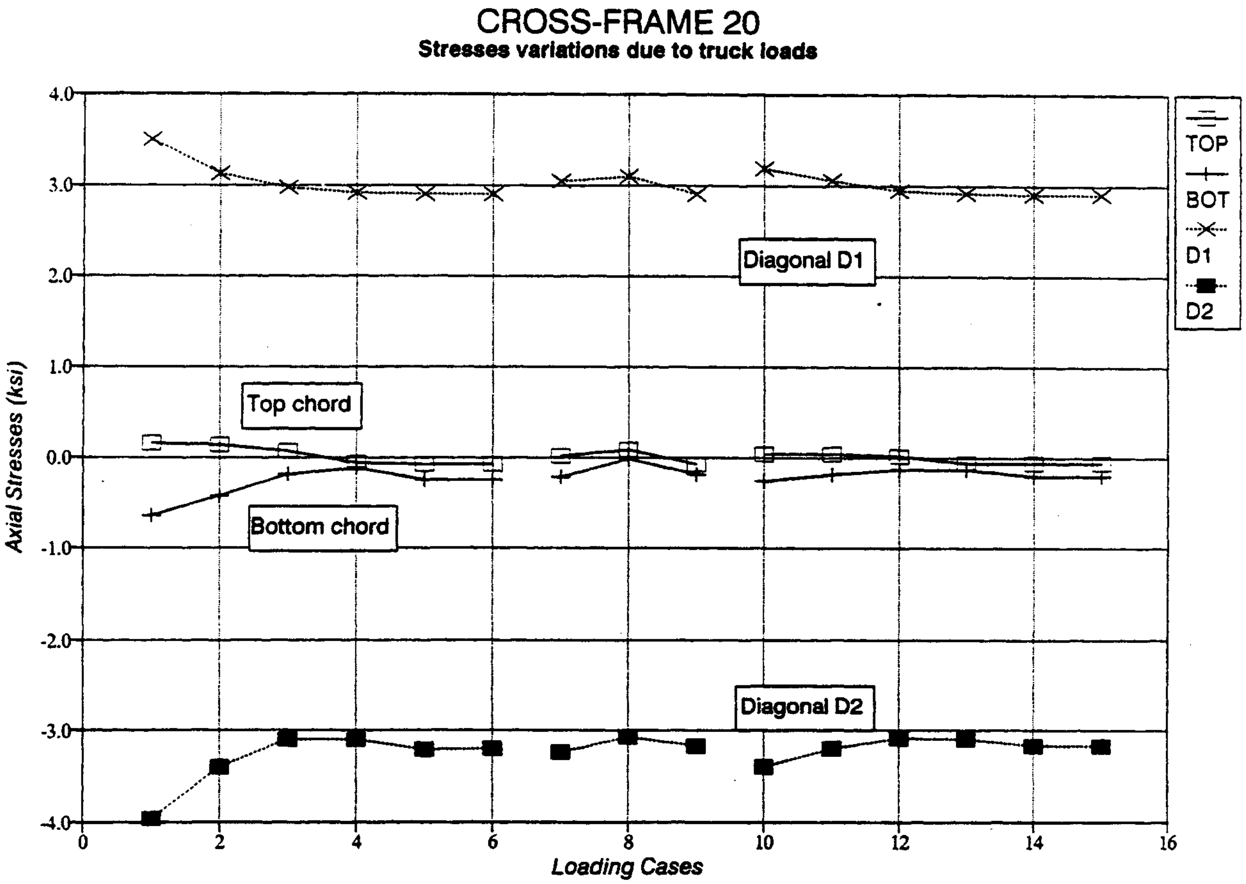

Figure 6.30. Stress variations due to truck loads in crossframe 20

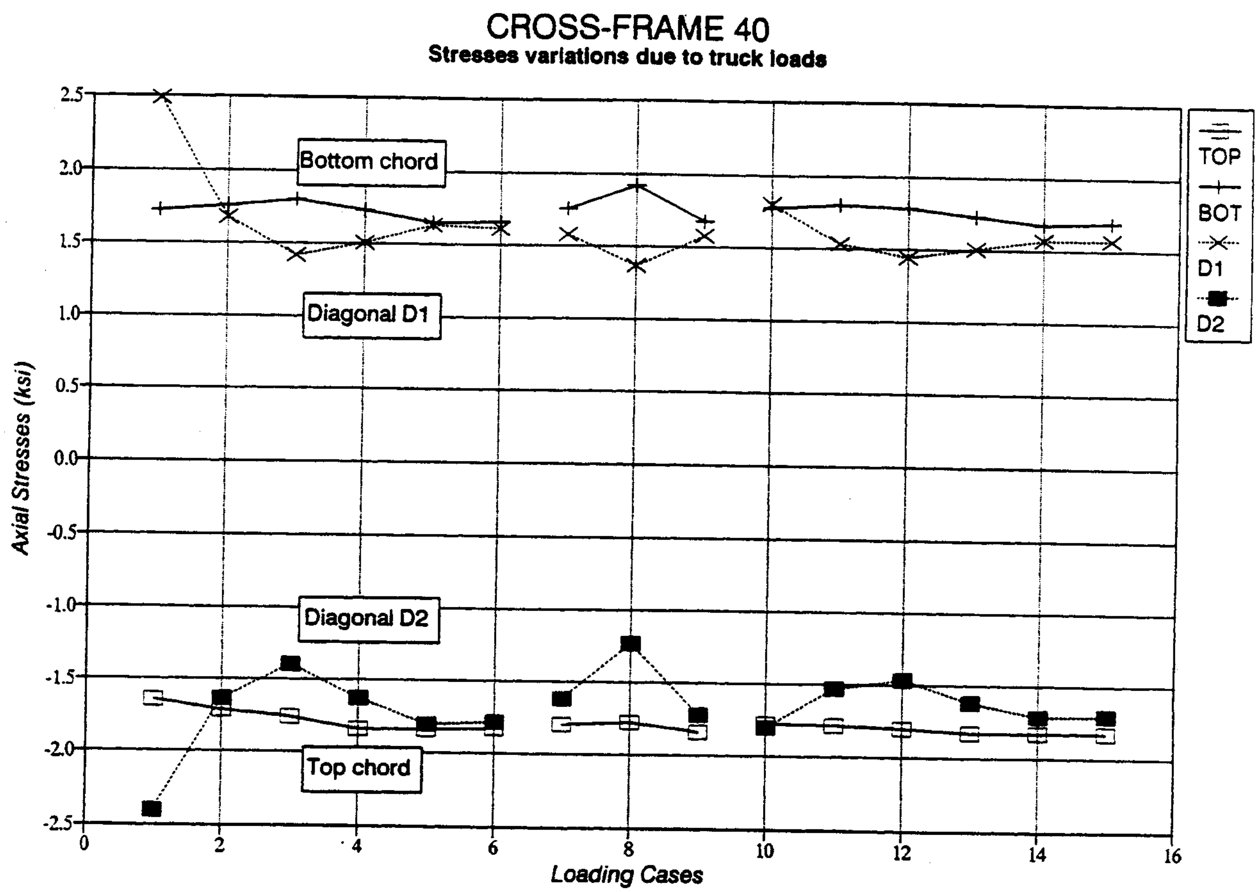

Figure 6.31. Stress variations due to truck loads in crossframe 40

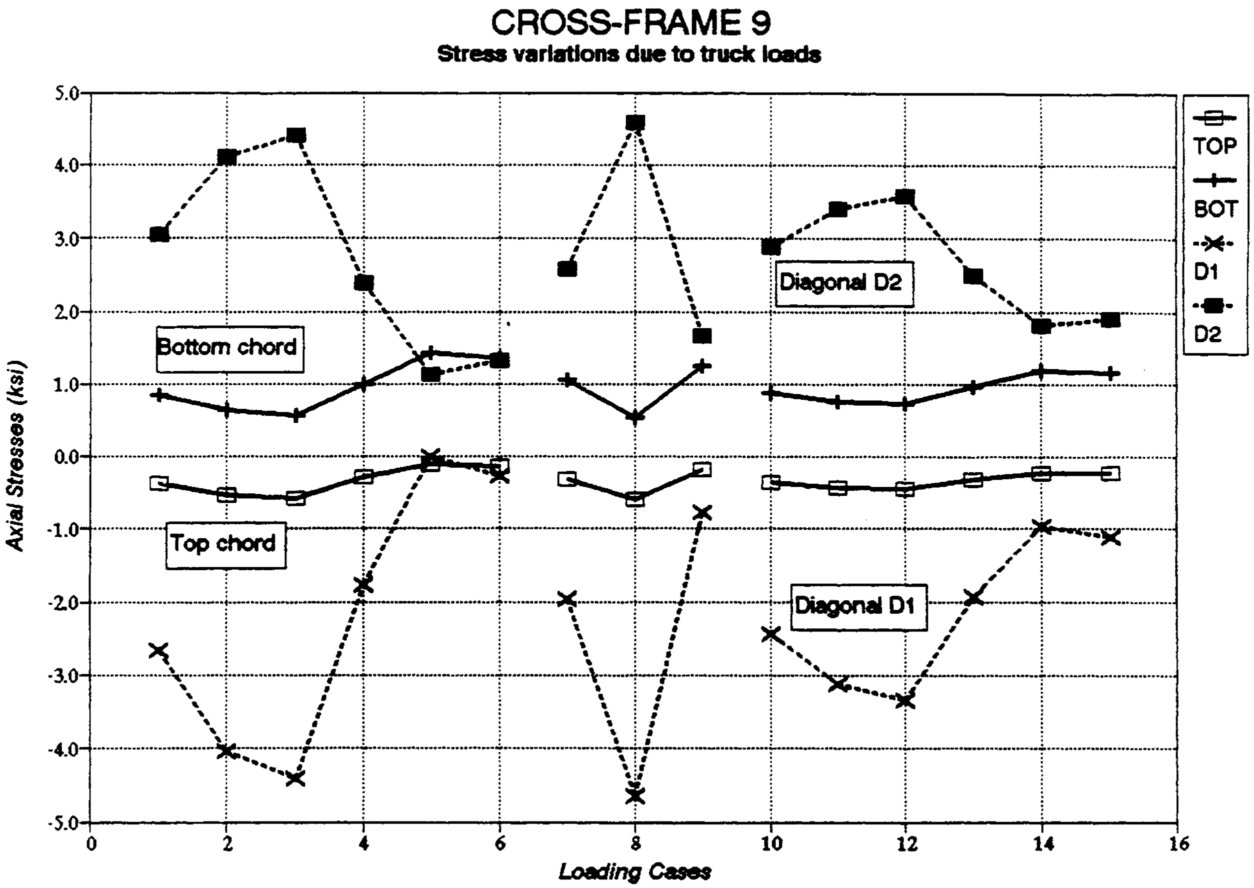

Figure 6.32. Stress variations due to truck loads in crossframe 9

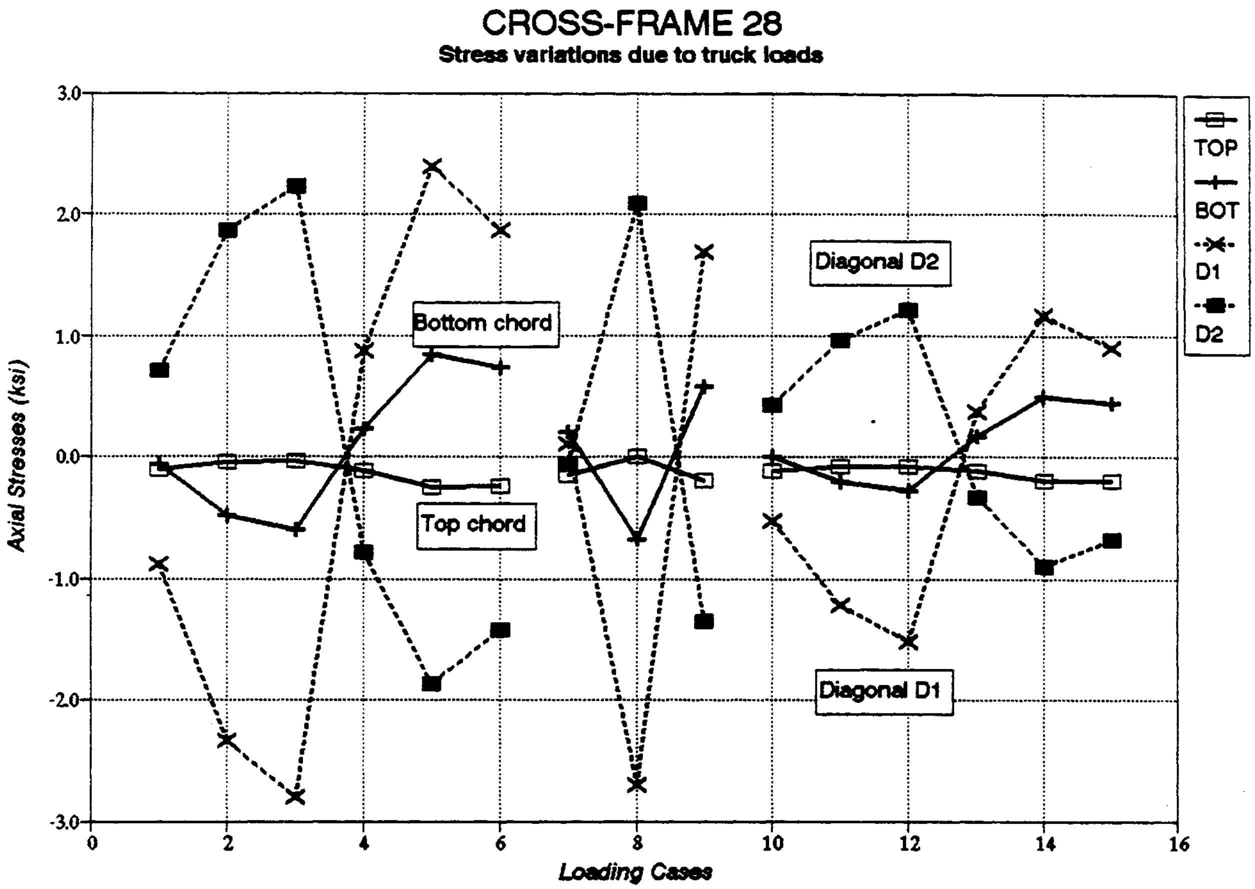

Figure 6.33. Stress variations due to truck loads in crossframe 28

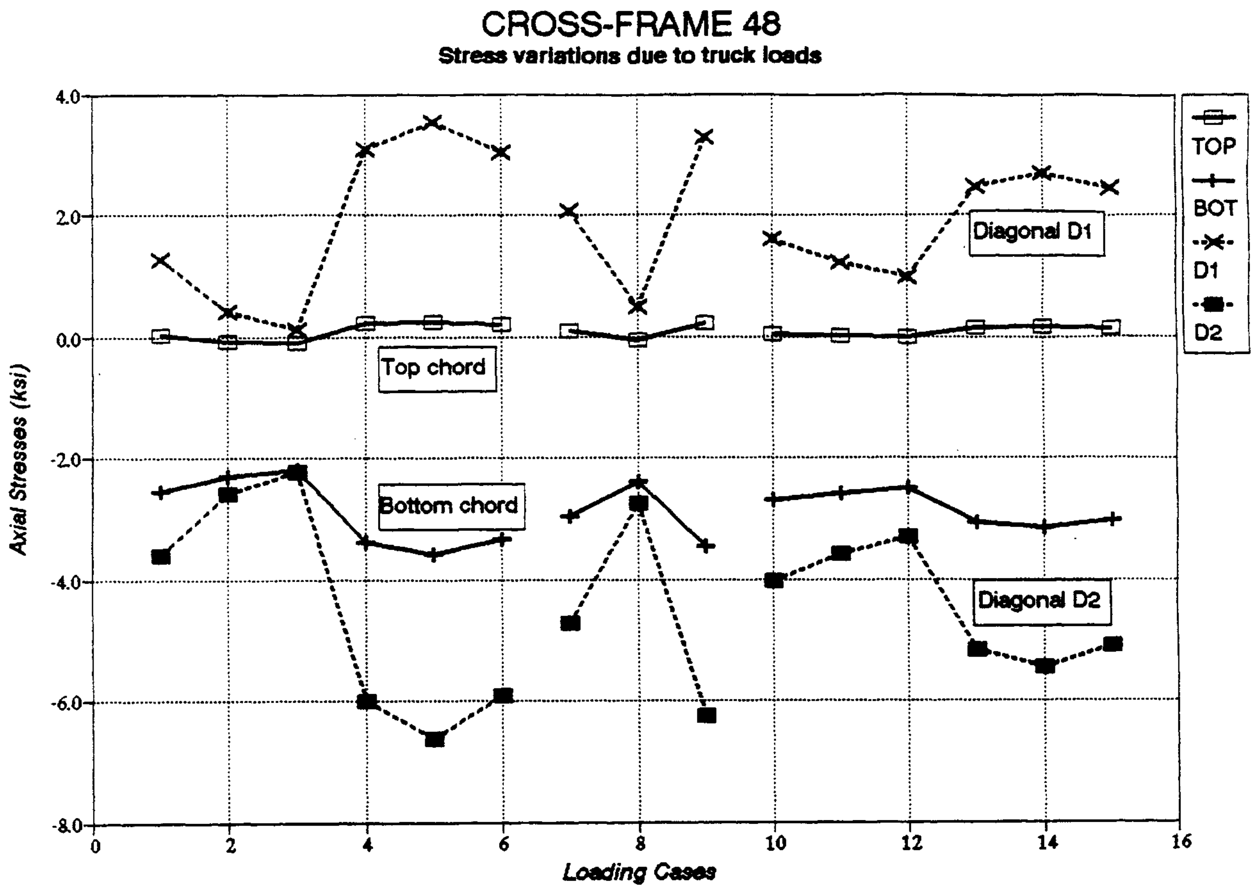

Figure 6.34. Stress variations due to truck loads in crossframe 48

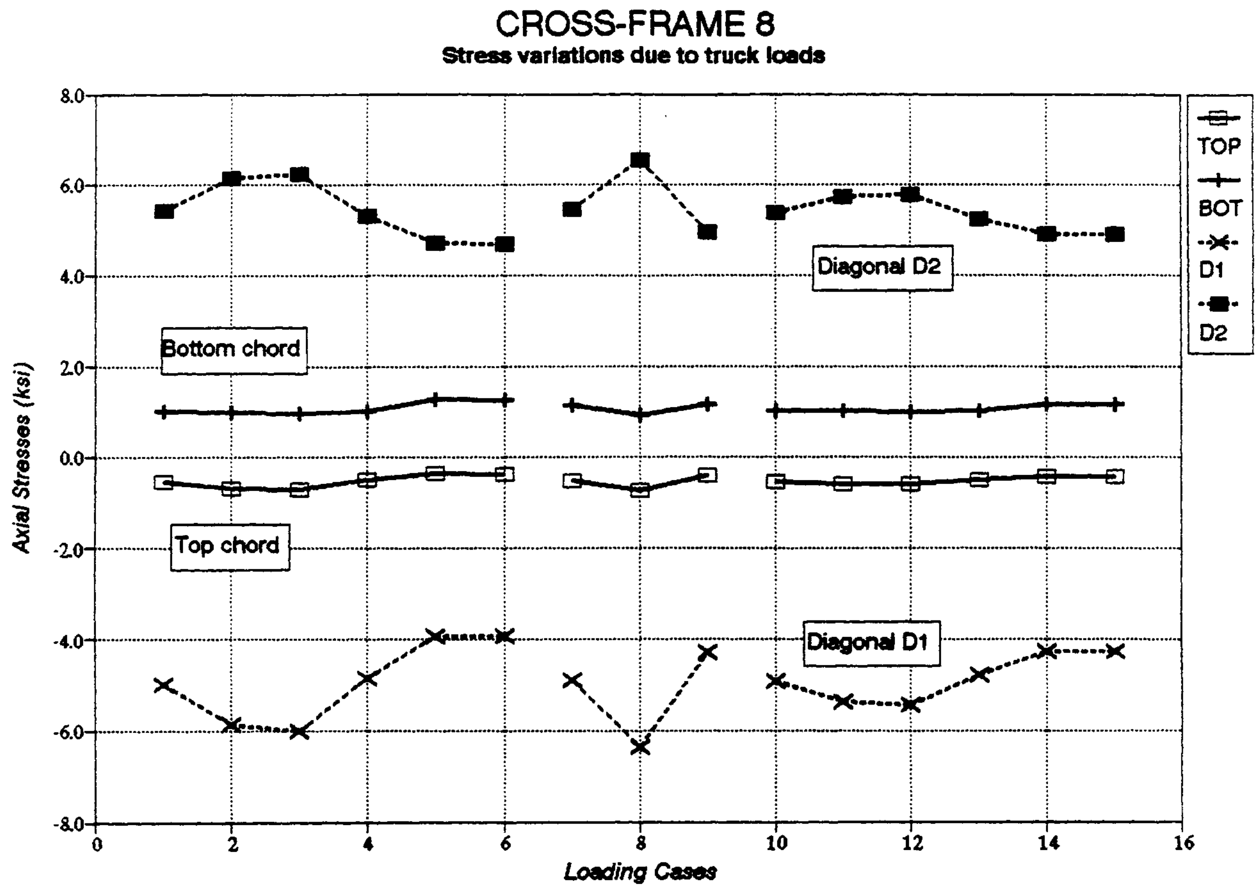

Figure 6.35. Stress variations due to truck loads in crossframe 8

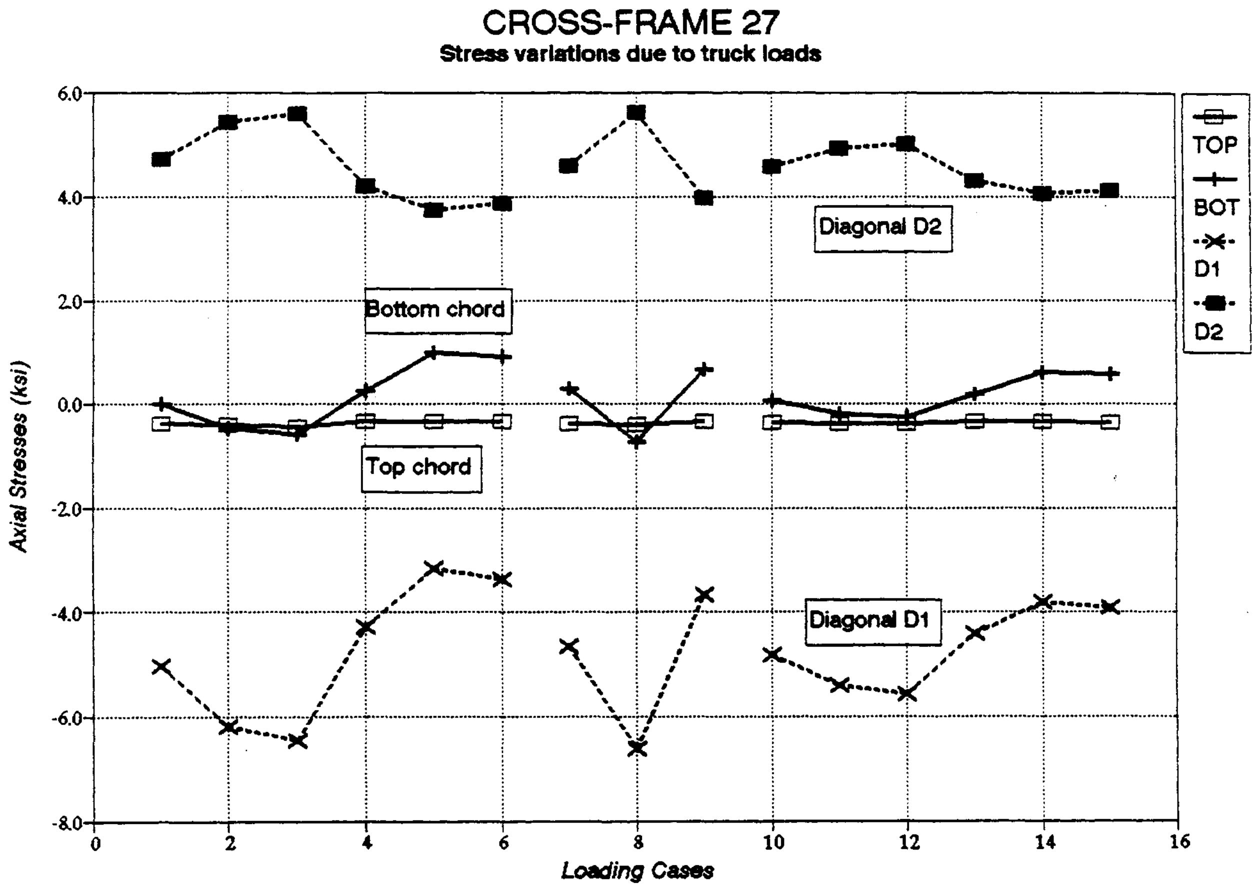

Figure 6.36. Stress variations due to truck loads in crossframe 27

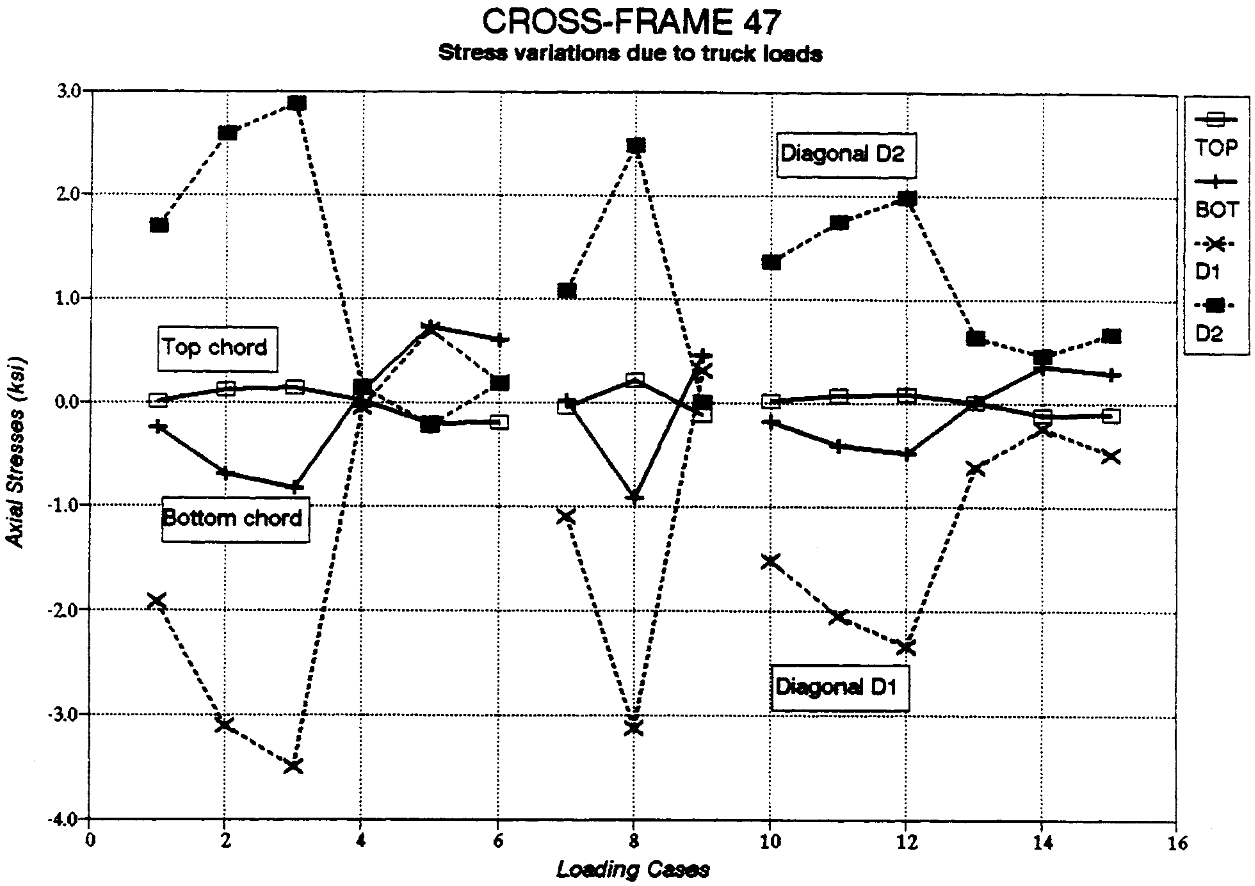

Figure 6.37. Stress Variations due to truck loads in crossframe 47

CHAPTER 7
CONCLUSIONS

This report has outlined: 1) the development of software at the University of Minnesota to analyze steel curved girder bridge systems; 2) the comparison of this program with the third party software, DESCUS-I, used by MN/DOT for these types of analyses; and 3) the comparison of this software with field measurements taken on MN/DOT Bridge No. 27998. Conclusions drawn from this study include:

1. This bridge was shored in the early stages of construction of the steel superstructure, and the bridge design was controlled by stiffness, not strength. Therefore, stresses well below the yield stress occurred throughout construction.

2. Computational results consistently matched well qualitatively and often quantitatively with measured results, both for stresses and deflections. The bridge behavior was predictable at all stages.

3. The primary difference between measured and computed results was due mainly to the erratic effects in the field of warping restraint and weak axis bending on the measured results.

4. The MN/DOT curved girder program, DESCUS-I, compares well to the UM program, which in turn compares well to the field measurements. Consequently, it may be concluded that the DESCUS-I program represents construction and final live load stresses and deflections well, both for the bare steel and the composite bridge system. It should be emphasized that DESCUS-I is geared towards modeling the bridge at just a few specific stages of construction, and that it makes minor modeling assumptions that are often less appropriate than those made in the UM program for permitting detailed modeling of a bridge. However, these assumptions are generally fine for analyses to be used for design, and, while the ability to

make direct comparisons between DESCUS-I and the field measurements is somewhat limited (due to constraints of specifying actual loading, etc. in DESCUS-I), it is felt that stresses obtained from DESCUS-I are representative of what is seen in the field.

5. Fit-up stresses were measured in the crossframes, but they dissipated as construction progressed, and they remained below 6 ksi.

6. There is evidence from the analysis results that the skew supports seem to have little effect on the distribution of stresses in the crossframes of this bridge. The crossframes near the stiffer, outer facia girder consistently have higher stresses from the analyses, regardless of their relation to the skew. However, this data is insufficient to extrapolate this conclusion to other steel curved girder bridges.

7. It is recommended that a minimum of 20 to 30 psf live loading for construction be included in analyses to capture maximum stresses.

8. While not discussed in this report, it may be mentioned that the University of Minnesota curved girder program accurately assesses the stability of curved girder bridge systems during construction: this bridge was shown to have adequate strength and stiffness using second-order inelastic analysis techniques [5].

Future research in this area should include further tests with increased live loading. The two trucks placed on this structure induced only approximately 2 ksi in the measured members. If additional trucks are placed on the structure, more substantial and reliable strain readings may be made, which will provide firmer evidence of the service load behavior of these types of structures. In addition, it may be possible to ascertain whether composite behavior diminishes over time.

REFERENCES

1. American Association of State Highway and Transportation Officials (1989). *Standard Specification for Highway Bridges*, 14th Edition, AASHTO, Washington, DC.
2. Hall, D. H. (1994). "Curved Girders are Special," *Structural Stability Research Council -- Link Between Research and Practice*, Proceedings of the 1994 SSRC 50th Anniversary Conference, 21-22 June 1994, SSRC, Bethlehem, Pennsylvania, pp. 101-117.
3. Fu, C. C. (1992). "DESCUS-I, Design and Analysis of Curved Girder Bridge System," Revision 2, Production Software Inc., Engineering Computer Services, College Park, Maryland.
4. Pulver, B. E. (1996). "Measured Stresses in a Steel Curved Girder Bridge System," M.C.E. Report, Department of Civil Engineering, University of Minnesota, Minneapolis, Minnesota.
5. Huang, W.-H. (1996). "Curved I-Girder Systems," Ph.D. dissertation, Department of Civil Engineering, University of Minnesota, Minneapolis, Minnesota.
6. Stegmann, T. H. and Galambos, T. V. (1976). "Load Factor Design Criteria for Curved Steel Bridges of Open Section," Report No. 43, Department of Civil Engineering, Washington University, St. Louis, Missouri, April.
7. Zureick, A., Naqib, R., and Yadlosky, J. M. (1993). "Curved Steel Bridge Research Project Interim Report I: Synthesis," Report No. FHWA-RD-93-129.
8. Dabrowski, R. (1968). *Curved Thin-Walled Girders,* Springer Verlag, Berlin, 1968 (in German).
9. Heins, C. P. (1975). *Bending and Torsional Design in Structural Members,* Lexington Books, New York.
10. Nakai, H. and Yoo, C. H. (1988). *Analysis and Design of Curved Steel Bridges,* McGraw-Hill, New York.
11. Minnesota Department of Transportation Bridge Division (1994). Documentation of MN/DOT Bridge No. 27998, Minnesota Department of Transportation, St. Paul, Minnesota.
12. Geokon Incorporated (1994). "Instruction Manual: VK-4100/4500 Vibrating Wire Strain Gages," Lebanon, New Hampshire.

13. Mondkar, D. P. and Powell, G. H. (1974). "CURVBRG -- A Computer Program for Analysis of Curved Open Girder Bridges," Internal Report, Division of Structural Engineering and Structural Mechanics, University of California at Berkeley, Berkeley, California, 171 pp.
14. Hambly, E. C. (1976). *Deck Behavior*, Halsted Press, John Wiley & Son, Inc., New York.
15. Lavelle, F.H. and Davidson, M.J. (1970). "Proposed Lateral Flange Bending Method," Department of Civil Engineering, University of Rhode Island, Kingston, Rhode Island, September.
16. Brennan, P.J. (1970). "Analysis of Horizontally Curved Girder Bridges Through Three-Dimensional Mathematical Method and Small-Scale Structural Testing," Research Project HPR 26111, Department of Civil Engineering, Syracuse University, Syracuse, New York, November.
17. Shore, S., Ali, S.A., and Wilson, J.L. (1970). "Preliminary Design of Horizontally Curved Girder Bridges by Equivalent Straight Beams," CURT Report T0170, Towne School Of Civil and Mechanical Engineering, University of Pennsylvania.
18. Bell, L.C. and Heins, C.P. (1968). "The Solution of Curved Bridge Systems Using the Slope-Deflection Fourier Series Method," Department of Civil Engineering, University of Maryland, College Park, Maryland, June.
19. Vlasov, V.Z. (1961). "Thin-Walled Elastic Beams," Second Edition, National Science Foundation, Washington, D.C..
20. McManus, P.F., Nasir, G.A., and Culver, C.G. (1969). "Horizontally Curved Girders - State of the Art," *Journal of the Structural Division*, ASCE, Vol. 95, No. ST5, May.
21. Dabrowski, R. (1964). "Zur Berechnung von Gekrummten dunnvandigen Tragern mit offenem Profil," *Der Stahlbau*, Vol. 33, No. 12, December.
22. United States Steel (1965). "Highway Structures Design Handbook, Volume I," Pittsburgh, Pennsylvania.
23. Kuo, J.T.C. and Heins, C.P. (1970). "Torsional Properties of Composite Steel Bridge Members," Report No. 37, Department of Civil Engineering, University of Maryland, College Park, Maryland, June.

24. Kuo, J.T.C. and Heins, C.P. (1971). "Behavior of Composite Beams Subjected to Torsion," Report No. 39, Civil Engineering Department, University of Maryland, College Park, Maryland, February.

APPENDIX A

STRESSES DUE TO CONSTRUCTION

APPENDIX A

STRESSES DUE TO CONSTRUCTION

This appendix presents the stresses due to construction of MN/DOT Bridge No. 27998, excluding the stresses produced during pouring of the concrete deck, which are reported in the following appendix.

OBSERVATIONS OF GIRDER STRESSES

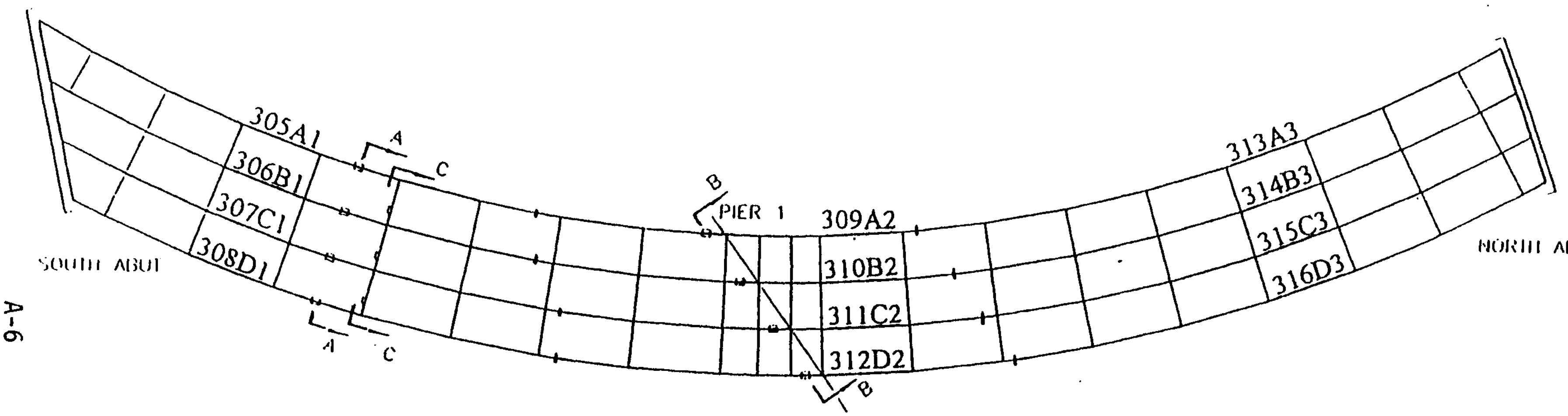

Figure A-1. Plan view of the girders displaying the girder nomenclature

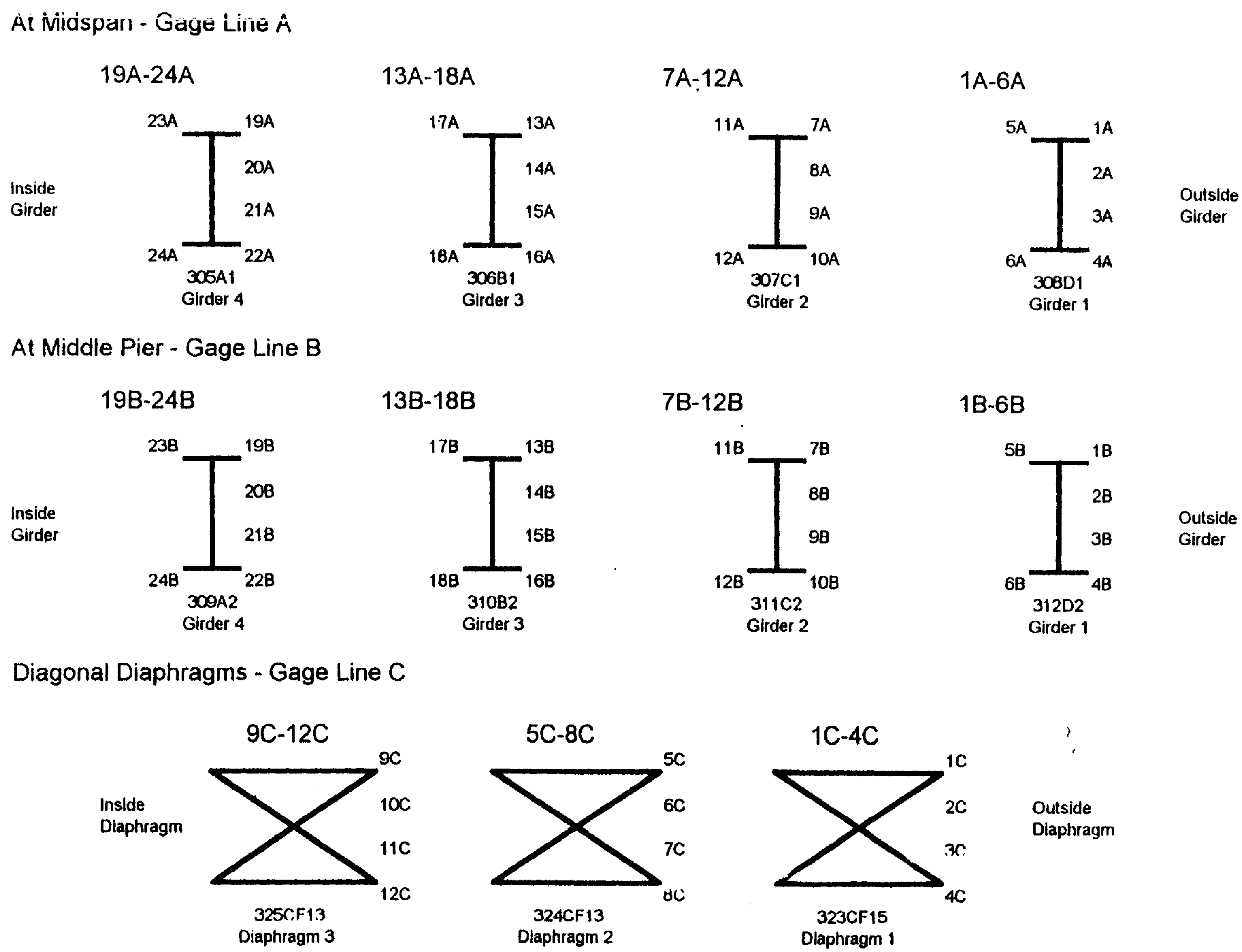

Figure A-2. Nomenclature used to describe gage locations, girders, and diaphragms.

Date and Time of Reading: July 19, 1995 at 11:00 p.m.

Temperature: 30 °C

Weather: Partly Cloudy

Loading Condition: The eight girders of span one, which runs from the southern abutment to the middle pier, were in place when this readings was taken. The diagonal diaphragms were in place and held with three to four bolts. The splices between the girders were fully tightened. Shoring towers were present at approximately the midspan of span one to enhance the stability of the girders until the diaphragms could be fully tightened and the remaining girders could be placed.

Objective of Reading: This reading was taken to determine the stresses present with only the first span in place. These observations are for the actual magnitudes of the stresses present.

General Observations: There does not appear to be a consistent pattern in the stresses for this stage. In some cases, a given flange registers a tensile stress present at one flange tip, and a compressive stress at the other flange tip. These erratic stresses could result from complex conditions present while the readings were taken. The shoring towers were put into place before the diaphragms were completely aligned. These towers were probably not perfectly level, so when they were tightened up to the bottom flange of the girder the alignment of the girder might have been affected, thus distorting the strain readings somewhat. Also when the diaphragms were placed, they were initially attached with three or four bolts, depending the accuracy of the alignment. If the alignment between the diaphragm bolt holes and the girder bolt holes was poor, then sometimes the bolts had to be hammered into place to create the proper alignment for the correct fit-up between the individual members of the structure. This procedure could have induced small, unpredictable stresses in the girders and diaphragms.

Notes on Specific Gages: Gage 11B was damaged during the placement of the girder.

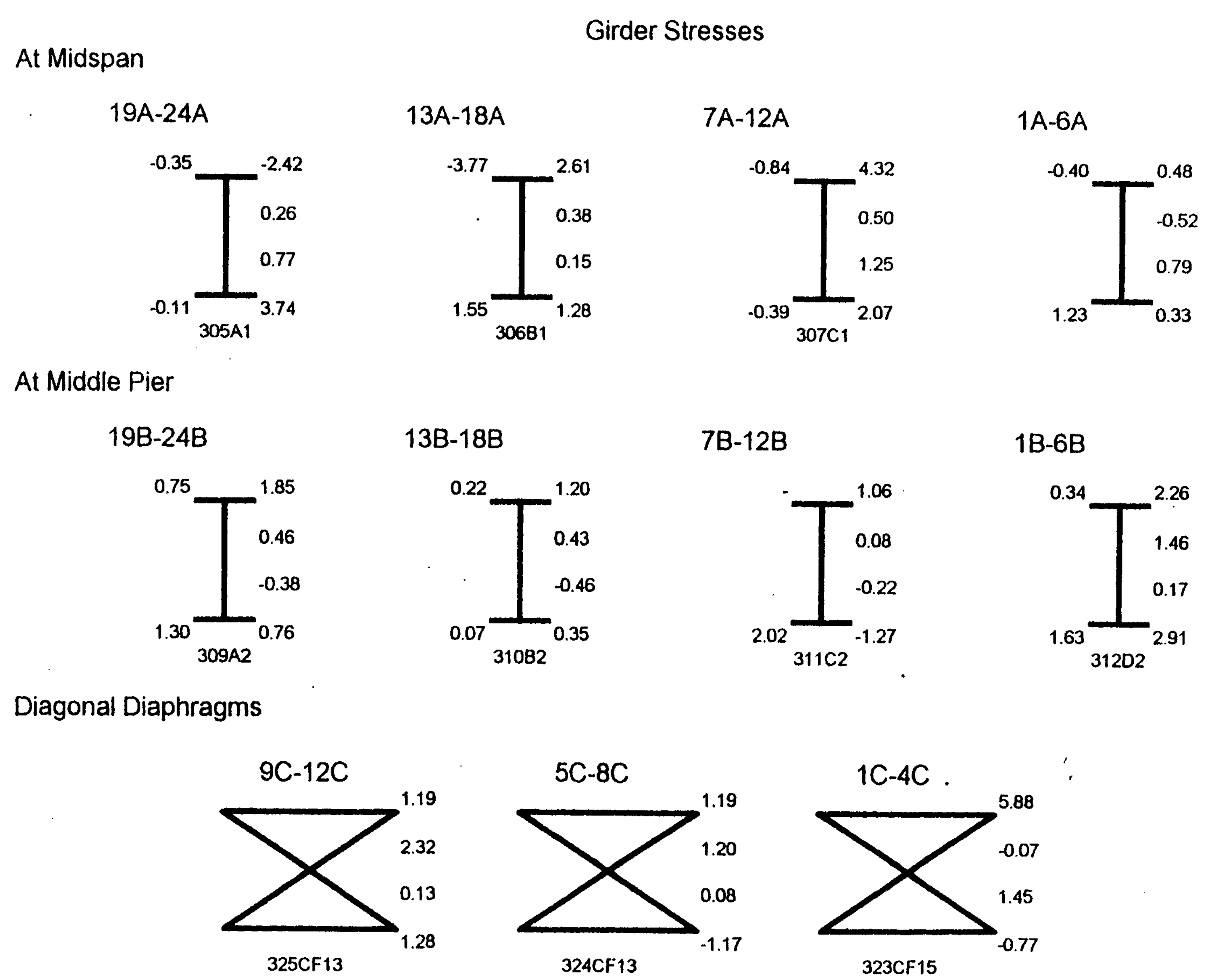

Figure A-3. Magnitude of girder stresses after erection of span 1

Date and Time of Reading: July 24, 1995 at 4:00 a.m.

Temperature: 21 °C

Weather: Clear

Loading Condition: Girder 315C3, the second from the outside facia girder, was being erected on the north span. This girder was held by the crane while the splice was tightened to girder 311D2. The outside facia girder, 316D3, was already in place, and the splice was fully tightened. The all of the diagonal diaphragms and end diaphragms in the south span were in place, and all of the bolts for all of the diaphragms were in place but not fully tightened.

Objective of Reading: This reading was taken to determine the stresses present during the erection of a girder. These observations describe the changes in the stress due to the given loading stage.

General Observations: Aside for the top inside flange tip of girders 1 and 4 and the top two flange tips of girder 3, compressive stresses were experienced by the girders at the midspan gages. At the middle pier, the girder 4 stresses demonstrated equivalent behavior to that of the stresses of girder 4 at the midspan. Girder 3 experienced compressive stress except for the outside bottom flange tip which experienced a minimal tensile stress. Girder 2 experienced compression in the bottom flange and minimal stresses in the top flange. This being the girder to which girder 315C3 is being spliced, this behavior is fairly reasonable. Aside for the inside top flange tip, girder 1 is reacting as expected. The bottom flange experienced an increase in compression, and the top flange experienced an increase in tension. This is behavior typical of a girder over a middle pier support, i.e. in a negative moment region. In regards to the other girders, the correlation of their behavior is not obvious. The same can be stated for the behavior of the diaphragms. The erection of the girders in span 2 was difficult because of the small tolerance between the girders being hoisted into place, the splice of the girders already in place, and the north abutment support. During the maneuvering of the girder into alignment with the splice, the crane could be forcing the girder back against the erected portion of the structure, and this could be a possible explanation for the compressive stresses observed. At the midspan, the range of stresses were -0.34 to -4.40 ksi (compression) and 0.11 to 1.76 ksi (tension). The largest change in compressive stress occurred at gage 22A, and the largest change in tensile stress occurred at gage 17A. At the middle pier, the ranges were -0.16 to -8.76 ksi and 0.06 to 5.64 ksi. The greatest change in stress occurred at gage 4B for compression and gage 1B for tension. The range of stress for the diaphragms was -0.44 to -3.74 ksi (largest at gage 1C) and 0.36 to 2.11 ksi (largest at gage 3C).

Notes on Specific Gages: Not applicable

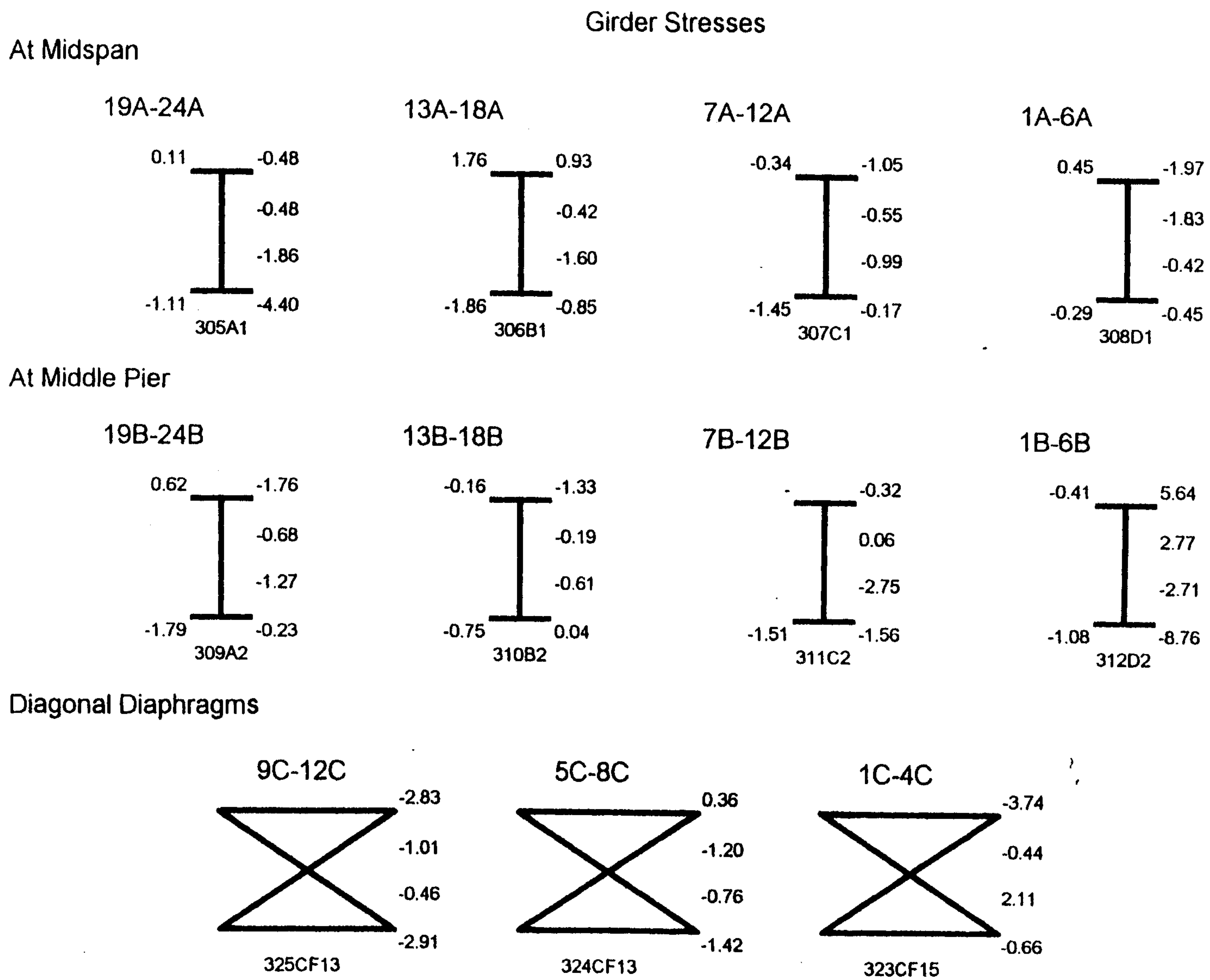

Figure A-4. Change in girder stresses between the erection of span 1 and the erection of half of span 2

Date and Time of Reading: July 24, 1995 at 4:00 a.m.

Temperature: 21 °C

Weather: Clear

Loading Condition: Girder 315C3, the second from the outside facia girder, was being erected on the north span. This girder was held by the crane while the splice was tightened to girder 311D2. The outside facia girder, 316D3, was already in place, and the splice was fully tightened. The all of the diagonal diaphragms and end diaphragms in the south span were in place, and all of the bolts for all of the diaphragms were in place but not fully tightened.

Objective of Reading: This reading was taken to determine the stresses present during the erection of a girder. These observations are for the actual magnitudes of the stresses present.

General Observations: For the observed stresses, there is no obvious correlation to the given loading stage. The readings for the gages at the middle pier for girder 1 were consistent with the behavior of a girder supported by a middle pier with two end supports under self weight. Warping across the flanges can also be observed, although it is of a greater stress range than was predicted by the computer analysis. The largest tensile stress observed at the middle pier was 7.90 ksi (at gage 1B), and the largest compressive stress was -5.86 ksi, at gage 4B. The largest tensile stress observed at the midspan was 3.27 ksi, at gage 7A, and the largest compressive stress was -2.91 ksi, at gage 19A. In the diaphragms, the largest tensile stress was 2.13 ksi, at gage 1C, and the largest compressive stress was -2.59 ksi, at gage 8C.

Notes on Specific Gages: Not applicable

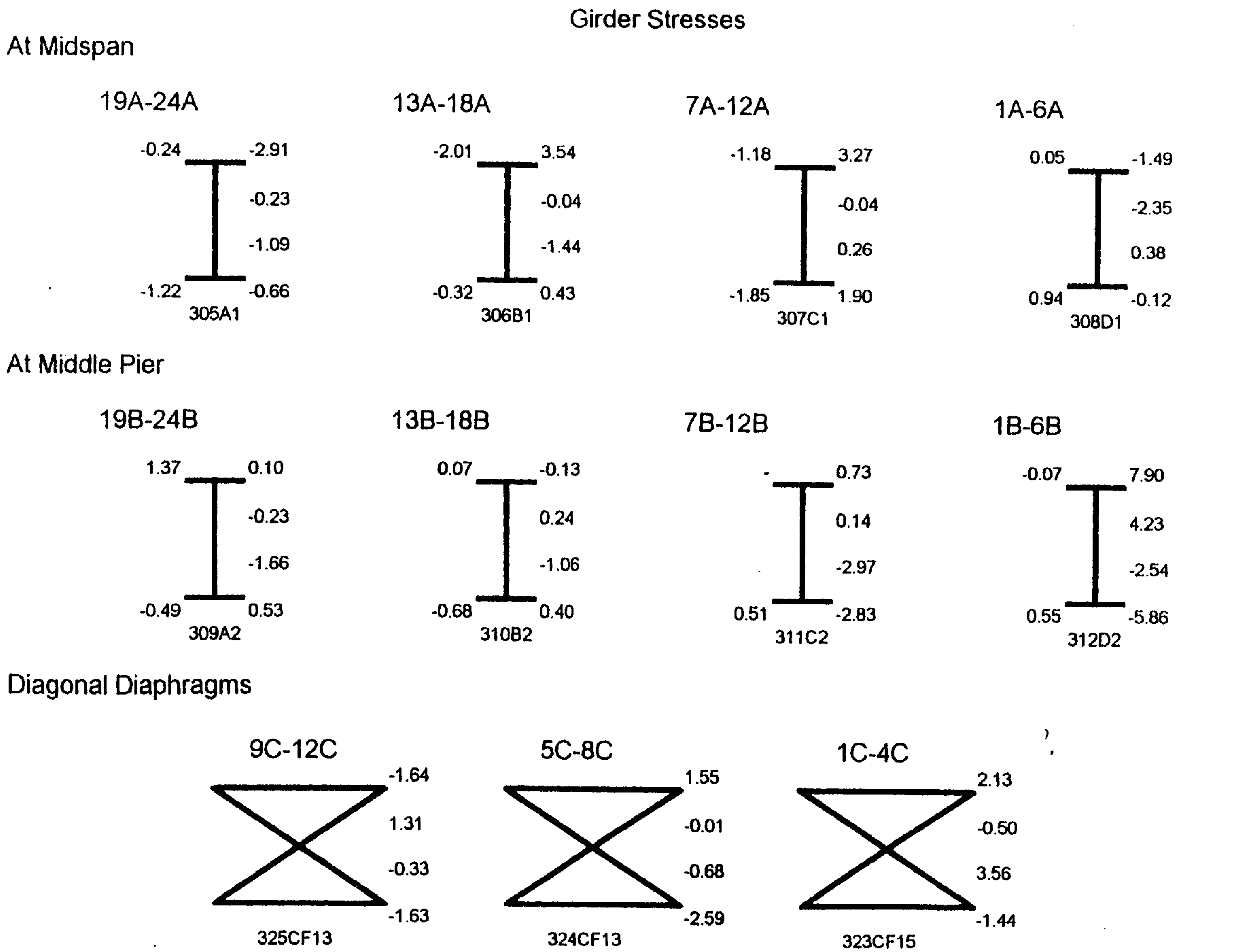

Figure A-5. Magnitude of girder stresses after the erection of half of span 2

Date and Time of Reading: July 26, 1995 at 11:00 p.m.

Temperature: 25 °C

Weather: Clear

Loading Condition: All of the girders were in place. The splices were fully tightened for all of the girders, and the diagonal diaphragms for span two were held in place with three to four bolts. In some cases the diaphragms were slightly skewed. These alignment problems were present in both spans, and this problem was remedied once all of the bolts were placed. Shoring towers were present at the approximate midspan of span two for all of the girders. The towers were used to increase the stability of the girders during the erection process. The bolts for all of the diagonals for span 1 had already been placed, and the whole structure will be "rattled up" after all of the bolts for span 2 are placed.

Objective of Reading: This reading was taken to determine the stresses with all of the girders in place before all of the diagonal diaphragms were fully tightened. These observations describe the changes in the stress due to the given loading stage.

General Observations: At the midspan, the bottom flanges experienced tensile stresses of ~ 1 to 2 ksi (with 2.11 ksi being the greatest magnitude), and the top flanges (except for the outside tip of girder 4) experienced compressive stresses of ~ 0.6 to 4 ksi (-3.98 ksi being the greatest magnitude). This behavior is expected in a positive moment region with the present loading being the self weight of the girders. At the middle pier, girders 2,3, and 4 behaved (except for a few gages) as would be expected for the girders in a negative moment region. This is an increase in tension for the top flanges and compression for the bottom flanges. Girder 1 displayed the opposite behavior for the middle and outside flange locations for both the top and bottom flanges. The range of stresses at the middle pier were 0.83 to 3.25 ksi and -0.35 to -2.27 ksi. At the middle pier, the largest increase in tensile stress, 5.00 ksi, occurred at the outside bottom flange tip of girder 1, and the largest increase in compressive stress, -2.27 ksi, occurred at gage 15B. Except for gage 12C, the top two members of the diaphragms experienced tension, ranging from 0.31 to 3.14 ksi, while the bottom two members experienced compression ranging from -0.13 to -2.12 ksi.

Notes on Specific Gages: Not Applicable

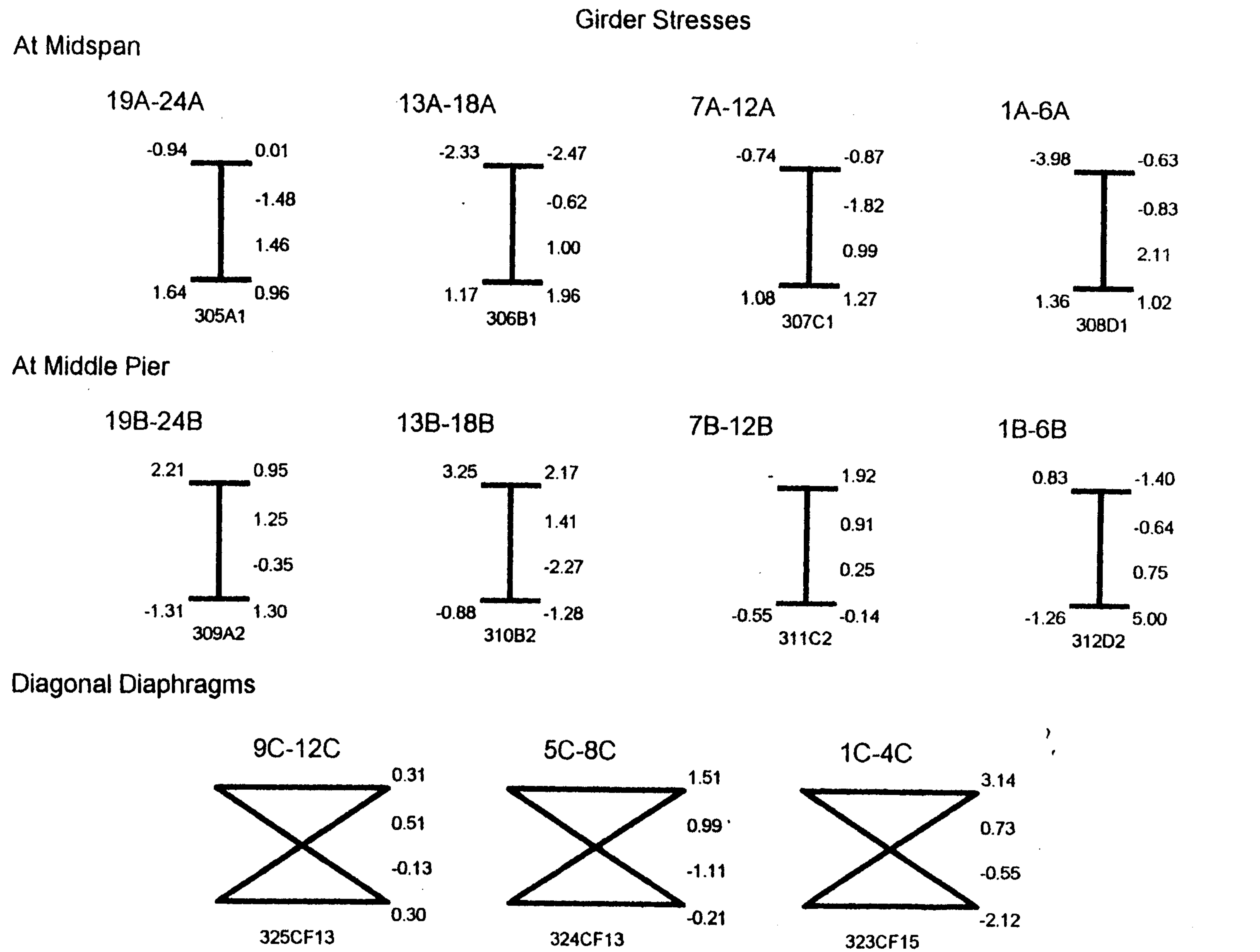

Figure A-6. Change in girder stresses between erection of half of span 2 and all of the girder and diaphragms in place with bolts loose

Date and Time of Reading: July 26, 1995 at 11:00 p.m.

Temperature: 25 °C

Weather: Clear

Loading Condition: All of the girders were in place. The splices were fully tightened for all of the girders, and the diagonal diaphragms for span two were held in place with three to four bolts. In some cases the diaphragms were slightly skewed. These alignment problems were present in both spans, and this problem was remedied once all of the bolts were placed. Shoring towers were present at the approximate midspan of span two for all of the girders. The towers were used to increase the stability of the girders during the erection process. The bolts for all of the diagonals for span 1 had already been placed, and the whole structure will be "rattled up" after all of the bolts for span 2 are placed.

Objective of Reading: This reading was taken to determine the stresses with all of the girders in place before all of the diagonal diaphragms were fully tightened. These observations are for the actual magnitudes of the stresses present.

General Observations: At the midspan except for gages 12A and 15A, the bottom flanges experience tensile stresses. The magnitude of these stresses ranges from 0.30 to 3.17 ksi. The top flanges (except for gages 7A and 13A) experienced compressive stresses. Warping can be observed across the top flanges of girders 1,2, and 3. Warping occurs because of the curvature of the girders. The curvature causes, the magnitude of the stress at the right flange tip to decrease across the width of the flange to a lessor value at the left flange tip. The range of compressive stresses is -0.66 to -4.34 ksi with the greatest value occurring at gage 17A. At the middle pier, the top flanges are in tension, as expected, ranging from 0.76 to 6.50 ksi. The largest magnitude of stress occurred at gage 1B. Except for gage 22B, the bottom flanges are in compression, as expected, ranging from -0.04 to -3.34 ksi. The largest magnitude of stress occurred at the gage 15B. There was not an observable pattern to the stresses present in the diaphragms. The largest tensile stress was 5.28 ksi at gage 1C and the largest compressive stress was -3.56 ksi at gage 4C.

Notes on Specific Gages: Not Applicable

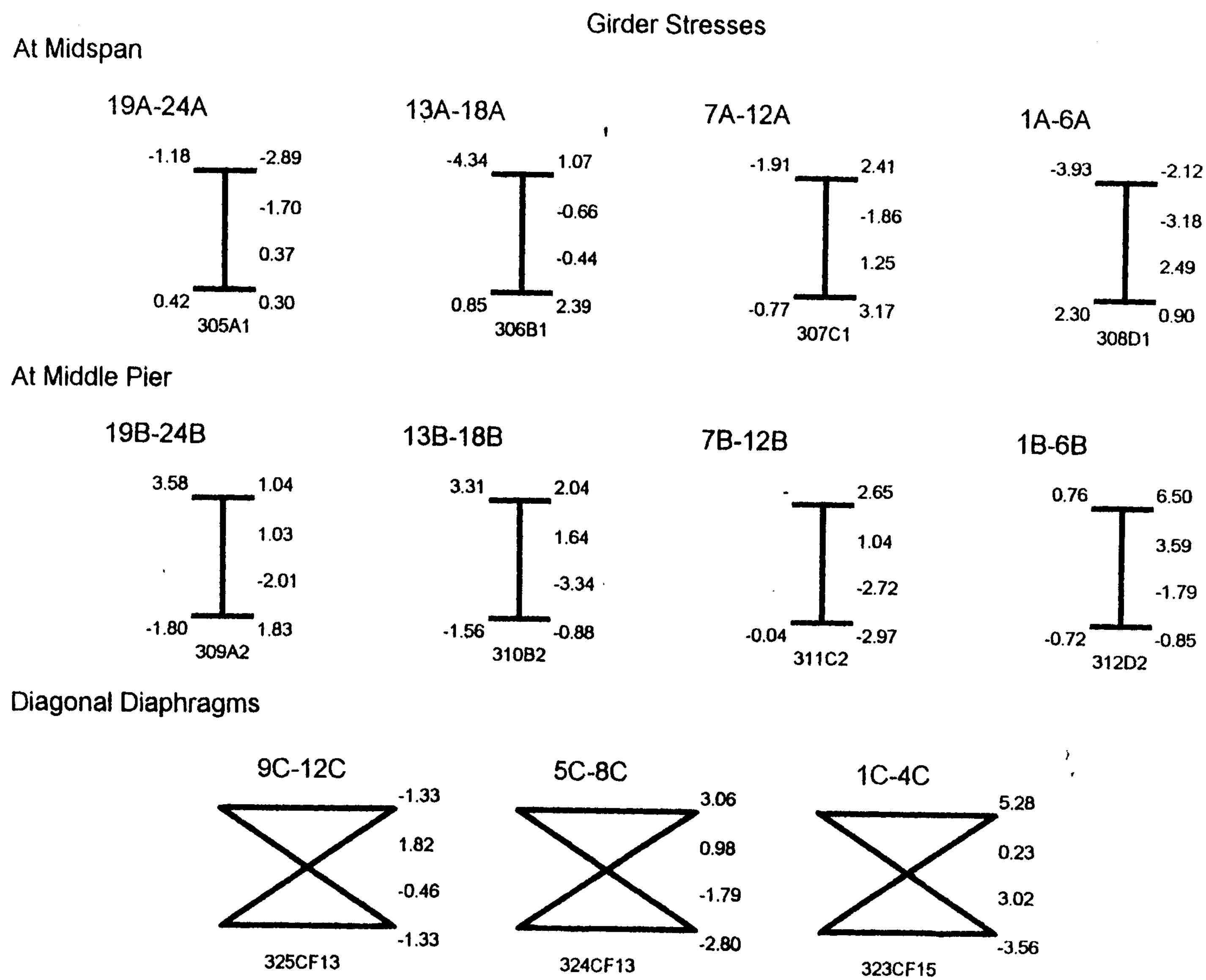

Figure A-7 Magnitude of girder stresses after all of the girders and diaphragms were in place with the bolts loose

Date and Time of Reading: July 28, 1995 at 11:00 p.m.

Temperature: 24 °C

Weather: Clear

Loading Condition: All of the girders were in place. All of the diaphragms, end and diagonal, were in place and fully tightened.

Objective of Reading: This reading was taken to determine the stresses that occur after the diagonals were placed and the bolts fully tightened. These observations describe the changes in the stress due to the given loading stage.

General Observations: At the midspan, it is observed that the bottom flanges experienced compressive stress, ranging from -0.01 to -0.47 ksi, while the top flanges (except for the top outside flange tip of girder 4) experienced tensile stress ranging from 0.04 to 1.15 ksi. This could be a result from the tightening of the diaphragms. The same behavior, tension in the top flanges and compression in the bottom flanges, was observed in the gages at the middle pier. Regarding the diaphragms, the top two members of diaphragms experienced compressive stress (-0.12 to -0.87 ksi) and the bottom two members experienced tensile stress (0.14 to 0.52 ksi).

Notes on Specific Gages: Not Applicable

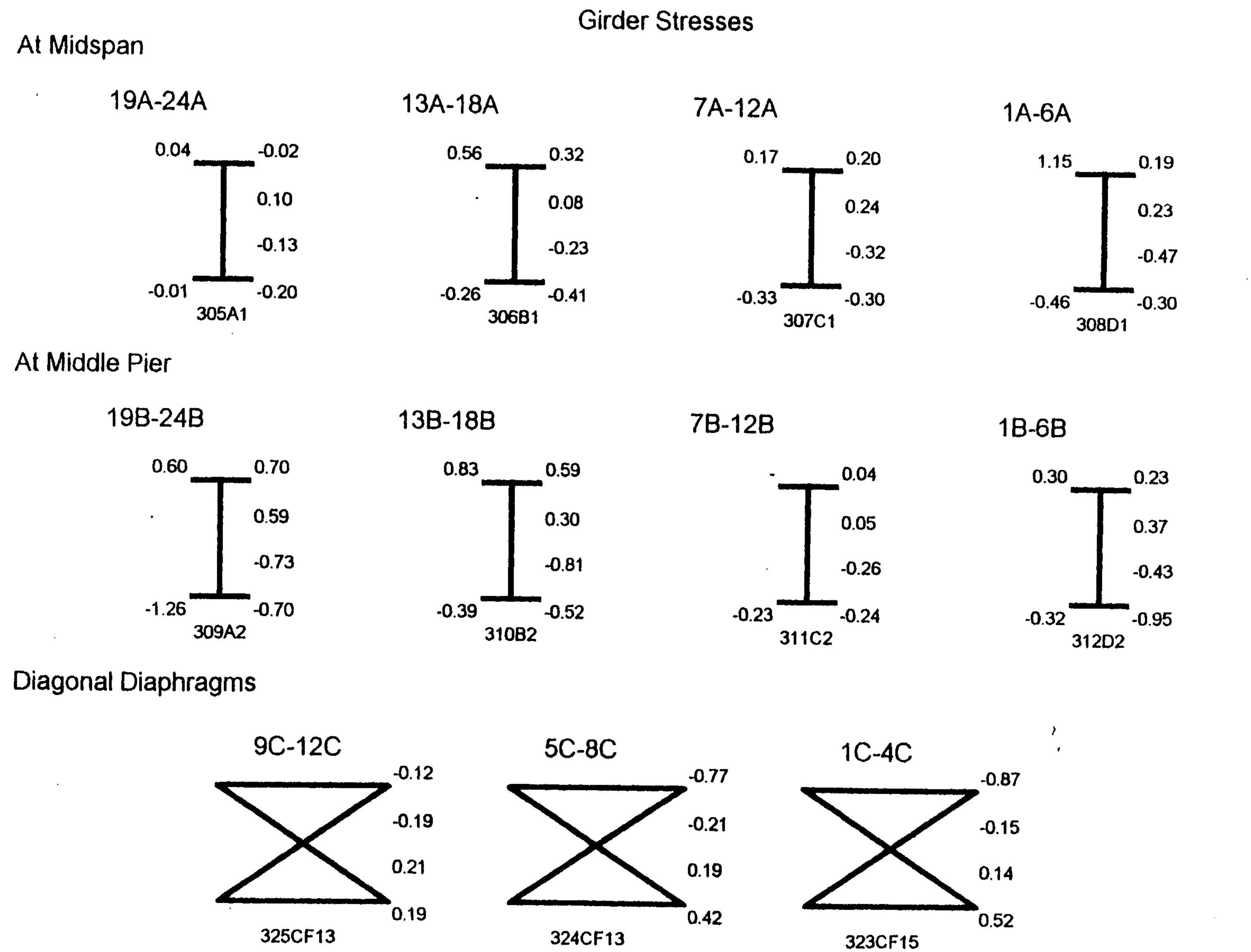

Figure A-8. Change in girder stresses between the erection of all of the girders and diaphragms with the bolts loose and after the structure was "rattled up"

Date and Time of Reading: July 28, 1995 at 11:00 p.m.

Temperature: 24 °C

Weather: Clear

Loading Condition: All of the girders were in place. All of the diaphragms, end and diagonal, were in place and fully tightened.

Objective of Reading: This reading was taken to determine the stresses after all diaphragms were placed and the bolts fully tightened. These observations are for the actual magnitudes of the stresses present.

General Observations: The process of putting all of the diagonals into place and fully tightening the bolts is called "rattling up" the bridge. This process involves, in many cases, hammering the bolts into place to properly align the diagonals. This might introduce residual stresses into the members. After each night of erection during the following day, the remaining bolts for the diaphragms erected were placed. After the all of the bolts were in place, the bolts for the entire structure were tightened and considered "rattled up". The shoring towers were removed, and the structure was then ready for the placement of the formwork. Except for gages 7A and 13A, the top flanges at the midspan experienced compressive stress as expected. Except for gages 12A and 15A, the bottom flanges at the midspan experienced tensile stress as expected. At the middle pier, the girders experienced tensile stress in the top flanges and compressive stress in the bottom flanges. This behavior is consistent for girders in a negative moment region. The top member and top diagonal, except for gage 9C, indicated that the change in stress was compressive, and the bottom two members, except for gage 3C, indicated the presence of a tensile force. At the midspan gages, the greatest compressive stress was -3.78 ksi (at gage 17A), and the greatest tensile stress was 2.87 ksi (at gage 10A). At the middle pier gages, the greatest compressive stress was -4.15 ksi (at gage 15B), and the greatest tensile stress was 6.74 ksi (at gage 1B). The greatest compressive and tensile stresses in the diaphragms were -3.04 ksi at gage 4C and 4.41 ksi at age 1C respectively.

Notes on Specific Gages: Not Applicable

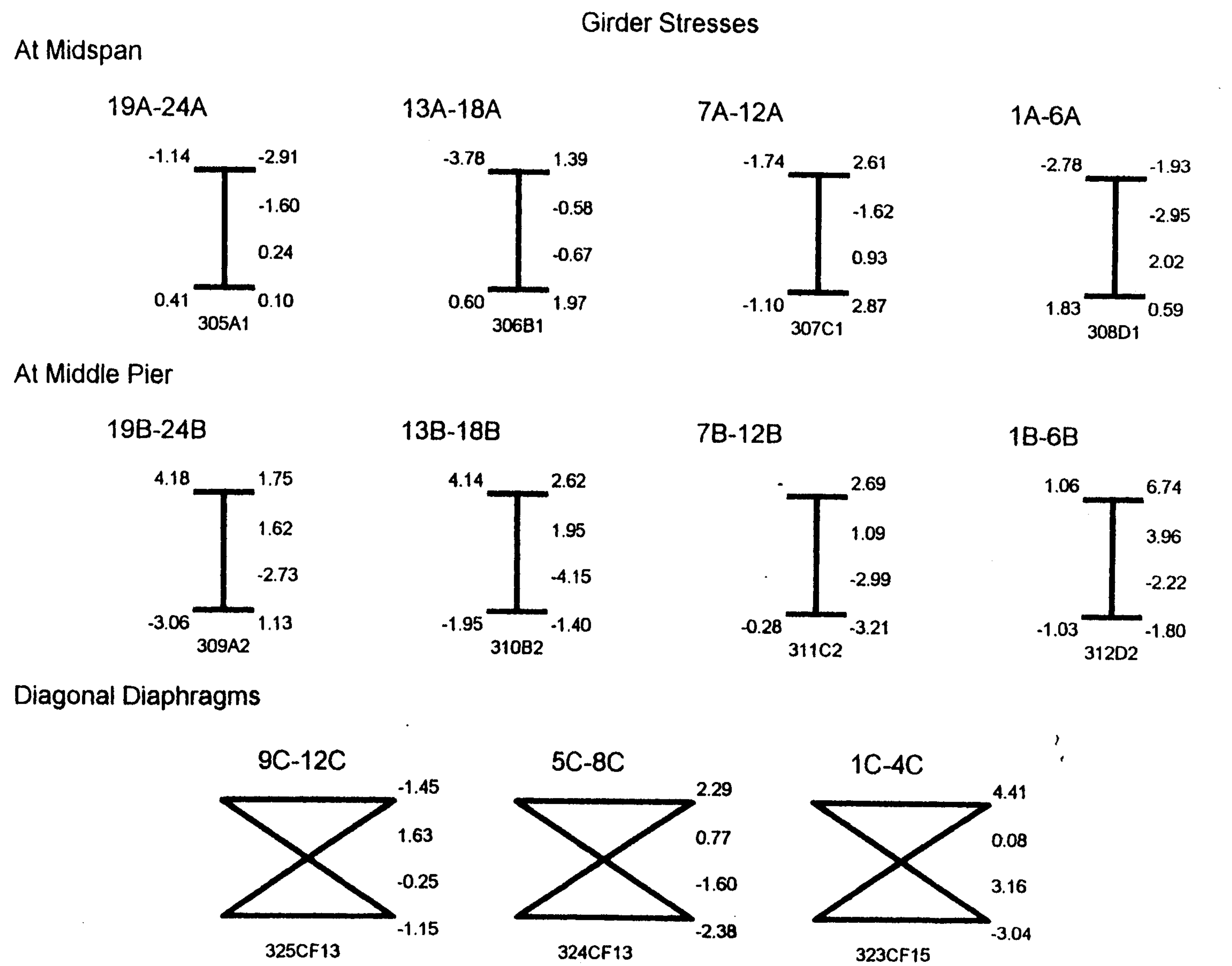

Figure A-9. Magnitude of girder stresses after all of the girders and diaphragms were erected and the structure was "rattled up"

Date and Time of Reading: August 7, 1995 at 7:00 a.m.

Temperature: 20 °C

Weather: Partly Cloudy

Loading Condition: The placement of the formwork was complete. All of the generators were removed from the deck. The shear connectors were attached.

Objective of Reading: This reading was taken to determine the stresses present with all of the formwork completed and the shear connectors present. These observations describe the changes in the stress due to the given loading stage.

General Observations: At the midspan gages, the top flanges for girders 2 and 4 experienced compression (-0.37 to -1.84 ksi) as expected, but the bottom flanges (except for gages 16A and 24A) also experienced compressive stress. This is not behavior consistent with girders in the positive moment region. Girders 1 and 3 experienced a minimal stress change at the flange tips (0.02, 0.00, 0.02, and -0.08 ksi) The stresses for the gages located on the webs (intended to predict the stresses at the middle of the flange) ranges from -0.17 to -0.50 ksi. For the gages on girders 1 and 4 this stress could be occurring because of the cantilevered support for the formwork outside of the girders. These supports transfer some portion of the load directly to the lower portion of the web. This maybe an explanation for the compressive stresses observed. The bottom flanges at the middle pier experienced compression (-0.44 to -0.85 ksi) as expected. The top flanges experienced both tension and compression (except for girder 4 which is in tension as expected) which does not seem to be explainable. The only change in stress greater than 1 ksi occurred at gage 23B, the inside top flange tip, with a magnitude of 3.08 ksi. The members of the diaphragms responded in a similar manner which was tension for the top members and compression for the bottom three members. The stress ranges for each of the bottom three members are similar. Starting with the top diagonal and proceeding to the bottom horizontal the ranges are as follows: -0.03 to -0.08, -0.22 to -0.33, and -0.80 to -0.87 ksi. This pattern of compression in the lower members once again could relate to the cantilevered formwork supports.

Notes on Specific Gages: During the placement of the formwork, gage 1A was damaged. This gage along with gage 11B was repaired, and the following readings are relative readings compared to the state of stress recorded after the gages were attached. Note the gray shading for the stress readings of these gages. Gage 17B and 12C did not register when the reading was taken.

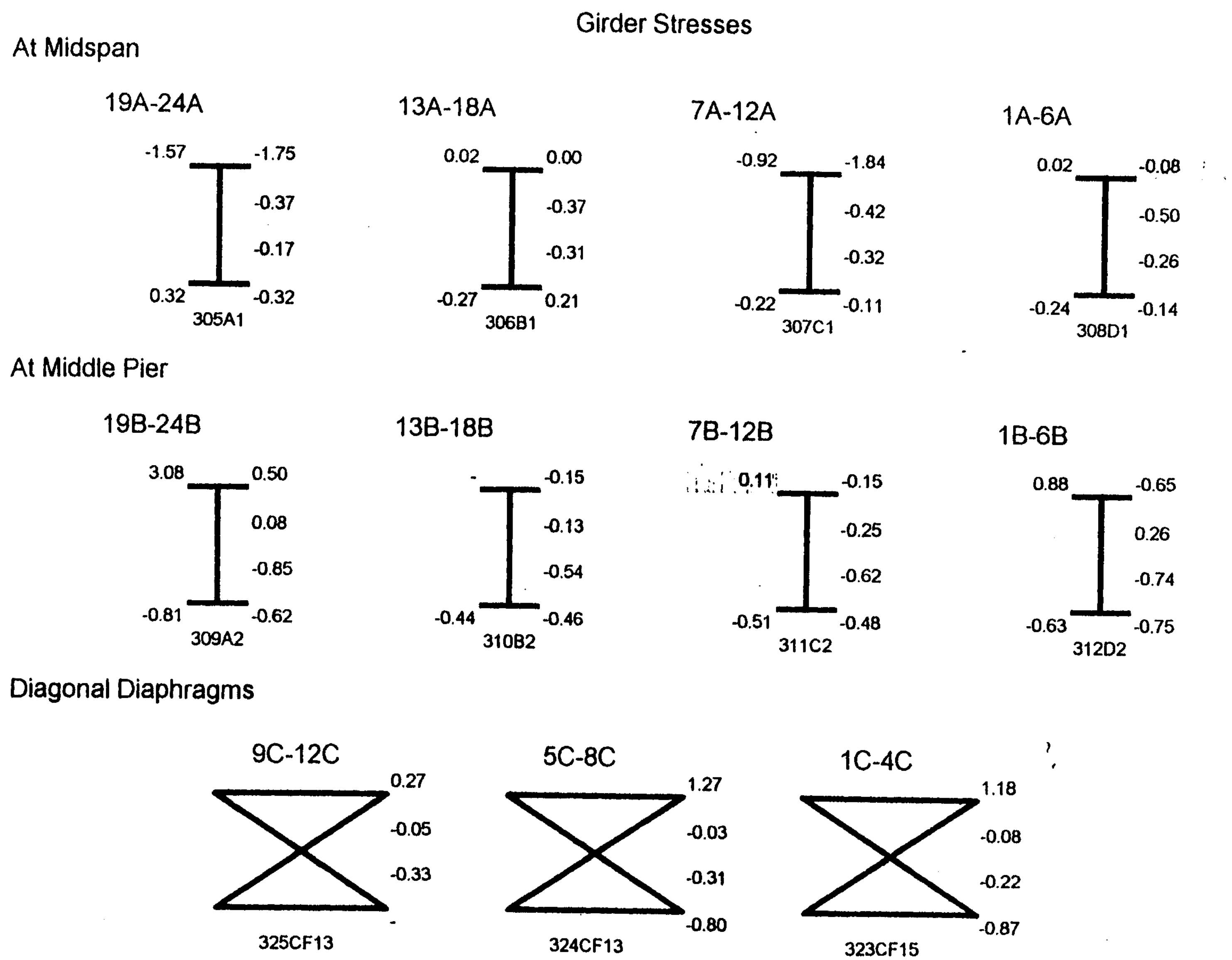

Figure A-10. Change in girder stresses between the "rattled up" structure and after the placement of the formwork

Date and Time of Reading: August 7, 1995 at 7:00 a.m.

Temperature: 20 °C

Weather: Partly Cloudy

Loading Condition: The placement of the formwork was complete. All of the generators were removed from the deck. The shear connectors were attached.

Objective of Reading: This reading was taken to determine the stresses present with all of the formwork completed and the shear connectors present. These observations are for the actual magnitudes of the stresses present.

General Observations: At the midspan, the compressive stress ranged from -0.08 to -4.66 ksi with the greatest value occurring at gage 19A.. The range of tensile stress was 0.07 to 2.76 ksi, and the largest stress occurred at gage 3A. At the middle pier, the range of compressive stress was -0.79 to -4.69 ksi, with the largest stress being located at 15B, and the range of tensile stress was 0.11 to 7.26 ksi, with the largest stress being located at gage 23B. The largest tensile stress in the diaphragms was 5.59 ksi at gage 1C, and the range of stress was 0.74 to 5.59 ksi. The largest compressive stress was -3.90 ksi at gage 4C with the range of stress being -0.01 to -3.90 ksi.

Notes on Specific Gages: During the placement of the formwork, gage 1A was damaged. This gage along with gage 11B was repaired, and the following readings are relative readings compared to the state of stress recorded after the gages were attached. Note the gray shading for the stress readings of these gages. Gage 17B and 12C did not register when the reading was taken.

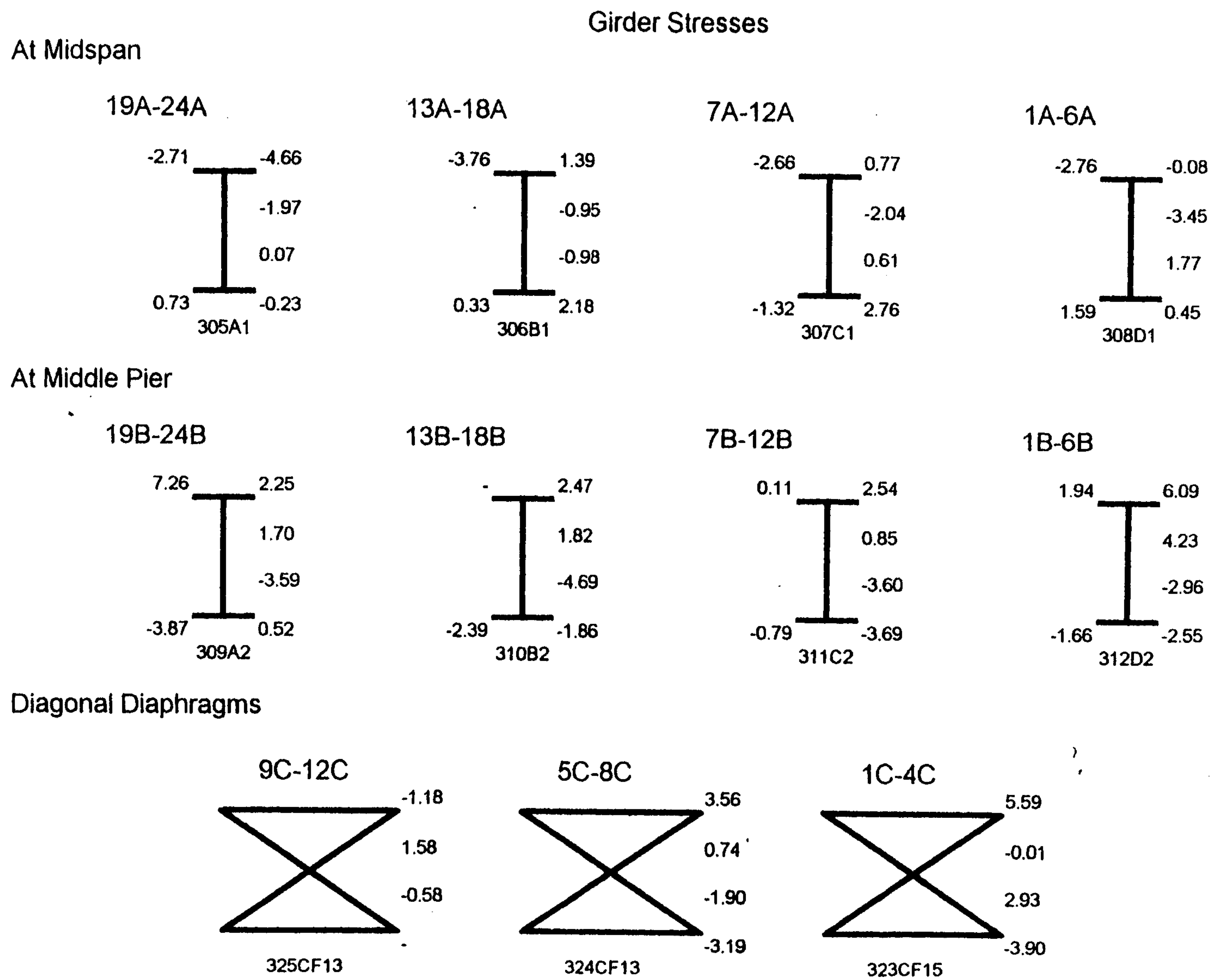

Figure A-11. Magnitude in girder stresses after the placement of the formwork

Date and Time of Reading: August 11, 1995 at 3:30 a.m.

Temperature: 20 °C

Weather: Overcast

Loading Condition: The loading for this set of readings consists of the self weight of the girders, the weight of the formwork, and the weight of all the reinforcement for the concrete bridge deck. This was the state of the bridge before the pouring of the concrete deck began.

Objective of Reading: This reading was taken to determine the stresses present with all of the deck reinforcement in place before the concrete deck was poured. These observations describe the changes in the stress due to the given loading stage.

General Observations: At the midspan, the bottom flanges experienced tension (0.11 to 0.55 ksi) as is expected in the positive moment region. The top flanges experienced both compressive and tensile stresses which does not have an obvious explanation. Except for girder 1, the change in stresses for these top flanges are minimal (ranging from -0.09 to 0.29 ksi), so these values are fairly insignificant. The top flanges at the middle pier experienced tension as expected ranging from 0.35 to 0.65 ksi. The bottom flanges experienced both compression and tension (-0.02 to -0.11 and 0.02 to 0.20 ksi). Except for gage 5C, all of the members of the diagonals experienced tensile stresses ranging from 0.01 to 0.63 ksi.

Notes on Specific Gages: Gage 12C and 17B did not register during this reading.

Date and Time of Reading: August 11, 1995 at 3:30 a.m.

Temperature: 20 °C

Weather: Overcast

Loading Condition: The loading for this set of readings consists of the self weight of the girders, the weight of the formwork, and the weight of all the reinforcement for the concrete bridge deck. This was the state of the bridge before the pouring of the concrete deck began.

Objective of Reading: This reading was taken to determine the stresses present with all of the deck reinforcement in place before the concrete deck was poured. These observations are for the actual magnitudes of the stresses present.

General Observations: At the midspan, the stress in the bottom flange gages increased in tension as expected with the additional dead load from the reinforcement. The top flange gages did not respond uniformly though. Approximately half of the gages showed an increase in compression as expected, but the remaining gages indicated a decrease. The range of compressive stress is -0.62 to -4.36 ksi (the largest value at gage 19A), and the range of tensile stress is 0.25 to 3.18 ksi (the largest value at gage 16A). At the middle pier, the top flanges increased in tensile stress, and a majority of the bottom flanges increased in compressive stress. The ranges of compressive and tensile stresses are -0.67 to -4.78 ksi and 0.67 to 7.75 ksi respectively. The largest stresses occurred at 15B (compression) and 23B (tension). Except for gage 5C the diaphragm members indicated an increase in tensile stress. The stress ranges for the diaphragms are as follows: -0.31 to -3.68 ksi and 0.22 to 5.60 ksi. Once again the largest stresses occur at 1C and 4C with the top member experiencing tension and the bottom horizontal experiencing compression.

Notes on Specific Gages: Gage 12C did not register during this reading.

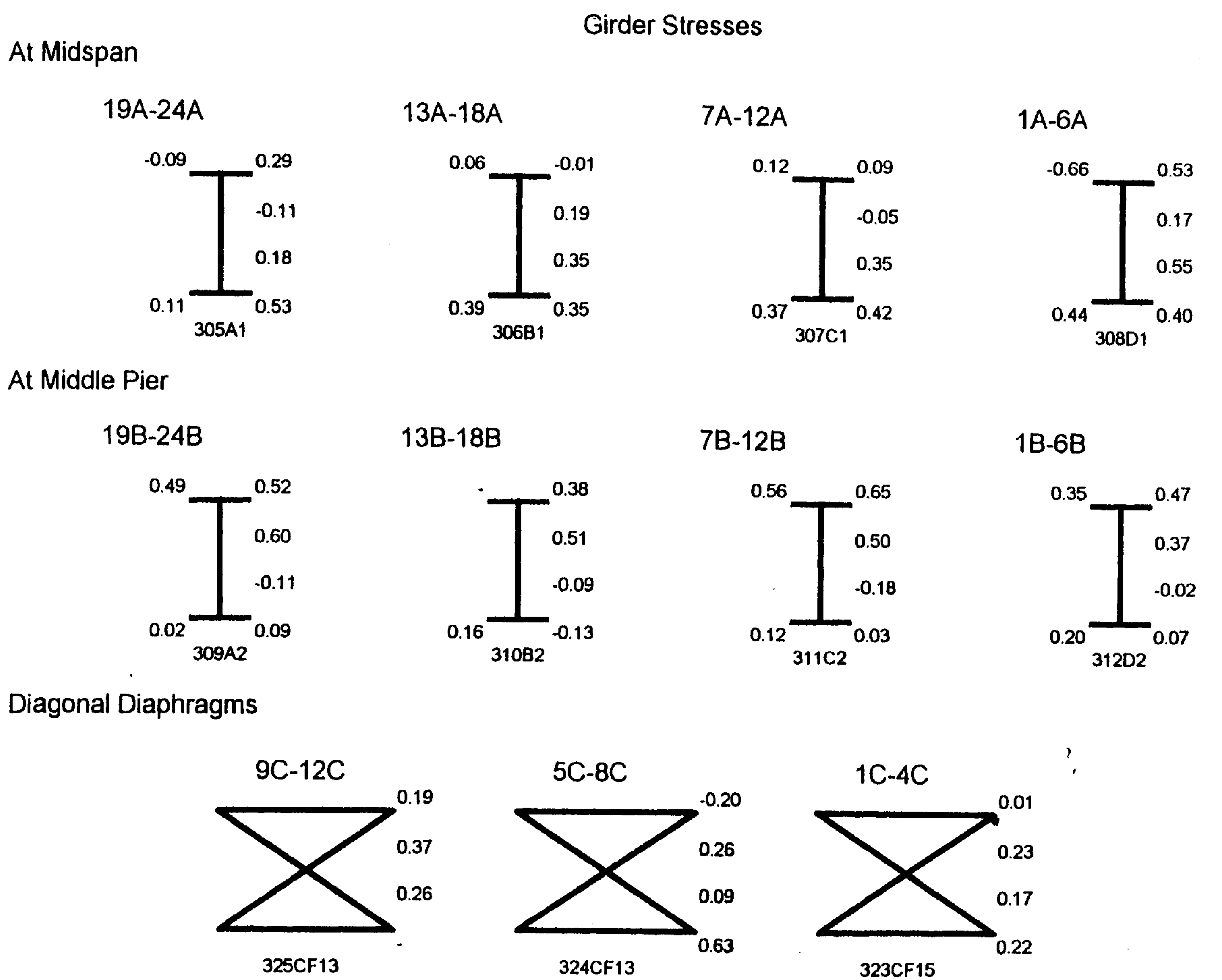

Figure A-12. Change in girder stresses between the placement of the formwork and the placement of the reinforcement

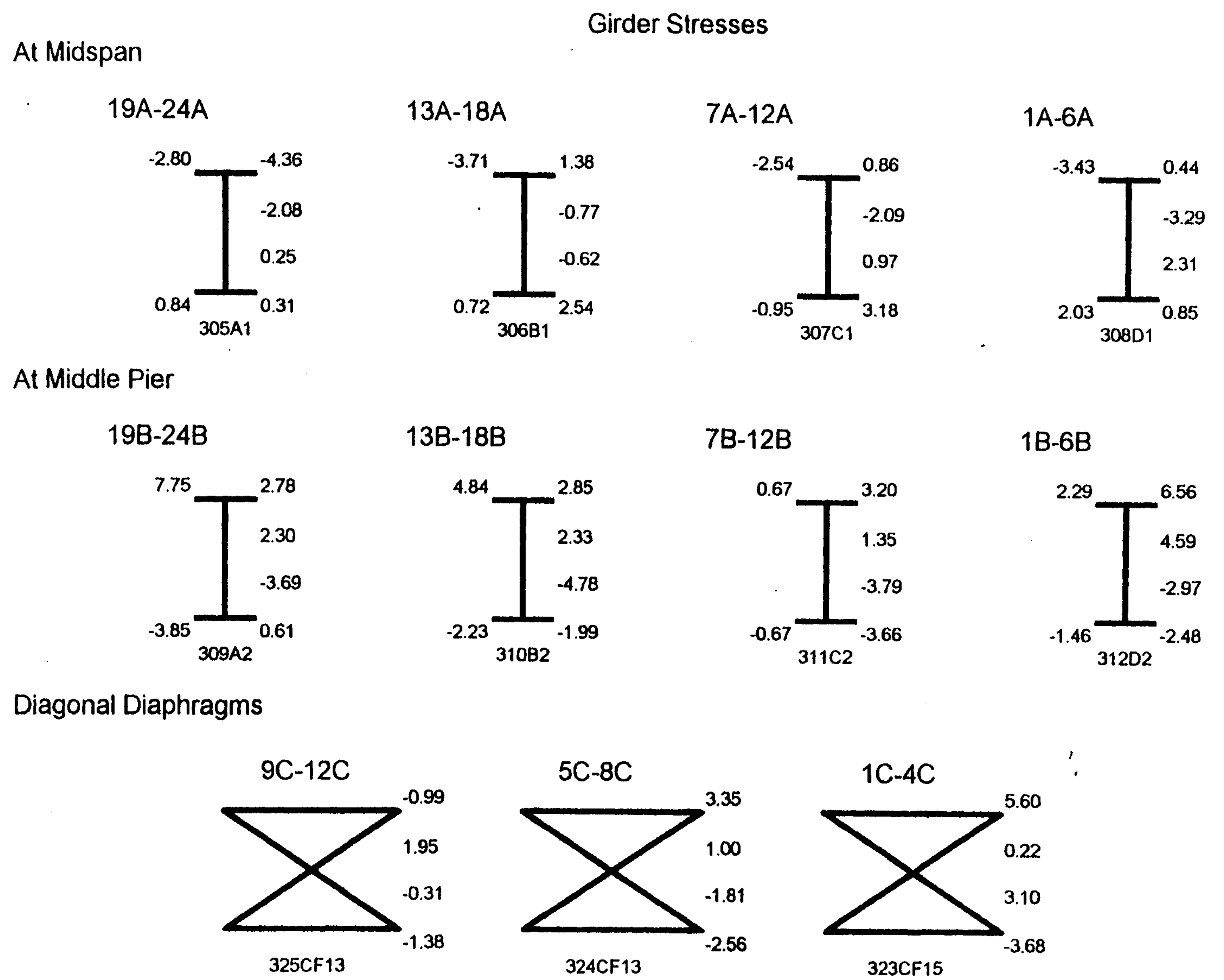

Figure A-13. Magnitude of girder stresses after the placement of the reinforcement

Date and Time of Reading: August 16, 1995 at 8:30 a.m.

Temperature: 23 °C

Weather: Clear

Loading Condition: The self weight of the bridge was the loading condition present when the reading was taken. The self weight for this loading stage includes the weight of the girders, the weight of the formwork, and weight of the concrete deck. The reinforcement for the side walls was being placed.

Objective of Reading: This reading was taken in order to examine the stresses present in the girders after the concrete deck had been poured and cured for five days. These stresses will be compared with the readings taken for the loading stage involving the stresses due to the presence of the formwork reinforcement. These observations describe the changes in the stress due to the given loading stage

General Observations: At the midspan, the top flanges experienced an increase in compressive stresses ranging from -1.83 to -6.22 ksi, and the bottom flanges experienced an increase in tensile stress ranging from 0.85 to 3.12 ksi. The largest change in tensile stress occurred at gage 6A and the largest change in compressive stress occurred at gage 5A. At the middle pier, the top flanges experienced tensile stress ranging from 4.05 to 6.00 ksi, and the bottom flanges experienced compressive stress ranging from -2.43 to -7.87 ksi. The largest change in tensile stress occurred at gage 17B, and the greatest change in compressive stress occurred at gage 24B. The stresses observed for the girders is consistent with the behavior that is expected for this loading stage. The range of stress changes for the diaphragms is -0.02 to -5.45 ksi (the largest stress occurring at gage 4C) and 0.51 to 5.14 ksi (the largest stress occurring at gage 1C).

Notes on Specific Gages: Gage 12C did not register.

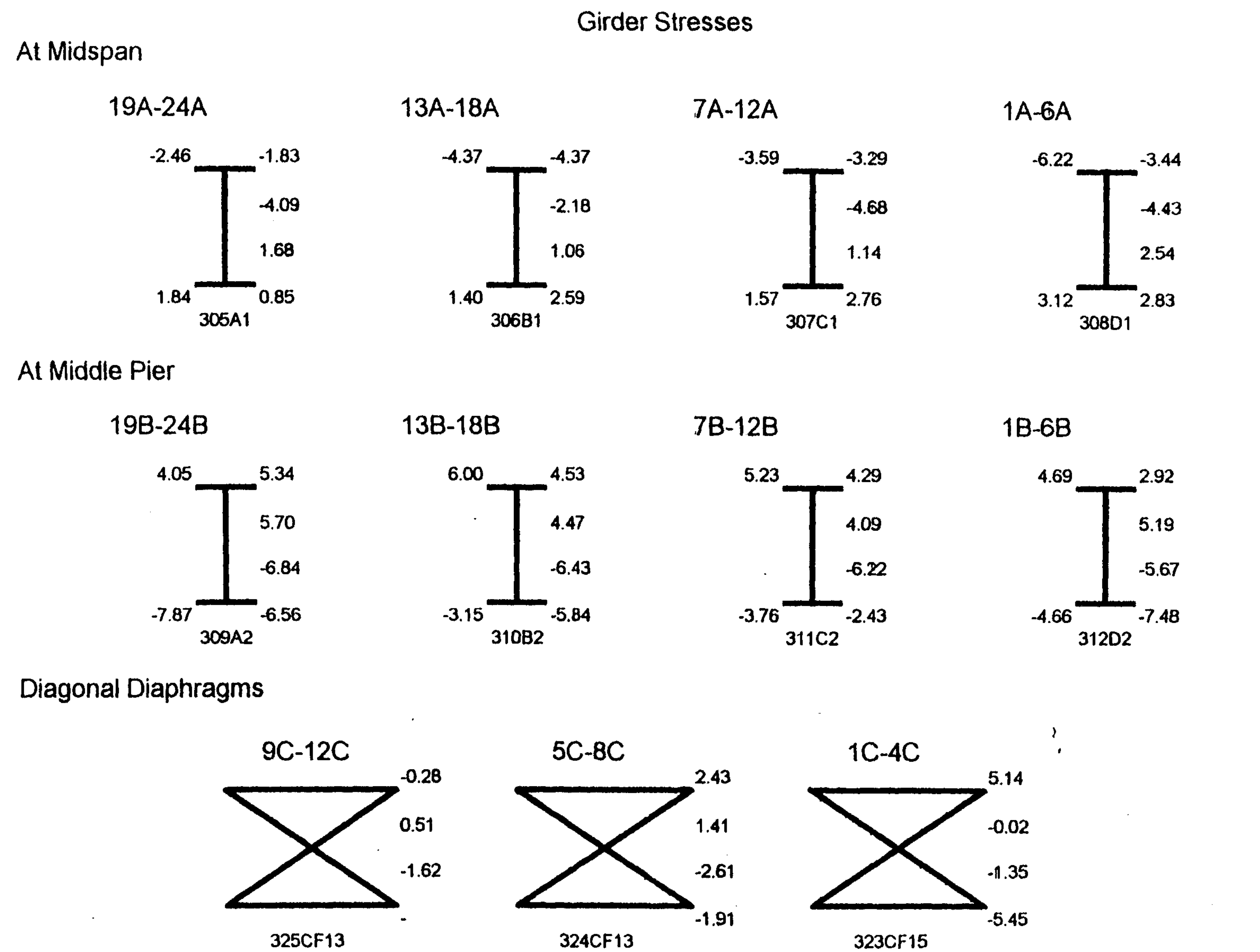

Figure A-14. Change in girder stresses between the placement of the reinforcement and the pouring of the reinforced concrete deck

Date and Time of Reading: August 16, 1995 at 8:30 a.m.

Temperature: 23 °C

Weather: Clear

Loading Condition: The self weight of the bridge was the loading condition present when the reading was taken. The self weight for this loading stage includes the weight of the girders, the weight of the formwork, and weight of the concrete deck. The reinforcement for the side walls was being placed.

Objective of Reading: This reading was taken in order to examine the stresses present in the girders after the concrete deck had been poured and cured for five days. These stresses will be compared with the readings taken for the loading stage involving the stresses due to the presence of the formwork reinforcement. These observations are for the actual magnitudes of the stresses present.

General Observations: The stresses observed in the midspan gages behaved as is expected in a positive moment region. The top flanges are in compression (ranging from -2.43 to -9.65 ksi), and the bottom flanges are in tension (ranging from 0.43 to 5.95 ksi). The largest stresses occur at gage 5A (compression) and gage 10A (tension). At the middle pier, the gages behaved as expected fro a girder in a negative moment region. The top flanges are in tension (ranging from 5.44 to 11.79 ksi), and the bottom flanges are in compression (ranging from -4.42 to -11.72 ksi). The largest stresses are at gage 23B (tension) and gage 24B (compression). The stresses in the diaphragms range from -1.26 to -9.13 ksi, with the largest stress occurring at gage 4C, in compression, and range from 0.20 to 10.75 ksi, with the largest stress occurring at gage 1C, in tension.

Notes on Specific Gages: Gage 12C did not register during this reading.

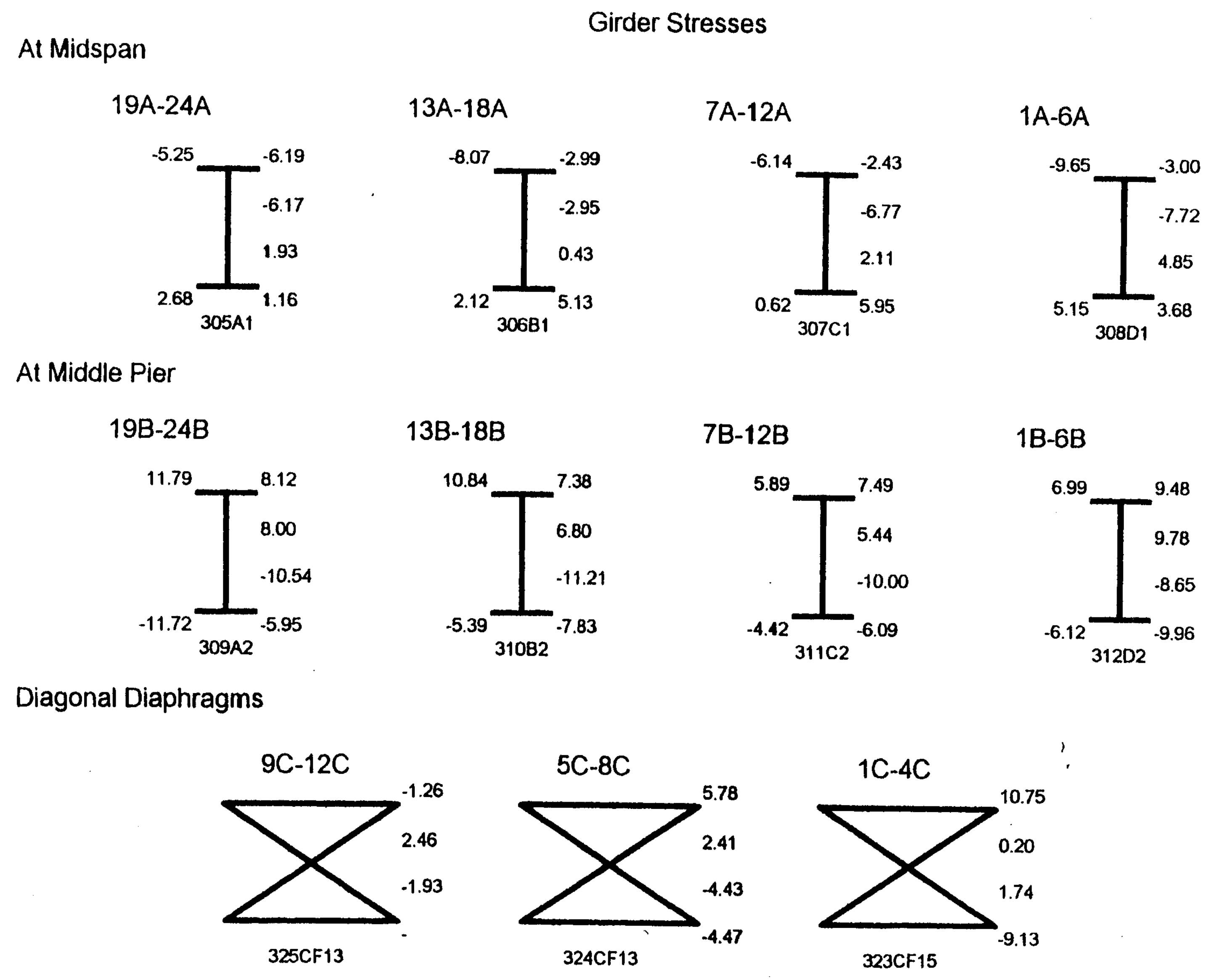

Figure A-15. Magnitude of girder stresses after the pouring of the reinforced concrete deck

Date and Time of Reading: August 25, 1995 at 8:30 a.m.

Temperature: 30 °C

Weather: Cloudy and Overcast

Loading Condition: The self weight of the bridge was the loading condition present when the reading was taken. The self weight for this loading stage includes the weight of the girders, the weight of the formwork, the weight of the concrete deck, and the weight of the newly poured parapet walls. Composite action was present between the slab and the girders.

Objective of Reading: This reading was taken in order to determine the effect that the side walls would have on members of the bridge. These observations describe the changes in the stress due to the given loading stage

General Observations: The stresses at the middle pier were as expected. The top flanges increasing in tension and the bottom flanges increasing in compression. The range of tensile stress was 0.41 ksi to 2.21 ksi, the largest of which occurred at gage 5B. The range of compressive stress was -0.29 to -2.34 ksi, the largest of which occurred at 21B. The bottom flanges at the midspan experienced an increase in tension ranging from 0.45 ksi to 1.82 ksi, the largest of which occurred at gage 3A. The top flange stresses were not as consistent. Girder 1 experienced an increase in tension across the top flange. The other girders registered an increase in both tension and compression stresses. This phenomonon does not have an obviuos explanation. Except for gage 23A, the largest change in stress for tension and compression is not greater than 0.35 ksi. This could be the observation of the distribution of the stress across the width of the bridge. The stresses observed in the members of the diaphragms were varied. The largest compressive stress was at gage location 11C while the largest tensile stress occurred at gage 10C, and the range of stresses were 0.54 to 1.08 ksi (tension) and -0.04 to -3.27 ksi (compression).

Notes on Specific Gages: Gage 12C did not register during this stage.

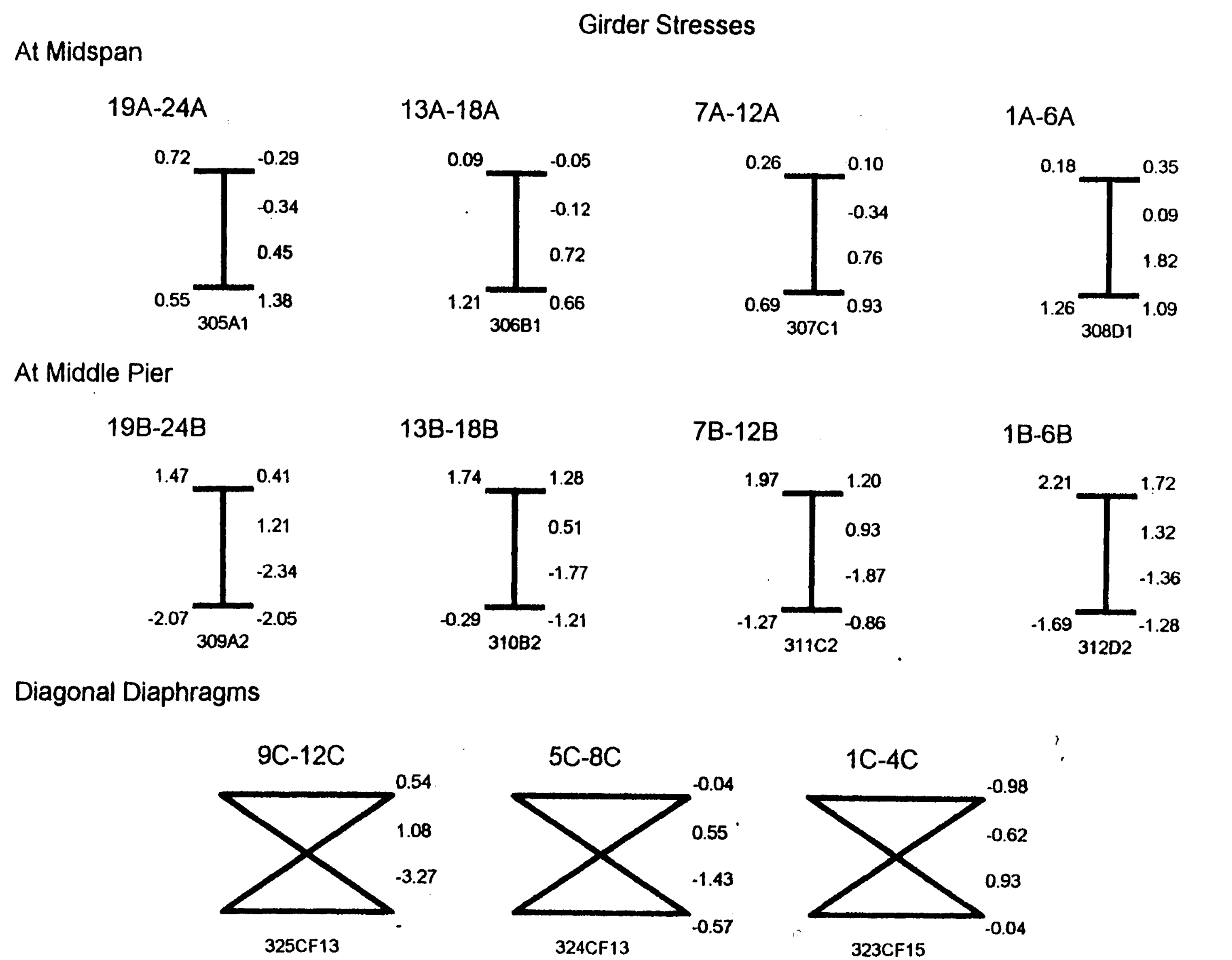

Figure A-16. Change in girder stresses between the pouring of the reinforced concrete deck and the pouring of the parapet walls

Date and Time of Reading: August 25, 1995 at 8:30 a.m.

Temperature: 30 °C

Weather: Cloudy and Overcast

Loading Condition: The self weight of the bridge was the loading condition present when the reading was taken. The self weight for this loading stage includes the weight of the girders, the weight of the formwork, the weight of the concrete deck, and the weight of the newly poured parapet walls. Composite action was present between the slab and the girders.

Objective of Reading: This reading was taken in order to determine the effect that the side walls would have on members of the bridge. These observations are for the actual magnitudes of the stresses present.

General Observations: At the midspan, the behavior of the girders was as expected. The top flanges were in compression, and the bottom flanges were in tension. The range of compressive stress was -2.32 to -7.99 ksi, and the range of tensile stress was 1.15 to 6.88 ksi. The largest compressive stress occurred at gage 17A, and the largest tensile stress occurred at gage 10A. The middle pier stresses were also as expected which is the top flanges in tension and the bottom flanges in compression. The tensile stress ranged from 6.37 to 13.26 ksi, and the compressive stress ranged from -5.68 to -13.79 ksi. The location of the greatest tensile stress was gage 23B and the greatest compressive stress was 24B. The stresses in the diaphragms did not have an identifiable pattern. The tensile stress ranged from 2.68 to 9.77 ksi, and the compressive stress ranged from -0.41 to -9.17 ksi. The greatest values of stress occurred once again at gage 1C (tension) and 4C (compression).

Notes on Specific Gages: Gage 12C did not register during this stage.

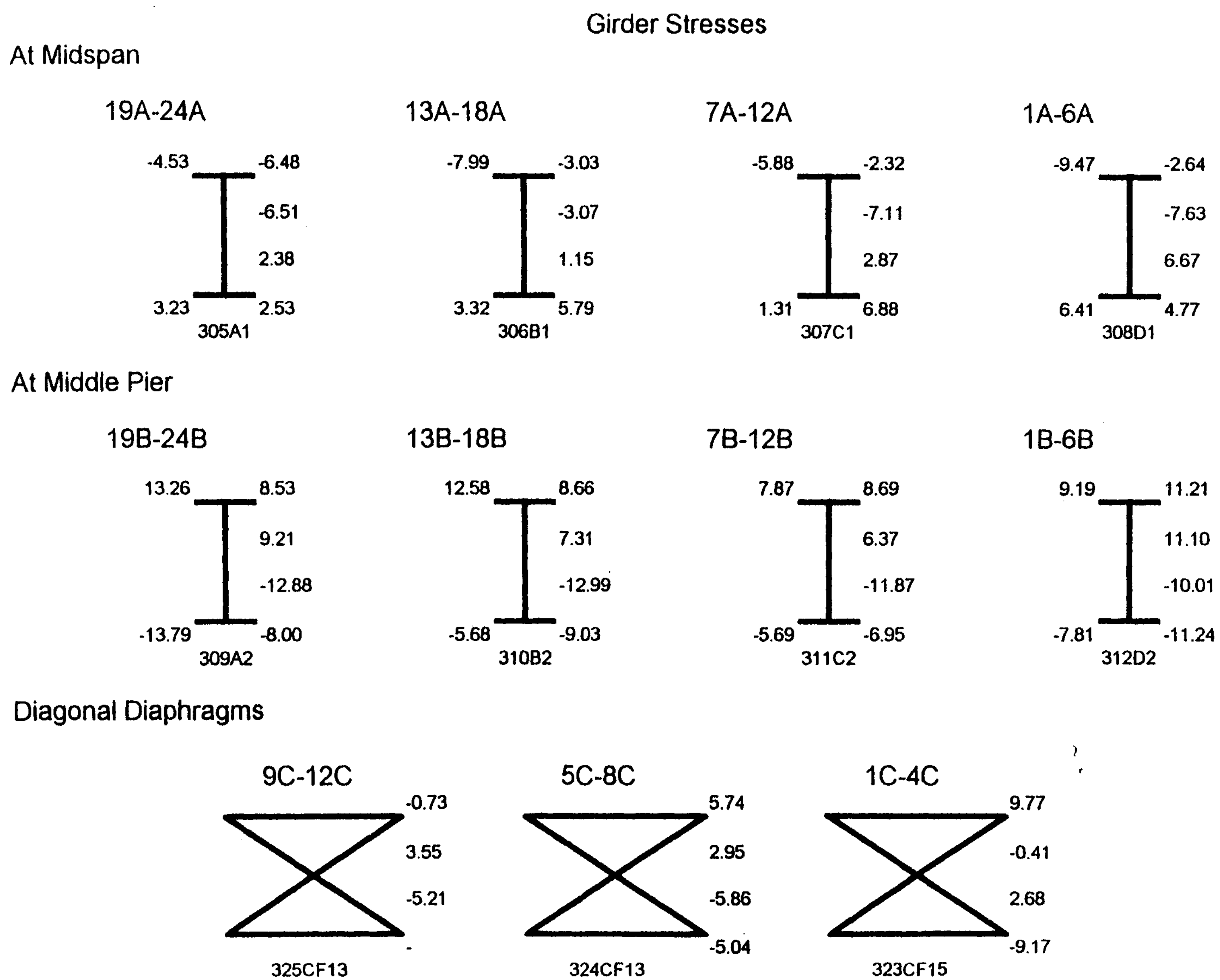

Figure A-17. Magnitude of girder stresses after the pouring of the parapet walls

Date and Time of Reading: October 7, 1995 at 11:30 p.m.

Temperature: 8 °C

Weather: Clear

Loading Condition: The loading condition for the bridge was the total dead load of the bridge which included self weight, formwork, the reinforced concrete deck and parapet walls, and the 2 inch overlay of low slump concrete. This was the final state of the bridge when it was opened to traffic.

Objective of Reading: This reading was taken to determine the final state of stress of the bridge before being put into service. This reading was also used as the base line to determine the live load stress induced by two 50 kip trucks in various loading positions. These observations describe the changes in the stress due to the given loading stage

General Observations: At the midspan, the top flanges continued to experience an increase in compression with the increased dead load. The change in stress for the bottom flange was not as uniform. There was both tensile and compressive stress experienced by the bottom flanges, but the majority of the stress changes were as expected for a positive moment region. The range of the increase in compression was -0.09 to -3.34 ksi with the largest change occurring at gage 1A. The range of tensile stress was 0.07 to 1.20 ksi with the largest change occurring at gage 24A. At the middle pier, the top flanges, except for gage 1B, were experiencing tension ranging from 0.01 to 1.08 ksi (the largest change at gage 11B). The bottom flanges were experiencing compression which ranged from -0.30 to -2.45 ksi (the largest change at gage 12B). Except for gages 6C and 1C, the diaphragms experienced compressive stress ranging from -0.02 to -4.03 ksi with the largest compressive stress occurring at gage 8C. The range of tensile stress was 0.09 to 0.80 ksi. The largest tensile stress occurred at gage 6C.

Notes on Specific Gages: Not Applicable

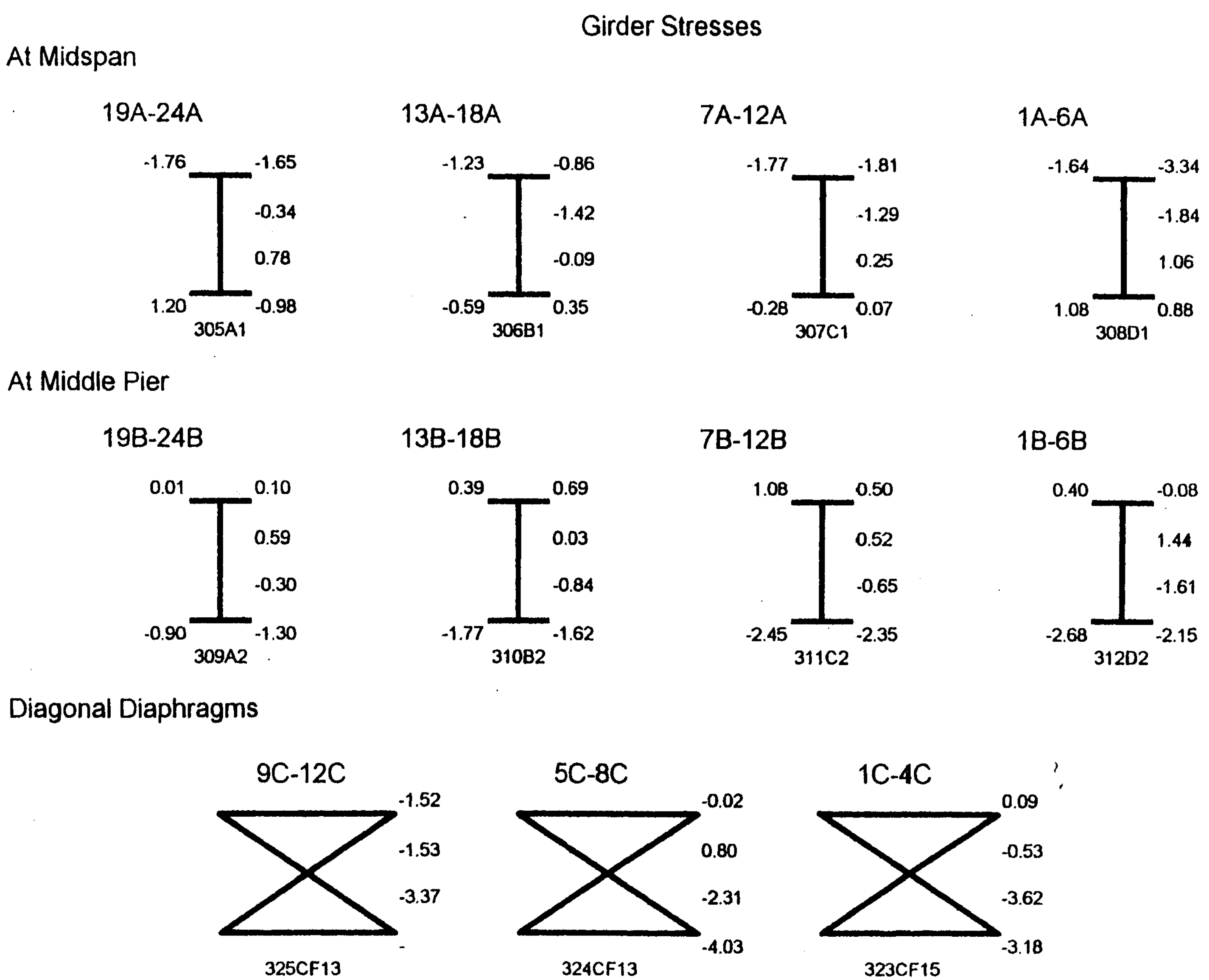

Figure A-18. Change in girder stresses between the pouring of the parapet walls and the final state of stress of the bridge before being opened for service

Date and Time of Reading: October 7, 1995 at 11:30 p.m.

Temperature: 8 °C

Weather: Clear

Loading Condition: The loading condition for the bridge was the total dead load of the bridge which included self weight, formwork, the reinforced concrete deck and parapet walls, and the 2 inch overlay of low slump concrete. This was the final state of the bridge when it was opened to traffic.

Objective of Reading: This reading was taken to determine the final state of stress of the bridge before being put into service. This reading was also used as the base line to determine the live load stress induced by two 50 kip trucks in various loading positions. These observations are for the actual magnitudes of the stresses present.

General Observations: At the midspan the stresses are as expected for members in a positive moment region. The top flange compressive stresses range from -4.13 to -11.10 ksi, and the bottom flange tensile stresses range from 1.06 to 7.73 ksi. The largest compressive stress occurred at gage 5A, and the largest tensile stress occurred at gage 3A. At the middle pier, the stress are as expected for members in a negative moment region. The top flange tensile stresses range from 6.89 to 13.27 ksi, and the bottom flange compressive stresses range from -8.14 to -14.68 ksi. The largest tensile stress occurred at gage 23B, and the largest compressive stress occurred at gage 24B. The final state of stress of the diaphragms once again did not have an obvious explanation. For diaphragm 1 the top member was in tension, and the lower three members were in compression. For diaphragm 2, the top two members were in tension, and the bottom two were in compression. For diaphragm 3, the top diagonal member was in tension, and the other three members were in compression. The range of tensile stress for the diaphragms was 2.02 to 9.87 ksi, and the range of compressive stress was -0.94 to -12.36 ksi. Once again the largest tensile stress occurred at gage 1C, and the largest compressive stress occurred at gage 4C.

Notes on Specific Gages: Not Applicable

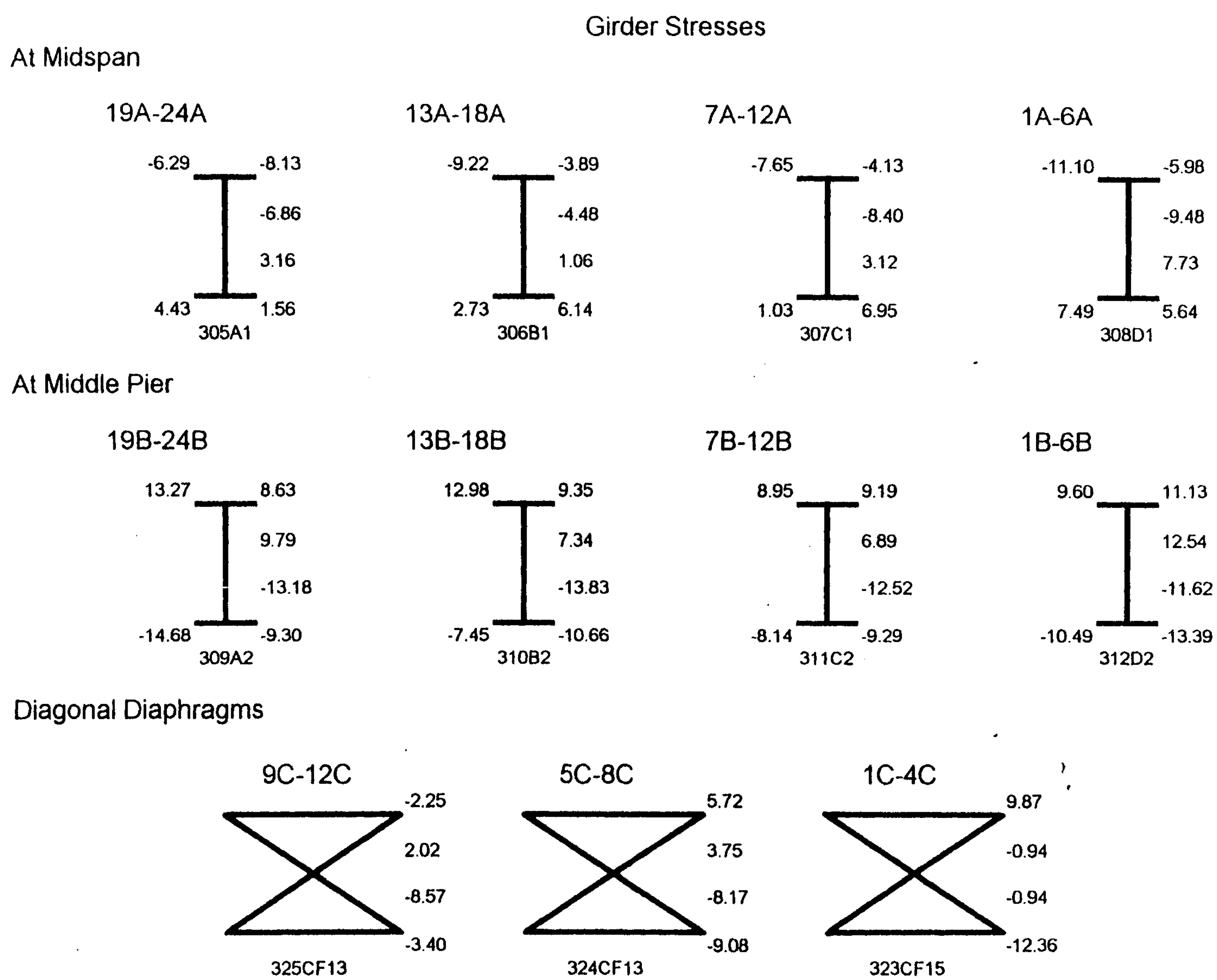

Figure A-19. Magnitude of girder stresses before the bridge was opened for service

APPENDIX B

STRESSES DUE TO POURING OF THE CONCRETE DECK

APPENDIX B
STRESSES DUE TO POURING OF THE CONCRETE DECK

This appendix presents the stresses due to pouring of the concrete deck on MN/DOT Bridge No. 27998.

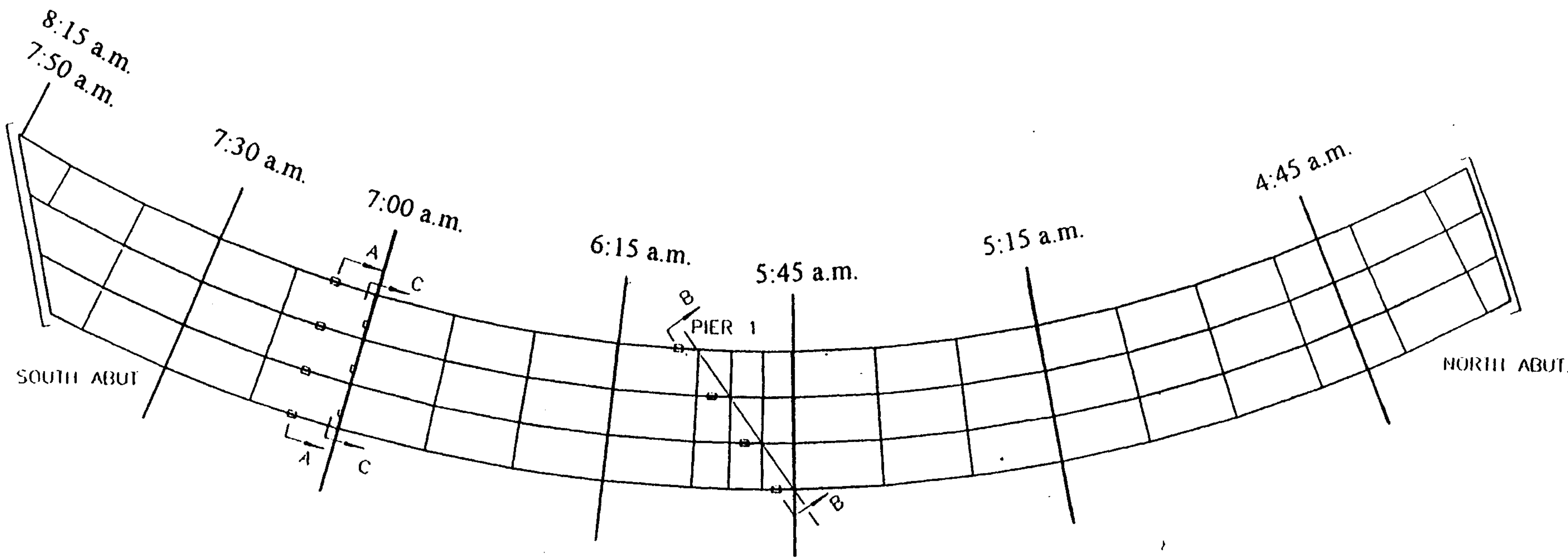

Figure B-1. Plan view of the bridge displaying the progression of the pouring of the concrete deck

OBSERVATIONS OF GIRDER STRESSES

Date and Time of Reading: August 11, 1995 at 4:45 a.m.

Temperature: 20 °C

Weather: Overcast

Loading Condition: The pouring of the concrete deck began at the north abutment at 4:15 a.m. Deck locations will be referenced from the north abutment. For this reading, the concrete was located at the first quarter point. Additional loading was provided from the finishing machine. There were ten to fourteen workers also present.

Objective of Reading: This reading was taken to determine the stresses present during the pouring of the concrete bridge deck.

General Observations: The three outside most girders, 306B1, 307C1, and 308D1, experienced an increase in tension on the top flange and compression on the bottom flange at the midspan of span one. Girder 305A1, the inside facia girder, experienced the opposite change in stress from the other three girders. This girder showed a maximum change in stress of only 0.06 ksi which is fairly negligible. The largest increase in stress, 1.08 ksi, occurred at gage 5A which is at the inside tip of the top flange of the outside facia girder. At the middle pier, the top flanges experienced an increase in tensile stress, and the bottom flanges experienced an increase in compressive stress. The range of stress changes at the middle pier were -0.25 to -0.83 ksi for compression and 0.39 to 0.83 ksi. The largest stress increases occurred at gage locations 5B (tension) and 24B (compression). The diaphragms showed ranges, in the change in the stresses, of -0.14 to -1.37 ksi and 0.23 to 0.79 ksi. The top two members experienced an increase in compressive stress while the bottom two experienced an increase tensile stress. The greatest compressive stress of -1.37 ksi occurred at gage location 1C, and the greatest tensile stress of 0.79 ksi occurred at gage 4C. All of the diagonals experienced a change in stress of approximately the same value. At the midspan gages, the stresses are smallest on the inside facia girder and increases in each girder as the outside facia girder is approached with the largest stresses being experienced by the outside girder. This behavior is not manifest in the gages at the middle pier. The behavior of the girders in span one is consistent with the what is expected when the loading is applied in the second span.

Notes on Specific Gages: Not Applicable

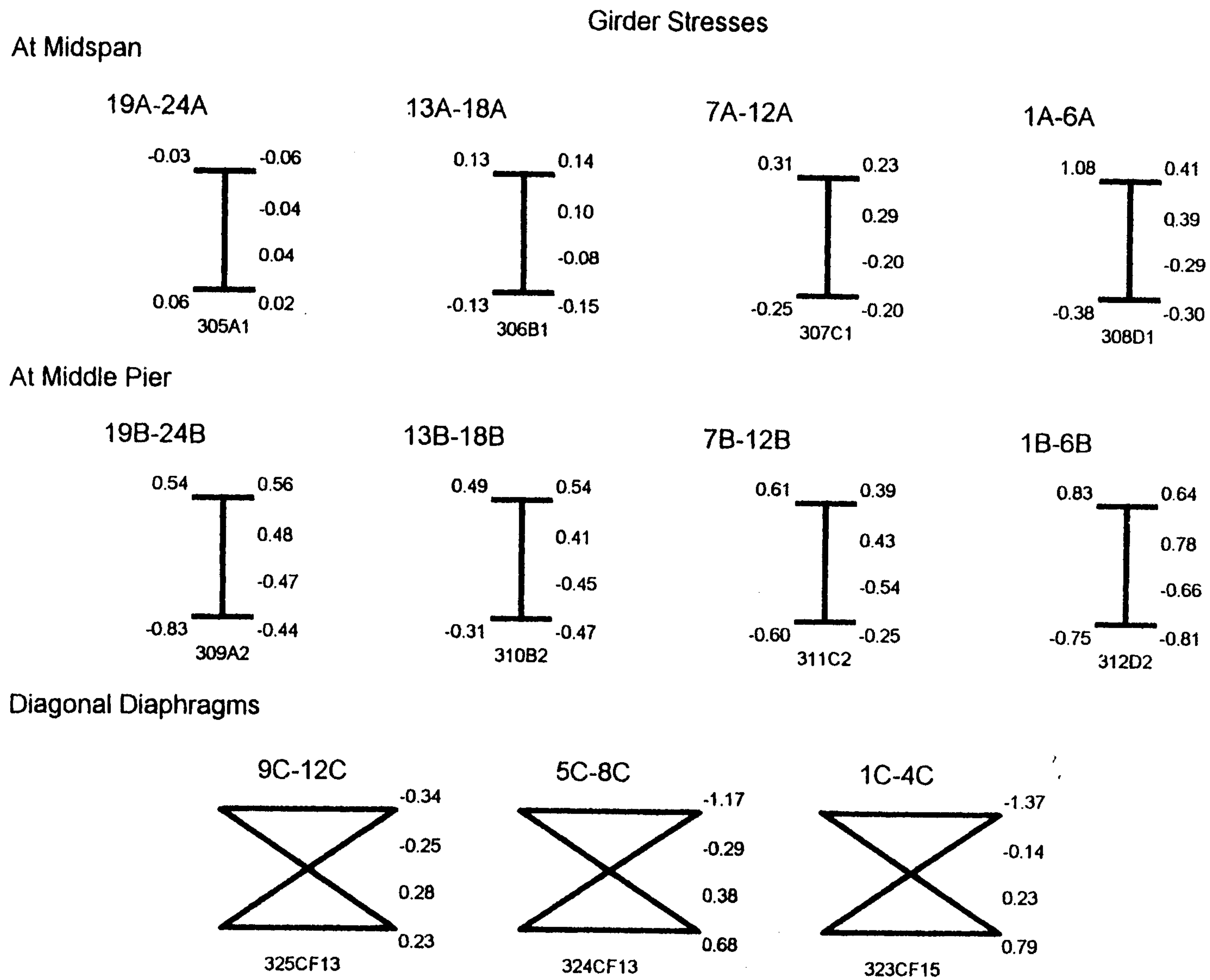

Figure B-2. Change in girder stresses between the initial reading and stage 1

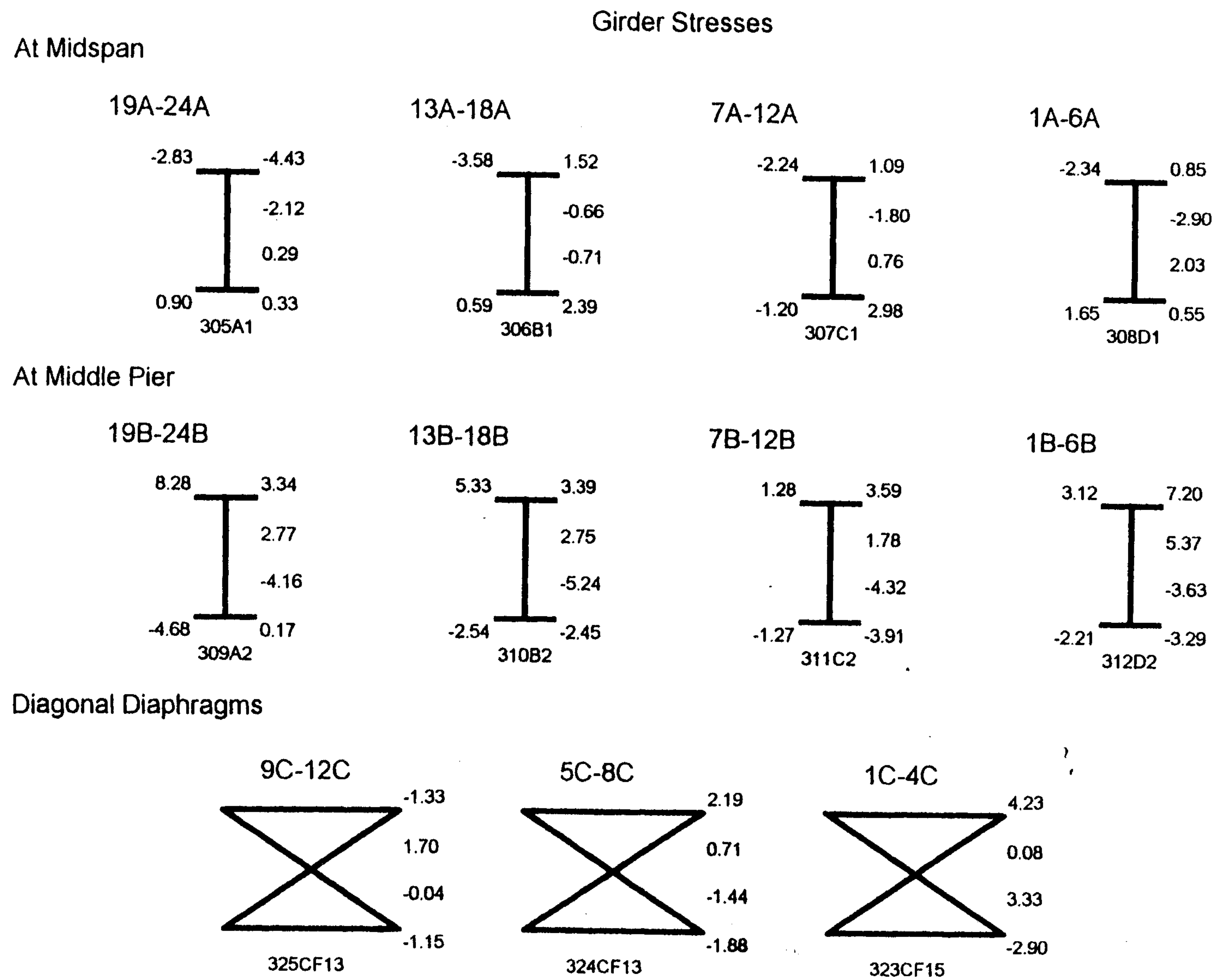

Figure B-3. Magnitude of girder stresses for stage 1 reading (4:45 a.m.)

Date and Time of Reading: August 11, 1995 at 5:15 a.m.

Temperature: 20 °C

Weather: Overcast

Loading Condition: The pouring of the deck had progressed to the midspan of span two.

Objective of Reading: This reading was taken to determine the stresses present during the pouring of the concrete bridge deck.

General Observations: The pattern of stress change observed for load stage 1 continued for this load stage. This pattern is compression in the top flange and tension in the bottom flange for girder 4 with girders 1,2, and 3 experiencing tension in the top flanges and compression in the bottom flanges. The stresses increased at the midspan, in most cases, by 2 to 2.5 times the increase observed previously. At the middle pier gages, the greatest increase in the change in stress was approximately 2.8 times the previous change in stress. The largest change in stress at the midspan, 2.64 ksi, occurred at gage location 5A. The greatest change in stress at the middle pier, 1.51 ksi, occurred at gage location 5B. The change in the stresses in the diaphragms did not increase appreciably. The largest compressive stress, -1.71 ksi, is still occurring at gage location 1C, and the greatest tensile stress is 1.25 ksi which occurs at location 4C. The inside diaphragm, 325CF13, is experiencing the least change in stress with the outside most diaphragm experiencing the greatest stress change. The middle diaphragm, 324CF13, experiences a stress change in between these two diaphragms. The top two members of the diaphragms experienced compression while the bottom two experienced tension.

Notes on Specific Gages: Not Applicable

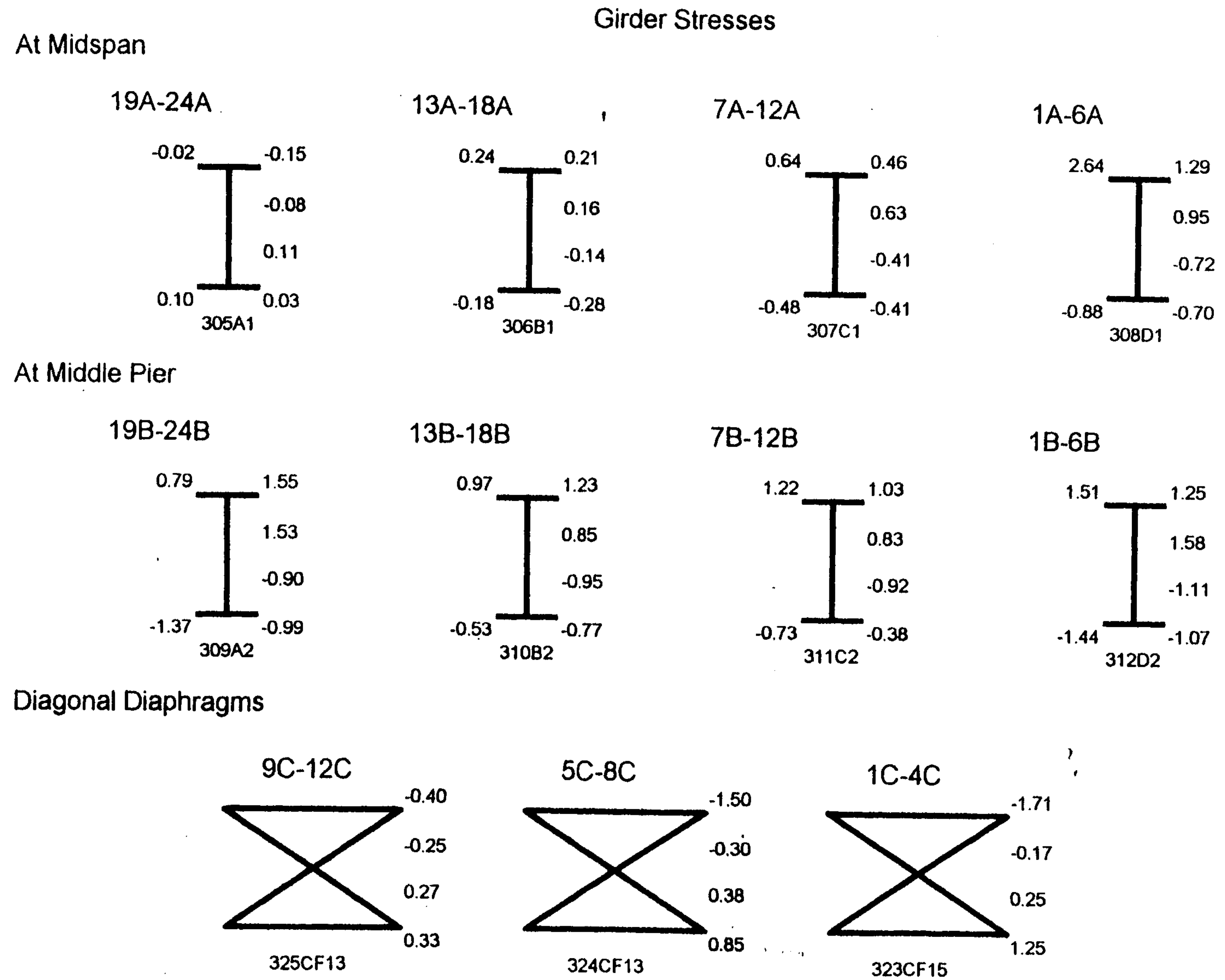

Figure B-4. Change in girder stresses between stage 1 and stage 2

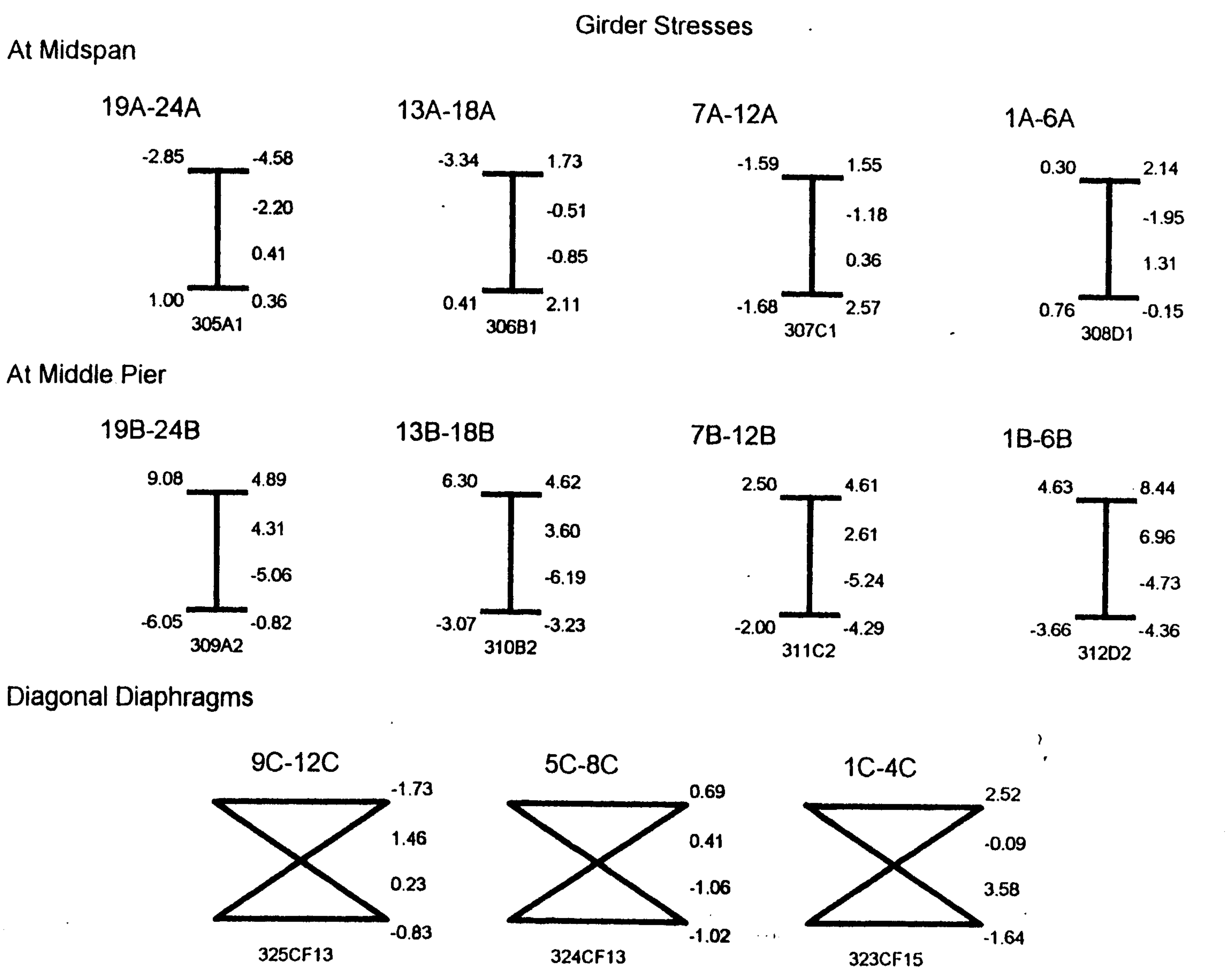

Figure B-5. Magnitude of girder stresses for stage 2 (5:15 a.m.)

Date and Time of Reading: August 11, 1995 at 5:45 a.m.

Temperature: 20 °C

Weather: Overcast

Loading Condition: The pouring of the deck had progressed to the middle pier.

Objective of Reading: This reading was taken to determine the stresses present during the pouring of the concrete bridge deck.

General Observations: There was a slight increase in the top flange tensile stresses and a decrease in the bottom flange compressive stresses at the midspan gages. The greatest change, once again at 5A, was 0.65 ksi. At the middle pier gages, the behavior continued as before with the tensile stresses increasing on the top flanges while the compressive stresses increase in the bottom flanges. The range in tensile stress change was 0.14 to 1.01 ksi. The range in compressive stress change was -0.19 to -0.78 ksi. There was not much change in the stresses in the diaphragms. Gage 9C was the only top horizontal to experience an increase in tensile stress, and the top two members experienced an increase in compressive stress. The bottom two members experienced an increase in tensile stress. The range of stress change was -0.07 to -0.49 ksi and 0.02 to 0.67 ksi..

Notes on Specific Gages: Not Applicable

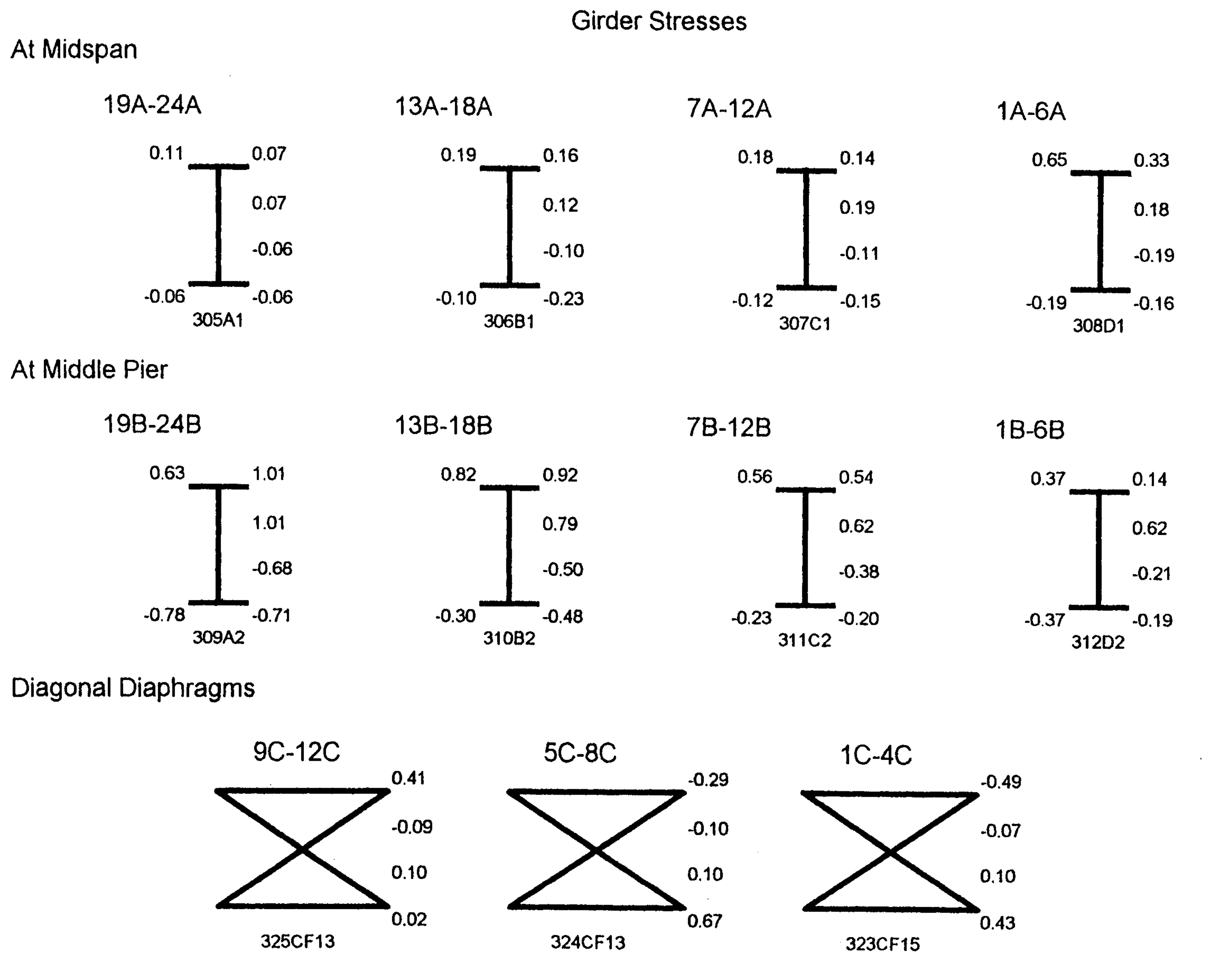

Figure B-6. Change in girder stresses between stage 2 and stage 3

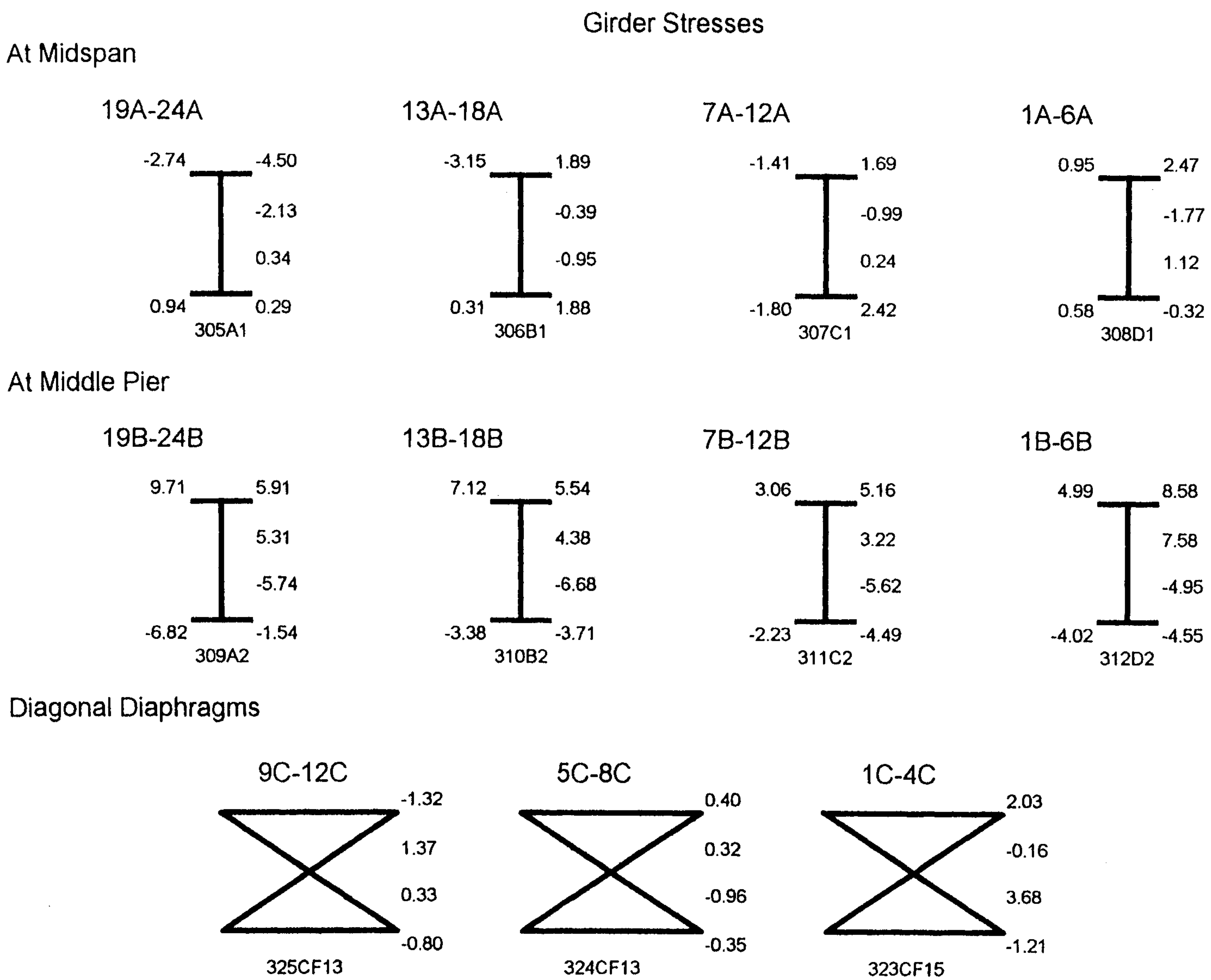

Figure B-7. Magnitude of girder stresses for stage 3 (5:45 a.m.)

Date and Time of Reading: August 11, 1995 at 6:15 a.m.

Temperature: 20 °C

Weather: Overcast

Loading Condition: The pouring of the deck had progressed to the first quarter point in span one.

Objective of Reading: This reading was taken to determine the stresses present during the pouring of the concrete bridge deck.

General Observations: The gages at the midspan began to register the reversal of stress (compression in the top flanges and tension in the bottom flanges) consistent with a positive moment region as the concrete was poured in span one. The absolute value of the change in stresses was minimal and ranged from 0.00 ksi to 0.59 ksi. Stress reversal also occurred in the diaphragms. The top two members, except for gage 9C, experienced tensile stresses with the bottom two experiencing compressive stresses. Except for girder 309A2 and gages 13B, the stresses at the middle pier experienced an increase in tensile stresses on the top flanges and increase in compressive stresses on the bottom flanges. Aside for gage 23B on girder 309A2, the gages registered a tensile stress increase for all of the locations. A possible explanation for this different behavior might result from the fact that these gages are located further away from the middle pier since gage line B is located along a diagonal line above the pier. Except for a compressive stress increase in gage 9C, the top two members of the diaphragms experienced an increase in tensile stress, and the bottom two members experienced an increase in compressive stress. This reaction resulting from the deck beginning to force the girders downwards as the deck is poured. When the deck was being poured in span two, the opposite reaction was observed.

Notes on Specific Gages: Not Applicable

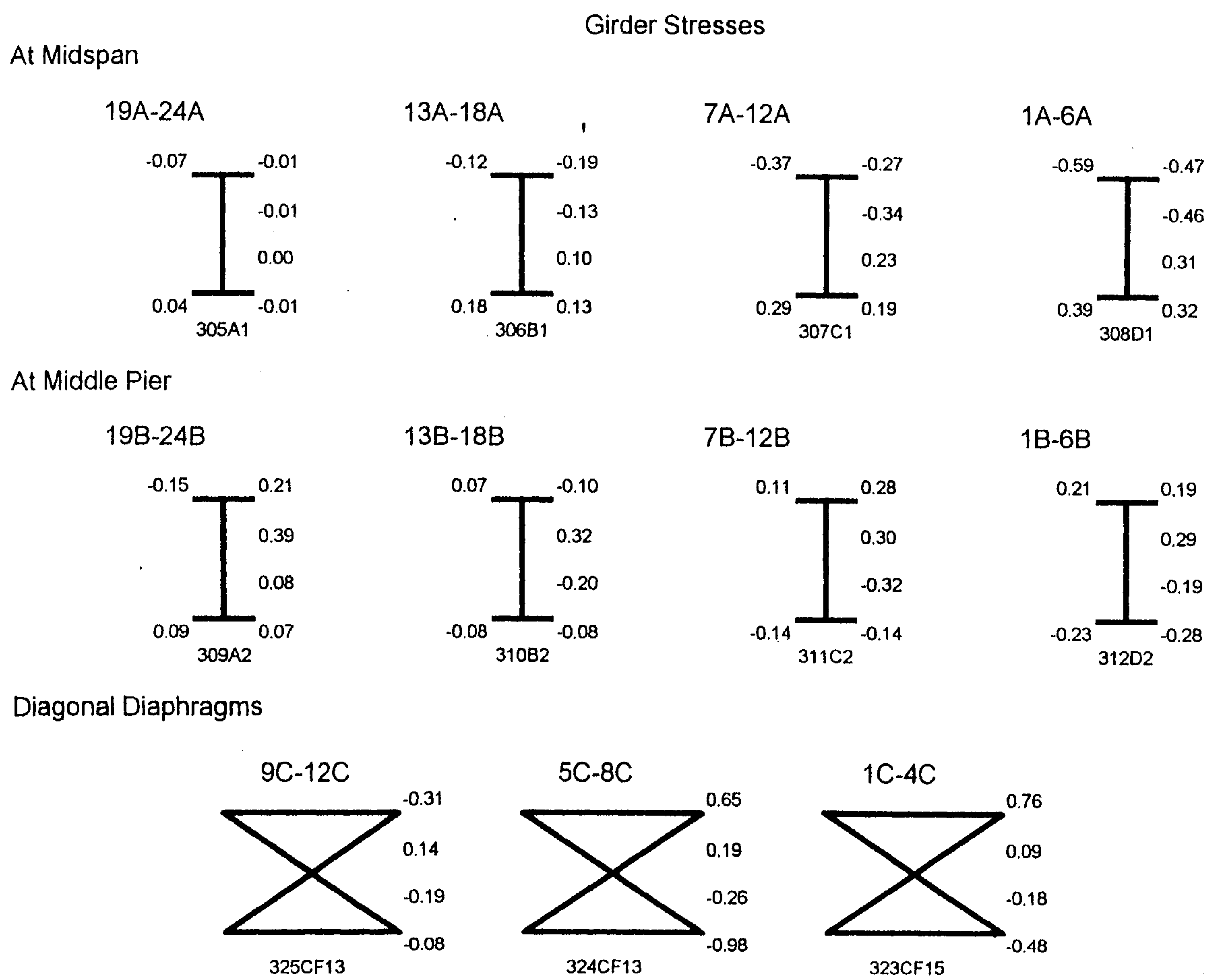

Figure B-8. Change in girder stresses between stage 3 and stage 4

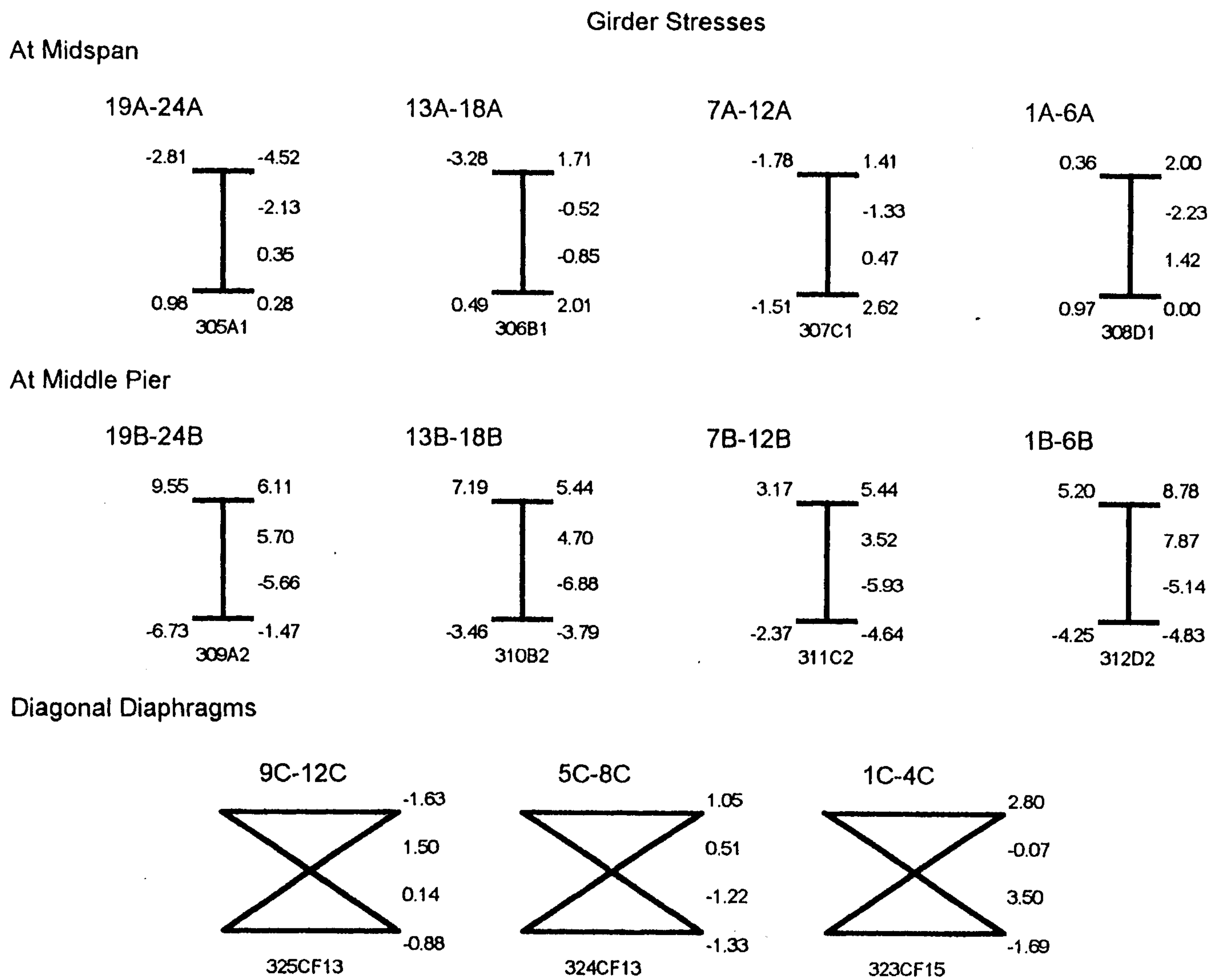

Figure B-9. Magnitude of girder stresses for stage 4 (6:15 a.m.)

Date and Time of Reading: August 11, 1995 at 7:00 a.m.

Temperature: 20 °C

Weather: Overcast

Loading Condition: The pouring of the deck had progressed to the midspan of span one.

Objective of Reading: This reading was taken to determine the stresses present during the pouring of the concrete bridge deck.

General Observations: The gages continued to respond in a manner consistent with the loading being present in the first span. At the midspan, the top flanges experienced an increase in compressive stress ranging from -0.60 ksi to -3.12 ksi The bottom flanges experienced an increase in tensile stress ranging from 0.58 ksi to 1.31 ksi. The middle pier gages experienced an increase in compressive stress on the bottom flanges and tensile stress on the top flanges. The tensile stress changes ranged from 0.58 ksi to 1.65 ksi, and the compressive stress changes ranged from -0.58 ksi to -1.52 ksi. The change in stresses at the middle pier are of approximately the same magnitude. The stresses in the diaphragms increased in tension in the top two members and compression in the bottom two. The ranges of increase were 0.74 ksi to ~4.35 ksi and -0.55 ksi to -2.94 ksi.

Notes on Specific Gages: Gage 1C did not register in the for the 6:15 a.m. reading, so the value of stress change for this stage was calculated by averaging the percentage of change of the other gages from the previous stage to this stage. The value used was 52%.

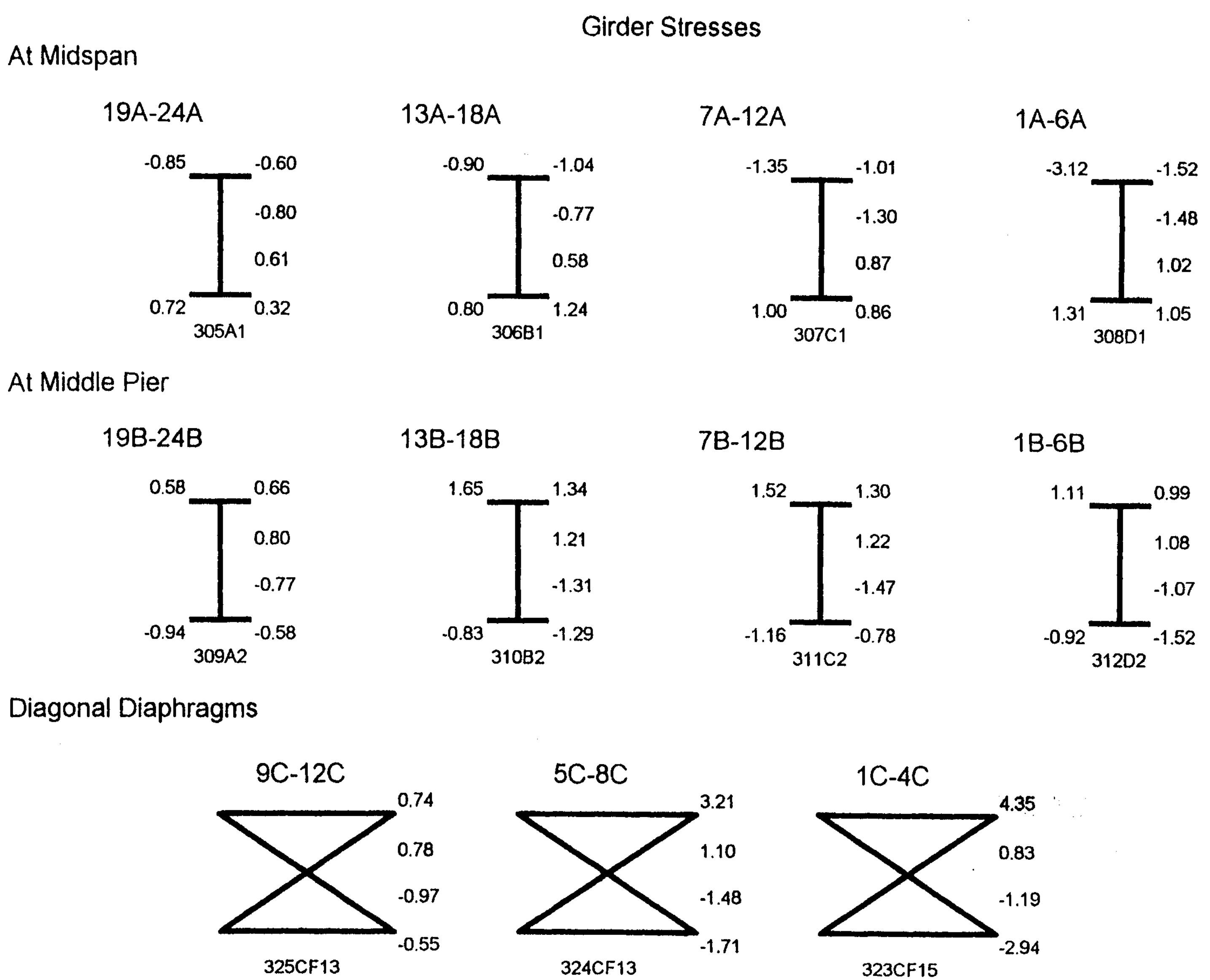

Figure B-10. Change in girder stresses between stage 4 and stage 5

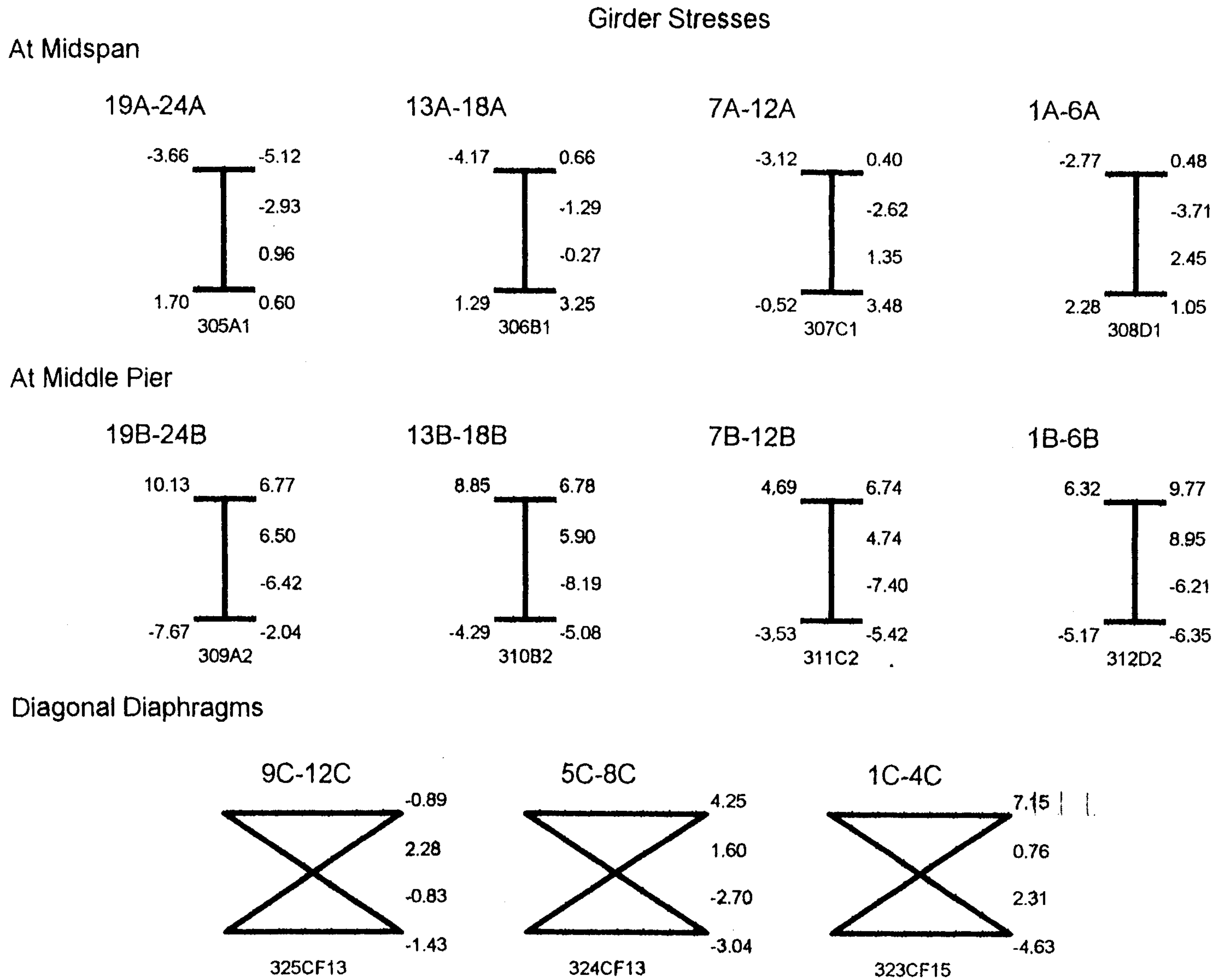

Figure B-11. Magnitude of girder stresses for stage 5 (7:00 a.m.)

Date and Time of Reading: August 11, 1995 at 7:30 a.m.

Temperature: 20 °C

Weather: Overcast

Loading Condition: The pouring of the deck had progressed to the third quarter point of span one.

Objective of Reading: This reading was taken to determine the stresses present during the pouring of the concrete bridge deck.

General Observations: The girders and diaphragms continued to respond in the same manner as described in the previous loading stage. The stress ranges at the midspan were -0.72 ksi to -6.05 ksi on the top flanges and 0.73 ksi to 2.80 ksi on the bottom flanges. At the middle pier the ranges were 0.93 ksi to 1.28 ksi on the top flanges and -0.44 ksi to -1.30 ksi on the bottom flanges. The tensile forces in the top two members ranged from 0.16 ksi to -4.01 ksi with the compressive forces in the other bottom members ranging from 0.96 ksi to 3.73 ksi.

Notes on Specific Gages: Gage 12C did not register for this loading stage. The change in stress for gage 1C was once again calculated for this stage.

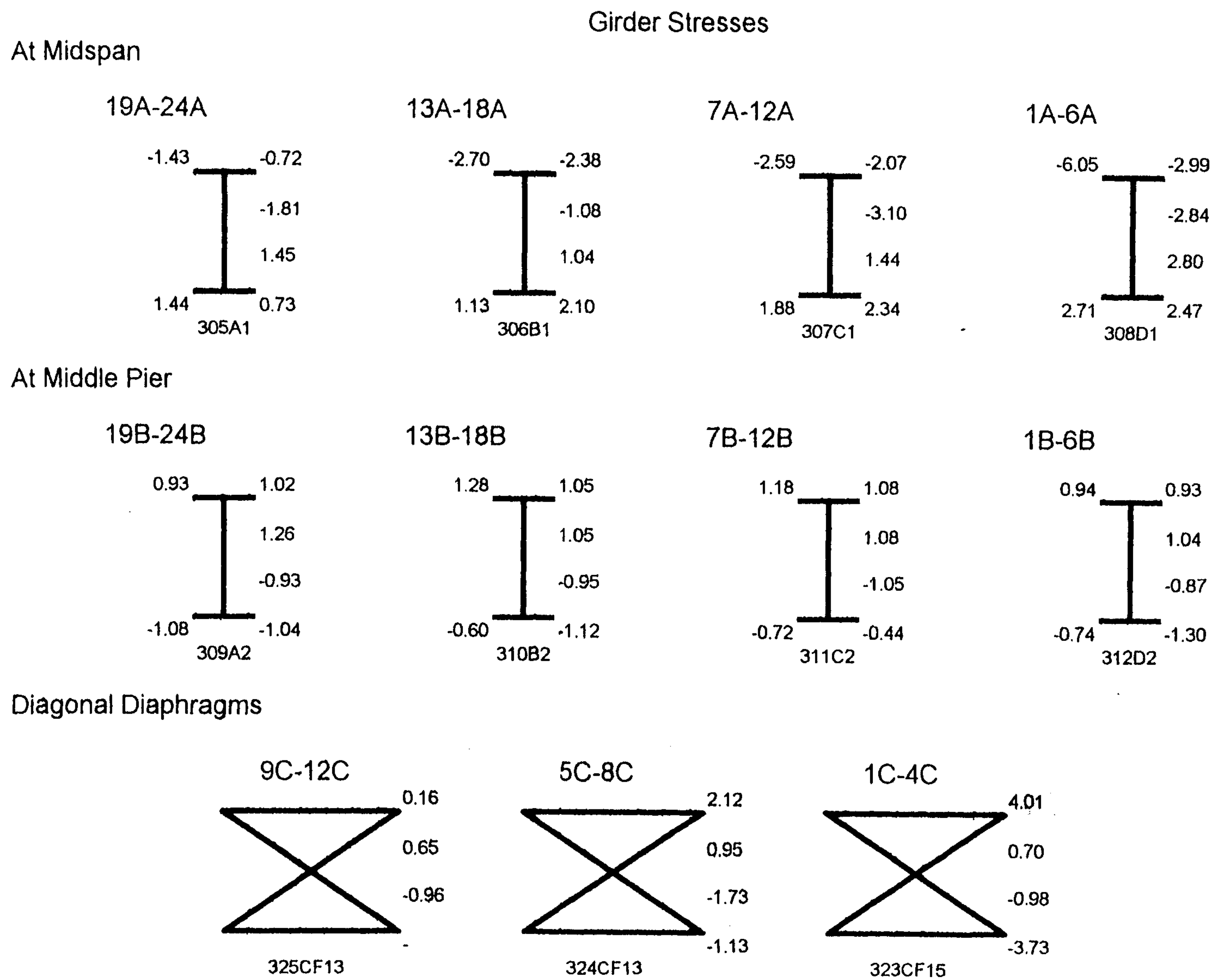

Figure B-12. Change in girder stresses between stage 5 and stage 6

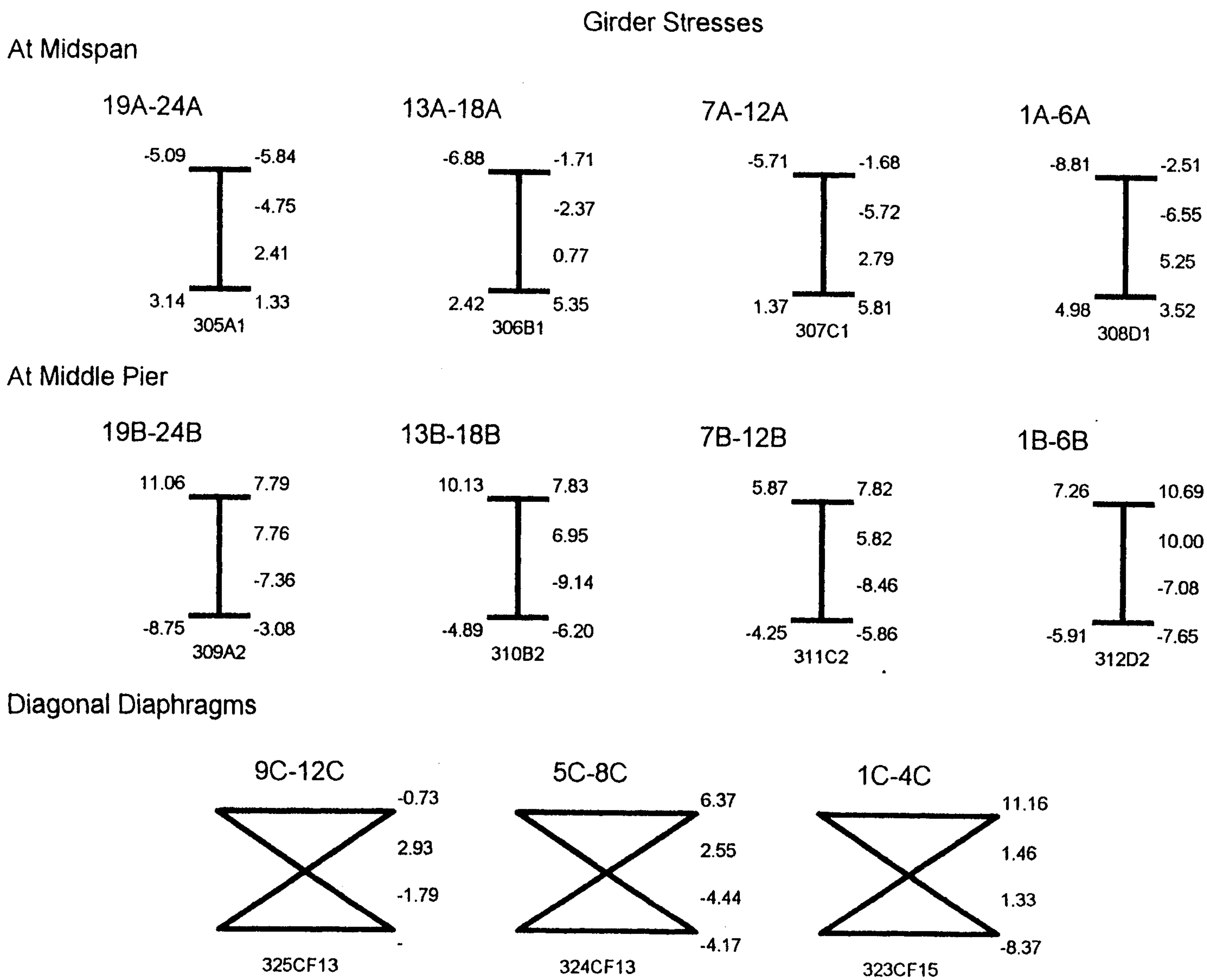

Figure B-13. Magnitude of girder stresses for stage 6 (7:30 a.m.)

Date and Time of Reading: August 11, 1995 at 7:50 a.m.

Temperature: 20 °C

Weather: Overcast

Loading Condition: The pouring of the deck was completed when this reading was taken.

Objective of Reading: This reading was taken to determine the stresses present during the pouring of the concrete bridge deck.

General Observations: The readings for this stage were erratic in most of the members, but a majority of the stress increases were consistent with the expected behavior. The changes in stress were minimal which could explain some of the discrepancies observed. This reading might be the perceiving some stress redistribution within the structure. The total range of the stress change was -0.46 ksi to 0.29 ksi at the midspan and -0.06 ksi to 0.12 ksi at the middle pier. The diaphragms experienced at change in stress that ranged from -0.19 ksi to 0.18 ksi.

Notes on Specific Gages: Gage 12C did register during this loading stage.

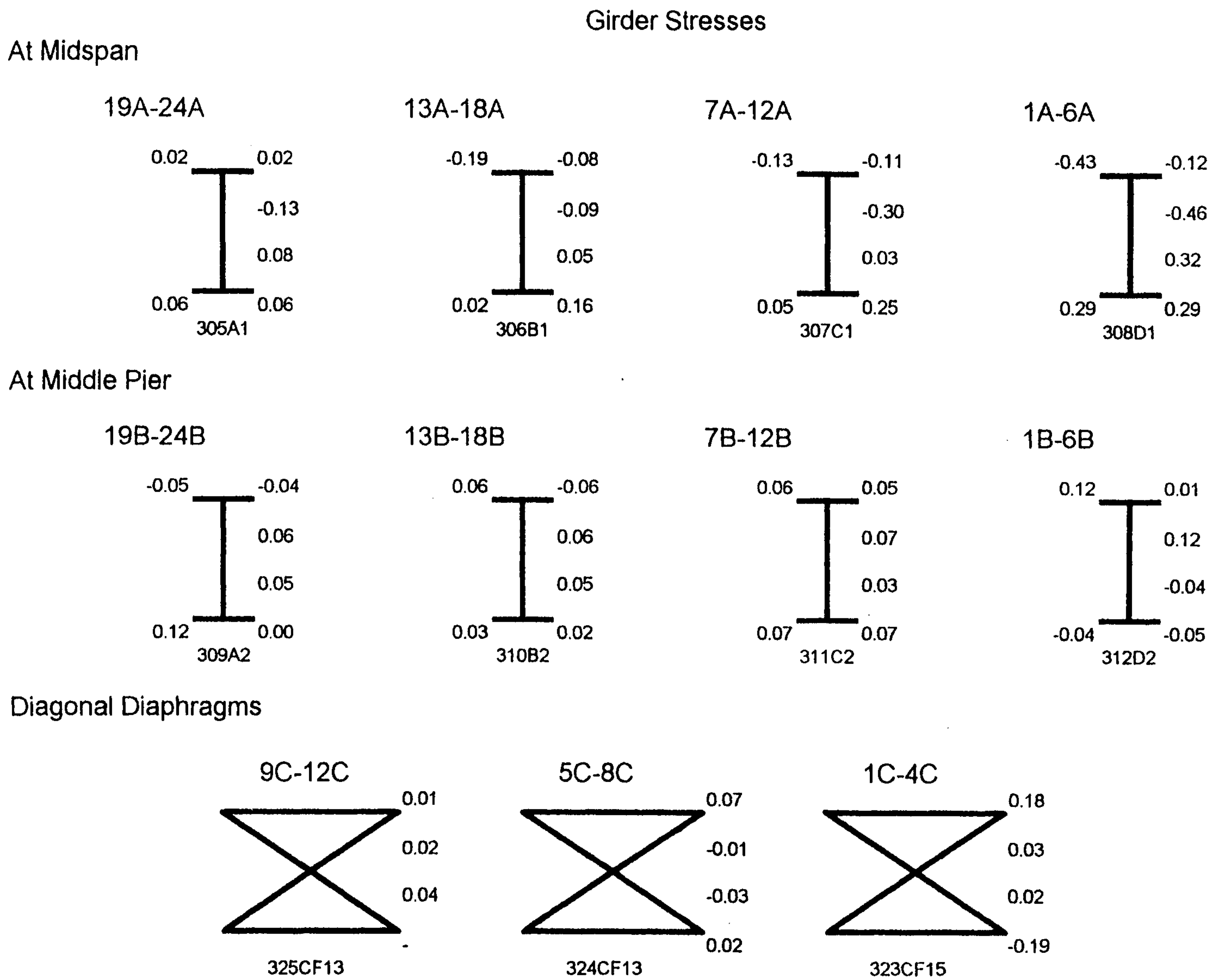

Figure B-14. Change in girder stresses between stage 6 and stage 7

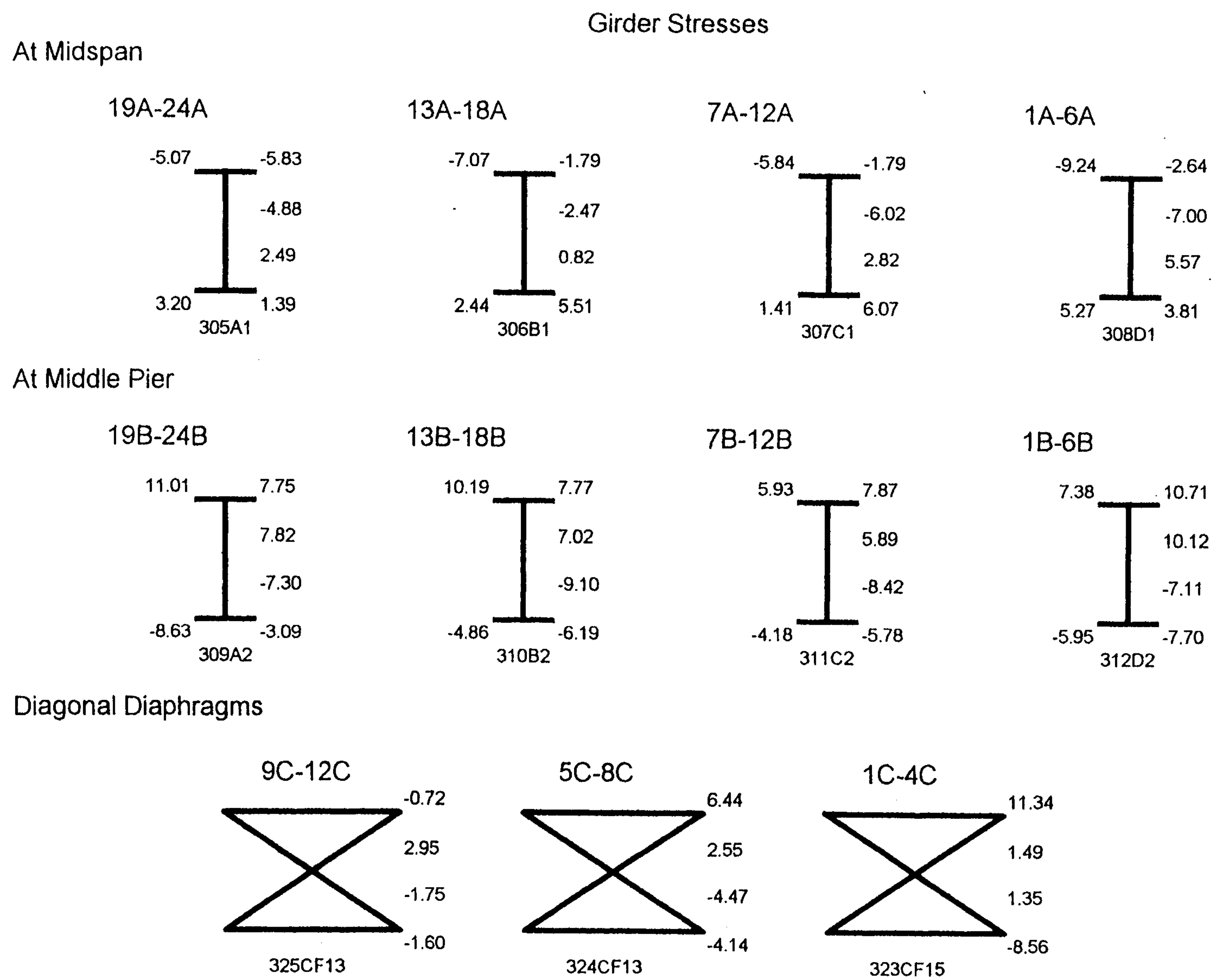

Figure B-15. Magnitude of girder stresses for stage 7 (7:50 a.m.)

Date and Time of Reading: August 11, 1995 at 8:15 a.m.

Temperature: 20 °C

Weather: Raining

Loading Condition: This reading was taken twenty-five minutes after the deck was completed.

Objective of Reading: This reading was taken to determine if a change occurs in the stresses within thirty minutes. This would help determine how long it takes for the composite action to begin.

General Observations: There was not an appreciable change in the stresses after twenty-five minutes.The greatest change in either tensile or compressive stresses was -0.47 ksi which was located in the diaphragm at gage location 8C. This reading was taken to observe if composite action began forming within 30 minutes of the completion of the pouring of the deck. Since there was a minimal change in the stresses, it appears that the composite action has yet to begin for this bridge.

Notes on Specific Gages: Gage 12C did not register during this loading stage.

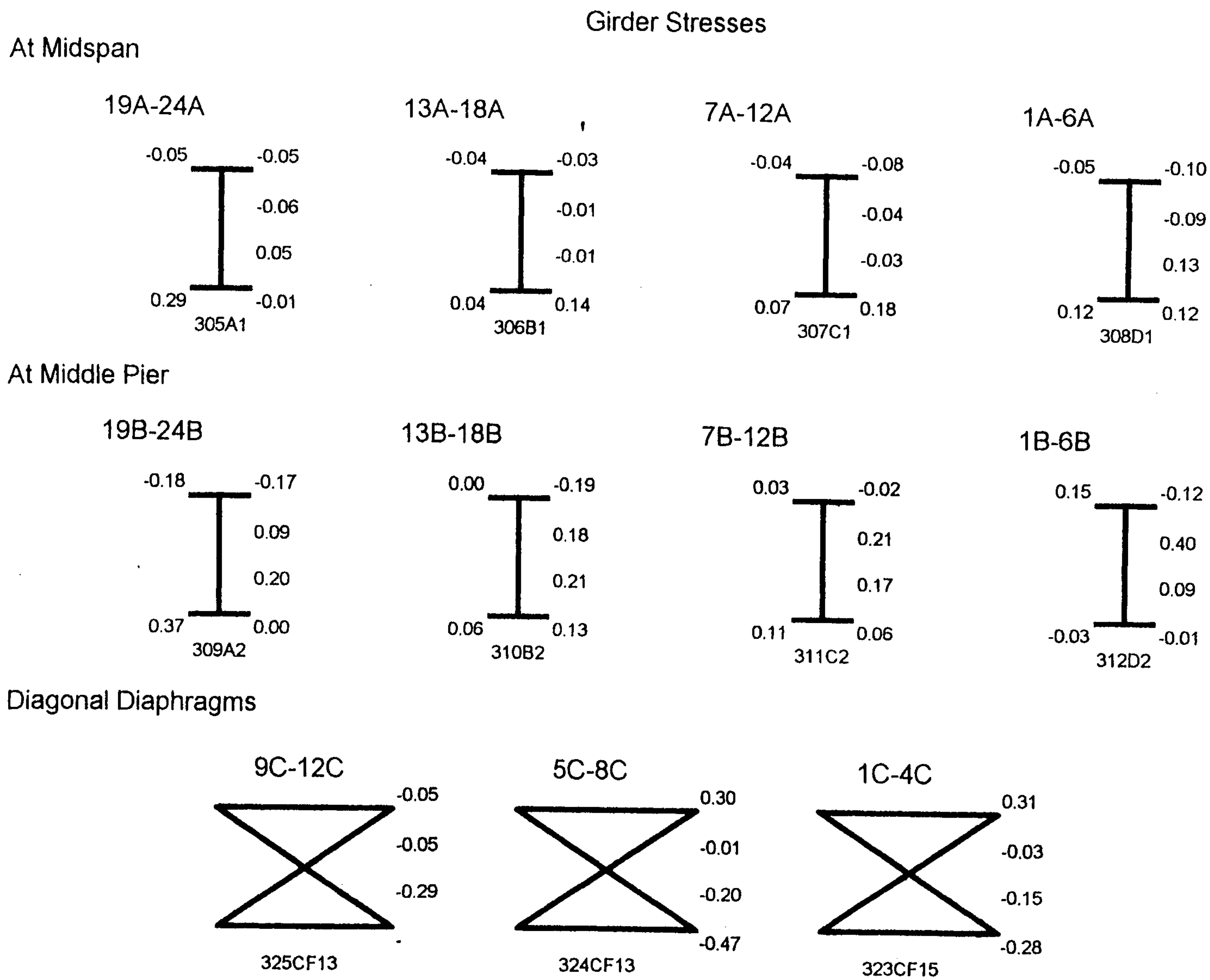

Figure B-16. Change in girder stresses between stage 7 and stage 8

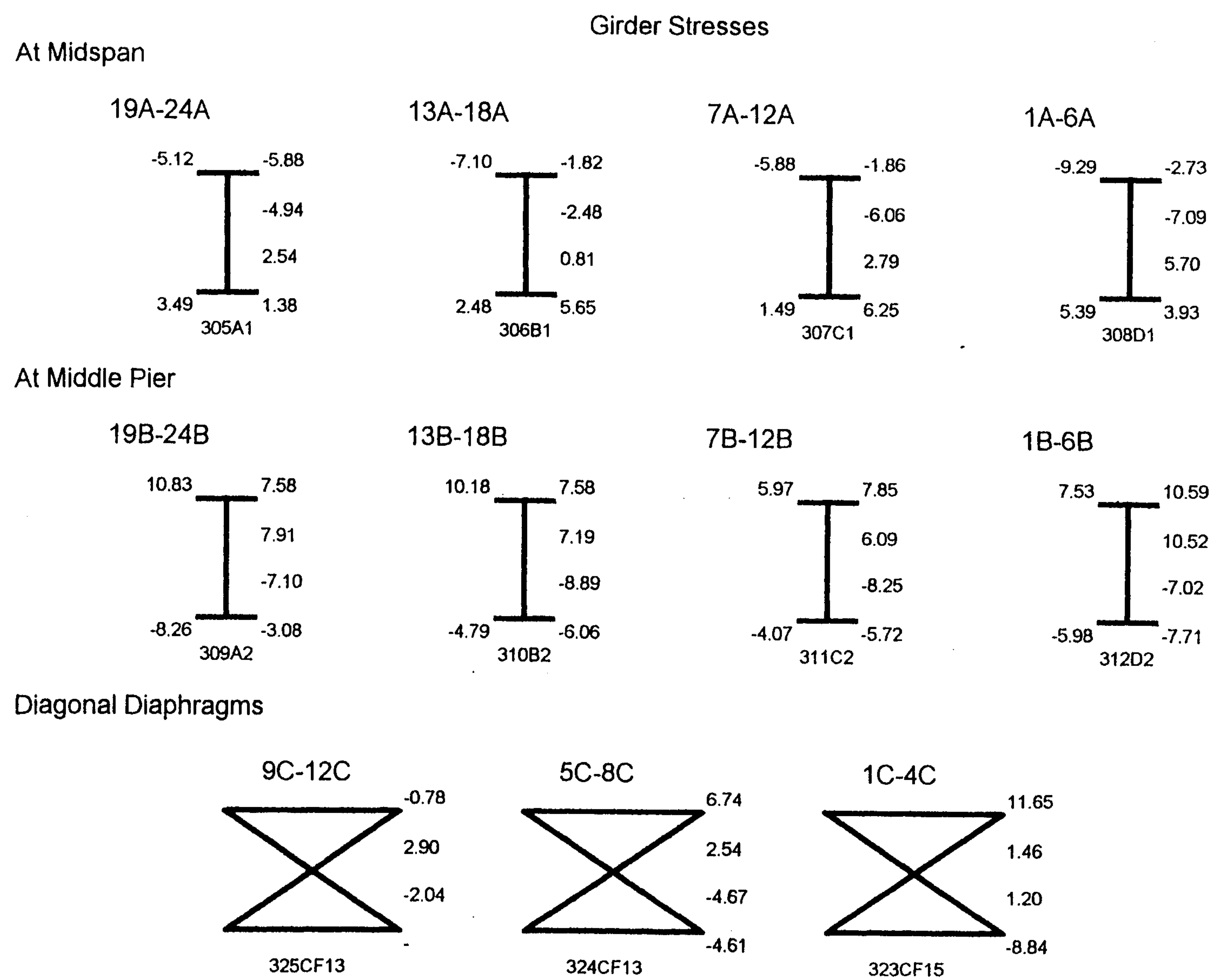

Figure B-17. Magnitude of girder stresses for stage 8 (8:15 a.m.)

POURING OF THE CONCRETE DECK PLOTS

CHANGE IN STRESSES OBSERVED

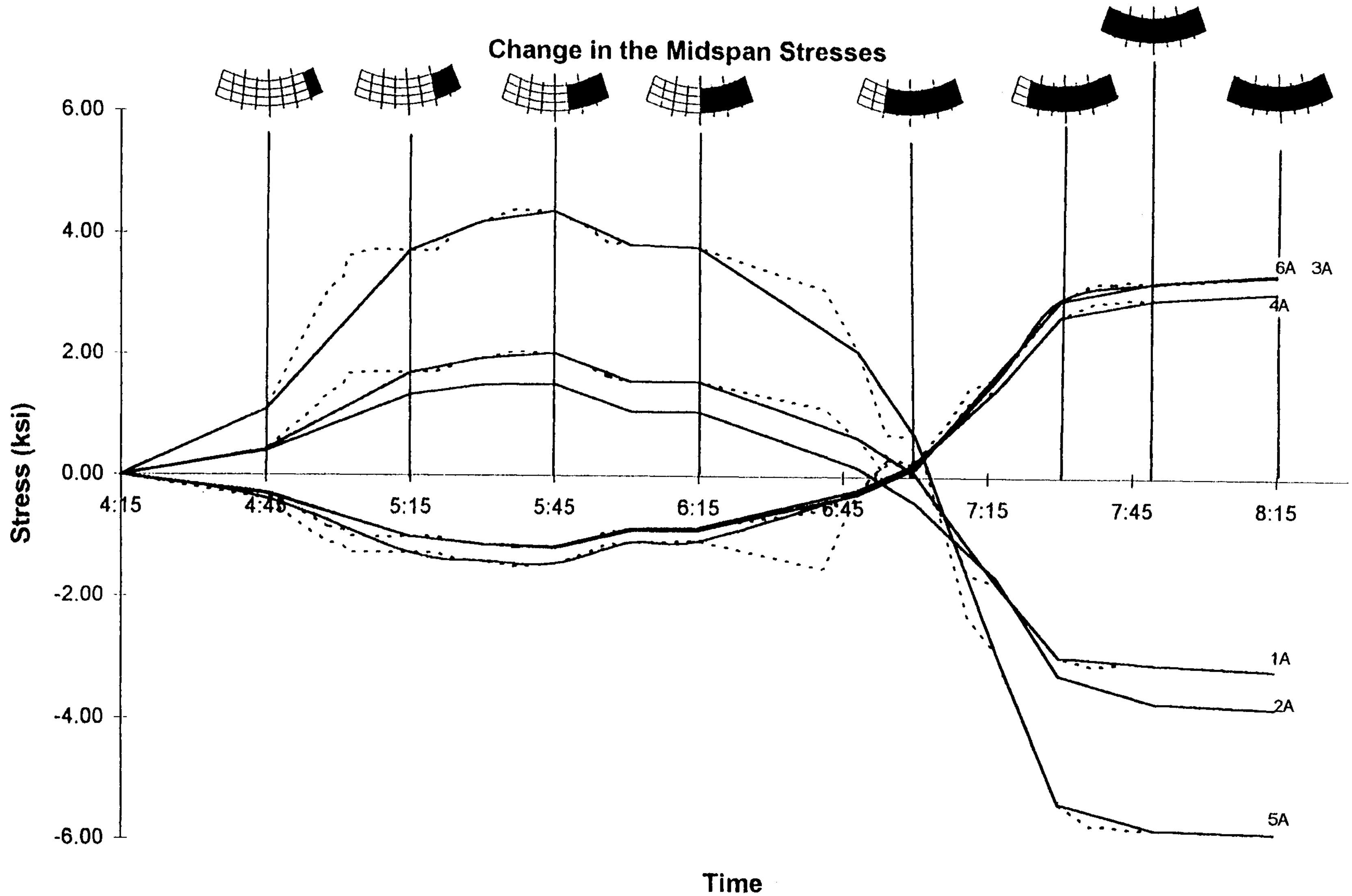

Figure B-18. Change in Stress for Gages 1A-6A During the Pouring of the Concrete Deck

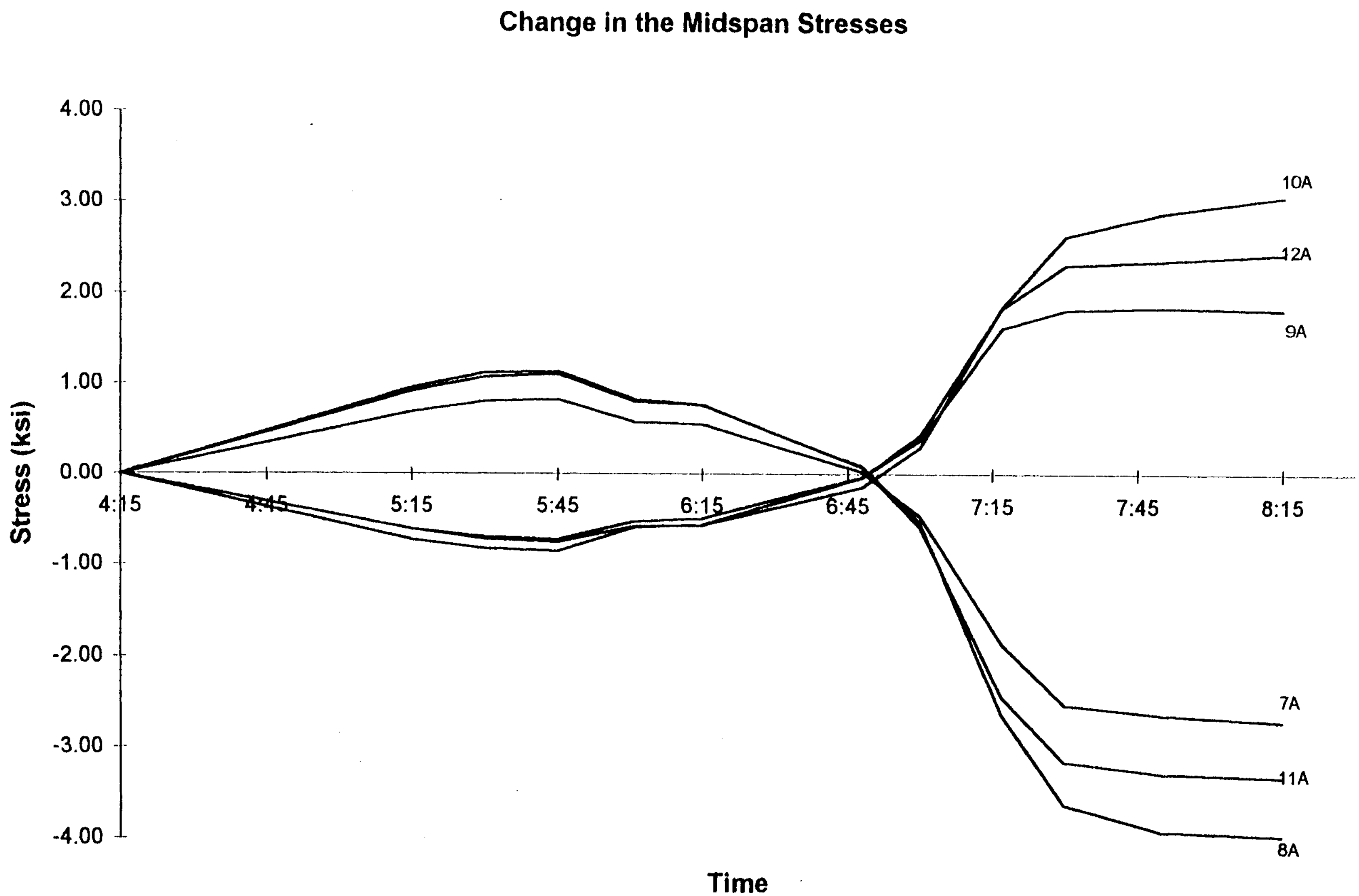

Figure B-19. Change in Stress for Gages 7A-12A During the Pouring of the Concrete Deck

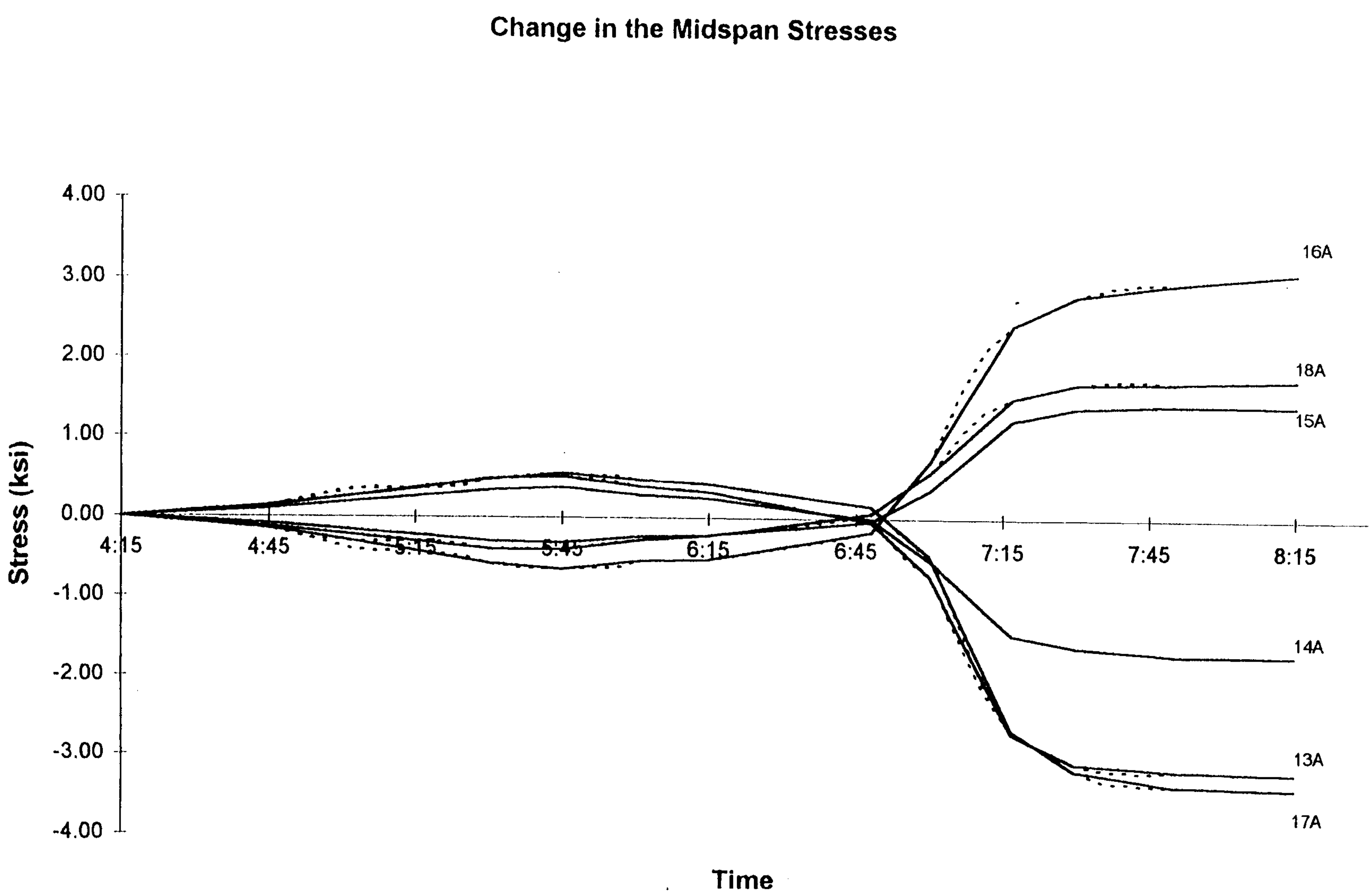

Figure B-20. Change in Stress for Gages 13A-18A During the Pouring of the Concrete Deck

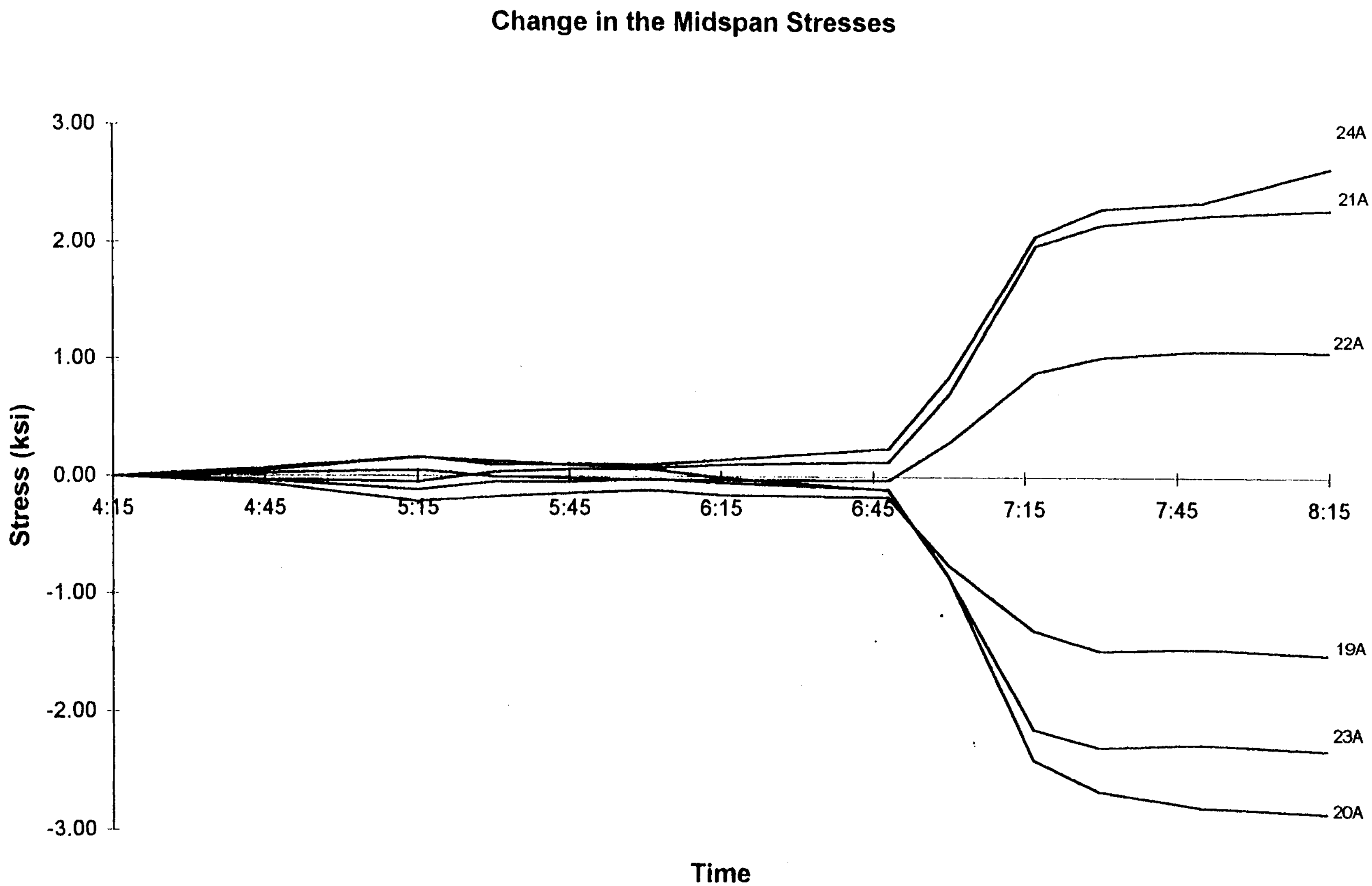

Figure B-21. Change in Stress for Gages 18A-24A During the Pouring of the Concrete Deck

Change in the Middle Pier Stresses

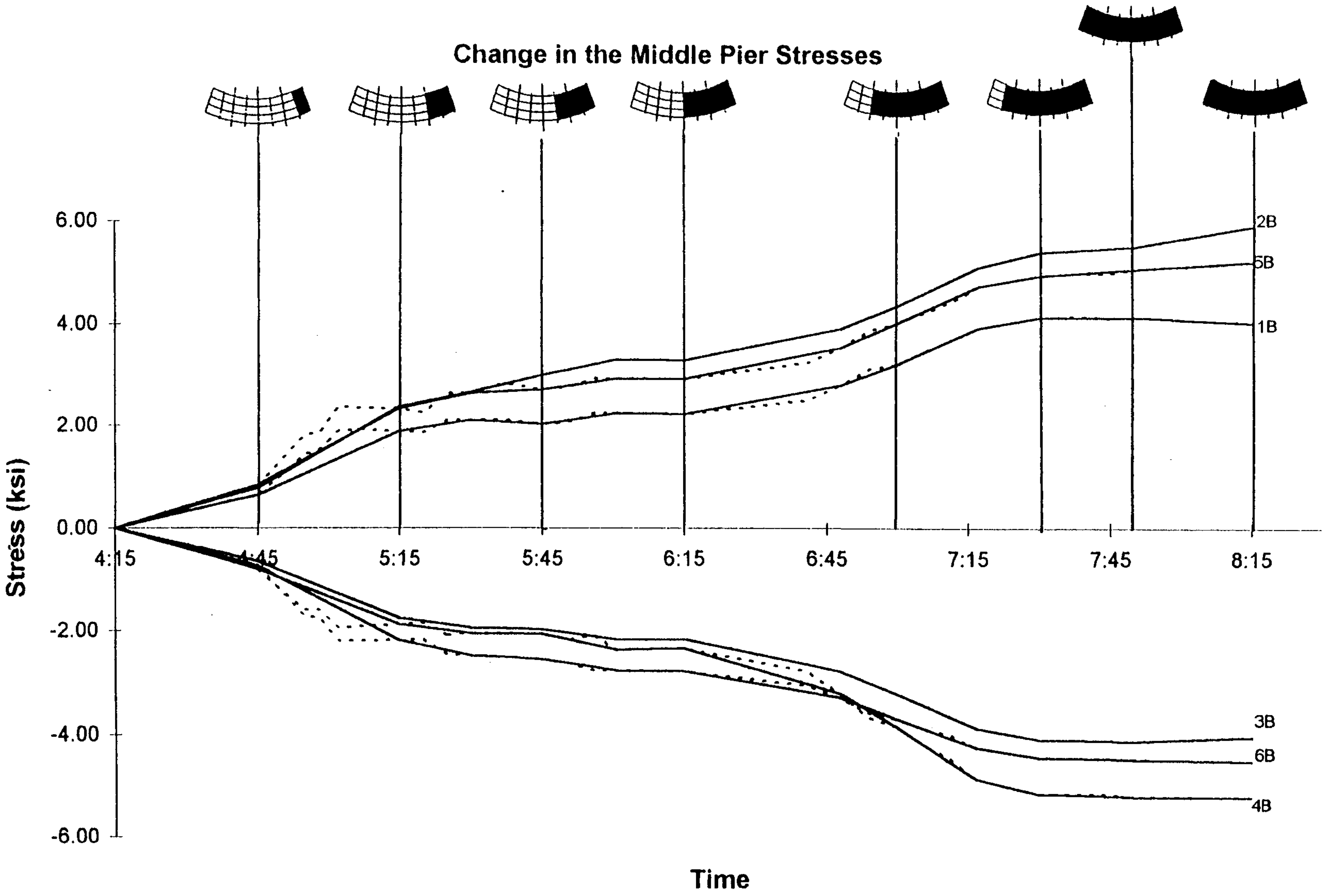

Figure B-22. Change in Stress for Gages 1B-6B During the Pouring of the Concrete Deck

Change in the Middle Pier Stresses

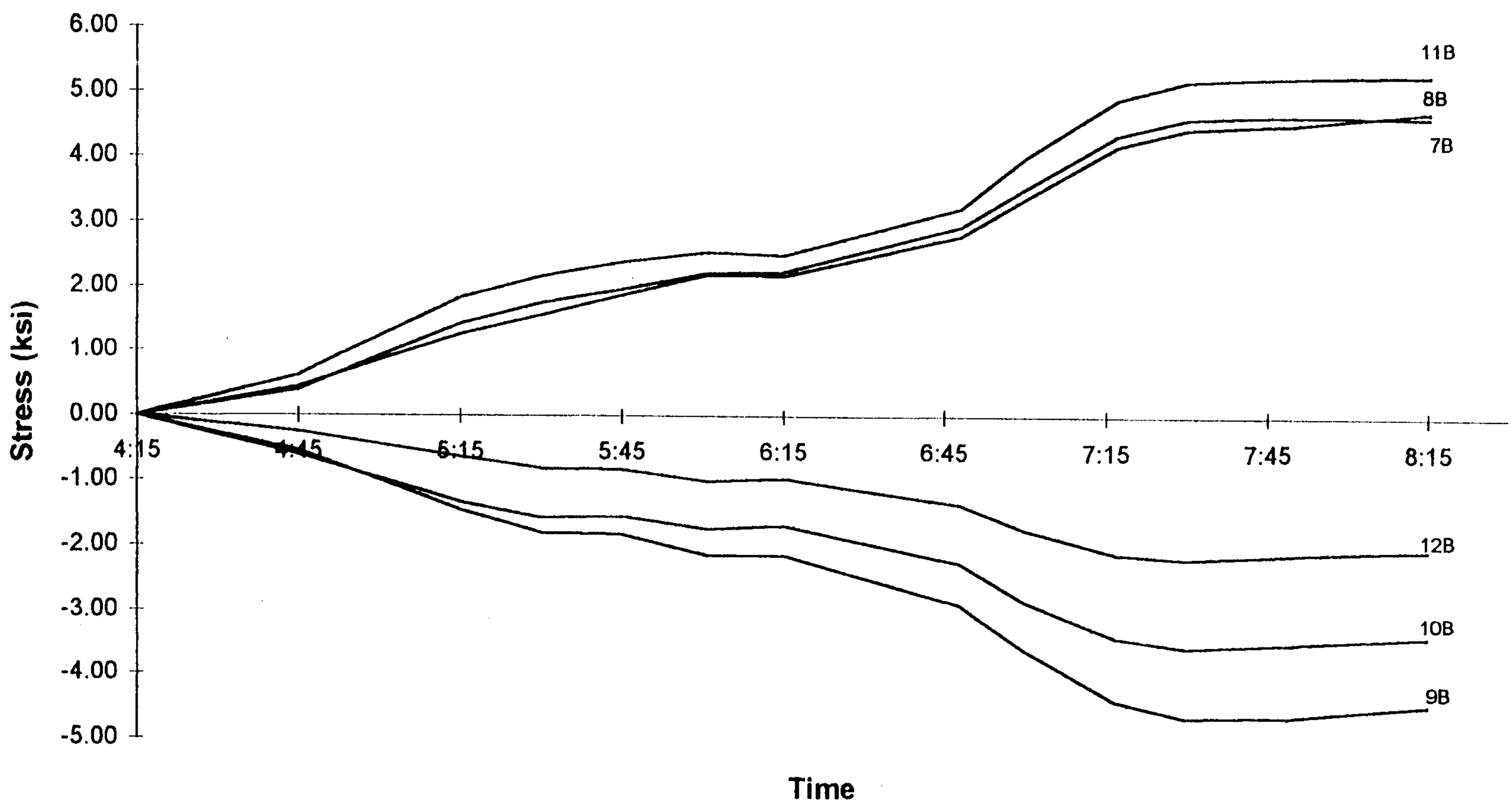

Figure B-23. Change in Stress for Gages 7B-12B During the Pouring of the Concrete Deck

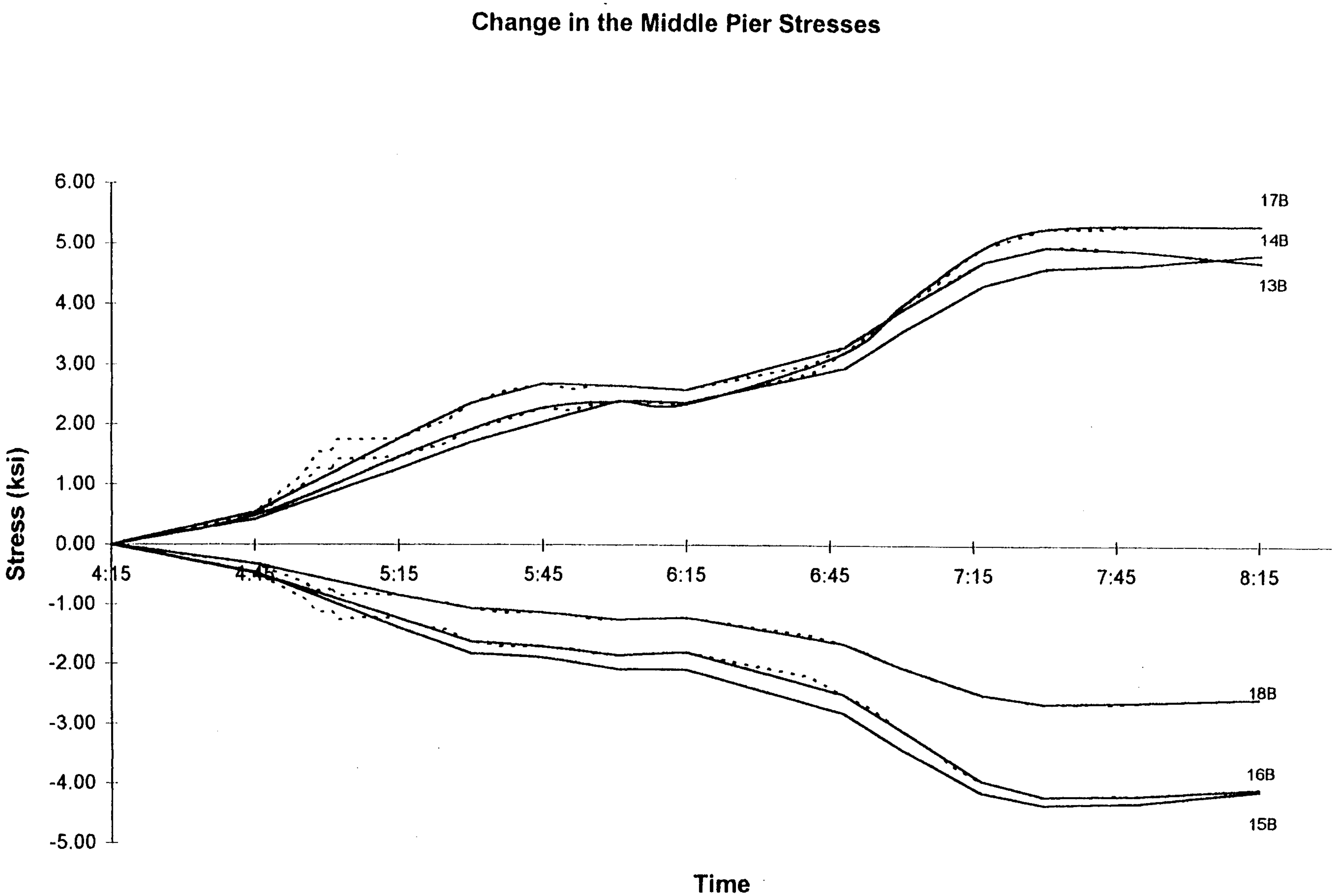

Figure B-24. Change in Stress for Gages 13B-18B During the Pouring of the Concrete Deck

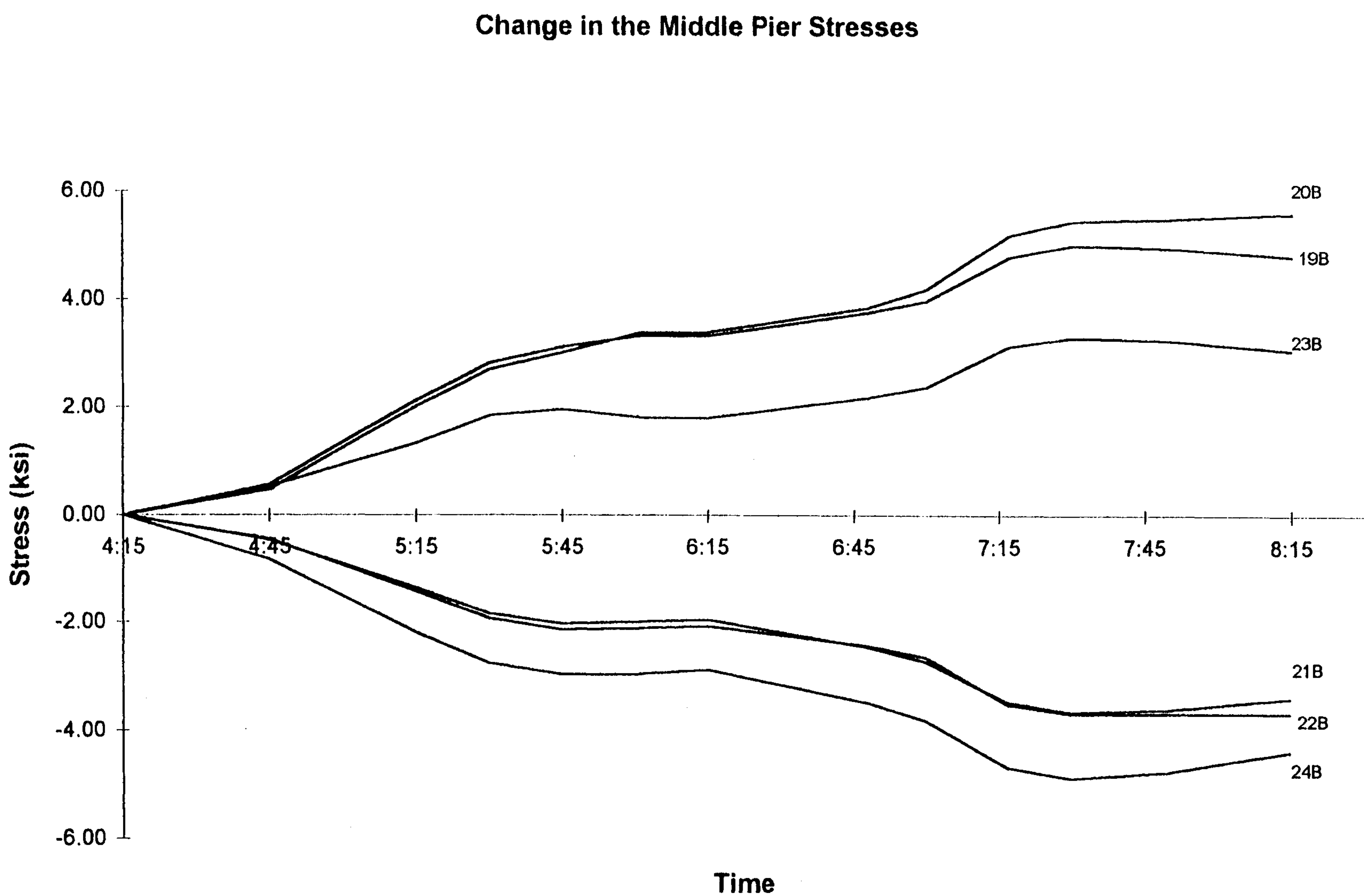

Figure B-25. Change in Stress for Gages 19B-24B During the Pouring of the Concrete Deck

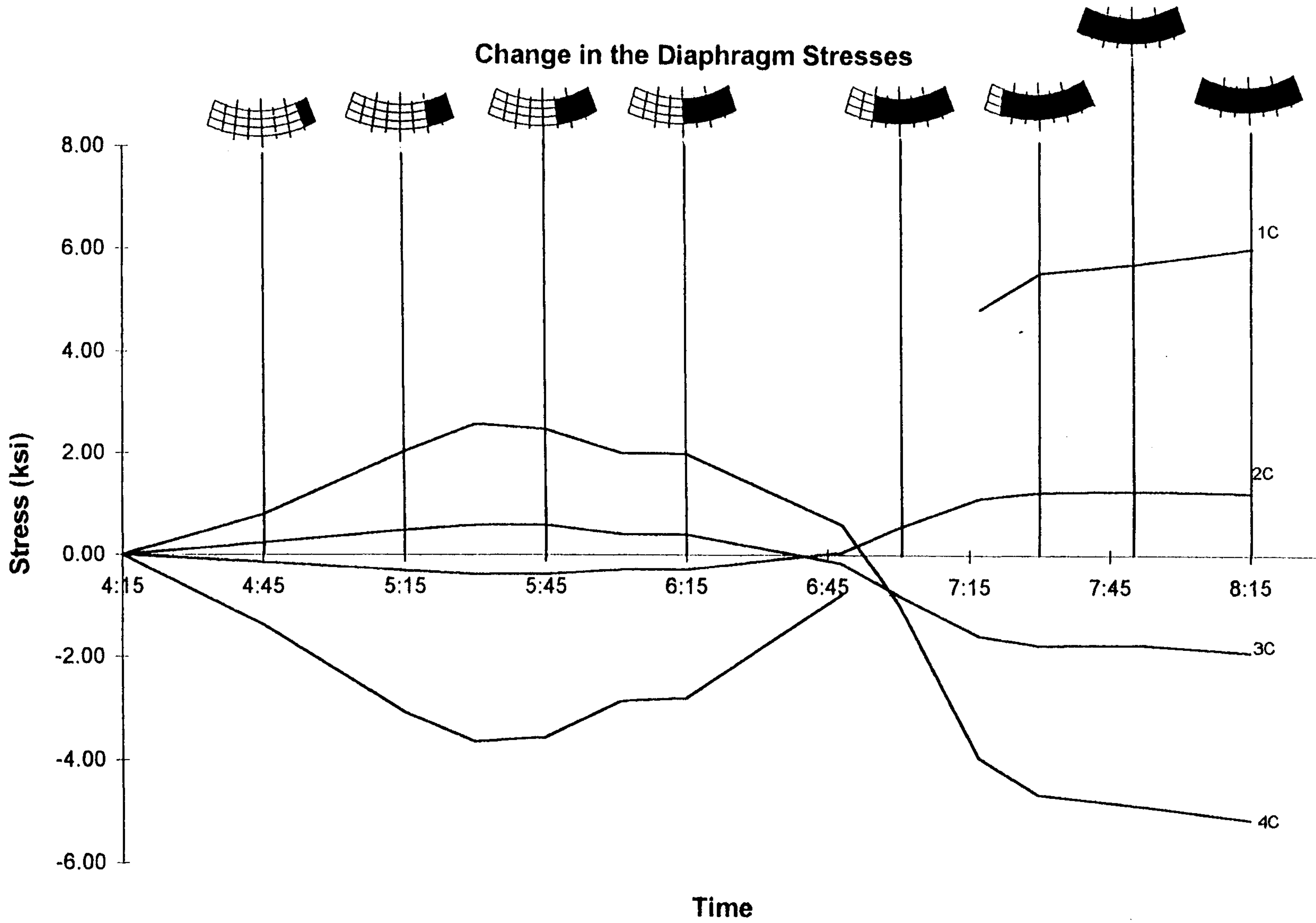

Figure B-26. Change in Stress for Gages 1C-4C During the Pouring of the Concrete Deck

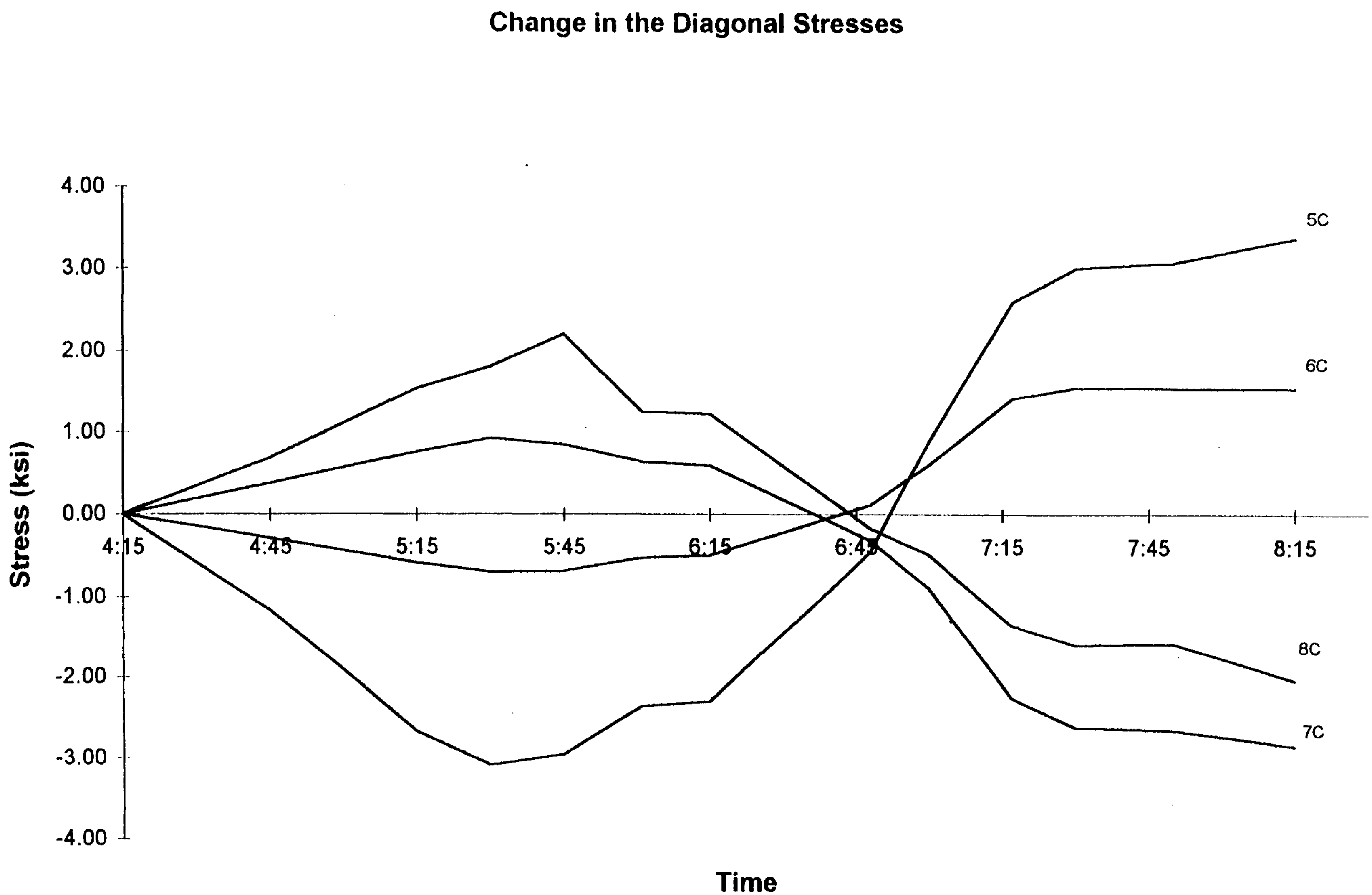

Figure B-27. Change in Stress for Gages 5C-8C During the Pouring of the Concrete Deck

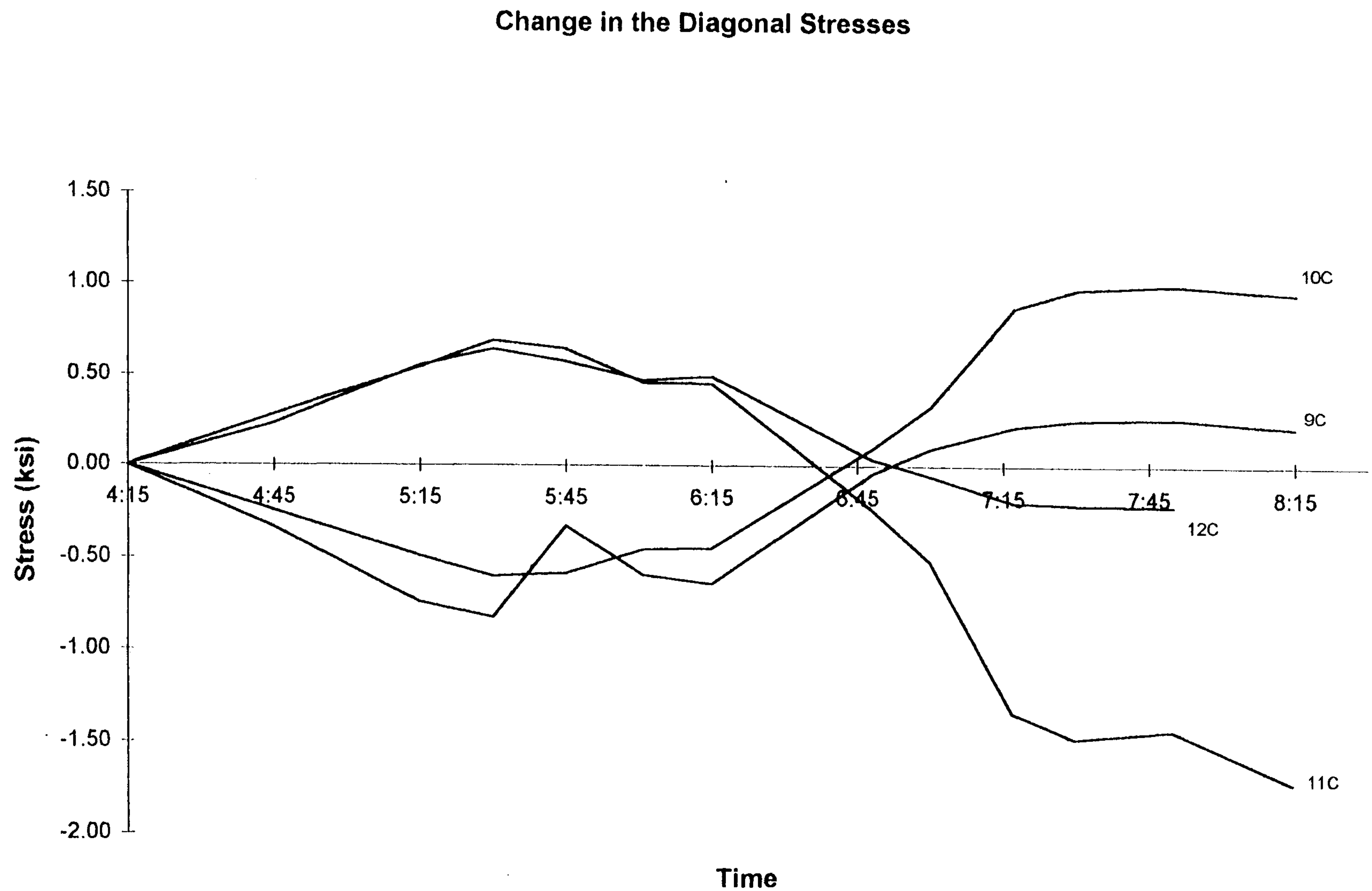

Figure B-28. Change in Stress for Gages 9C-12C During the Pouring of the Concrete Deck

POURING OF THE CONCRETE DECK PLOTS

ACTUAL STRESSES OBSERVED

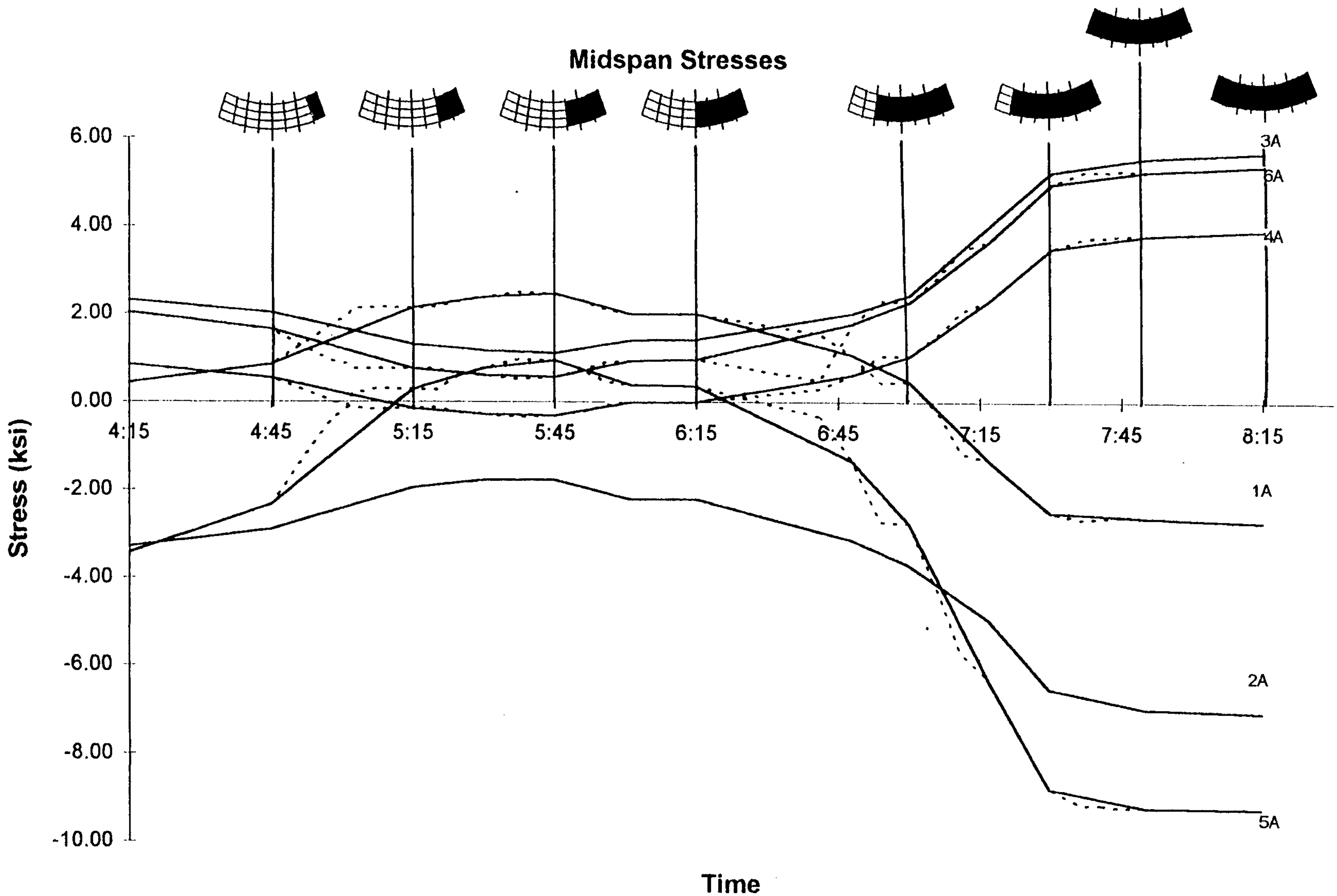

Figure B-29. - Magnitude of Stress for Gages 1A-6A Measured During the Pouring of the Concrete Deck

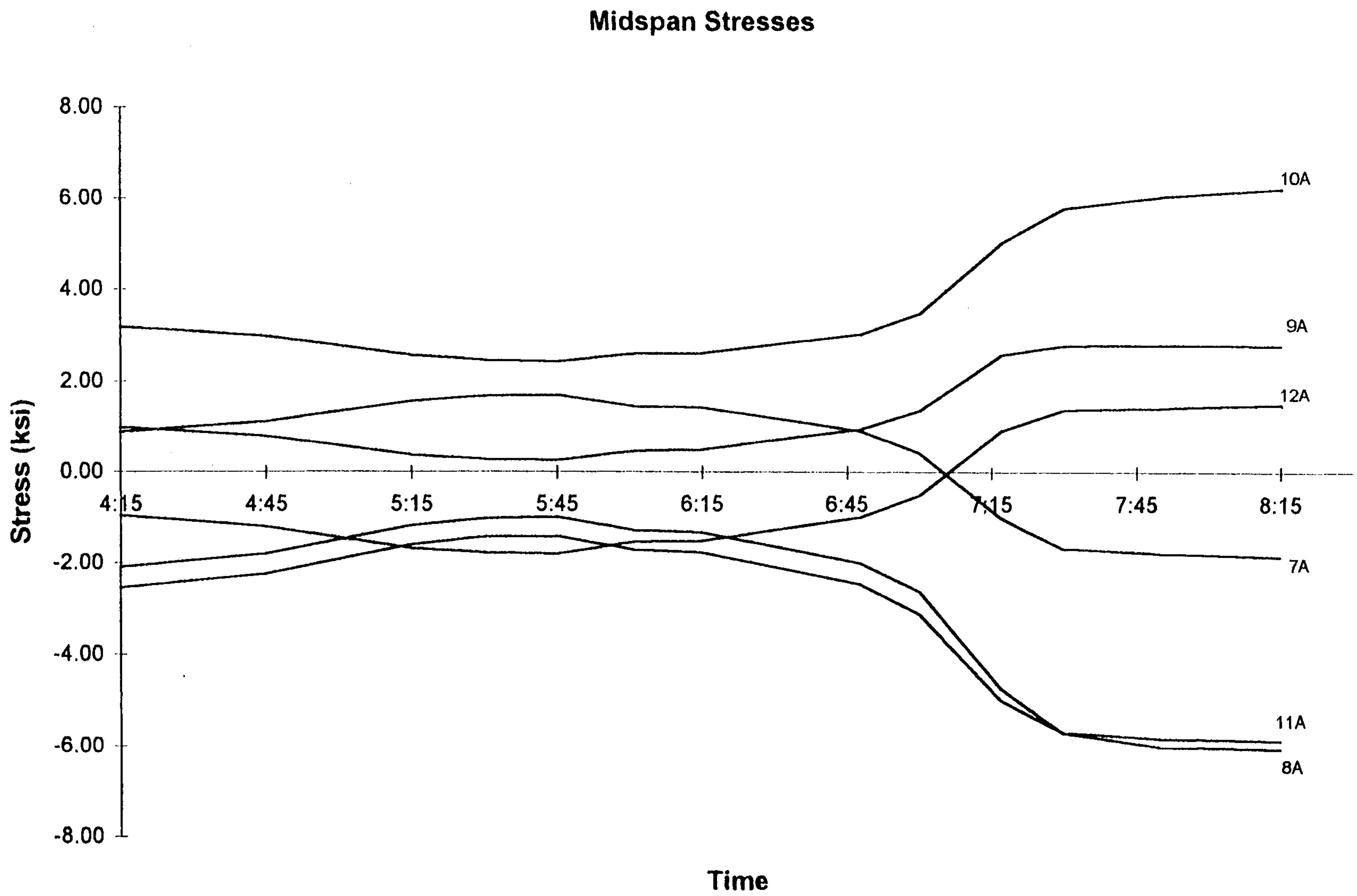

Figure B-30. Magnitude of Stress for Gages 7A-12A Measured During the Pouring of the Concrete Deck

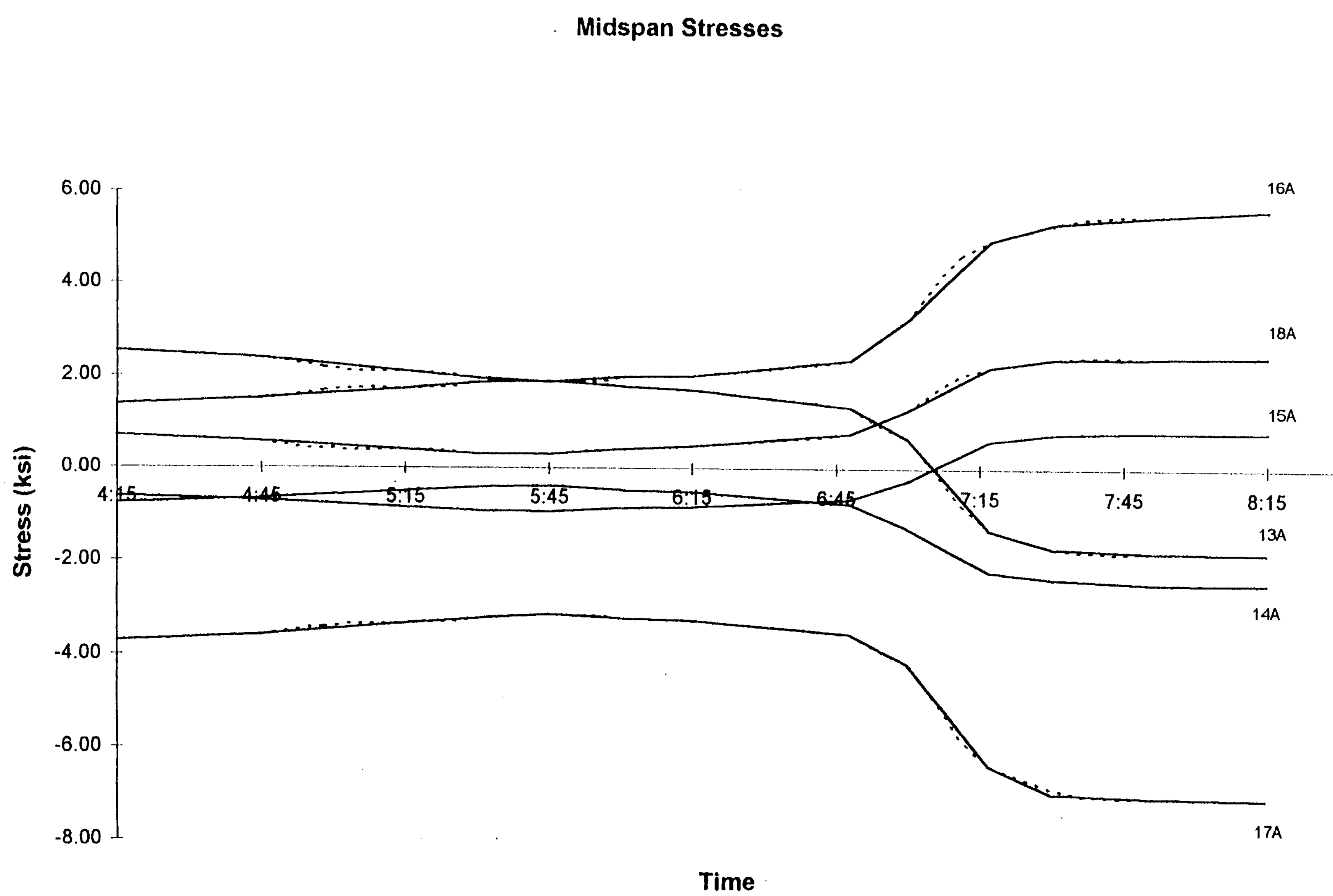

Figure B-31. Magnitude of Stress for Gages 13A-18A Measured During the Pouring of the Concrete Deck

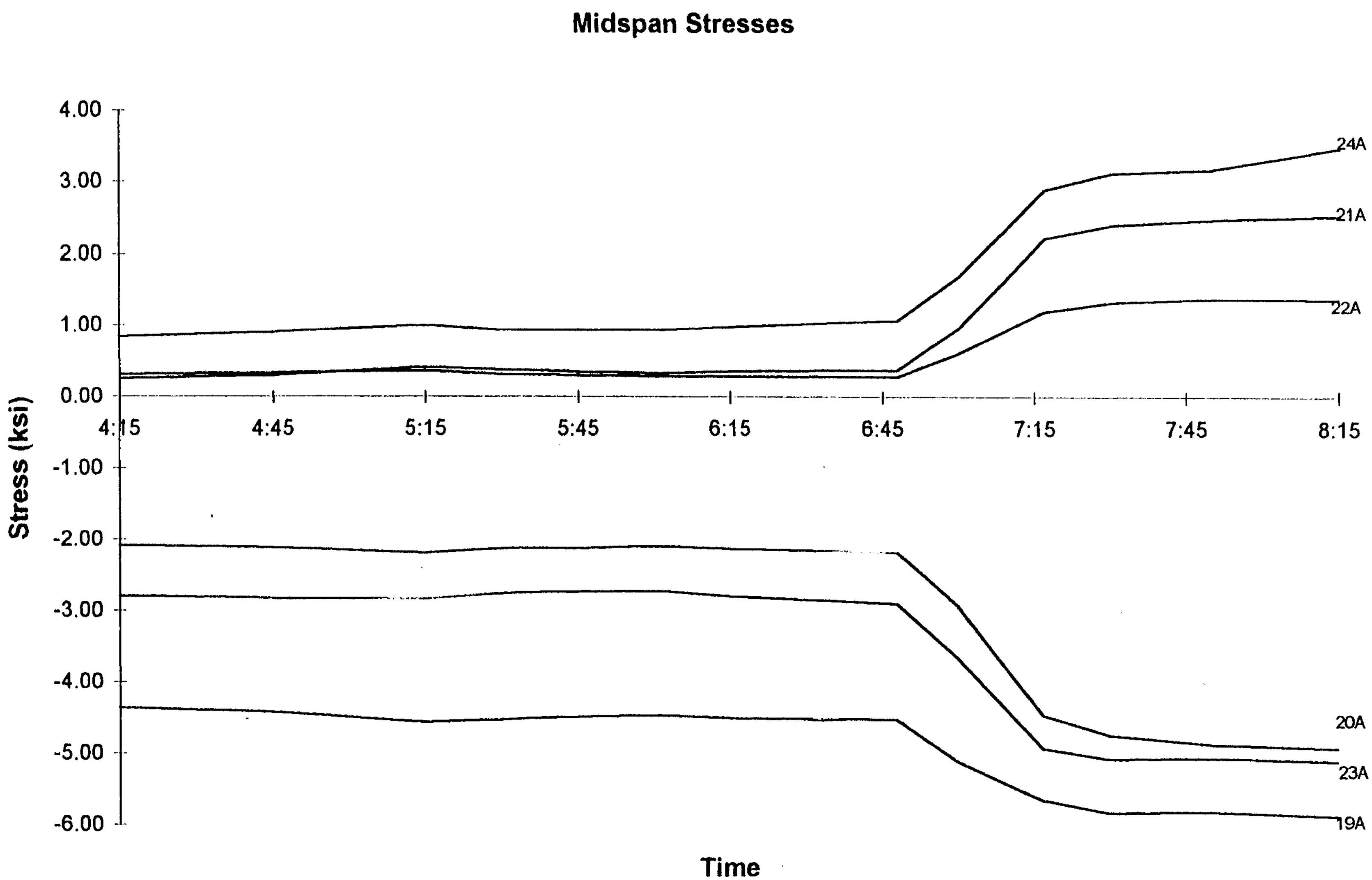

Figure B-32. Magnitude of Stress for Gages 19A-24A Measured During the Pouring of the Concrete Deck

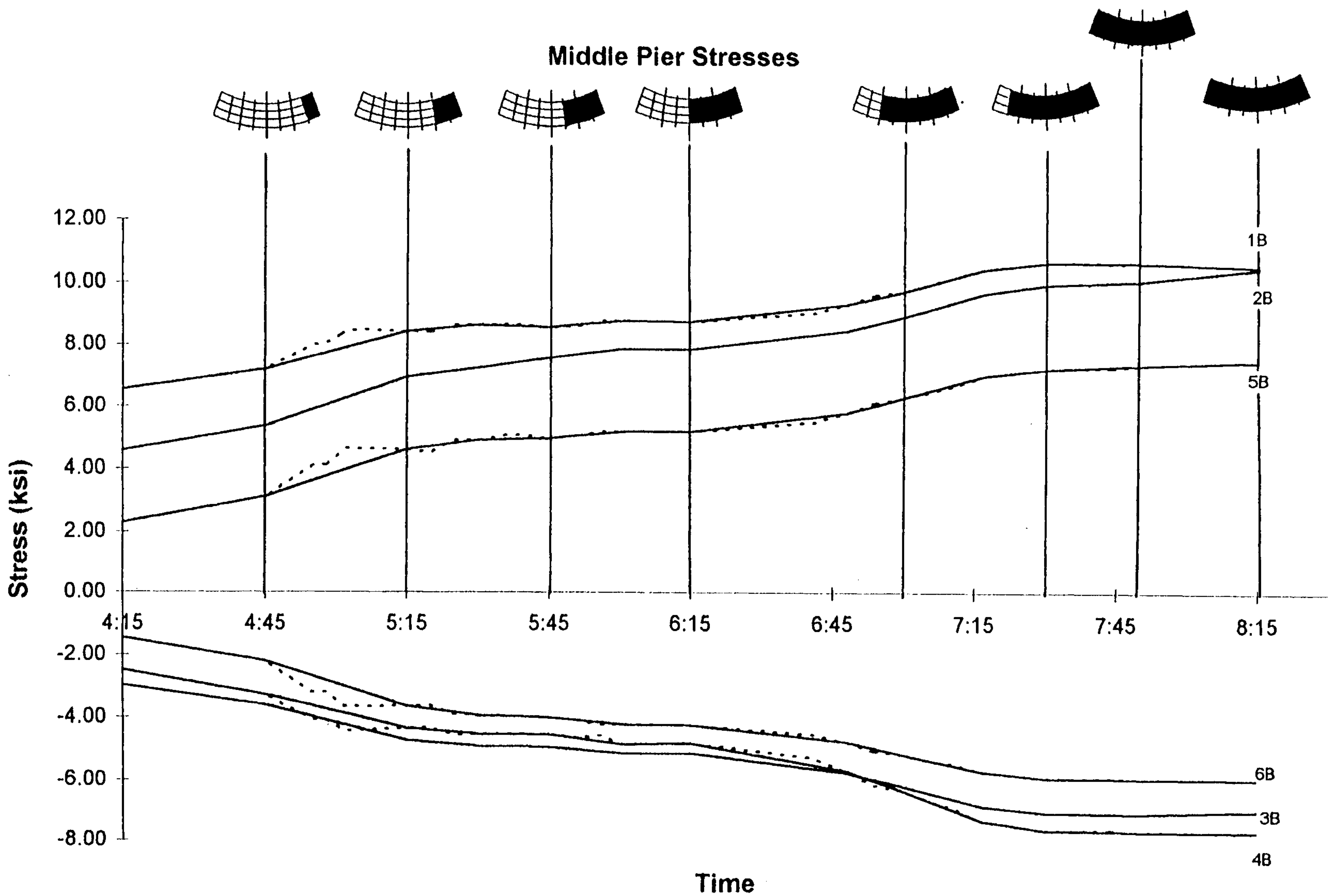

Figure B-33. Magnitude of Stress for Gages 1B-6B Measured During the Pouring of the Concrete Deck

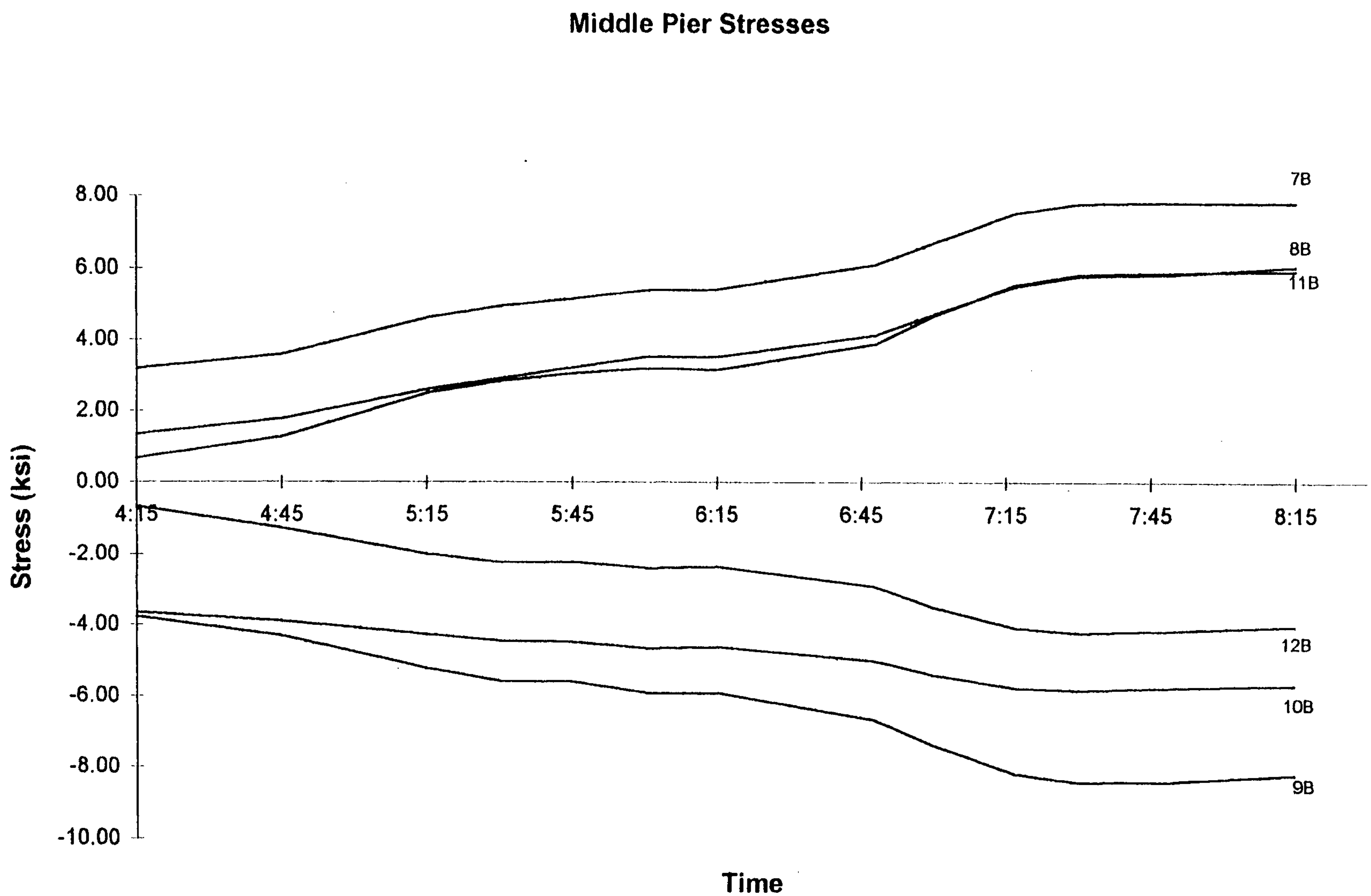

Figure B-34. Magnitude of Stress for Gages 7B-12B Measured During the Pouring of the Concrete Deck

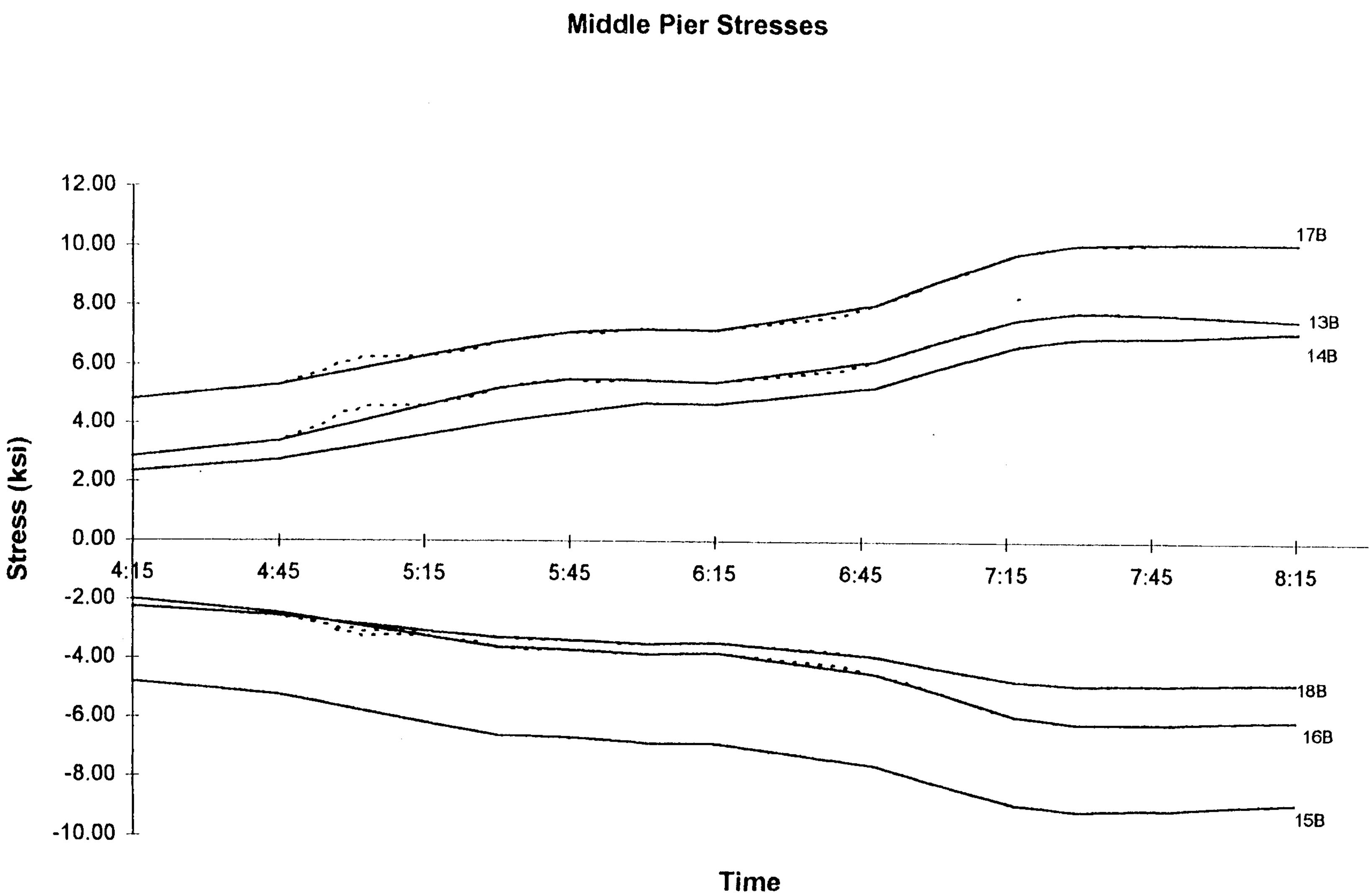

Figure B-35. Magnitude of Stress for Gages 13B-18B Measured During the Pouring of the Concrete Deck

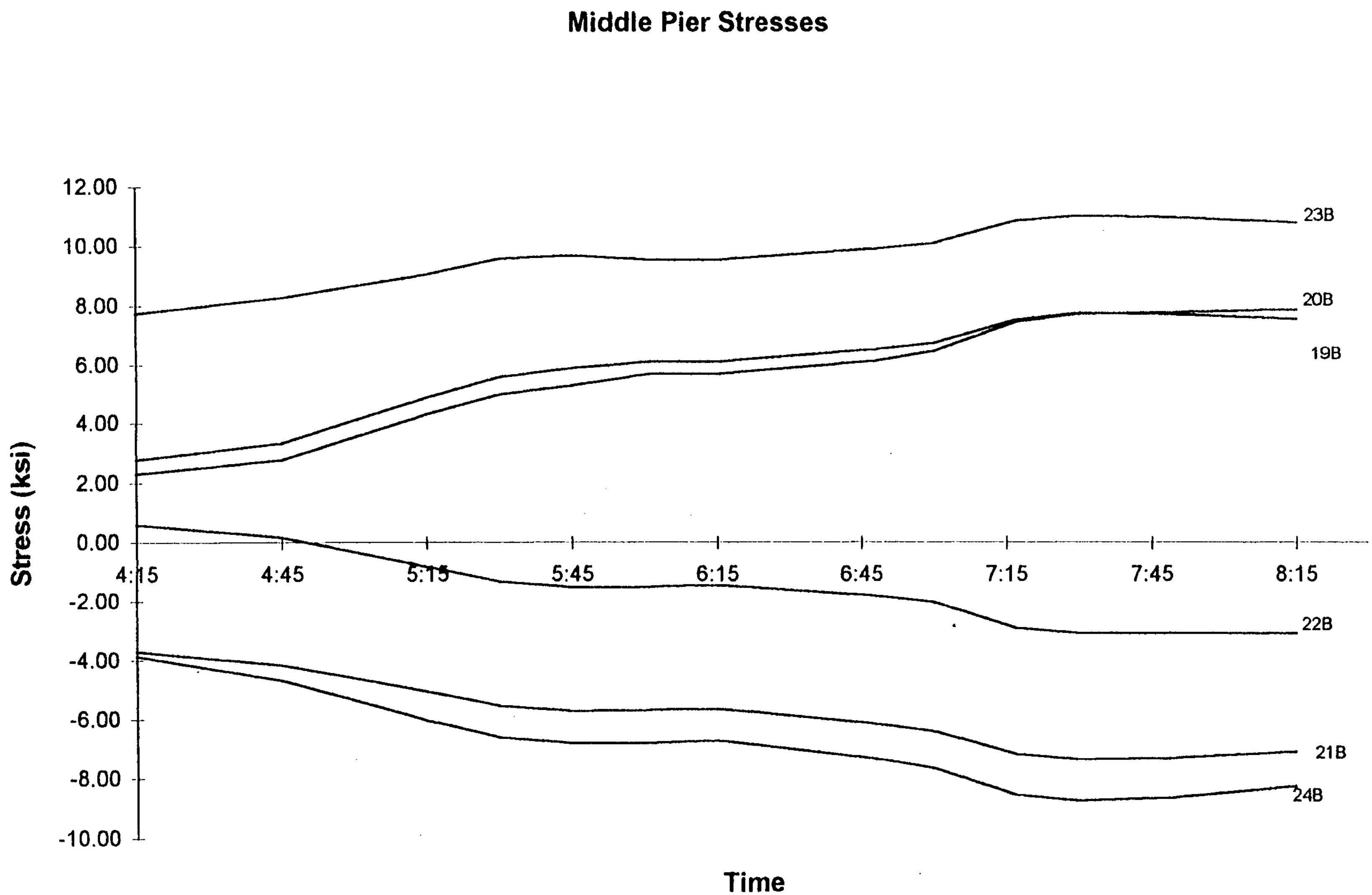

Figure B-36. Magnitude of Stress for Gages 19B-24B Measured During the Pouring of the Concrete Deck

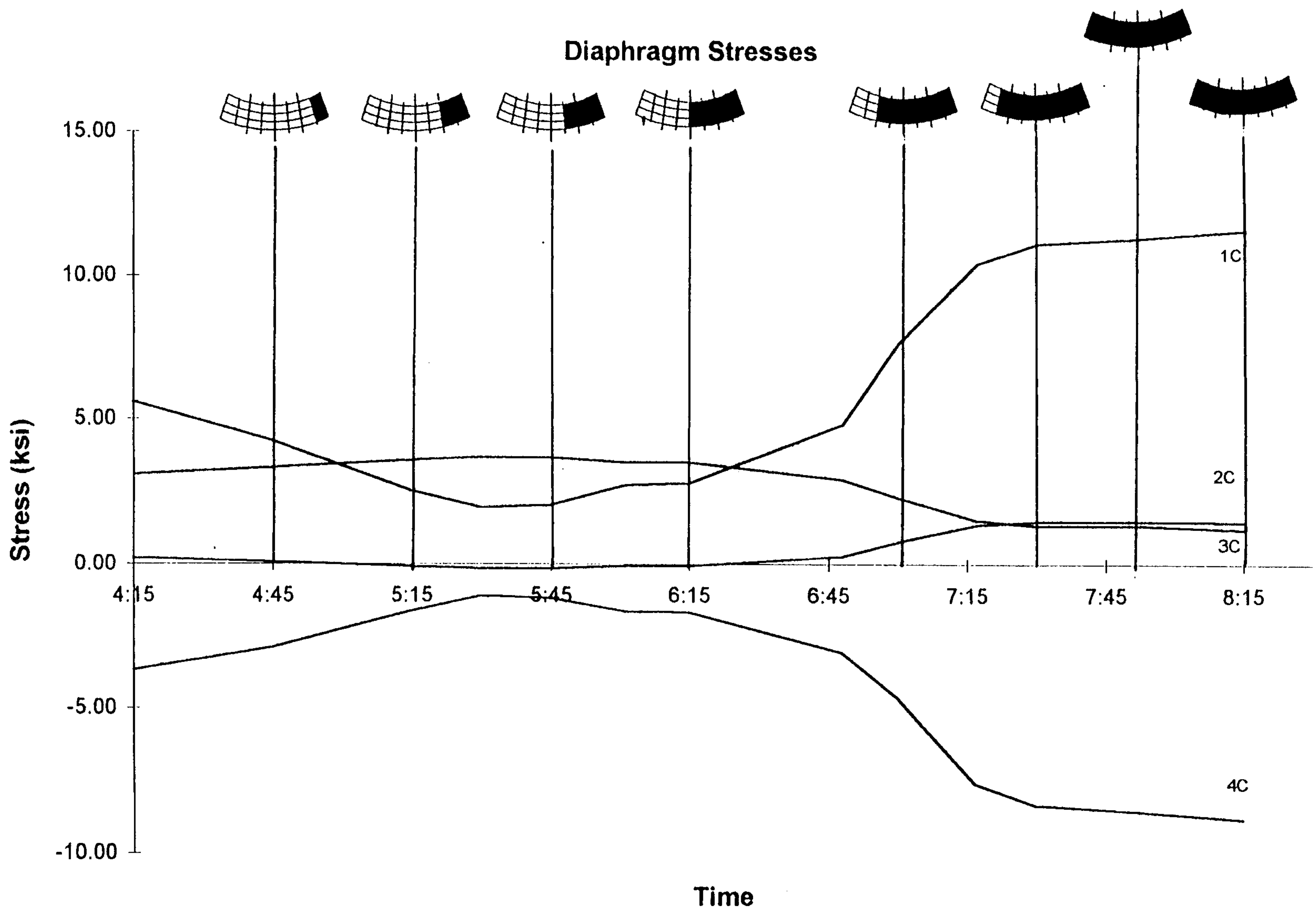

Figure B-37. Magnitude of Stress for Gages 1C-4C Measured During the Pouring of the Concrete Deck

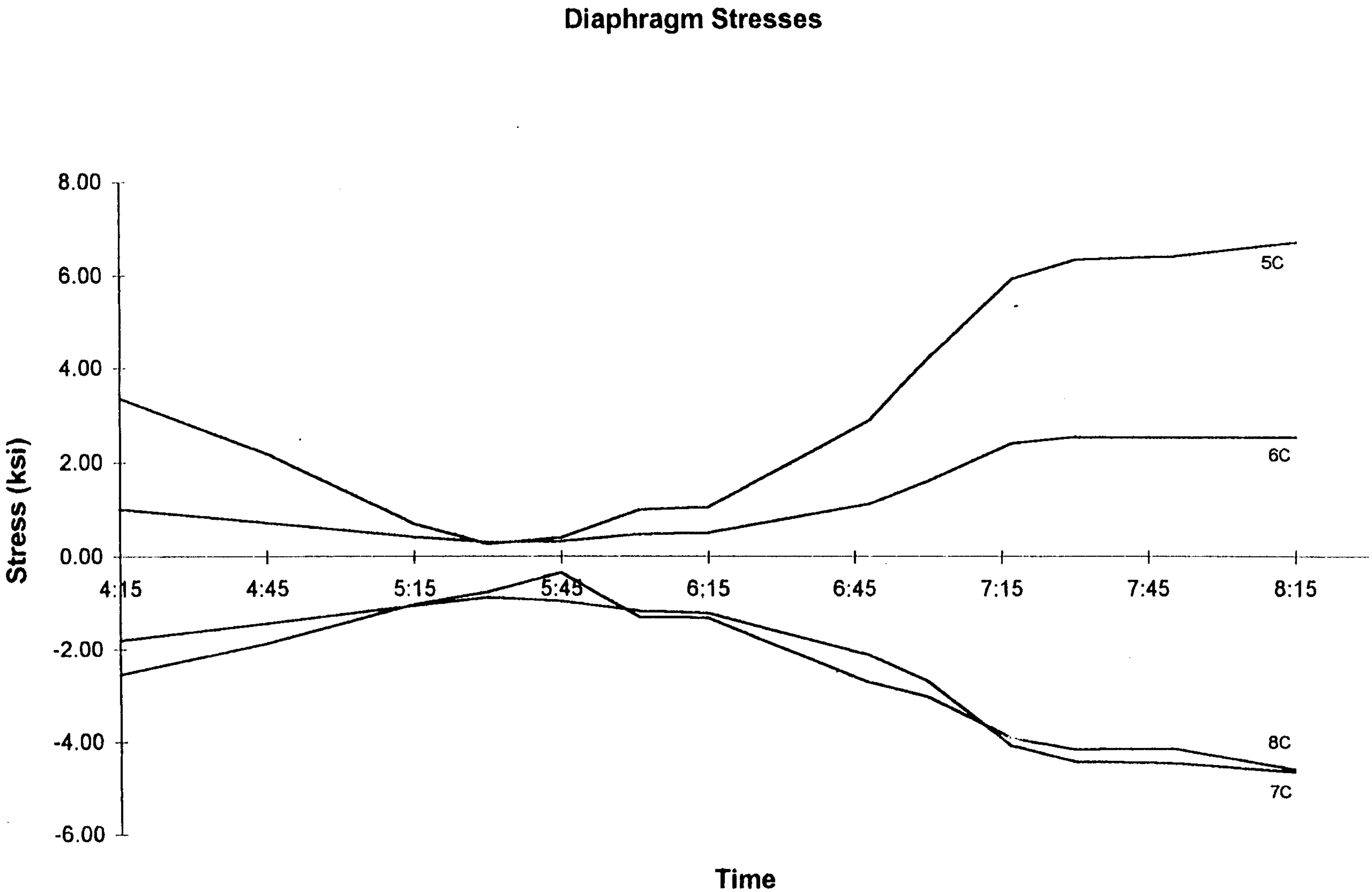

Figure B-38. Magnitude of Stress for Gages 5C-8C Measured During the Pouring of the Concrete Deck

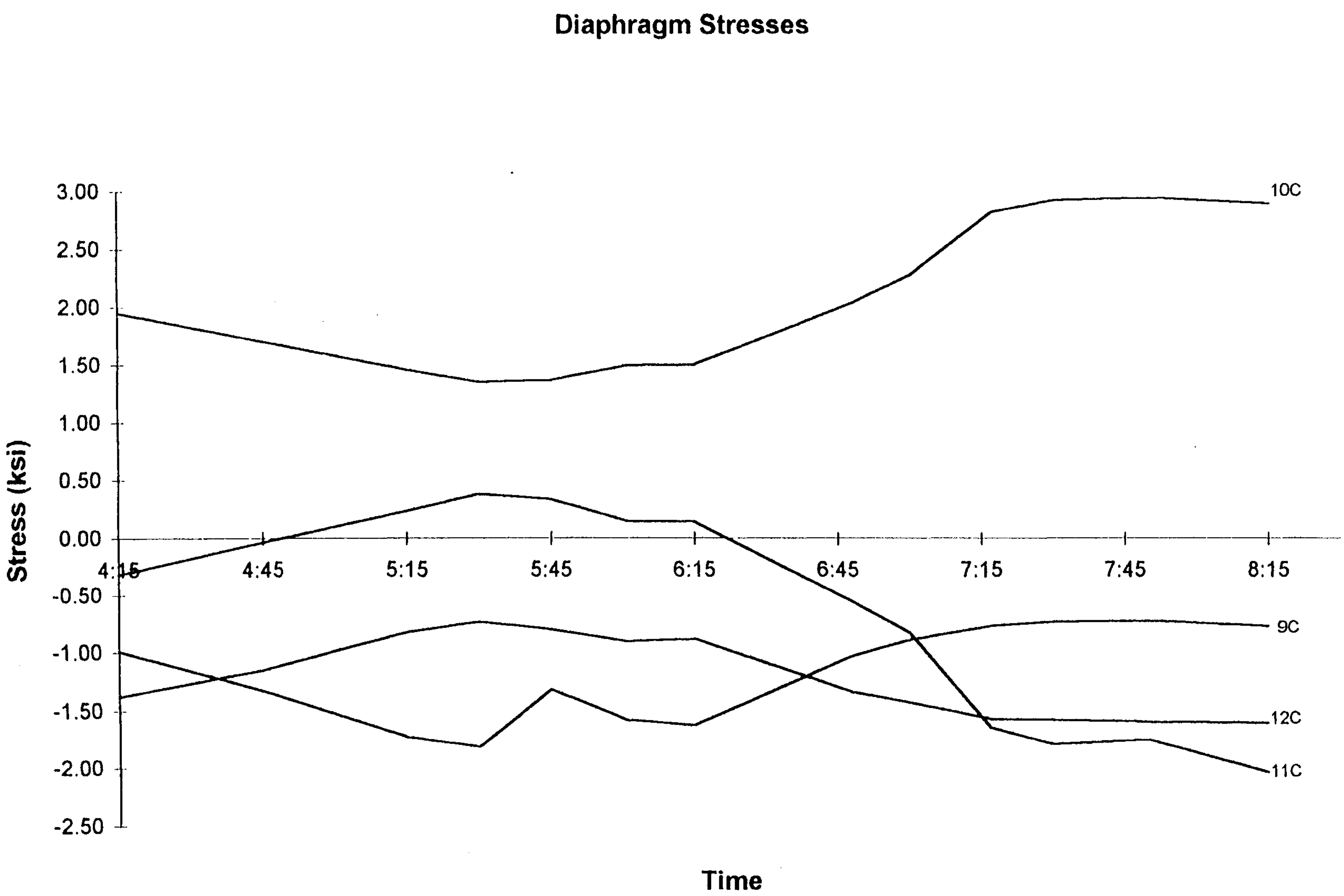

Figure B-39. Magnitude of Stress for Gages 9C-12C Measured During the Pouring of the Concrete Deck

APPENDIX C

STRESSES DUE TO TRUCK LIVE LOADING

APPENDIX C

STRESSES DUE TO TRUCK LIVE LOADING

This appendix presents the stresses due to truck live loading applied to MN/DOT Bridge 27998.

OBSERVATIONS OF GIRDER STRESSES

Notes:

The centerline of front wheels of each truck coincides with the line of crossframe; e.g., Case 2 on line 5.

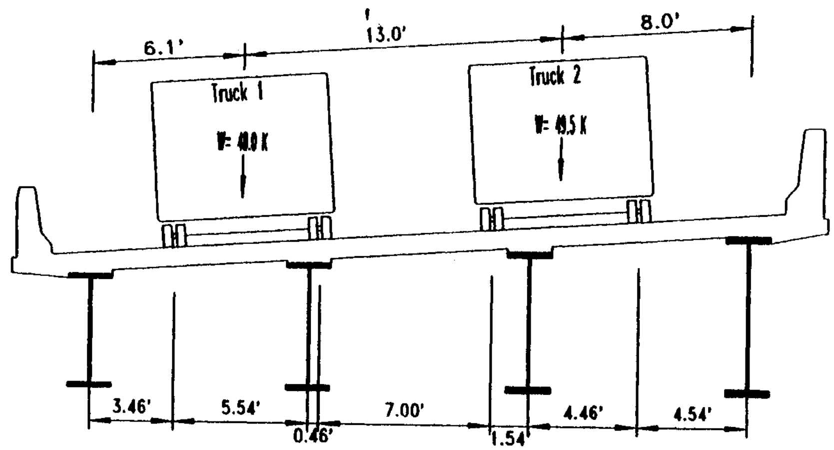

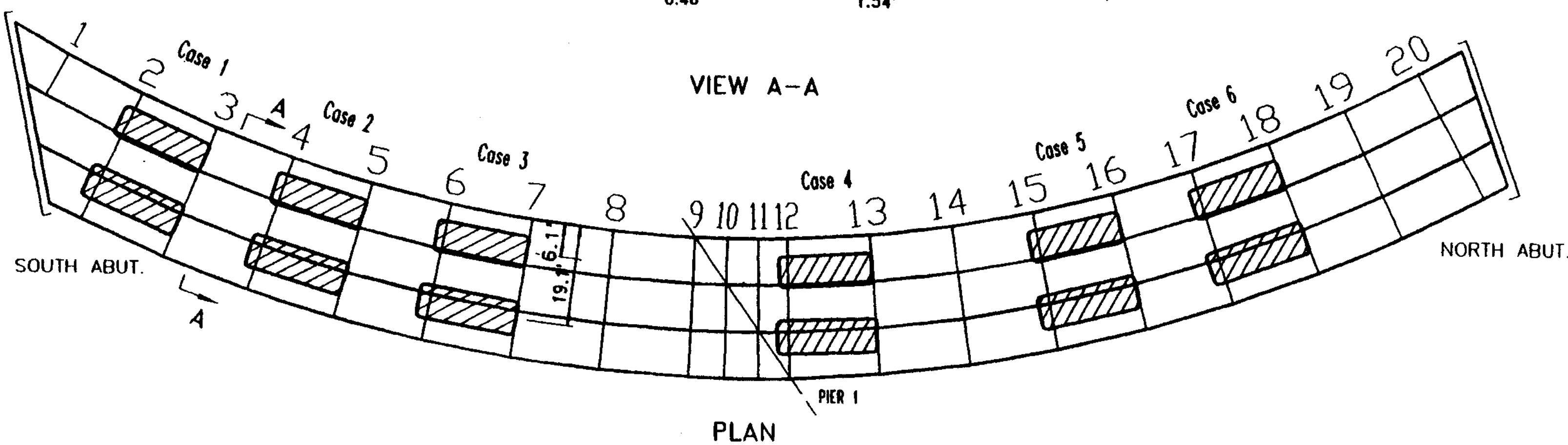

Figure C-1a. Plan of field tests for cases 1 to 6

Notes:

The centerline of front wheels of each truck coincides with the line of crossframe; e.g., Case 8 on lines 5 & 7 for trucks 1 and 2 respectively

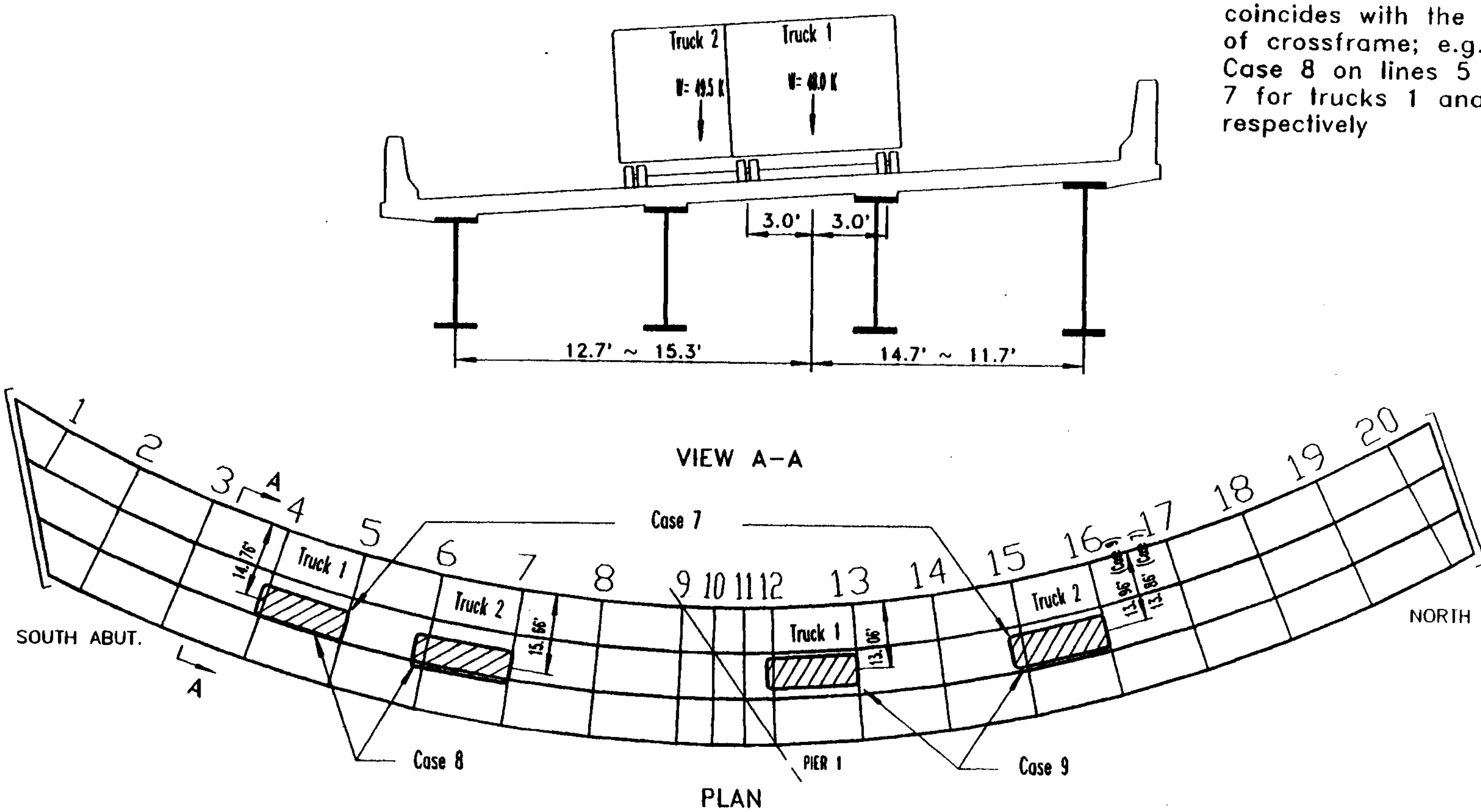

Figure C-1b. Plan of field tests for cases 7 to 9

Notes:

The centerline of front wheels of each truck coincides with the line of crossframe; e.g., Case 11 on line 5.

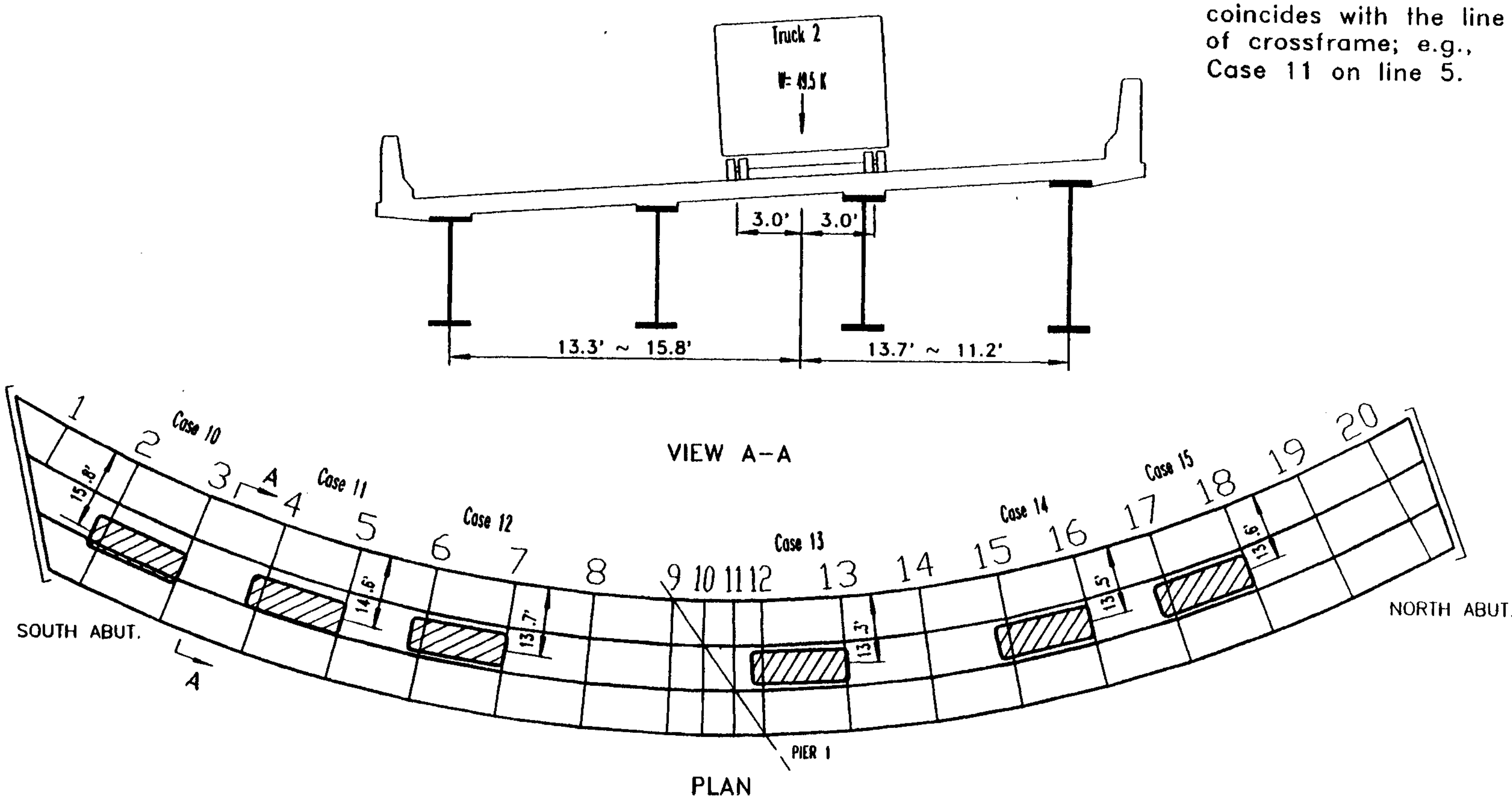

Figure C-1c. Plan of field tests for cases 10 to 15

Date and Time of Reading: October 7, 1995 at 11:25 p.m.

Temperature: 8 °C

Weather: Partly Cloudy

Loading Condition: Two 50 kip trucks were placed side by side at the first quarter point of span 1.

Objective of Reading: This reading was taken to observe the change in stress due to the loading condition mentioned above

General Observations: At the midspan gages except for girder 4, the top flanges experienced compression, and the bottom flanges experienced tension. This behavior is as expected for loading in span 1 which results in a positive moment region being formed at the midspan of the girders. It appears that the loading was not significant enough to cause the entire top flange of girder 4 to experience compressive forces. The range for stress increase was -0.03 to -0.15 ksi for the top flanges and 0.31 to 0.53 ksi for the bottom flanges. The stresses in the top flanges did not increase appreciably which could be due to the composite action in this region. At the middle pier gages, as expected for a negative moment region, the top flanges experienced tension and the bottom flanges experienced compression. The range of stress increase was 0.01 to 0.06 ksi in the top flanges and -0.15 to -0.37 ksi in the bottom flanges. It appears that there is some composite action occurring at the top flanges and the concrete. There are no shear connectors in this region, so this might be resulting from friction between the two materials. The loading appears to not have been significant enough to break the bond between the top of the girders and the concrete deck. The top two members in the diaphragms displayed an increase in tension, 0.09 to 0.26 ksi, and the bottom two members displayed an increase in compression, -0.05 to -0.60 ksi.

Notes on Specific Gages: Not Applicable

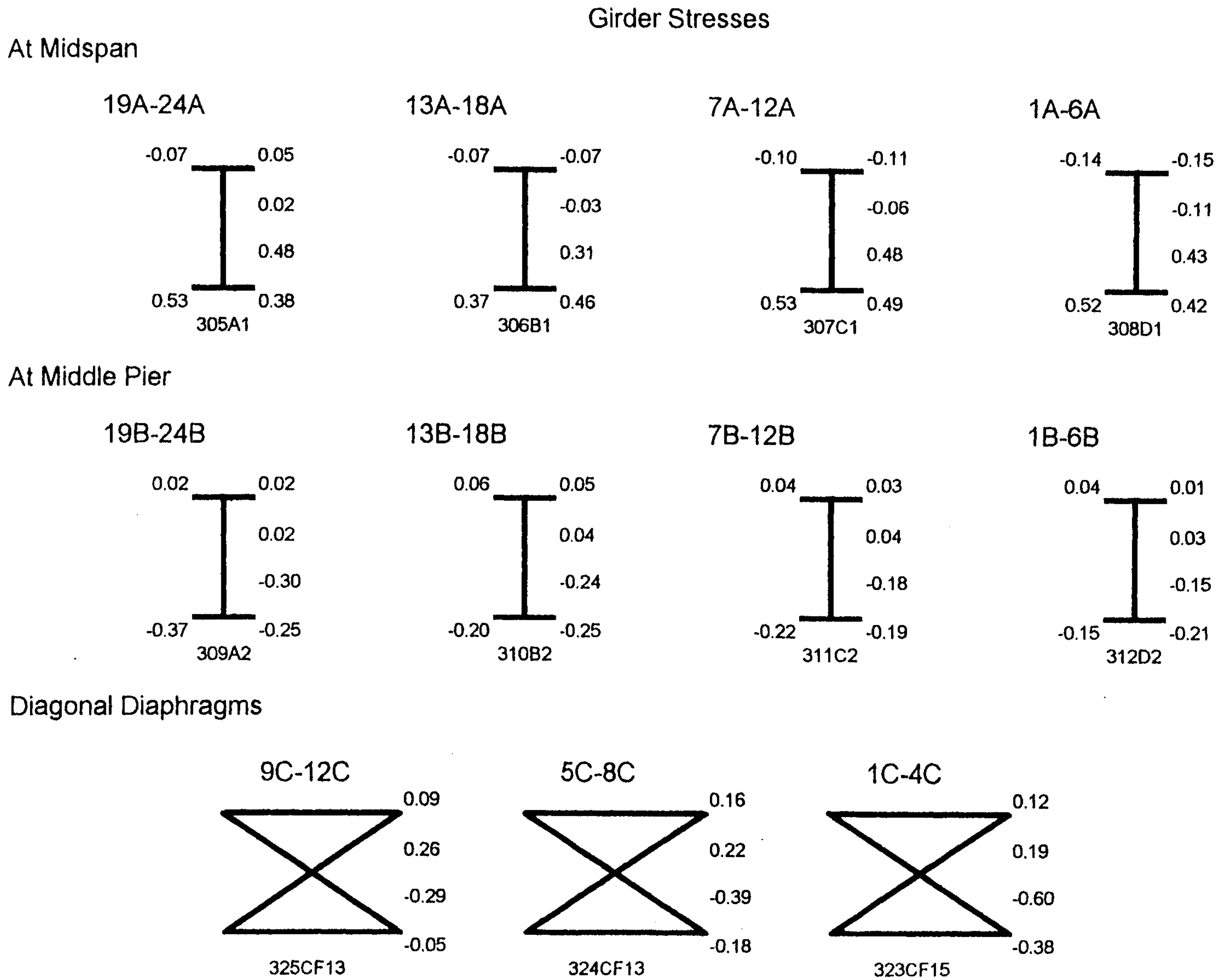

Figure C-2. Change in Stress For Two 50 kip Trucks Placed Side by Side at the First Quarter Point of Span 1

Date and Time of Reading: October 7, 1995 at 11:55 p.m.

Temperature: 8 °C

Weather: Partly Cloudy

Loading Condition: Two 50 kip trucks were placed side by side at the midspan of span 1.

Objective of Reading: This reading was taken to observe the change in stress due to the loading condition mentioned above

General Observations: As observed in the previous loading position, except for girder 4, the top flanges experienced compression, and the bottom flanges experienced tension at the midspan gages. These stress changes ranged from -0.07 to -0.31 ksi in the top flanges and 0.79 to 1.48 ksi in the bottom flanges. The behavior of the girders at the middle pier was equivalent to the previous loading stage which is an increase in tension in the top flanges and compression in the bottom flanges. The range of the stress changes was 0.07 to 0.13 ksi for the top flanges and -0.38 to -0.72 ksi for the bottom flanges. The top two members of the diaphragms increased in tension while the bottom two members, except for gages 8C and 12C, increased in compression. The stress changes ranges were 0.14 to 0.92 ksi and -0.14 to -1.76 ksi.

Notes on Specific Gages: Not Applicable

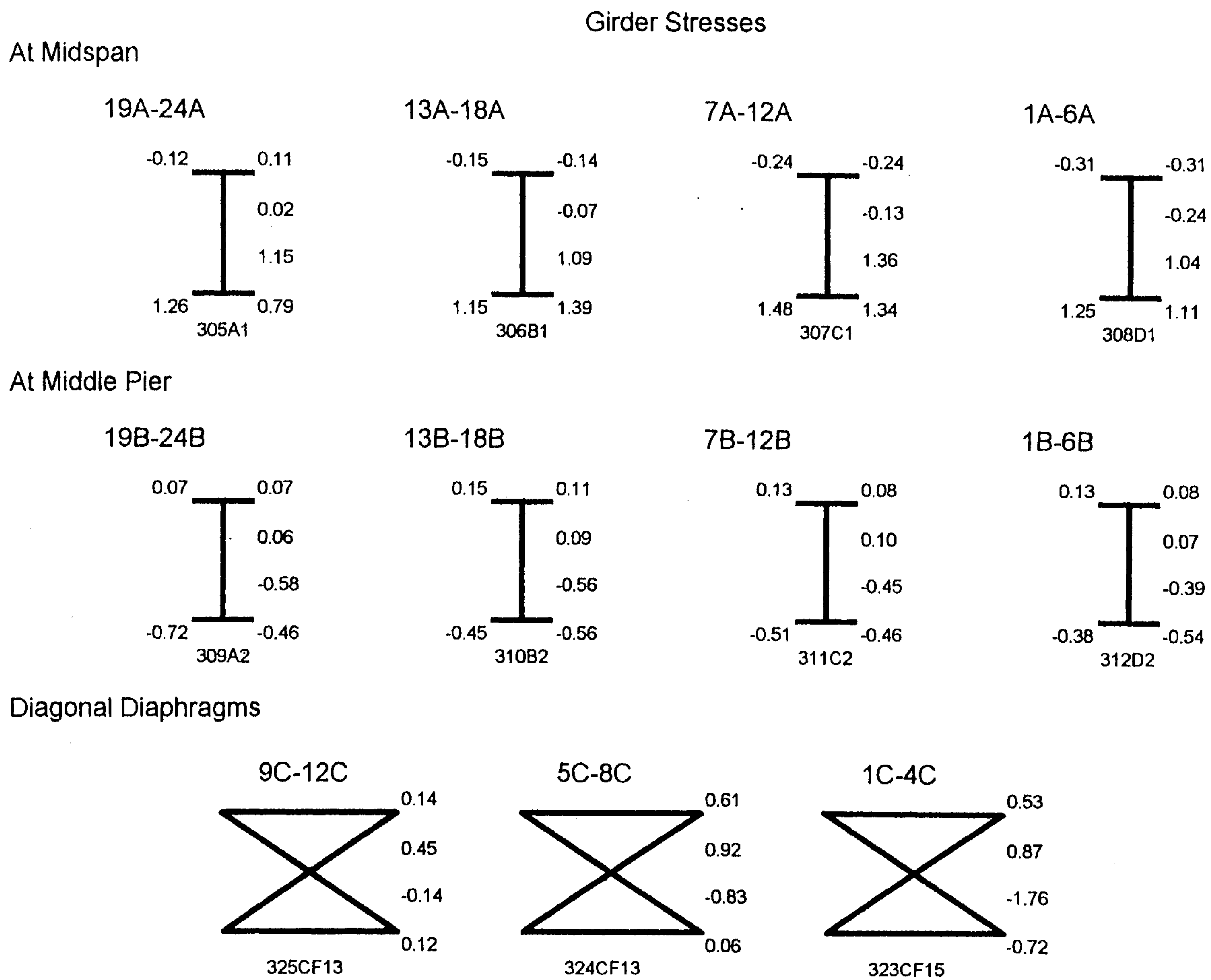

Figure C-3. Change in Stress for Two 50 kip Trucks Placed Side by Side at the Midspan of Span 1

Date and Time of Reading: October 8, 1995 at 12:10 a.m.

Temperature: 8 °C

Weather: Partly Cloudy

Loading Condition: Two 50 kip trucks were placed side by side at the third quarter point of span 1.

Objective of Reading: This reading was taken to observe the change in stress due to the loading condition mentioned above

General Observations: The stresses at the midspan decreased from the previous loading condition which is expected. Except for girder 4, the top flanges are still experiencing compression while the bottom flanges are experiencing tension. These stresses range from -0.03 to -0.25 ksi in the top flanges and 0.39 to 1.13 ksi in the bottom flanges. The bottom flanges at the middle pier continued to experience compressive stresses. For this loading condition, the bottom flange stresses in girders 1,2, and 3 continued to increase in compression. The changes in the top flange stresses were varied, but the flanges continued to experience tension. The range in the top flange stresses was 0.05 to 0.16 ksi, and the range for the bottom flanges was -0.44 to -0.70 ksi. The top two members in the diaphragms experienced tensile stress, ranging from 0.13 ksi to 0.54 ksi, and the bottom flanges experienced compressive stress, ranging from -0.04 ksi to -1.39 ksi.

Notes on Specific Gages:

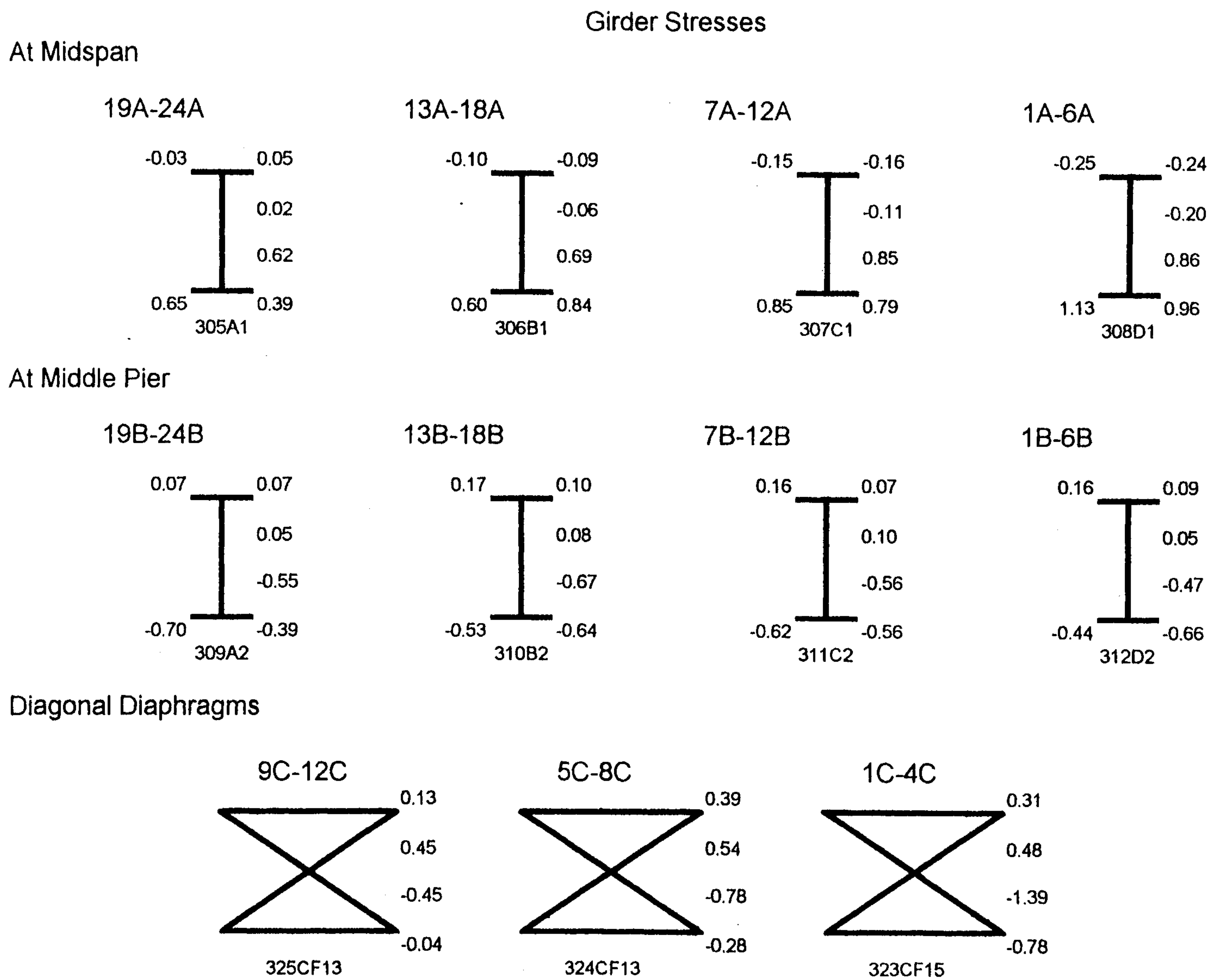

Figure C-4. Change in Stress for Two 50 kip Trucks Placed Side By Side at the Third Quarter Point of Span 1

Date and Time of Reading: October 8, 1995 at 12:35 a.m.

Temperature: 8 °C

Weather: Partly Cloudy

Loading Condition: Two 50 kip trucks were placed side by side at the first quarter point of span 2.

Objective of Reading: This reading was taken to observe the change in stress due to the loading condition mentioned above

General Observations: The loading moved into span 2, and for most of the midspan gages a stress reversal could be observed. Therefore, the top flanges began to experience tension while the bottom flanges began to experience compression. The total range of stress was -0.13 ksi to 0.06 ksi. These stresses are quite small which could explain the lack of uniform behavior across the girders. Except for gages 1B, 2B, and 7B, the middle pier stresses continued to experience tension in the top flange and compression in the bottom flanges. The magnitude of the stresses experienced decreased as the loading crossed into the other span. Since the loading is now on the other side of the support, a majority of the load must be resisted by the support which then decreases the stress being observed by the gages. The range of stress observed was 0.00 to 0.11 ksi in the top flanges and -0.09 to -0.36 ksi in the bottom flanges. The largest stress for the bottom flanges was observed in girder four. There was not an explainable pattern in the stress changes observed for the diaphragms, but a majority of the members experienced compressive stress. The total range of stress for the members was -0.24 ksi to 0.22 ksi.

Notes on Specific Gages: Not Applicable

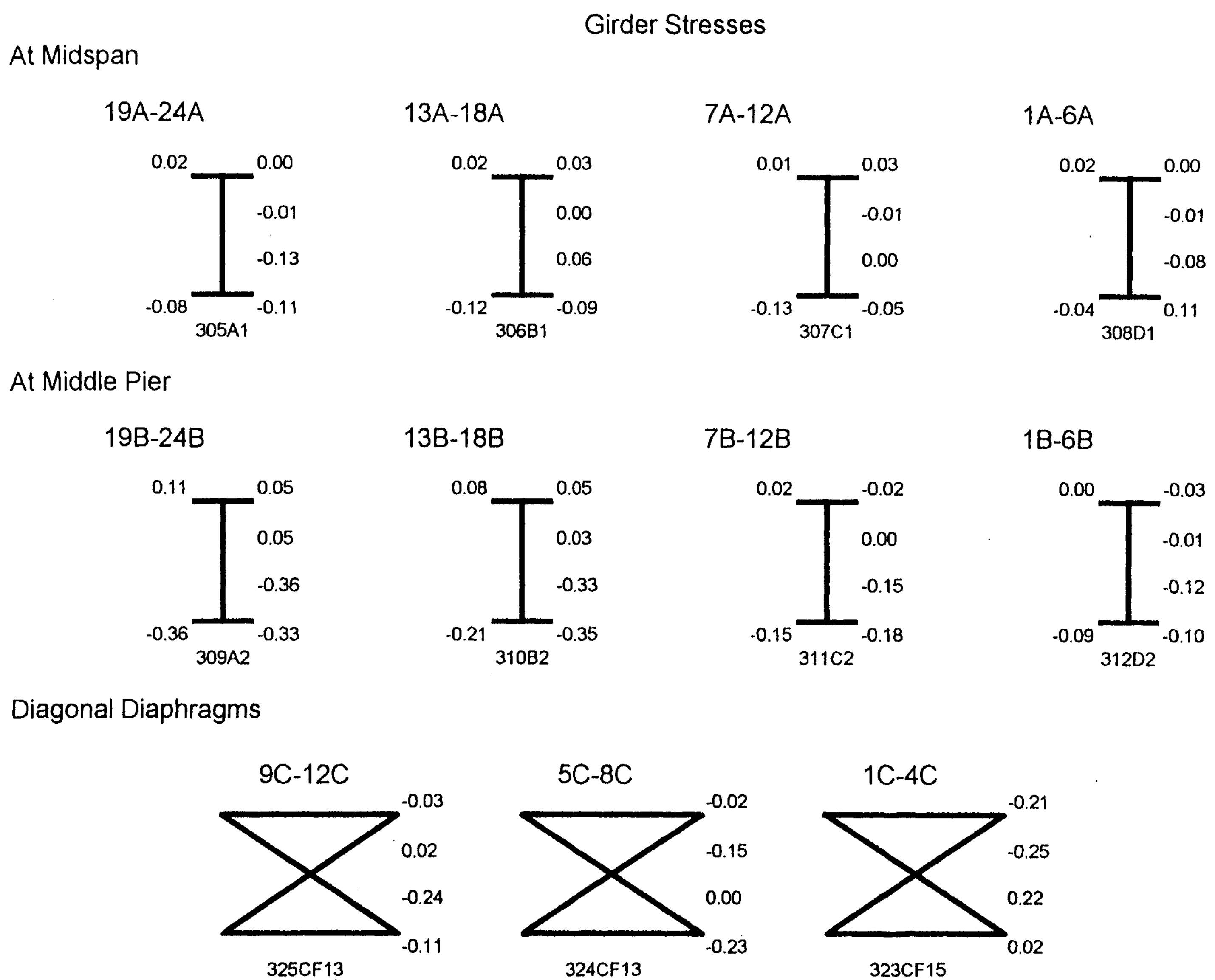

Figure C-5. Change in Stress for Two 50 kip Trucks placed Side by Side at the First Quarter Point of Span 2

Date and Time of Reading: October 8, 1995 at 12:45 a.m.

Temperature: 8 °C

Weather: Partly Cloudy

Loading Condition: Two 50 kip trucks were placed side by side at the midspan of span 2.

Objective of Reading: This reading was taken to observe the change in stress due to the loading condition mentioned above

General Observations: Except for gages 15A and 20A, the midspan gages behaved, as expected, which is as girders in a negative moment region. This negative moment was created by the truck loading located in the second span of the bridge. The top flanges experienced tension, ranging from 0.01 to 0.07 ksi, and the bottom flanges experienced compression, ranging from -0.05 to -0.28 ksi. The middle pier stresses increased to approximately the same magnitude experienced when the trucks were located at the third quarter point of span 1. The top flanges experienced tension, ranging from 0.05 to 0.16 ksi, and the bottom flanges experienced compression, ranging from -0.34 ksi to -0.67 ksi. Except for gages 3C, 4C, and 7C, the diaphragm members experienced compressive stress. The range of stresses were -0.06 to -0.28 ksi for compression and 0.18 to 0.45 ksi for tension. Diaphragm 1 did display a reversal in stress with the top two members experiencing compression while the bottom two members experienced tension.

Notes on Specific Gages:

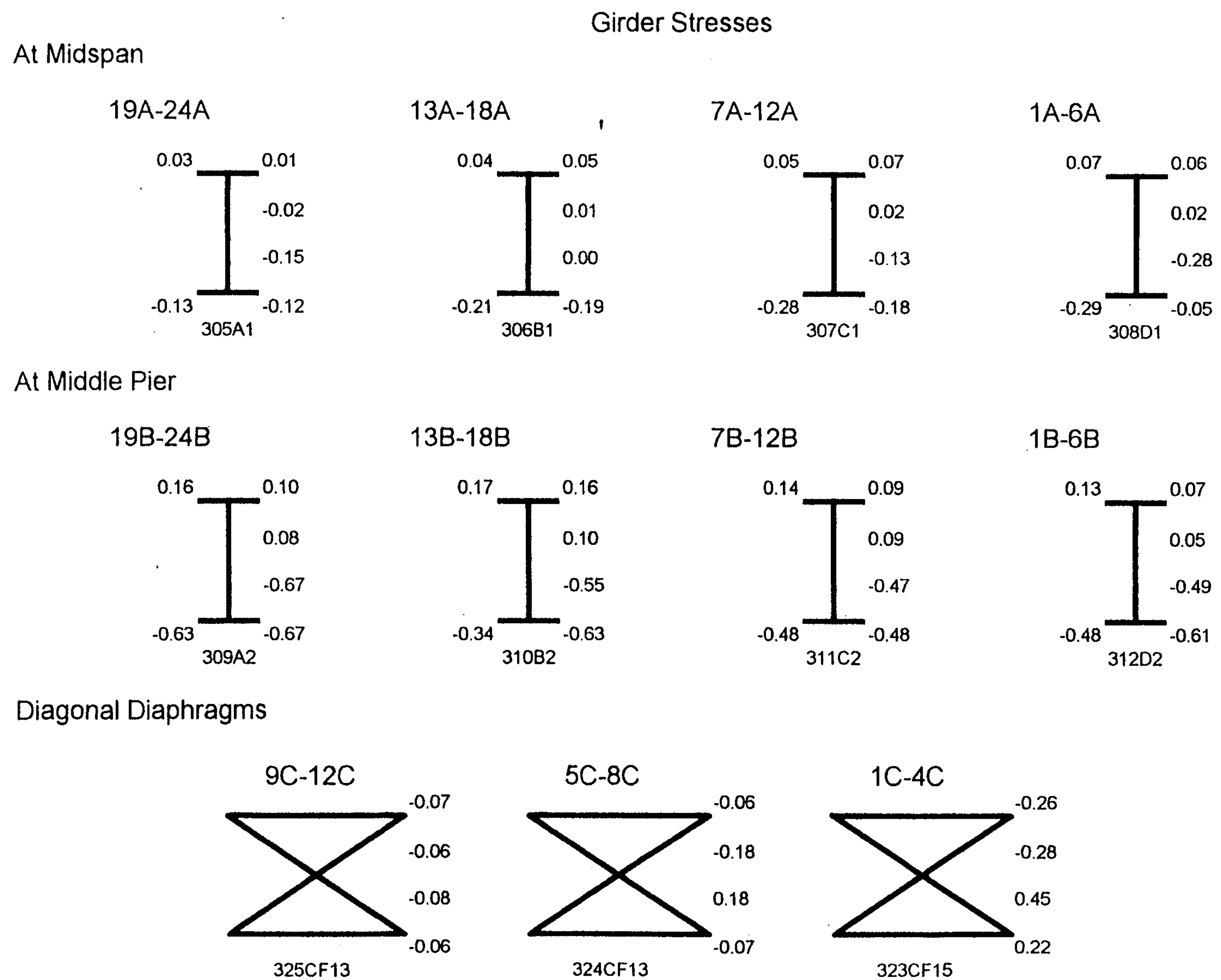

Figure C-6. Change in Stress for Two 50 kip Trucks Placed Side by Side at the Midspan of Span 2

Date and Time of Reading: October 8, 1995 at 12:55 a.m.

Temperature: 8 °C

Weather: Partly Cloudy

Loading Condition: Two 50 kip trucks were placed side by side at the third quarter point of span 2.

Objective of Reading: This reading was taken to observe the change in stress due to the loading condition mentioned above

General Observations: In general the stresses at the midspan continued to decrease as the loading was located further away from the gages. Except for gages 15A and 20A, the top flanges experienced tension, ranging from 0.00 to 0.07 ksi, and the bottom flanges experienced compression, ranging from -0.01 to -0.23 ksi. At the middle pier except for girder 1, the stresses decreased in the girders as the load was location further away from the middle pier. The top flanges continued to experience tension, ranging from 0.02 to 0.013 ksi, and the bottom flanges continued to experience compression, ranging from -0.22 to -0.62 ksi. The same stress patterns continued to be observed in the diaphragms. Diaphragm 1 experienced compression in the top two members with tension in the bottom two, diaphragm 2 experienced compression in its members except for gage 7C, and diaphragm 3 experienced compressive stress in all of its members. The total range of stress for the diaphragms was -0.28 ksi to 0.38 ksi.

Notes on Specific Gages: Not Applicable

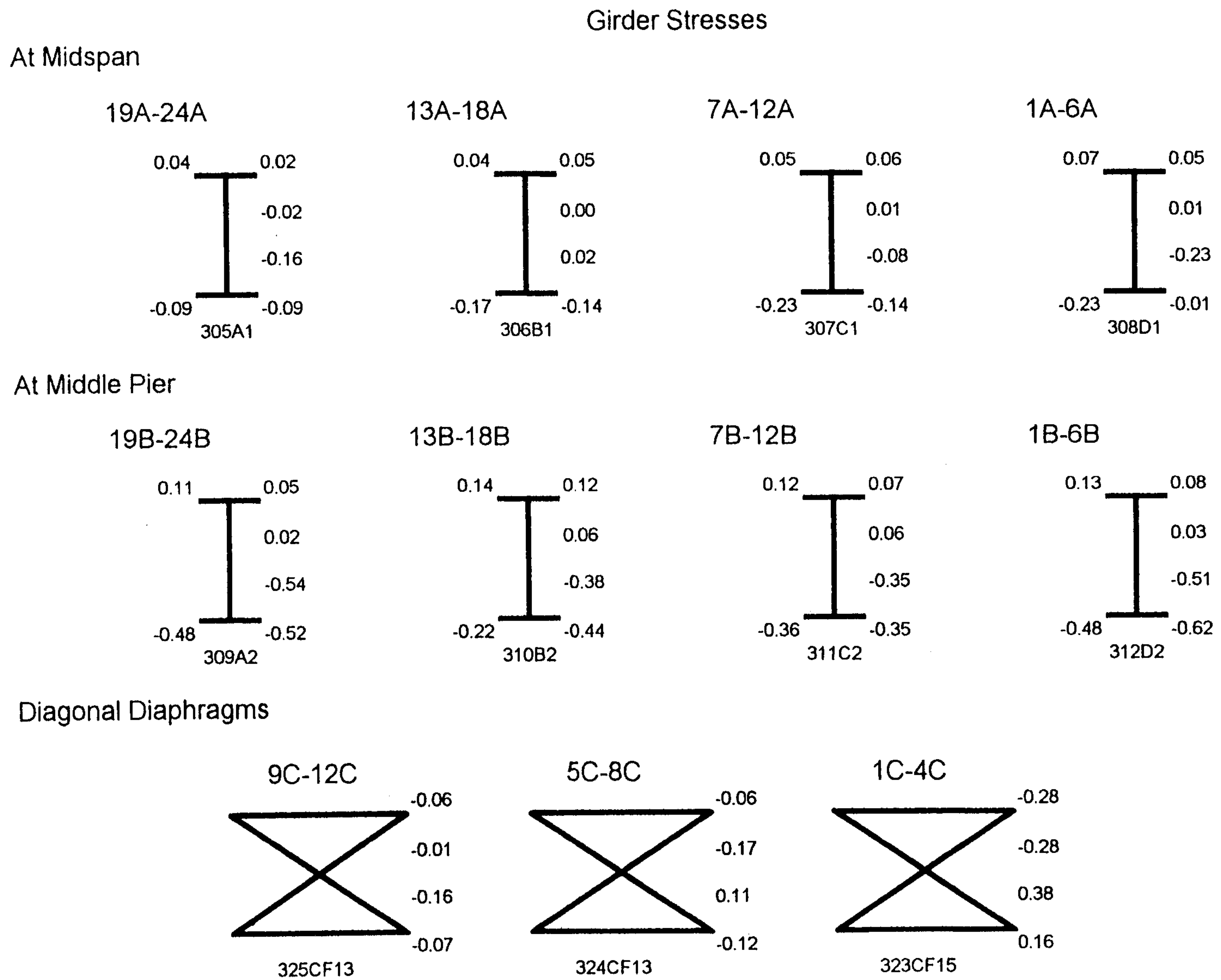

Figure C-7. Change in Stress for Two 50 kip Trucks Placed Side by Side at the Third Quarter Point of Span 2

TRUCK LIVE LOADING PLOTS

TWO TRUCKS SIDE BY SIDE PLACED AT THE QUARTER POINTS

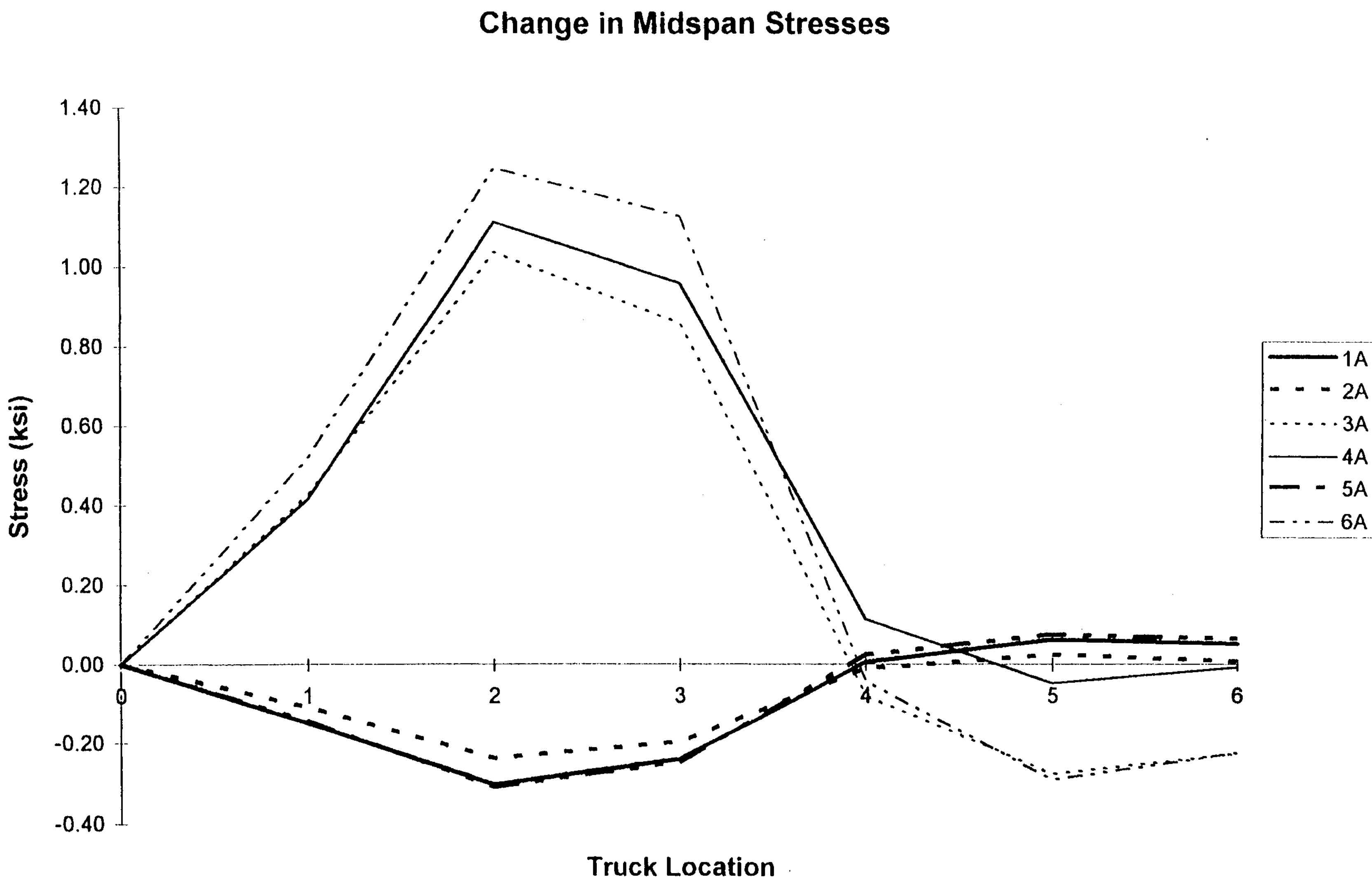

Figure C-8. Change in Stress for Gages 1A-6A with Two 50 kip Trucks Placed Side by Side at the Quarter Points of the Bridge

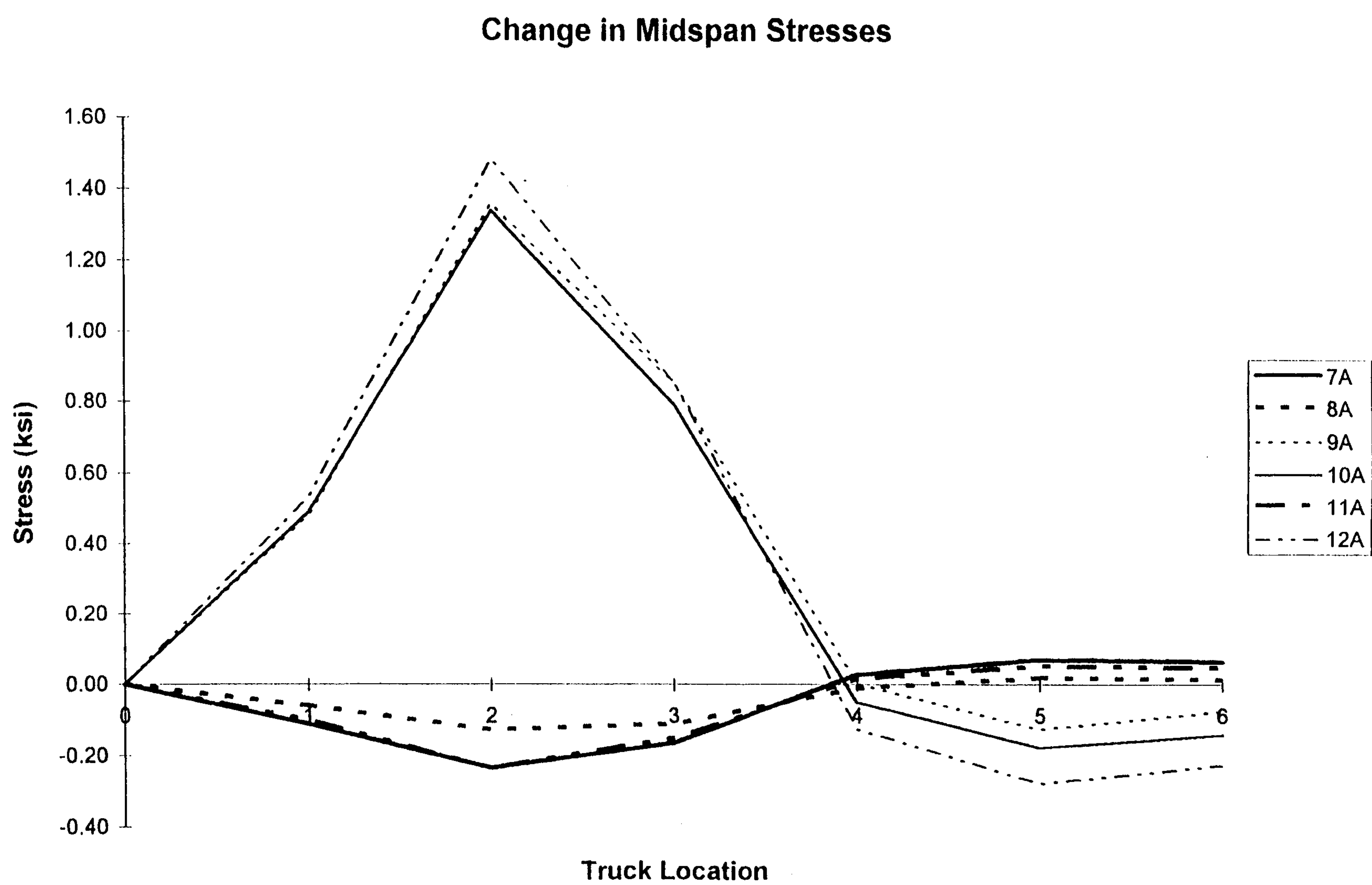

Figure C-9. Change in Stress for Gages 7A-12A with Two 50 kip Trucks Placed Side by Side at the Quarter Points of the Bridge

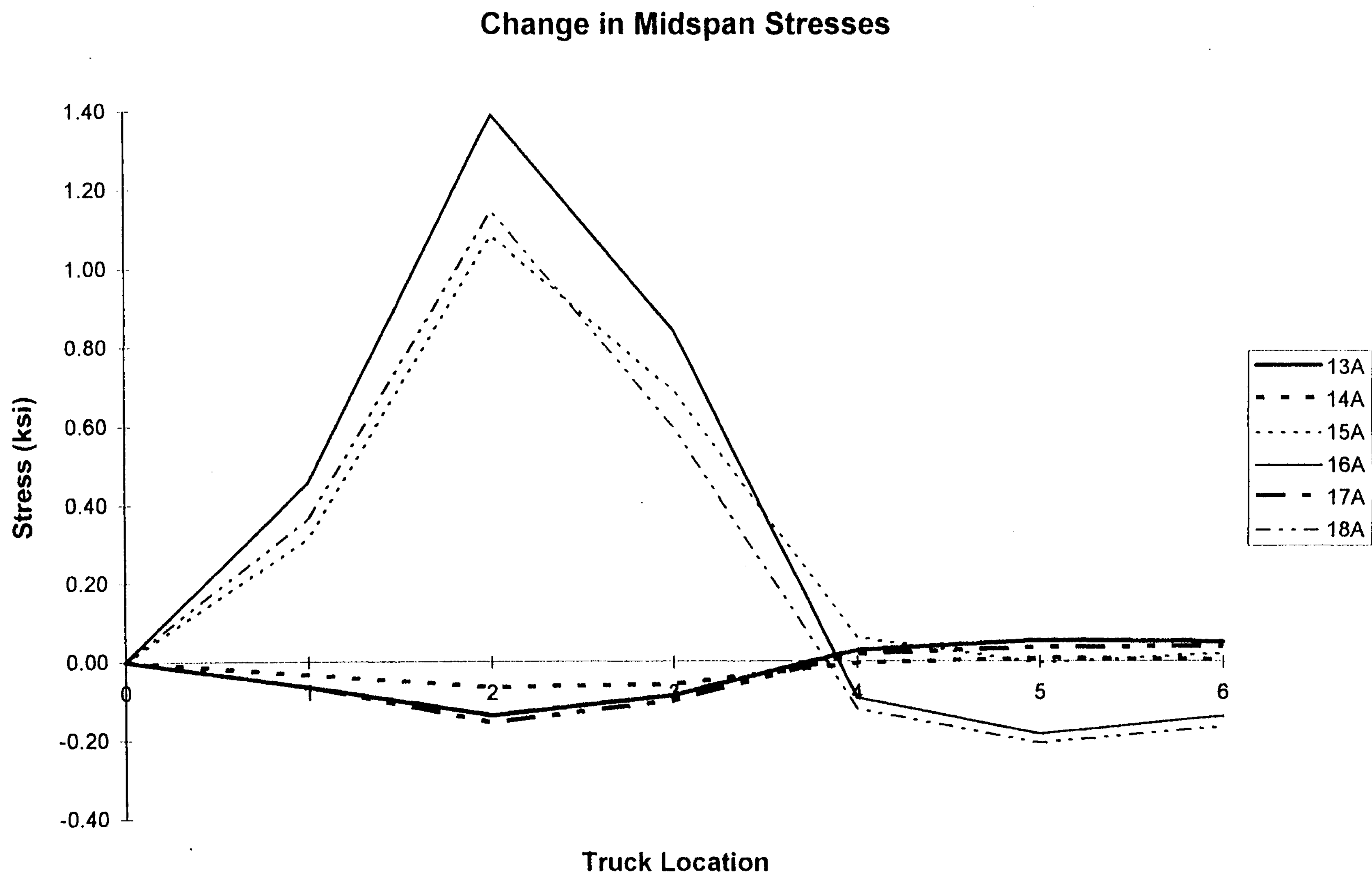

Figure C-10. Change in Stress for Gages 13A-18A with Two 50 kip Trucks Placed Side by Side at the Quarter Points of the Bridge

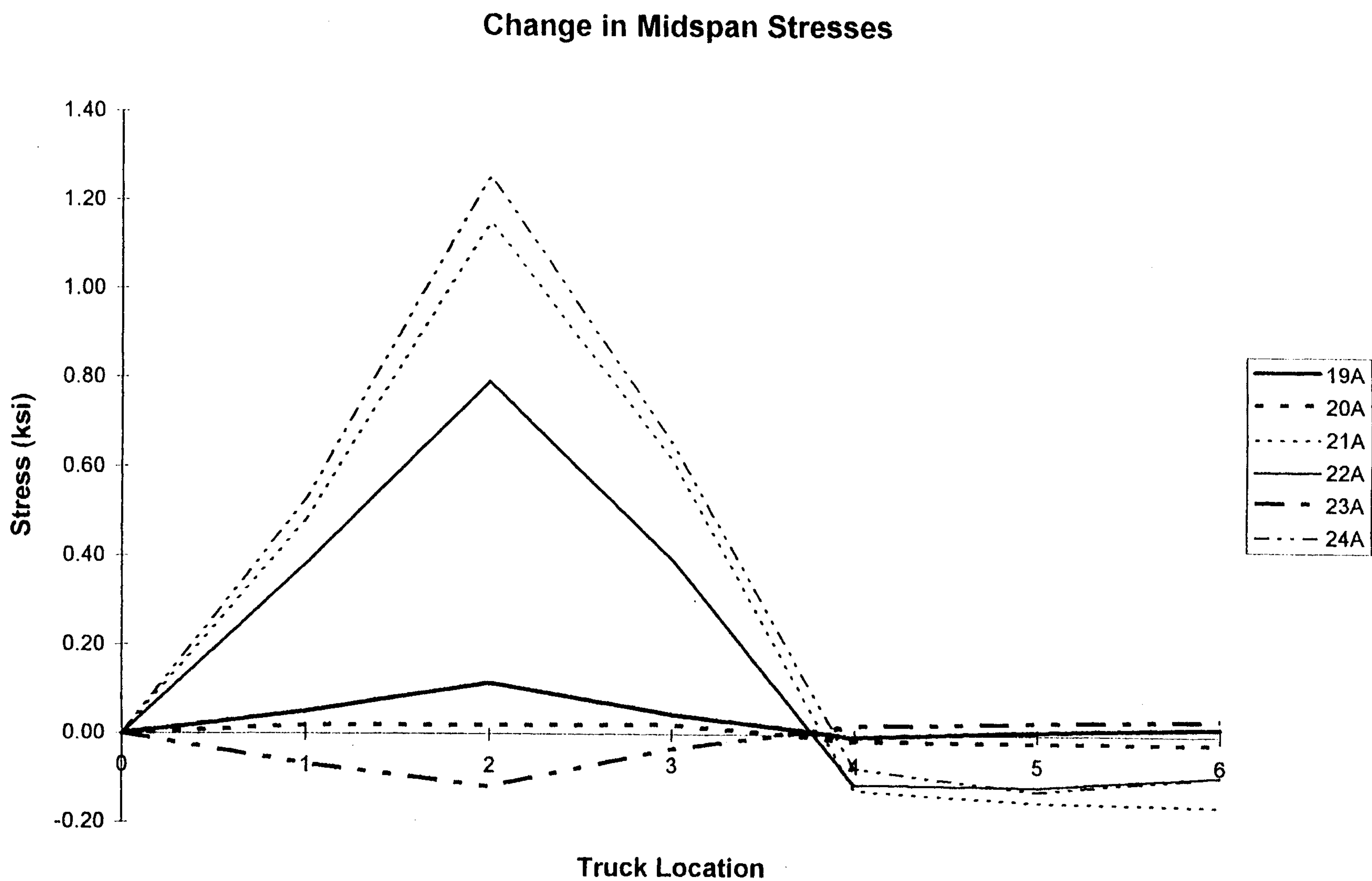

Figure C-11. Change in Stress for Gages 19A-24A with Two 50 kip Trucks Side by Side Placed at the Quarter Points of the Bridge

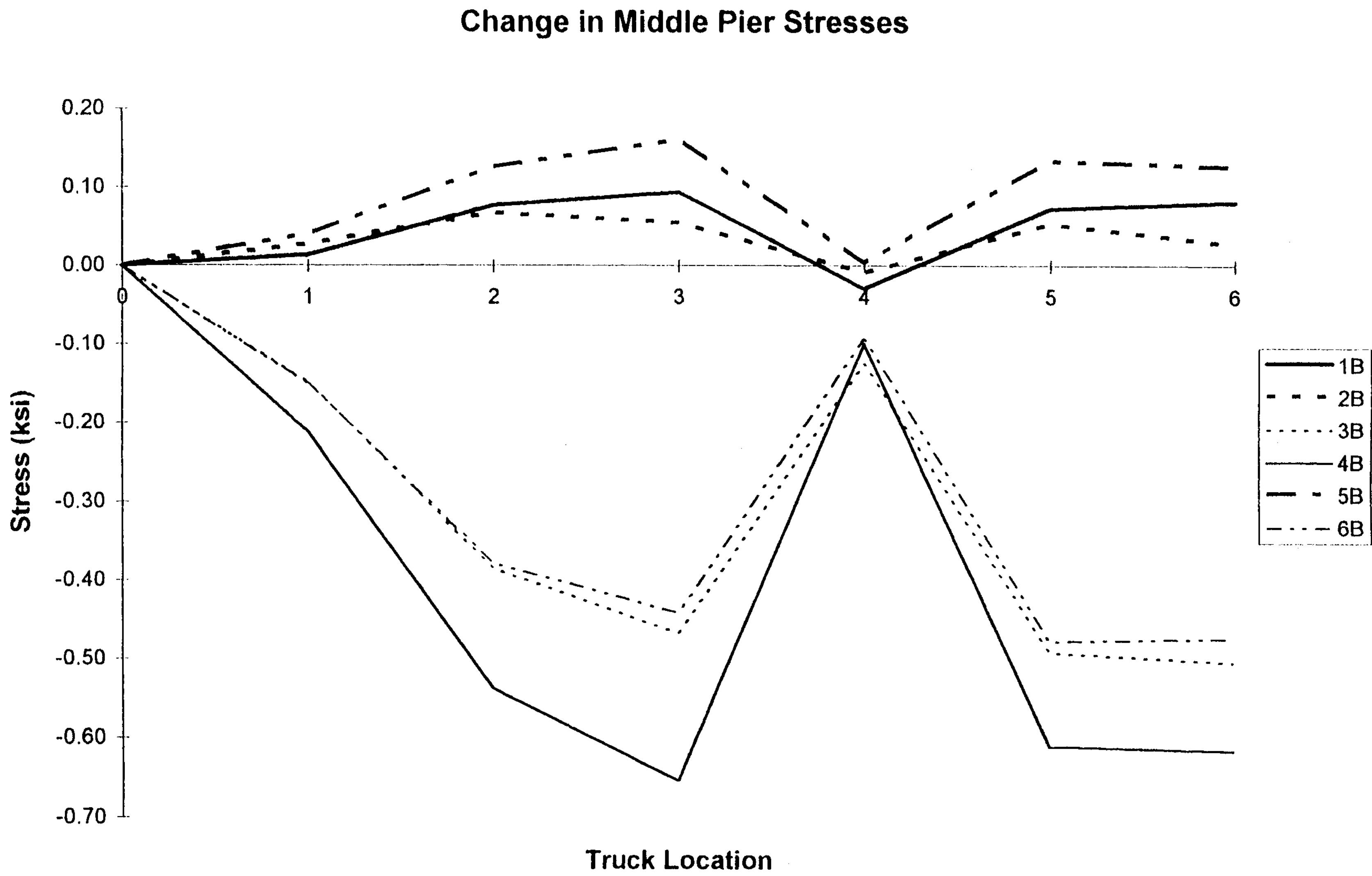

Figure C-12. Change in Stress for Gages 1B-6B with Two 50 kip Trucks Placed Side by Side at the Quarter Points of the Bridge

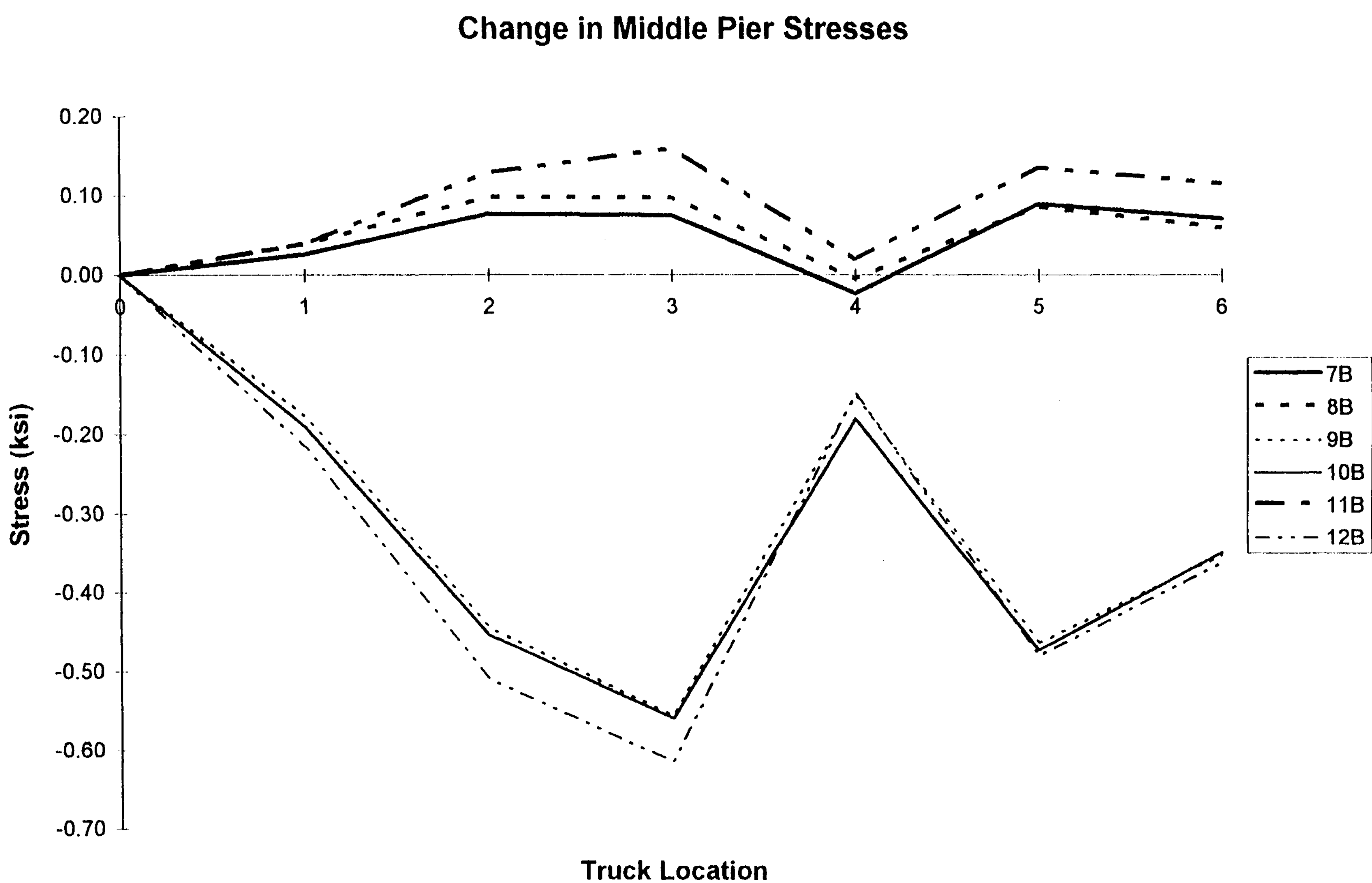

Figure C-13. Change in Stress for Gages 7B-12B with Two 50 kip Trucks Placed Side by Side at the Quarter Points of the Bridge

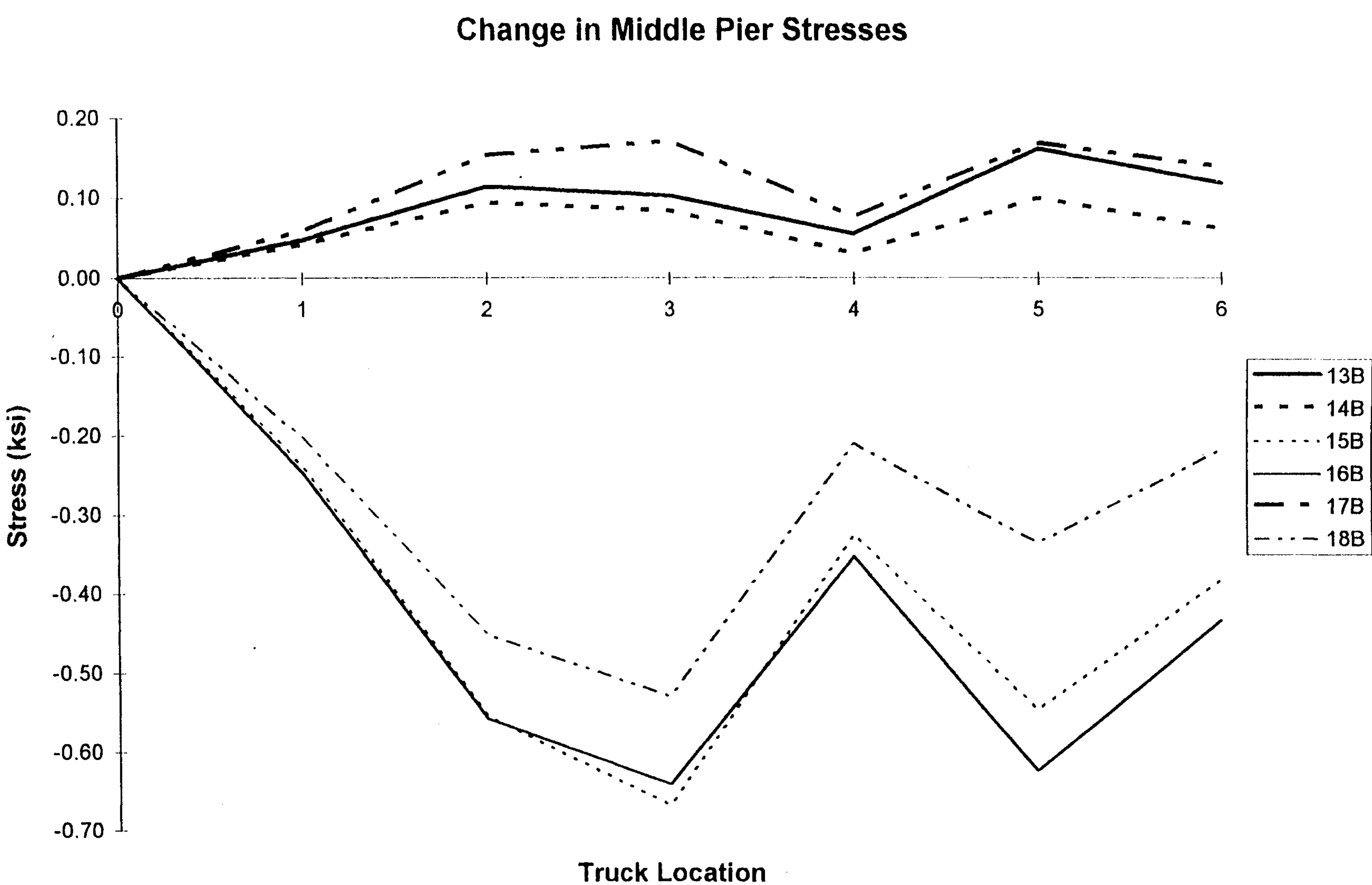

Figure C-14. Change in Stress for Gages 13B-18B with Two 50 kip Trucks Placed Side by Side at the Quarter Points of the Bridge

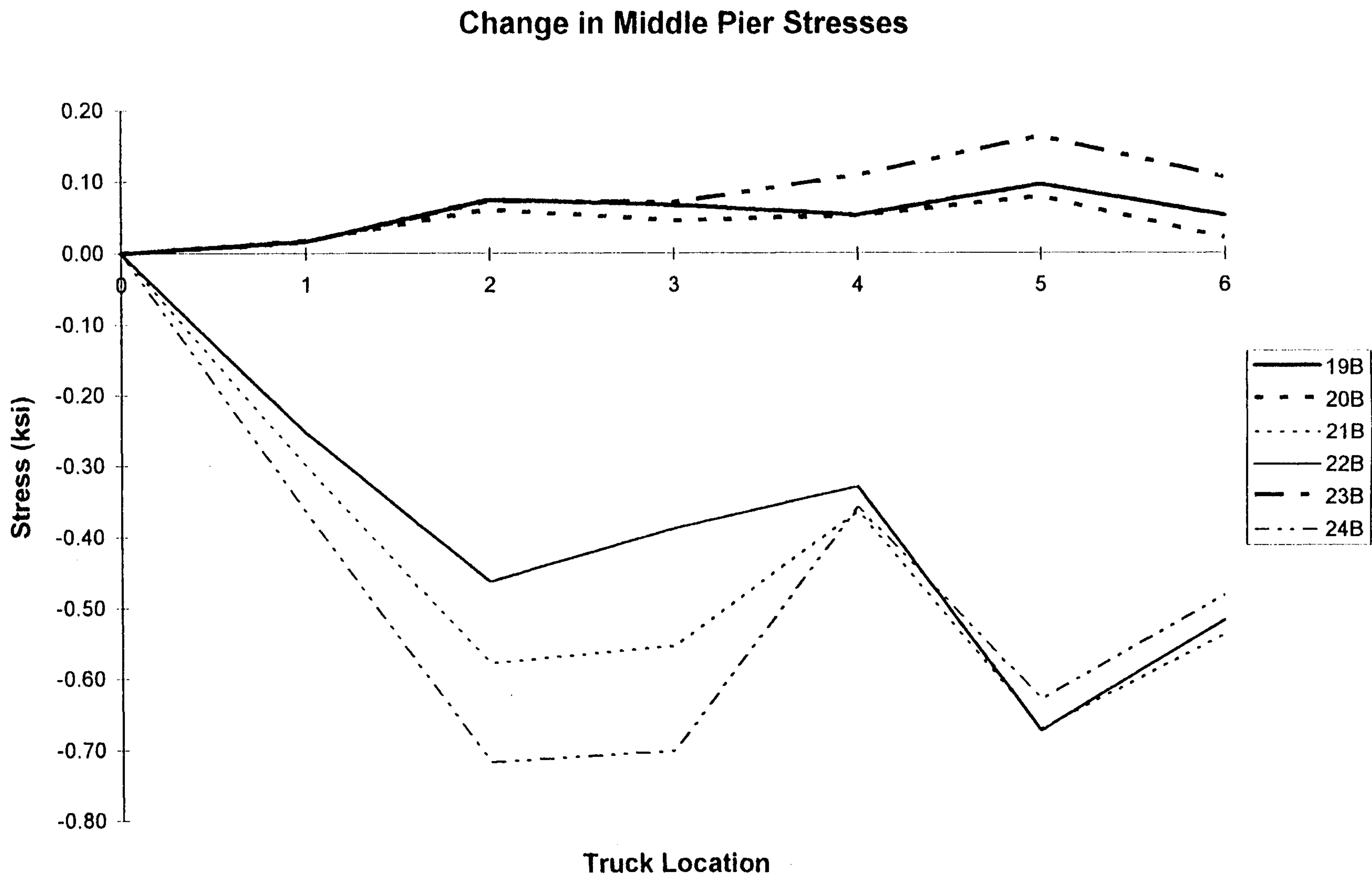

Figure C-15. Change in Stress for Gages 19B-24B with Two 50 kip Trucks Side by Side at the Quarter Points of the Bridge

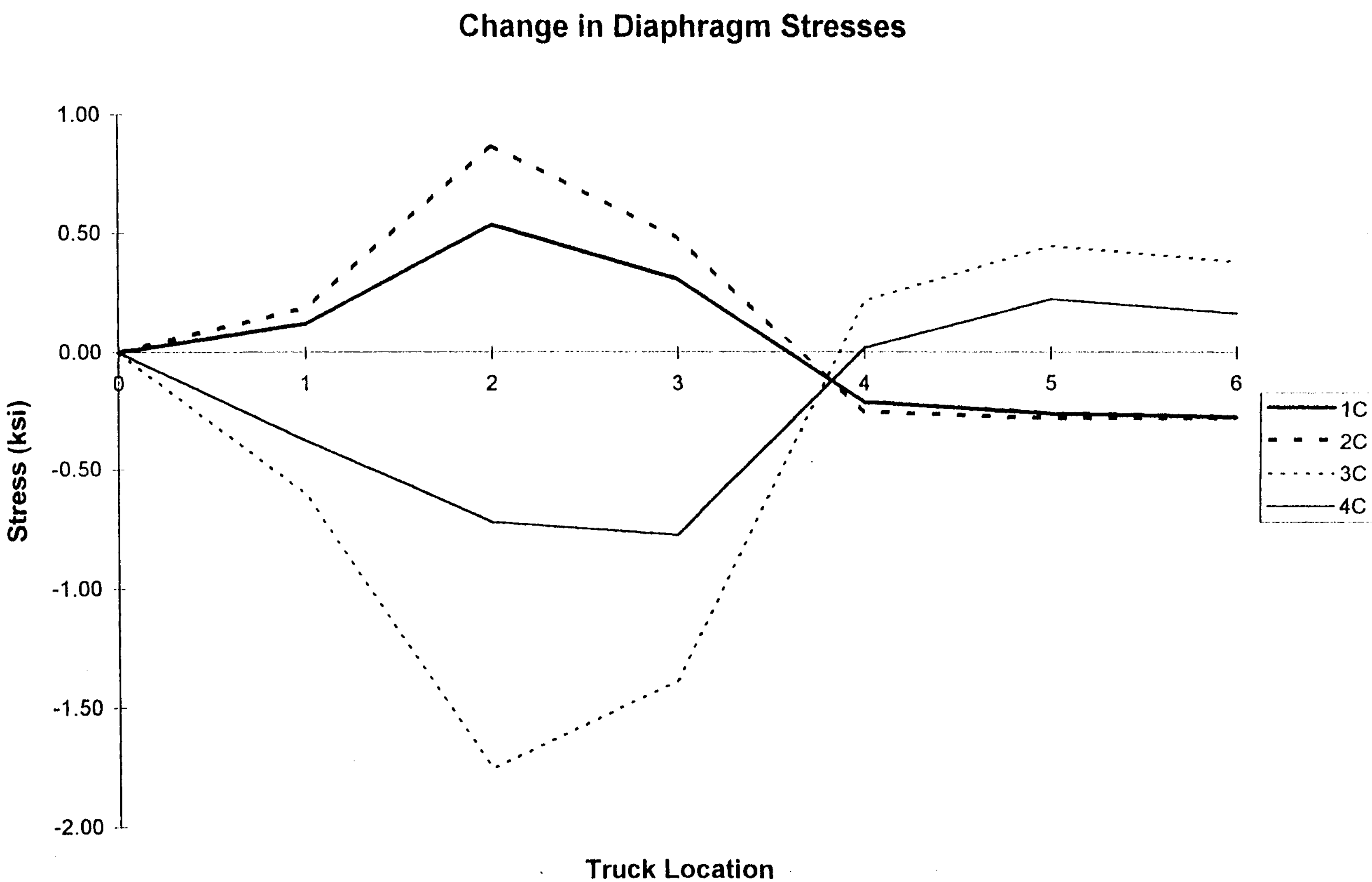

Figure C-16. Change in Stress for gages 1C-4C with Two 50 kip Trucks Placed Side by Side at the Quarter Points of the Bridge

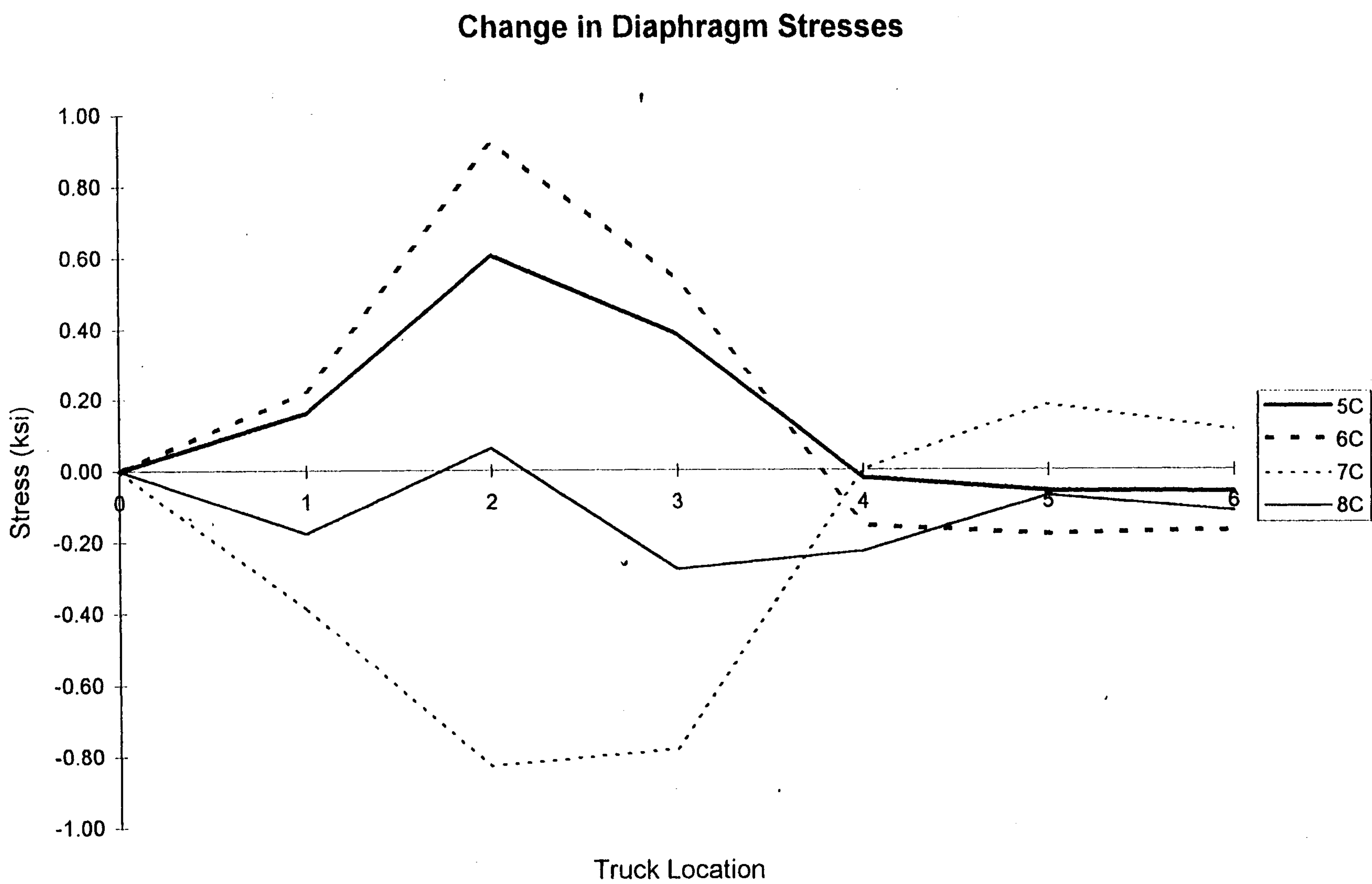

Figure C-17. Change in Stress for gages 5C-8C with Two 50 kip Trucks Placed Side by Side at the Quarter Points of the Bridge

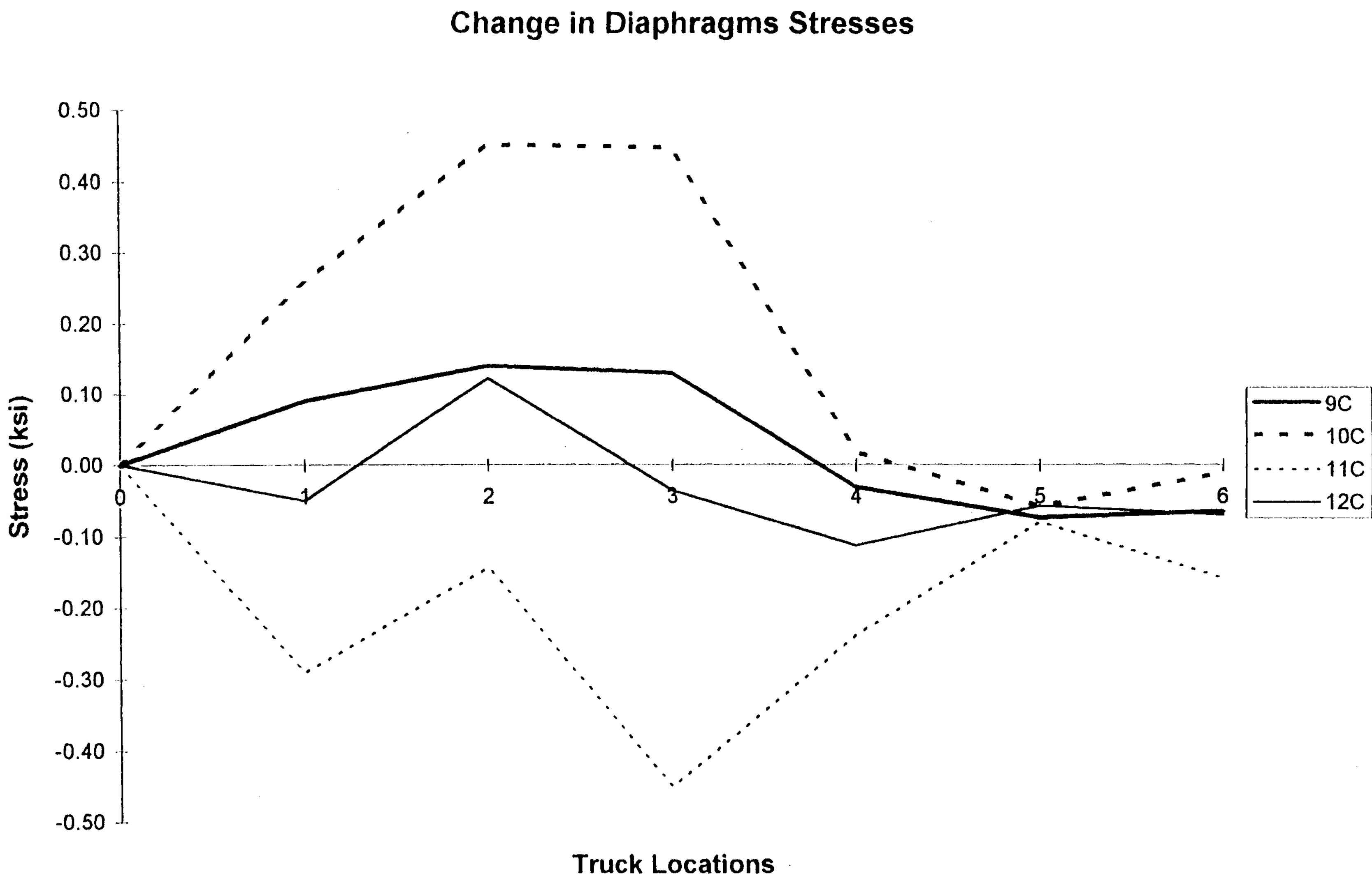

Figure C-18. Change in Stress for Gages 9C-12C with Two 50 kip Trucks Placed Side by Side at the Quarter Points of the Bridge

OBSERVATIONS OF GIRDER STRESSES

Date and Time of Reading: October 8, 1995 at 2:10 a.m.

Temperature: 8 °C

Weather: Partly Cloudy

Loading Condition: One 50 kip truck was placed at the first quarter point of span 1.

Objective of Reading: This reading was taken to observe the change in stress due to the loading condition mentioned above

General Observations: At the midspan gages, girder 1 was the only girder to behave as a girder in a positive moment region which is compression in the top flange and tension in the bottom flange. Girders 2,3, and 4 experienced tensile stresses at their inside and outside flange tips while the gage affixed to the web registered compressive stress. This behavior could result from the composite behavior present at this location. The one truck does not appear to have a significant enough load to properly stress the three inside girders at the midspan. The stresses observed in these top flanges were fairly insignificant and ranged from 0.00 ksi to 0.08 ksi. The bottom flanges, which are in tension, experienced stresses ranging from 0.07 to 0.45 ksi. The largest stresses occurred in girder 1, so it appears that this being the stiffest girder means that it is carrying a greater portion of the load. There is not an observable pattern to the middle pier stresses. Gages 1B, 5B, 11B, 13B, 17B, and 23B displayed an increase in tension, which would be expected for these gage locations, and the remaining gages displayed an increase in compressive stress. Except for six gages the girder is behaving as expected for a girder in a negative moment region. The range of tensile stress was 0.01 to 0.07 ksi, and the range of compressive stress was -0.04 to -0.25 ksi. Except for gage 10C, the members of the diaphragms experienced compression ranging from -0.01 to -0.55 ksi. The lone tensile stress was 0.21 ksi.

Notes on Specific Gages: Not Applicable

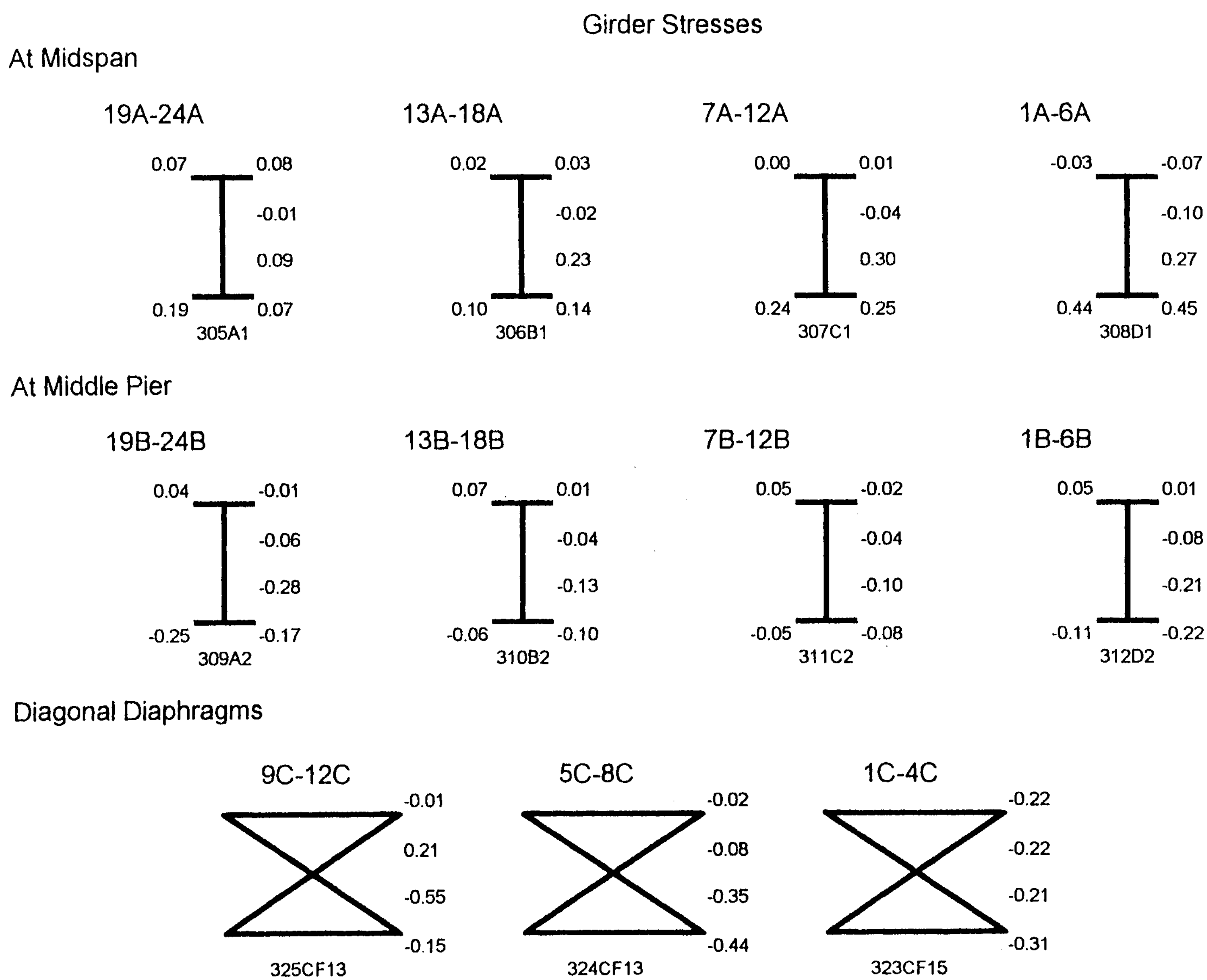

Figure C-19. Change in Stress for One 50 kip Truck Placed at the First Quarter Point of Span 1

Date and Time of Reading: October 8, 1995 at 2:25 a.m.

Temperature: 8 °C

Weather: Partly Cloudy

Loading Condition: One 50 kip truck was placed at the midspan of span 1.

Objective of Reading: This reading was taken to observe the change in stress due to the loading condition mentioned above

General Observations: Having the load located directly over the gages caused, except for the two flange tips of girder 4, the girders to respond in the manner expected for a load present in span 1. The top flange compressive stresses increased and ranged from -0.01 to -0.18 ksi while the bottom flange tensile stress range increased to 0.25 to 0.79 ksi. The gages affixed to the top of the web at the middle pier continued to display compressive stress, but the flange tips experienced tensile stress ranging from 0.00 to 0.12 ksi. The bottom flanges experienced compression ranging from -0.21 to -0.43 ksi. The top members for diaphragms 1 and 2 experienced tensile stress while the bottom two experienced compression. For diaphragm 3, the top member displayed compressive stress, the next member down displayed tension, the next member down displayed compression, and the bottom member displayed tension. The stress ranges for these members were -0.10 to -0.96 ksi and 0.01 to 0.31 ksi.

Notes on Specific Gages: Not Applicable

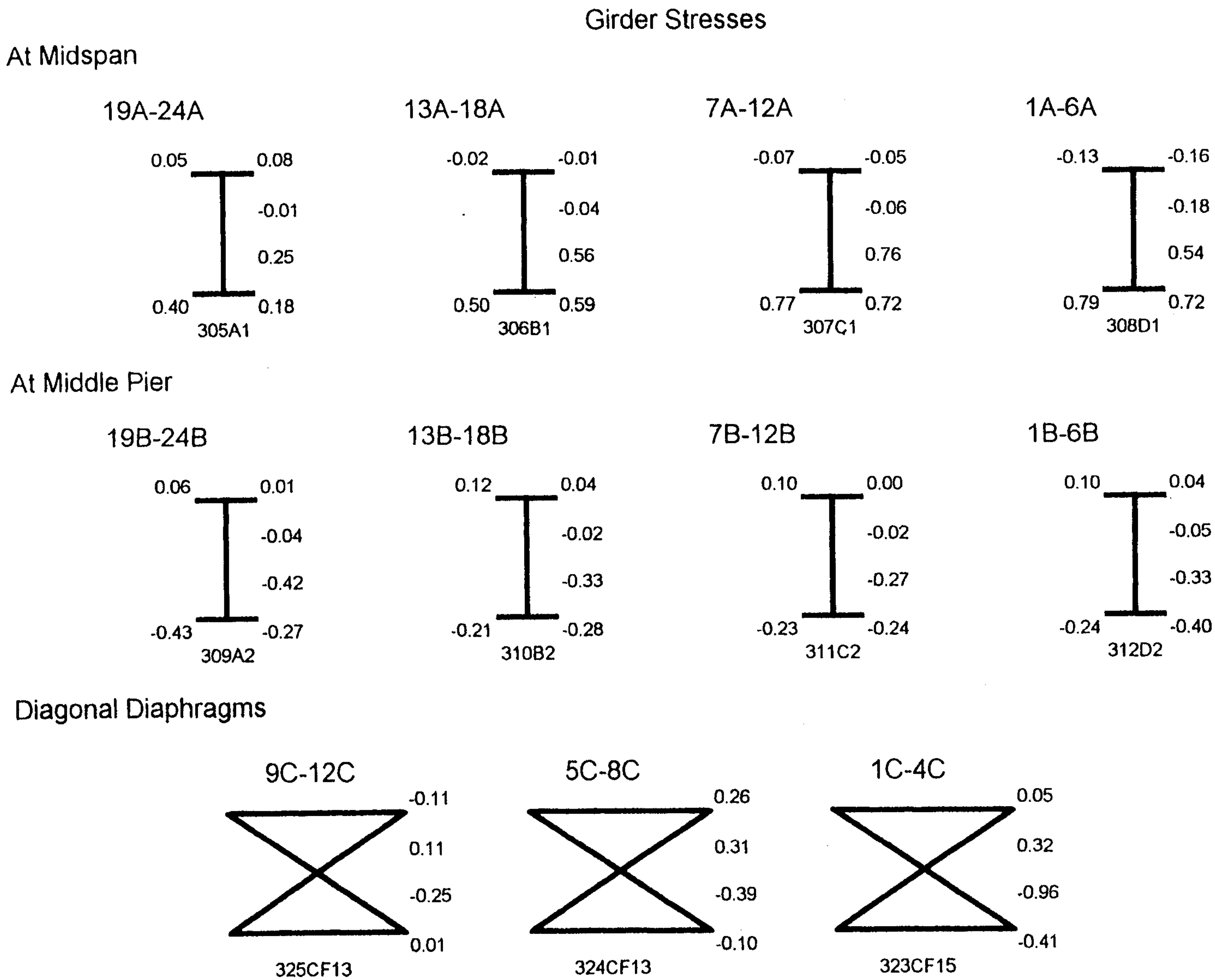

Figure C-20. Change in Stress for One 50 kip Truck Placed at the Midspan of Span 1

Date and Time of Reading: October 8, 1995 at 2:40 a.m.

Temperature: 8 °C

Weather: Partly Cloudy

Loading Condition: One 50 kip truck was placed at the third quarter point of span 1.

Objective of Reading: This reading was taken to observe the change in stress due to the loading condition mentioned above

General Observations: Girders 1 and 2 at the midspan continued to respond in a manner consistent with a girder in a positive moment region. The range of compressive stress experienced by all of the midspan girders ranged from -0.01 to -0.14 ksi. The tensile stress in the bottom flanges decreased as the loading moved beyond the midspan of span 1. These stresses ranged from 0.16 ksi to 0.66 ksi. The same behavior described for the middle pier gages in the previous loading stage continued for the girders. The tensile stresses ranged from 0.01 to 0.12 ksi, and the compressive stress for the bottom flanges ranged from -0.24 to -0.44 ksi. The stresses for the diaphragms ranged from -0.04 to -0.67 ksi and 0.08 to 0.20 ksi.

Notes on Specific Gages: Not Applicable

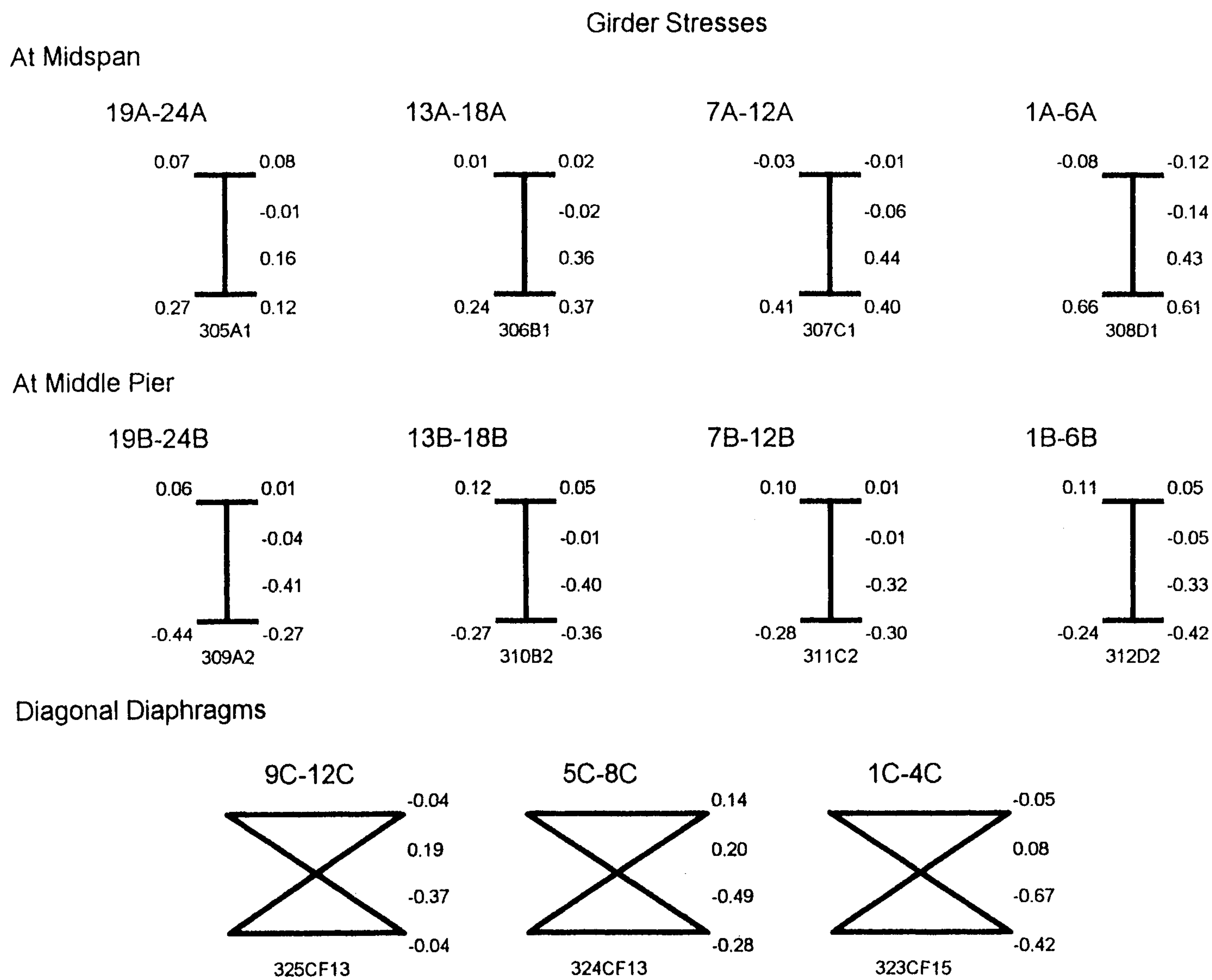

Figure C-21. Change in Stress for One 50 kip Truck Placed at the Third Quarter Point of Span 1

Date and Time of Reading: October 8, 1995 at 2:45 a.m.

Temperature: 8 °C

Weather: Partly Cloudy

Loading Condition: One 50 kip truck was placed at the first quarter point of span 2.

Objective of Reading: This reading was taken to observe the change in stress due to the loading condition mentioned above

General Observations: A partial stress reversal, tension in the top flanges and compression in the bottom flanges, can be observed in the midspan gages. The term partial was used because there was not a uniform stress reversal across the cross section, but there is the beginning of an observable trend in girders 2,3, and 4. Once again, it appears that there is not enough load to cause uniform behavior across the girders at the midspan. The range of stress experienced was 0.00 to 0.17 ksi in tension and -0.01 to -0.14 ksi in compression. Except for gages 11B, 13B, 17B, 19B, and 23B, the gages at the middle pier displayed compressive stress. These stresses ranged from -0.03 to -0.29 ksi. The tensile stress ranged from 0.00 to 0.09 ksi. Except for gages 3C and 10C, the members of the diaphragms experienced compression ranging from -0.04 to -0.44 ksi. The tensile stresses were 0.09 ksi and 0.23 ksi.

Notes on Specific Gages: Not Applicable

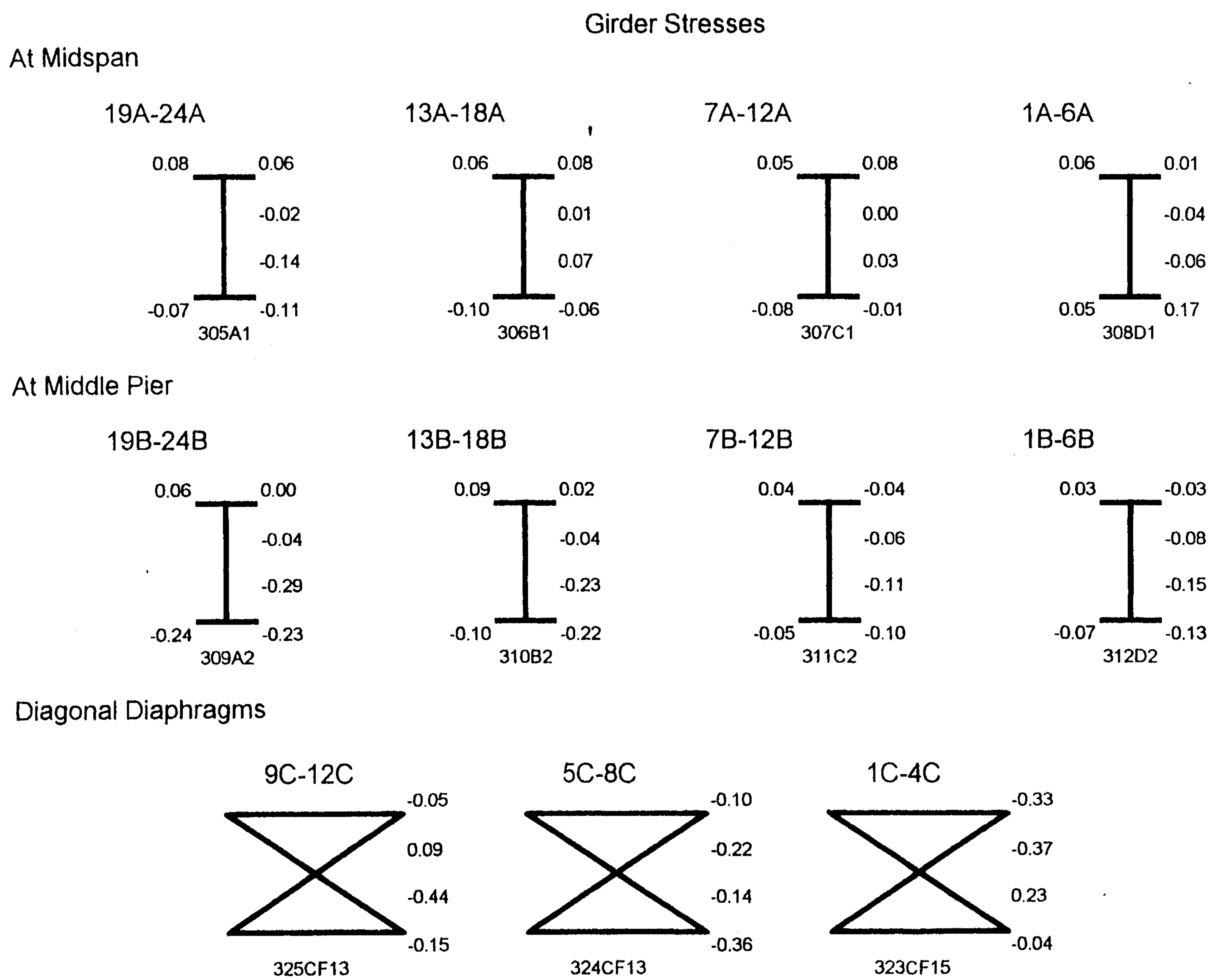

Figure C-22. Change in Stress for One 50 kip Truck Placed at the First Quarter Point of Span 2

Date and Time of Reading: October 8, 1995 at 2:55 a.m.

Temperature: 8 °C

Weather: Partly Cloudy

Loading Condition: One 50 kip truck was placed at the midspan of span 2.

Objective of Reading: This reading was taken to observe the change in stress due to the loading condition mentioned above

General Observations: The midspan gages are basically displaying stresses consistent with girders in a negative moment region. The range of tensile stress is 0.00 to 0.08 ksi, and the range of compressive stress is -0.02 to -0.17 ksi. The equivalent statement can be made for the gages located at the middle pier. Theses stresses range from 0.01 to 0.09 ksi in tension and -0.01 to -0.46 ksi in compression. The range of stress for the diaphragms is 0.02 to 0.32 ksi in tension and -0.02 to -0.35 ksi in compression.

Notes on Specific Gages: Not Applicable

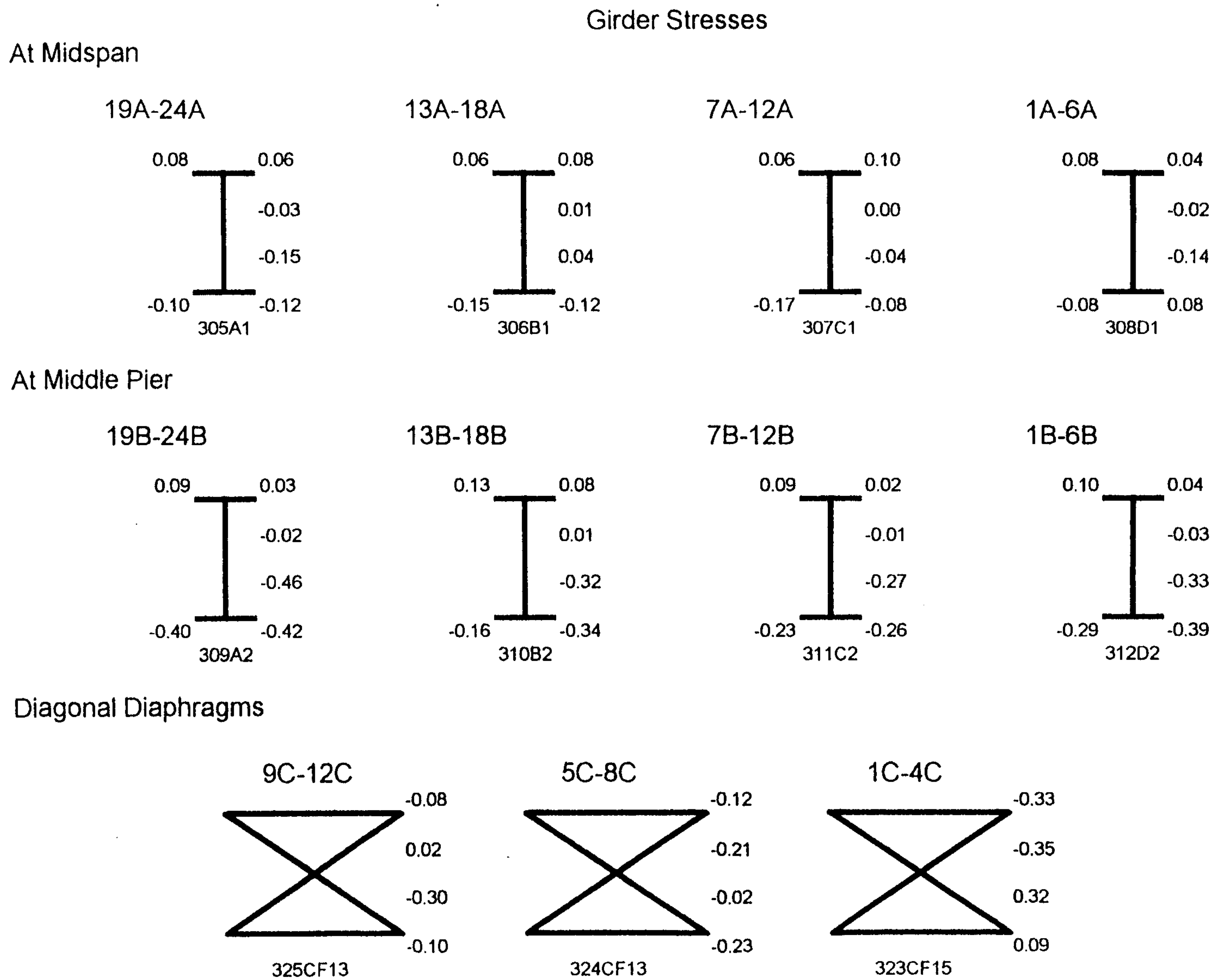

Figure C-23. Change in Stress for One 50 kip Truck Placed at the Midspan of Span 2

Date and Time of Reading: October 8, 1995 at 3:00 a.m.

Temperature: 8 °C

Weather: Partly Cloudy

Loading Condition: One 50 kip truck was placed at the third quarter point of span 2.

Objective of Reading: This reading was taken to observe the change in stress due to the loading condition mentioned above

General Observations: The same behavior as described in the previous loading stage continued at the midspan. The stresses ranged from 0.00 to 0.09 ksi in tension and -0.01 to -0.14 ksi in compression. At the middle pier, the gages continued to display stresses basically consistent with the behavior previously described. These stress ranges were 0.00 to 0.09 ksi in tension and -0.01 to -0.37 ksi in compression. The stress ranges observed in the diaphragms were 0.02 to 0.25 ksi in tension and -0.03 to -0.32 ksi in compression.

Notes on Specific Gages: Not Applicable

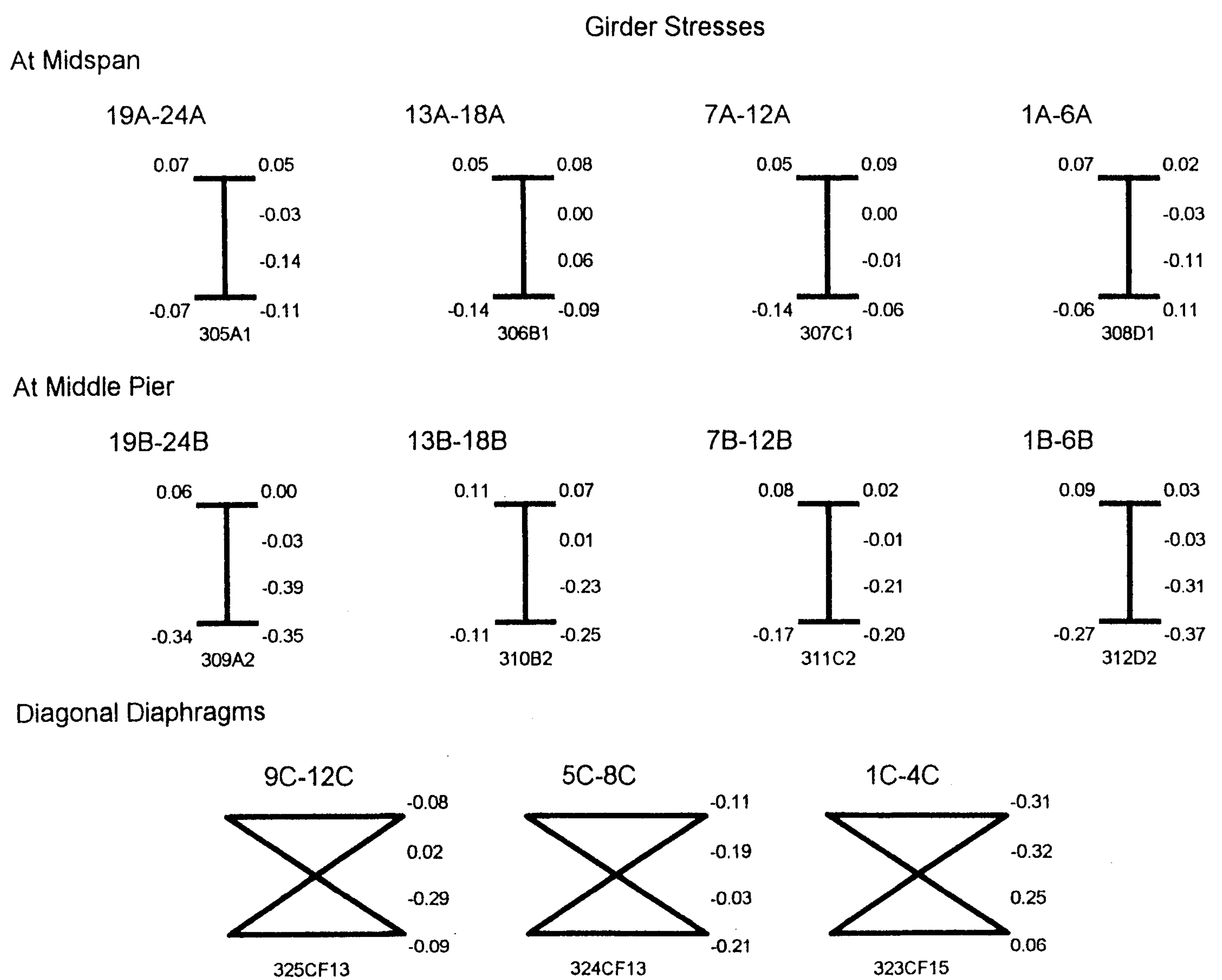

Figure C-24. Change in Stress for One 50 kip Truck Placed at the Third Quarter Point of Span 2

TRUCK LIVE LOADING PLOTS

ONE TRUCK PLACED AT THE QUARTER POINTS

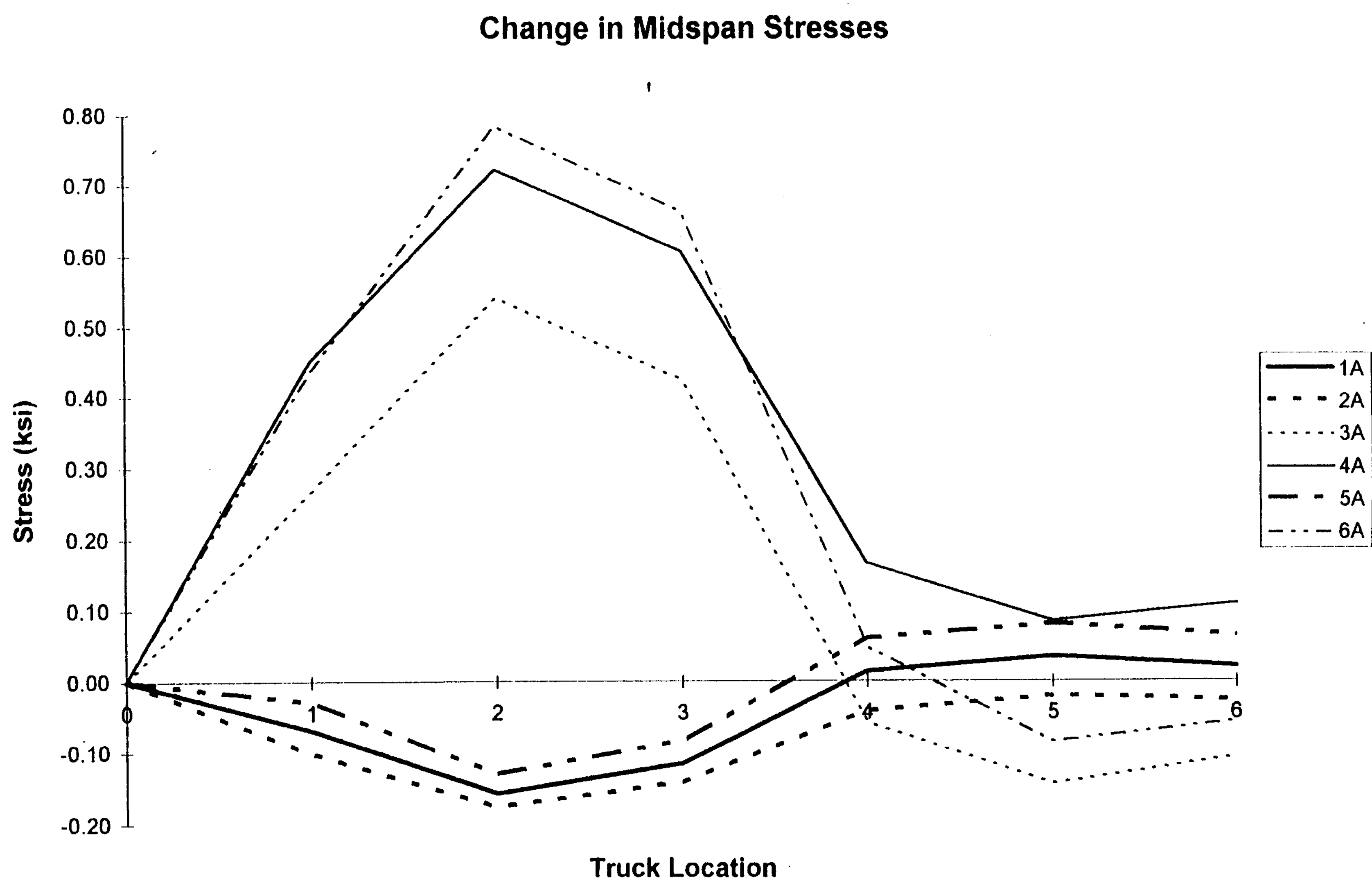

Figure C-25. Change in Stress for Gages 1A-6A with One 50 kip Trucks Placed at the Quarter Points of the Bridge

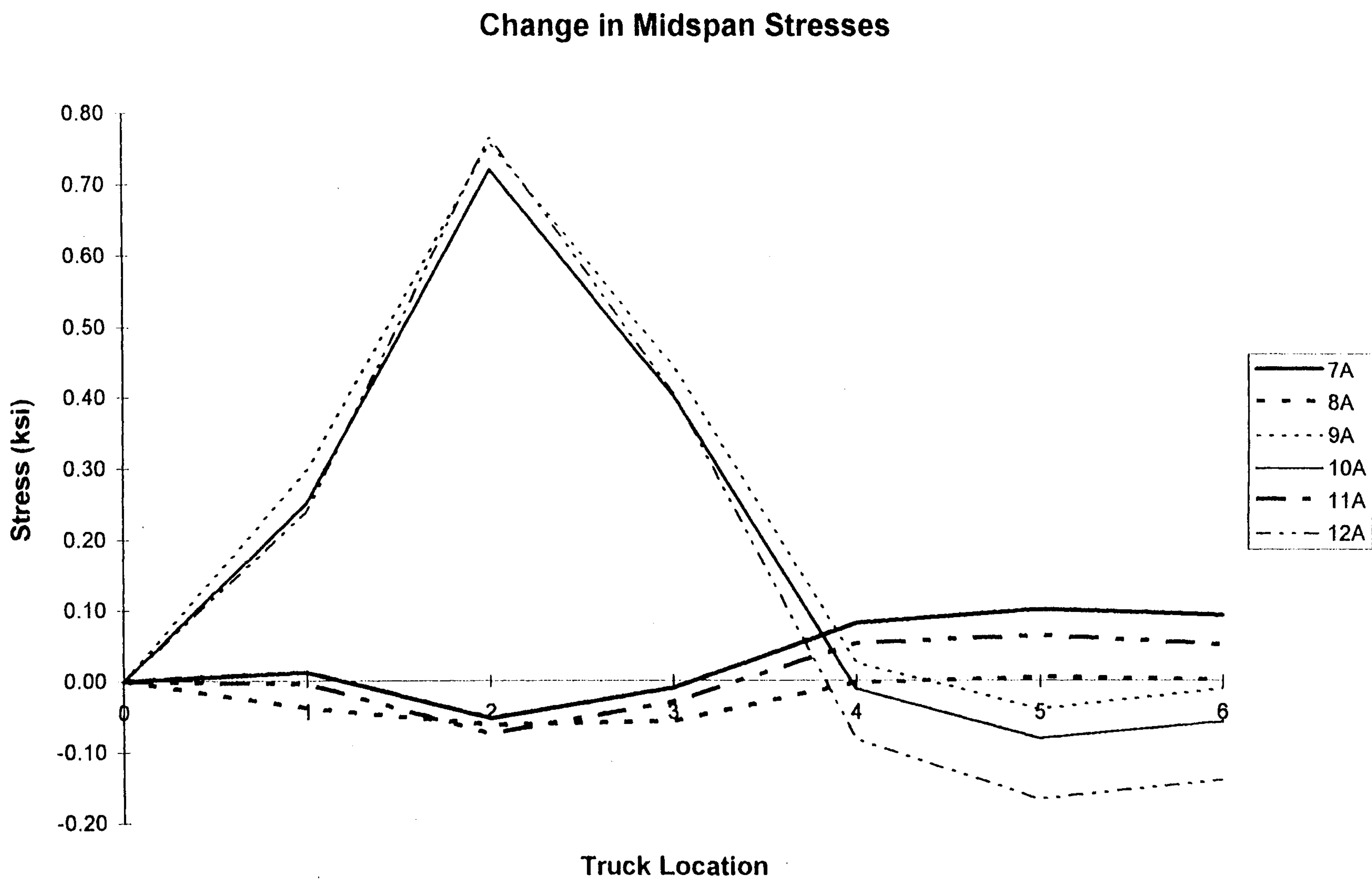

Figure C-26. Change in Stress for Gages 7A-12A with One 50 kip Truck Placed at the Quarter Points of the Bridge

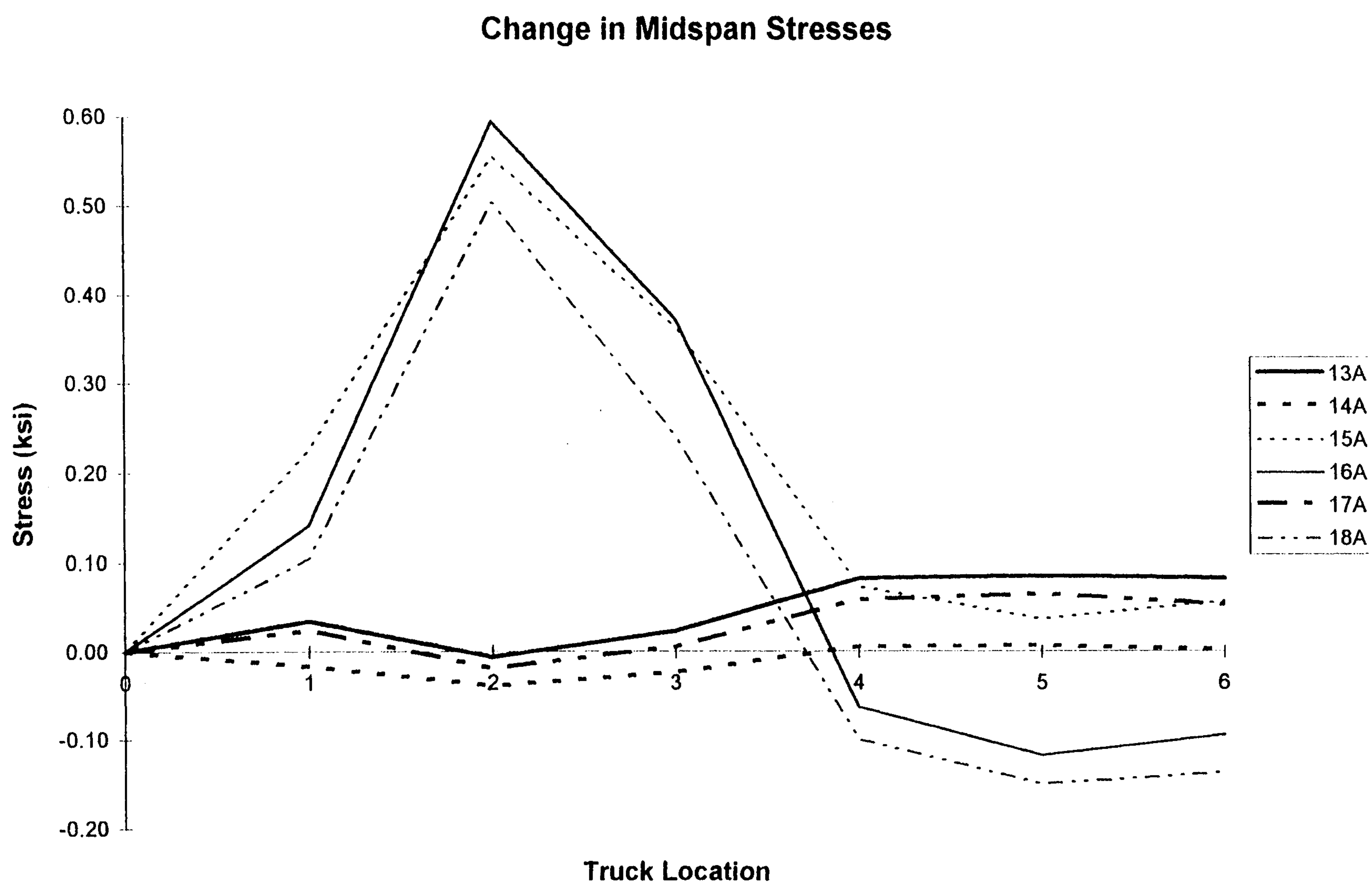

Figure C-27. Change in Stress for Gages 13A-18A with One 50 kip Placed at the Quarter Points of the Bridge

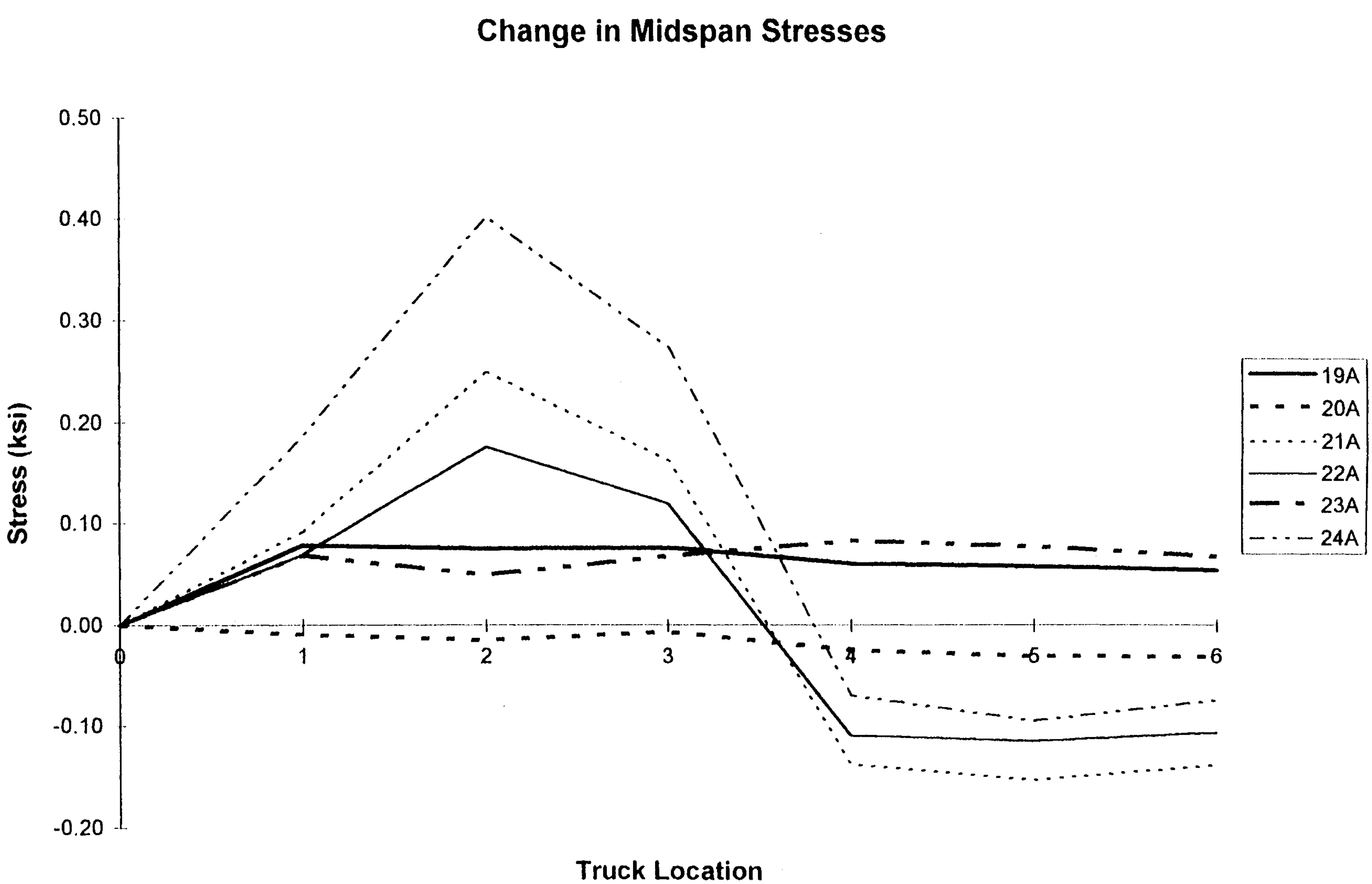

Figure C-28. Change in Stress for Gages 19A-24A with One 50 kip Truck Placed at the Quarter Points of the Bridge

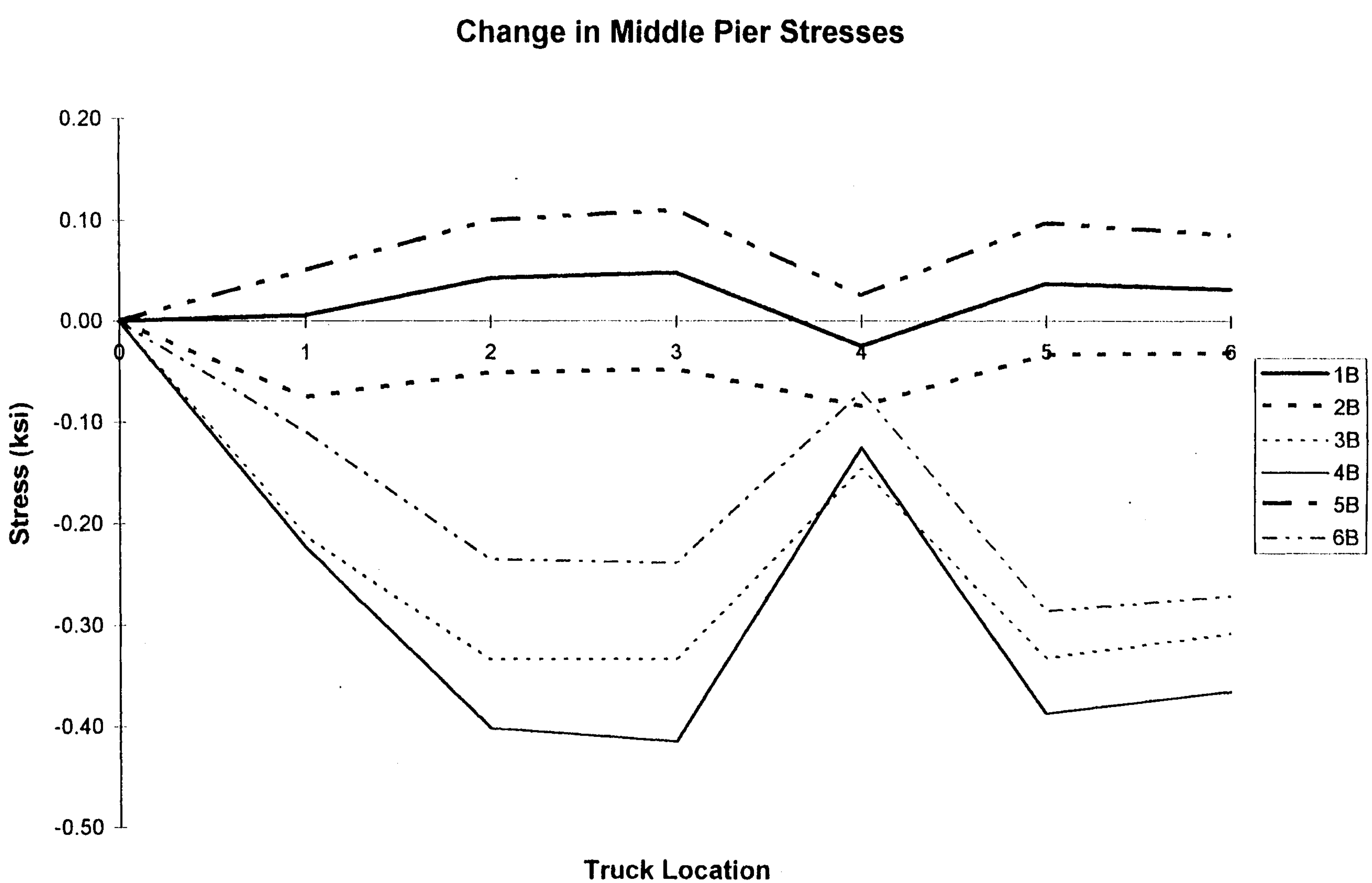

Figure C-29. Change in Stress for Gages 1B-6B with One 50 kip Truck Placed at the Quarter Points of the Bridge

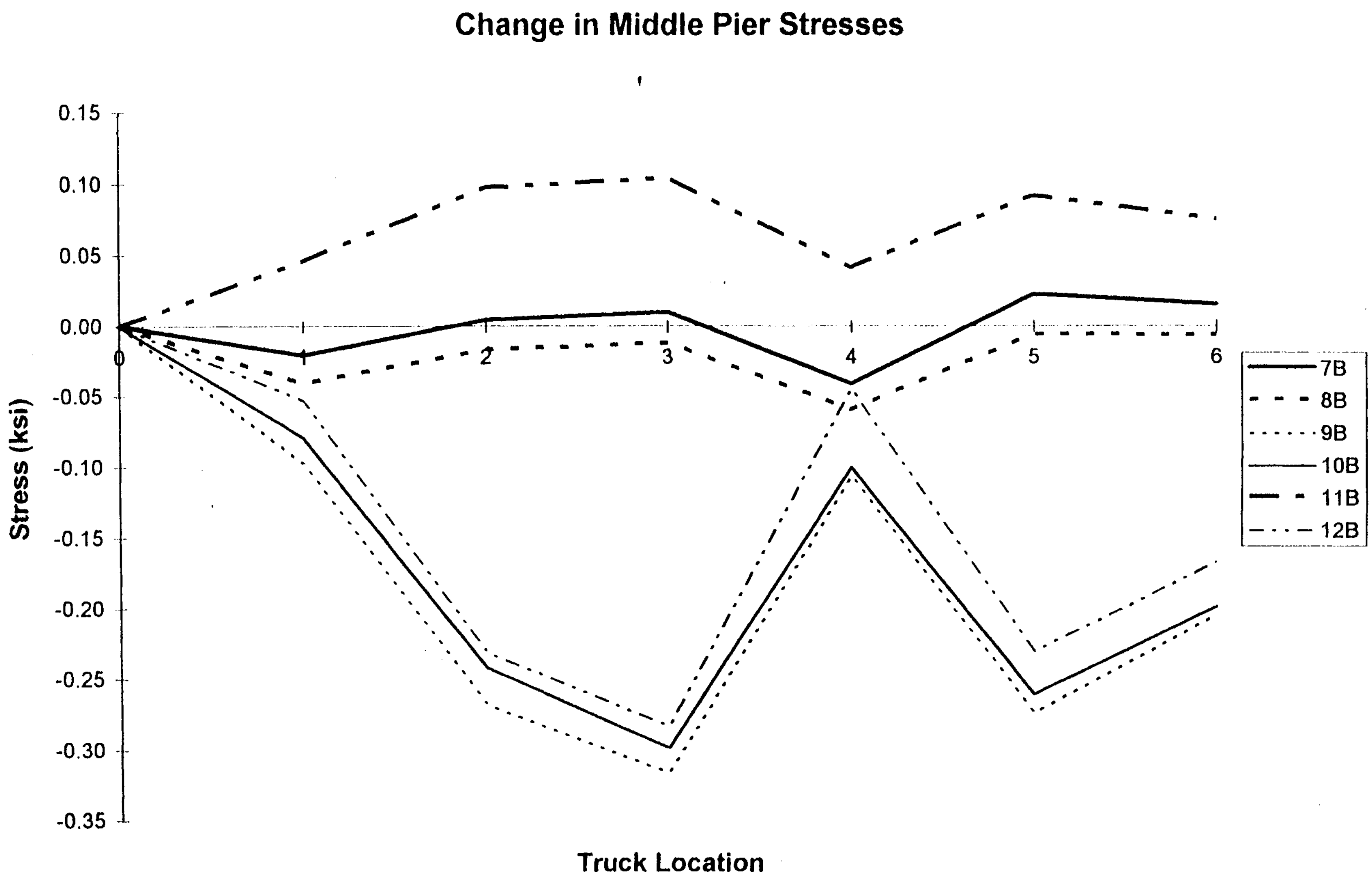

Figure C-30. Change in Stress for gages 7B-12B with One 50 kip Truck Placed at the Quarter Points of the Bridge

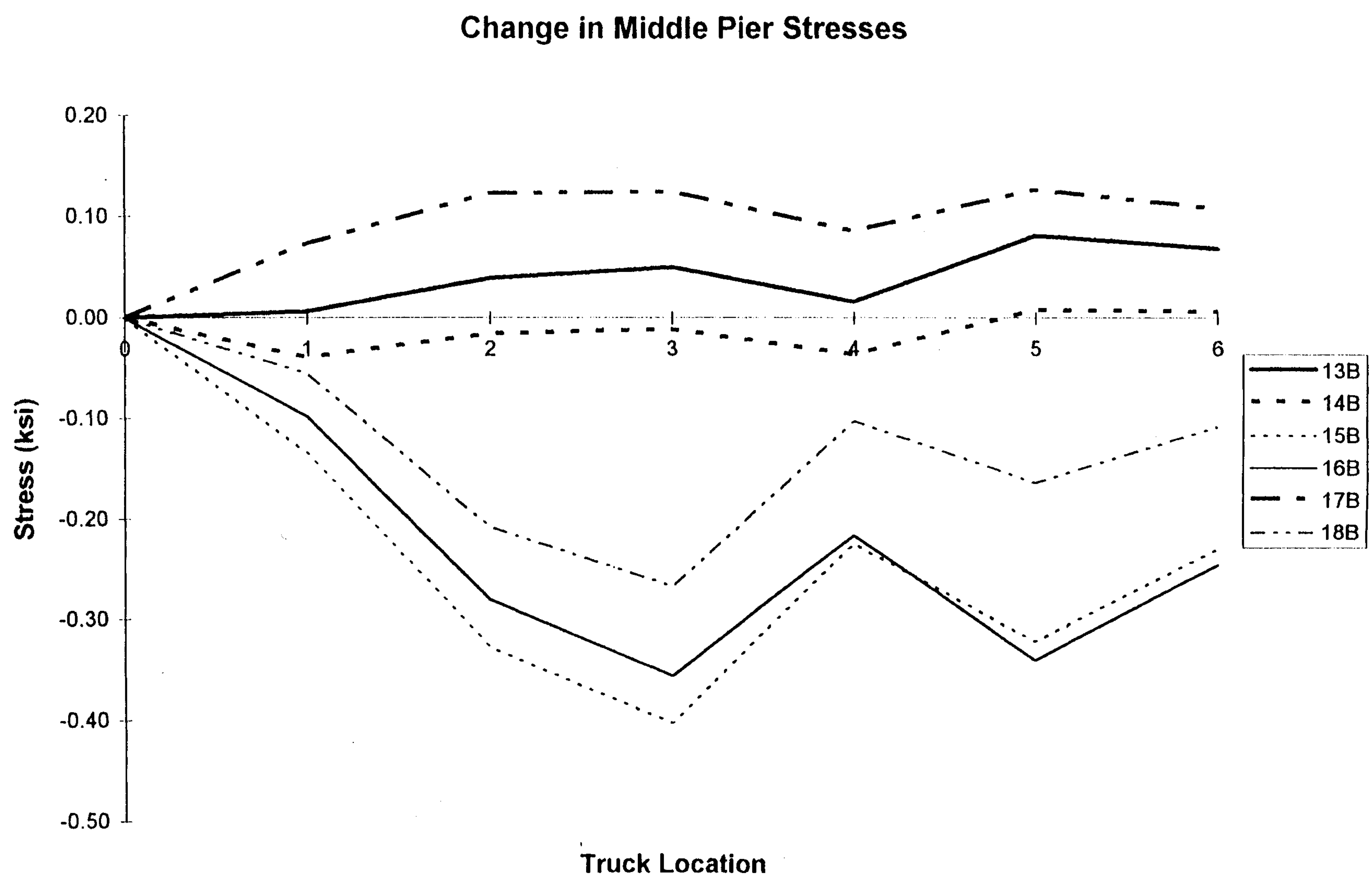

Figure C-31. Change in Stress for Gages 13B-18B with One 50 kip Truck Placed at the Quarter Points of the Bridge

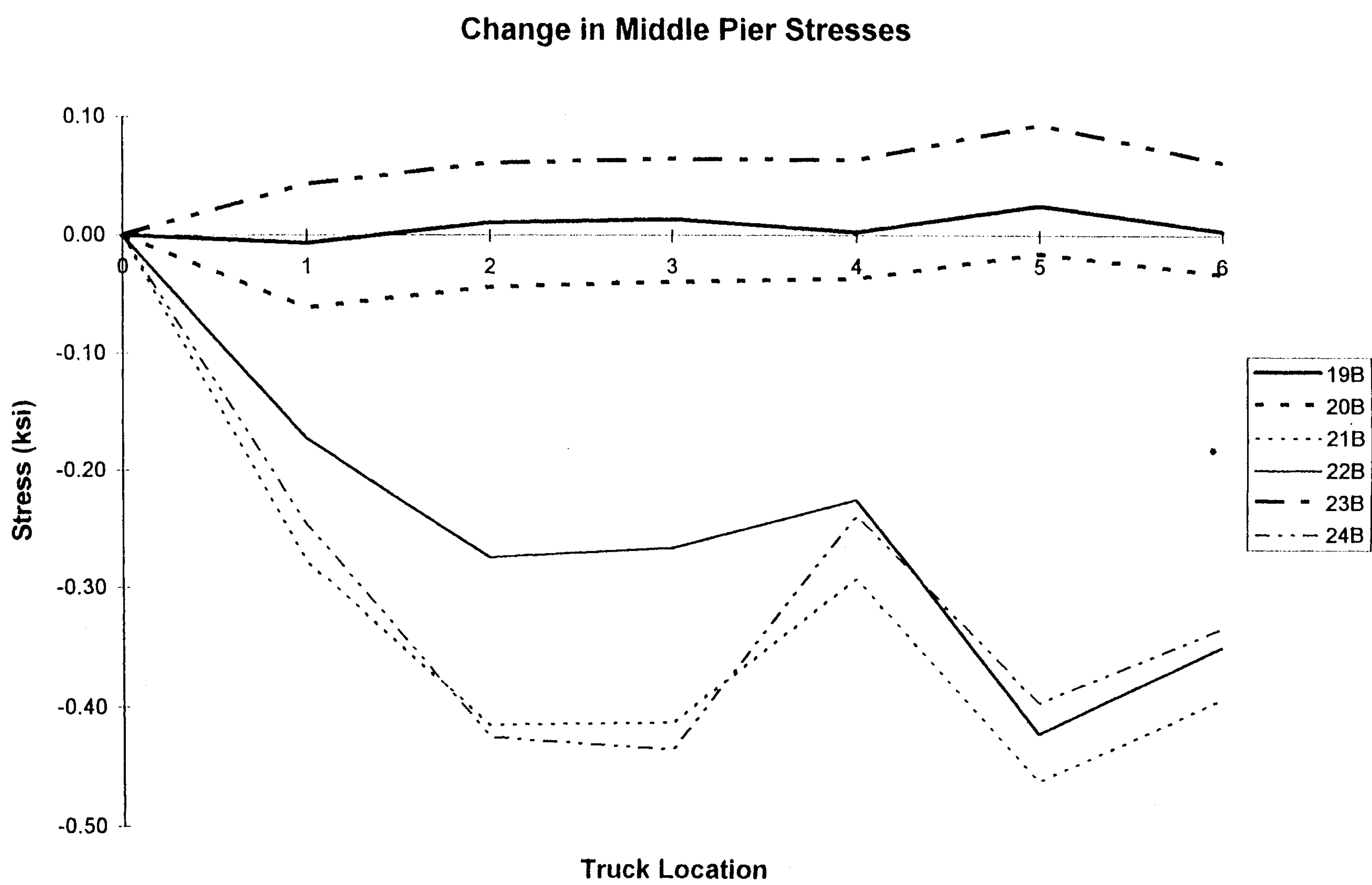

Figure C-32. Change in Stress for Gages 19B-24B with One 50 kip Truck Placed at the Quarter Points of the Bridge

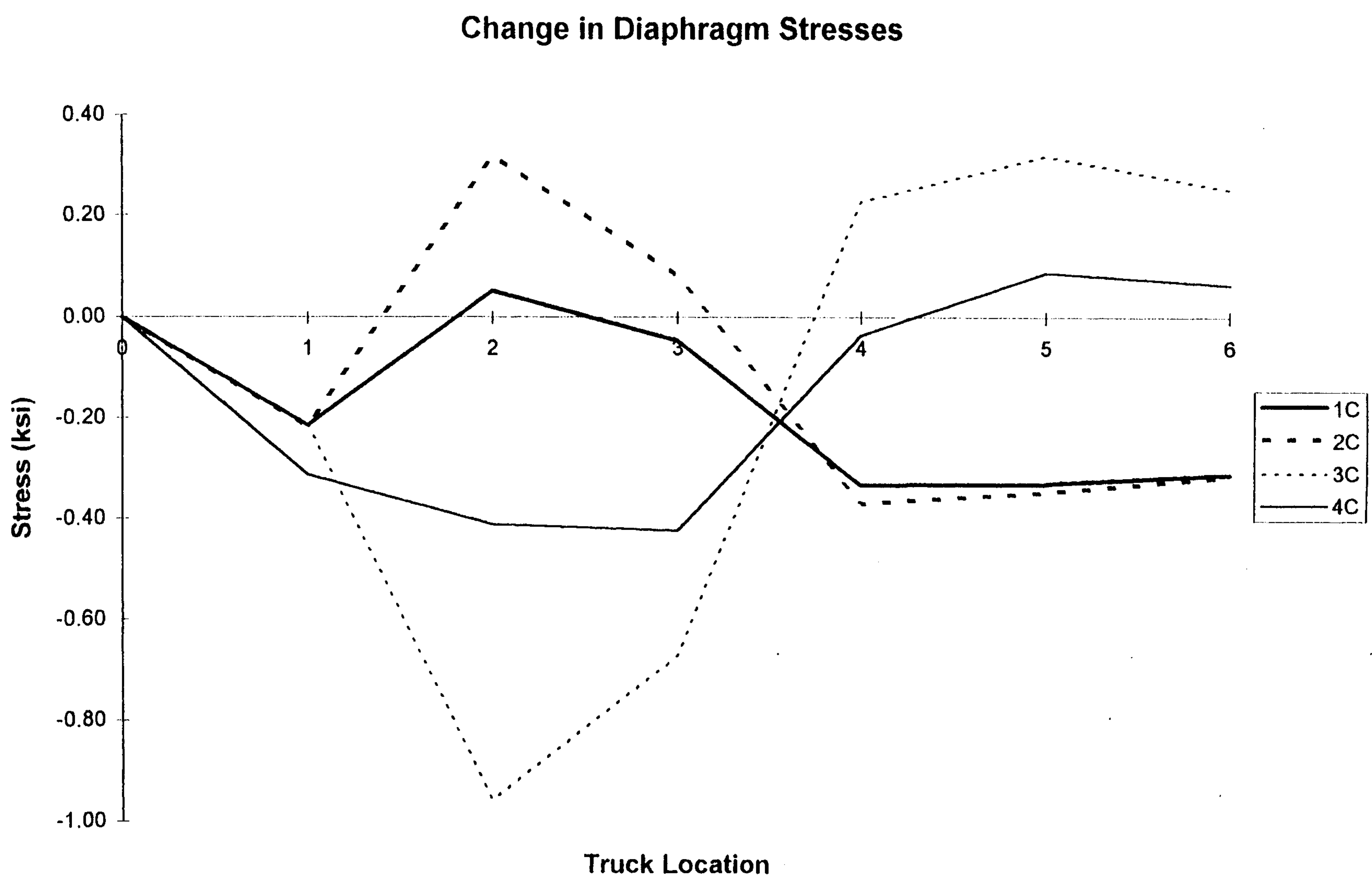

Figure C33. Change in Stress for Gages 1C-4C with One 50 kip Truck Placed at the Quarter Points of the Bridge

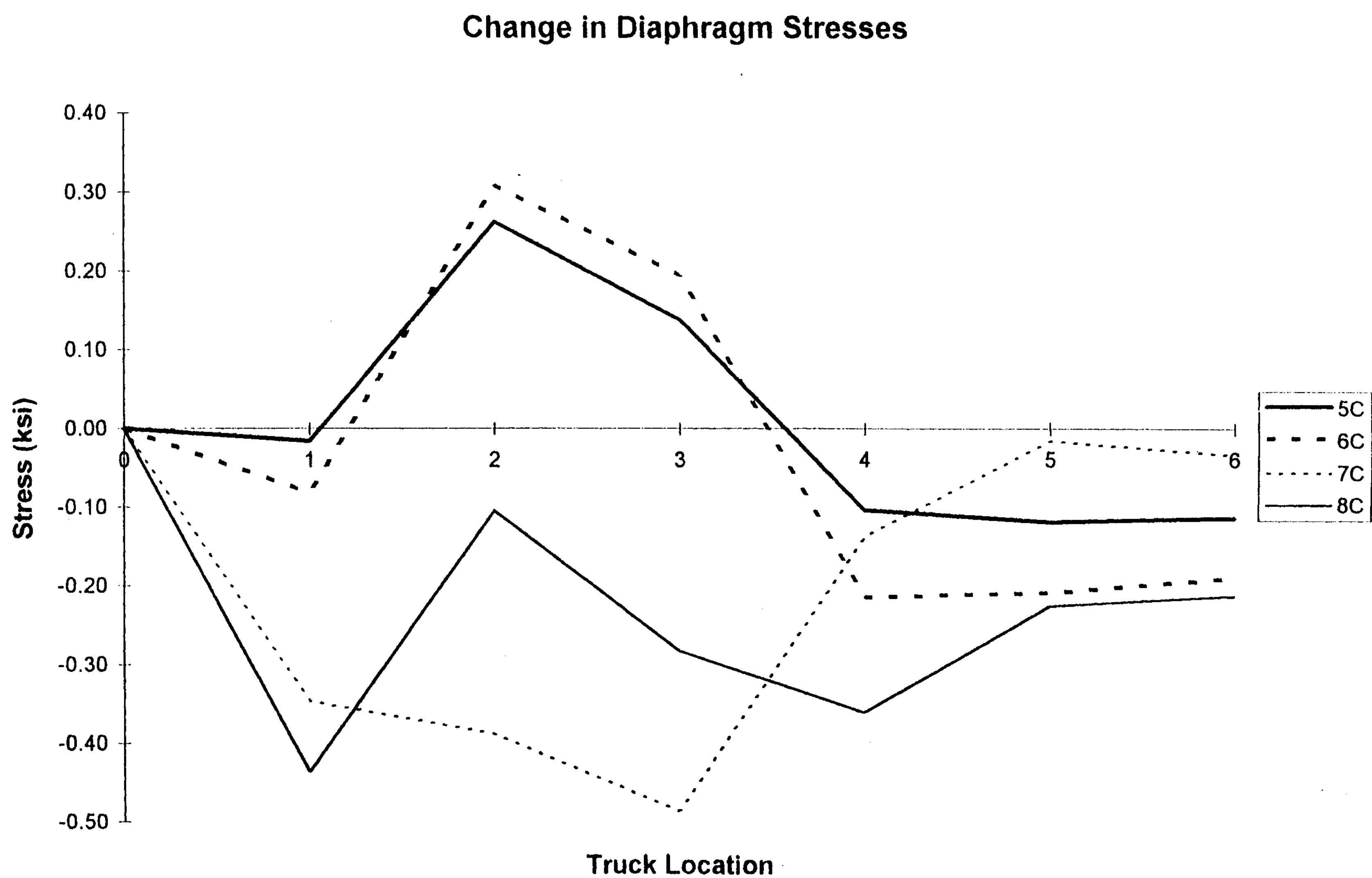

Figure C-34. Change in Stress for gages 5C-8C with One 50 kip Truck Placed at the Quarter Points of the Bridge

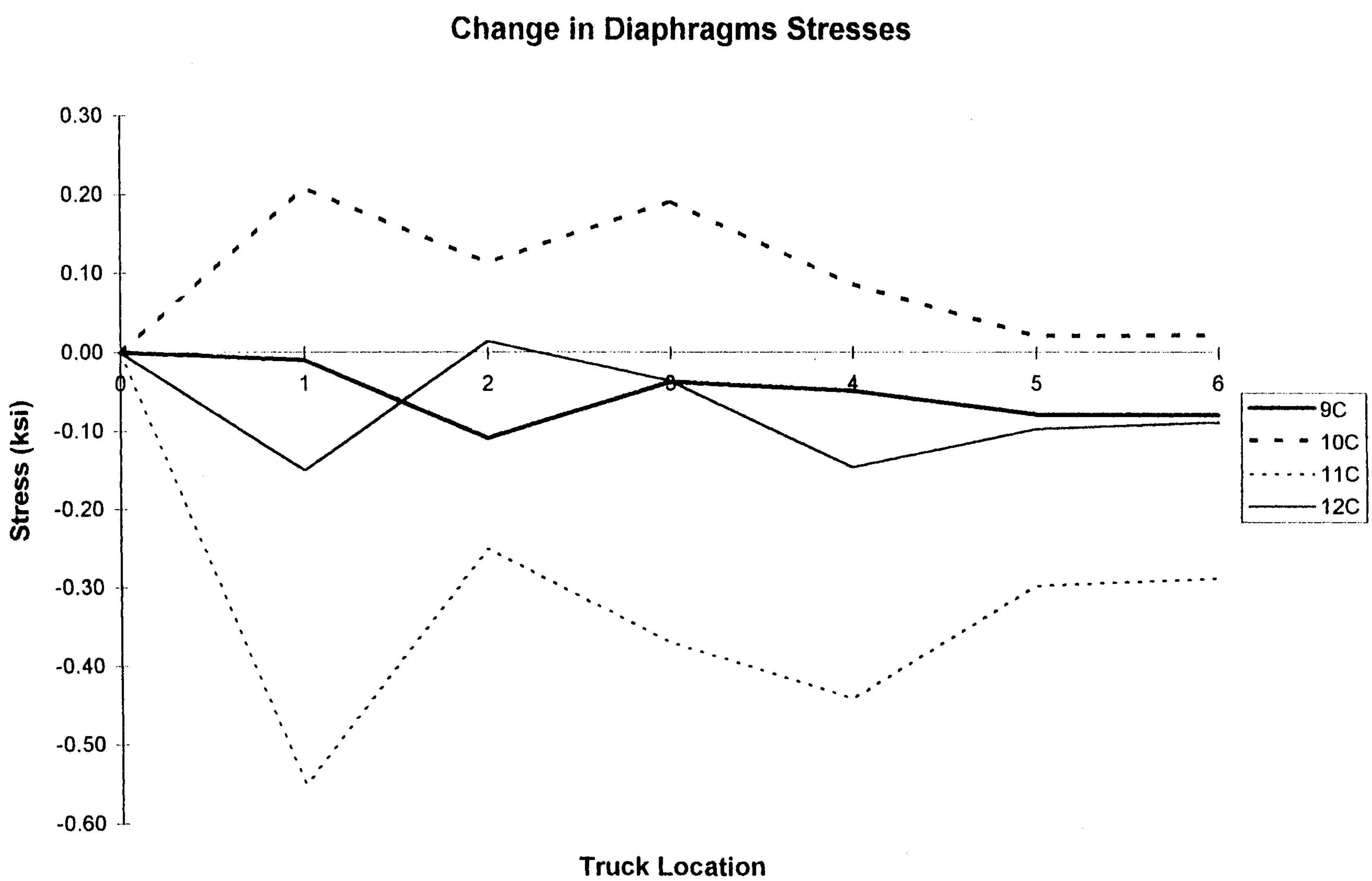

Figure C-35. Change in Stress for Gages 9C-12C with One 50 kip Truck Placed at the Quarter Points of the Bridge

OBSERVATIONS OF GIRDER STRESSES

Date and Time of Reading: October 8, 1995 at 1:45 a.m.

Temperature: 8 °C

Weather: Partly Cloudy

Loading Condition: Two 50 kip trucks placed end to end at the midspan of span 1.

Objective of Reading: This reading was taken to observe the change in stress due to the loading condition mentioned above

General Observations: Except for the two flange tip gages on girder 4, the midspan gages registered tension for the bottom flanges and compression for the top flanges. Beginning at girder 1 and progressing towards girder 4, warping can be observed across the width of the bridge. At each gage location, except for gage 4A, the largest stress occurred in girder 1 and progressively decreased as girder 4 was approached. This warping could be one explanation for the tensile stresses observed in the inside and outside flange tips of girder 4. The stresses ranged from 0.02 to 1.37 ksi in tension and -0.01 to -0.26 ksi in compression. At the middle pier, tension was experienced in the top flanges, and compression was experienced in the bottom flanges (except for the compressive force at gage 20A). The range of stresses were 0.05 to 0.21 ksi and -0.33 to -0.74 ksi. Diaphragm 1 experienced tension in the top two members and compression in the bottom two members. This pattern did not continue in the other two diaphragms. The stress range for the diaphragms was 0.03 to 0.82 ksi and -0.10 to -1.81 ksi.

Notes on Specific Gages: Not Applicable

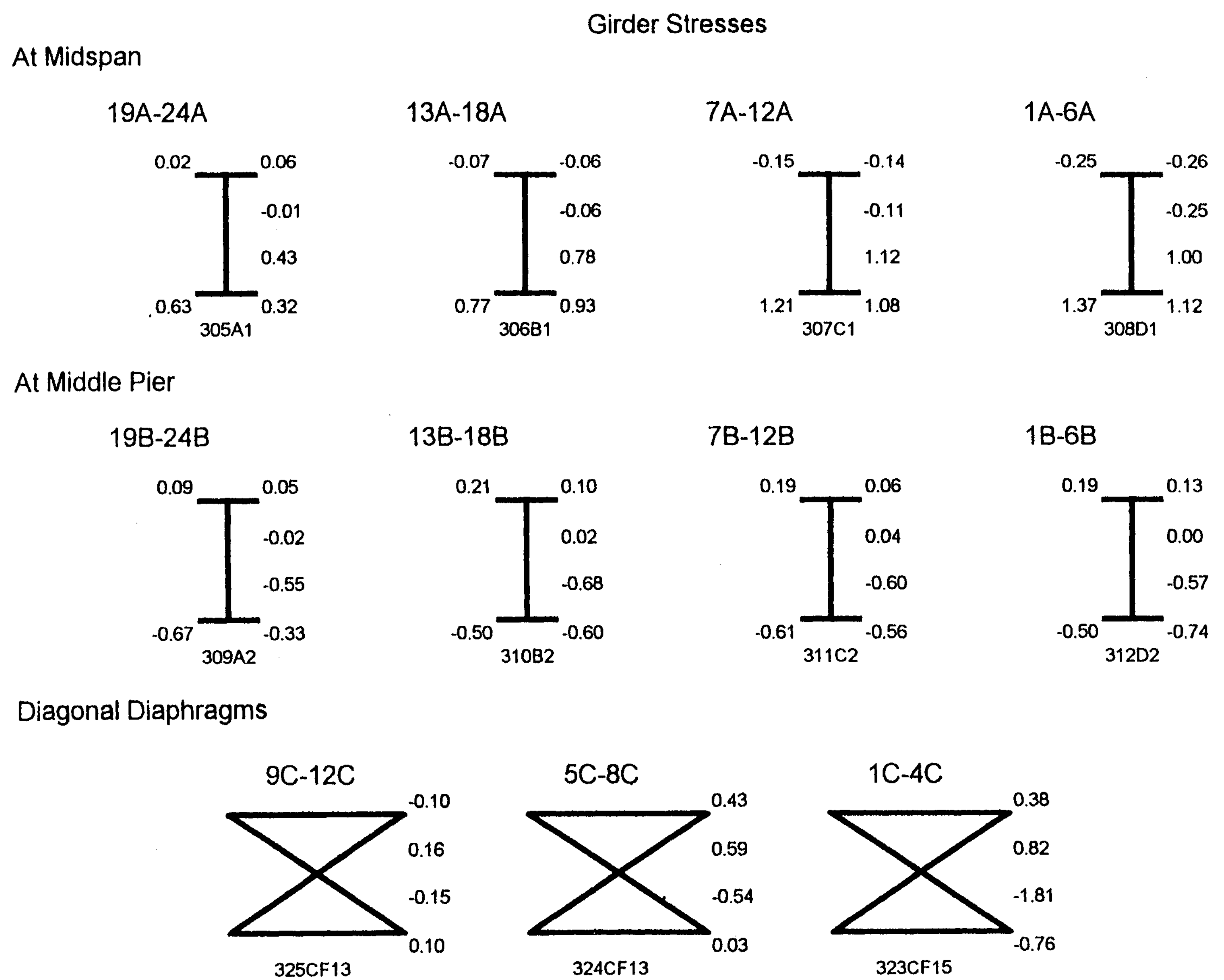

Figure C-36. Change in Stress for Two 50 kip Trucks Placed End to End at the Midspan of Span 1

Date and Time of Reading: October 8, 1995 at 2:00 a.m.

Temperature: 8 °C

Weather: Partly Cloudy

Loading Condition: Two 50 kip trucks placed at the midspan of span 2.

Objective of Reading: This reading was taken to observe the change in stress due to the loading condition mentioned above

General Observations: The stresses observed at the midspan gages with the load in span 2 were fairly insignificant, but a basic trend of tension in the top flanges and compression in the bottom flanges could be identified. The range of stresses was 0.00 to 0.10 ksi and -0.03 to -0.23 ksi. At the middle pier, the top flanges, except for gage 2B, experienced tensile stress, ranging from 0.00 to 0.15 ksi, and the bottom flanges experienced compression ranging from -0.27 to -0.56 ksi. Diaphragm 1 experienced tension in the bottom two members and compression in the top two members. This pattern did not continue in the other two diaphragms. The stress range for the diaphragms was 0.01 to 0.46 ksi and -0.07 to -0.40 ksi.

Notes on Specific Gages: Not Applicable

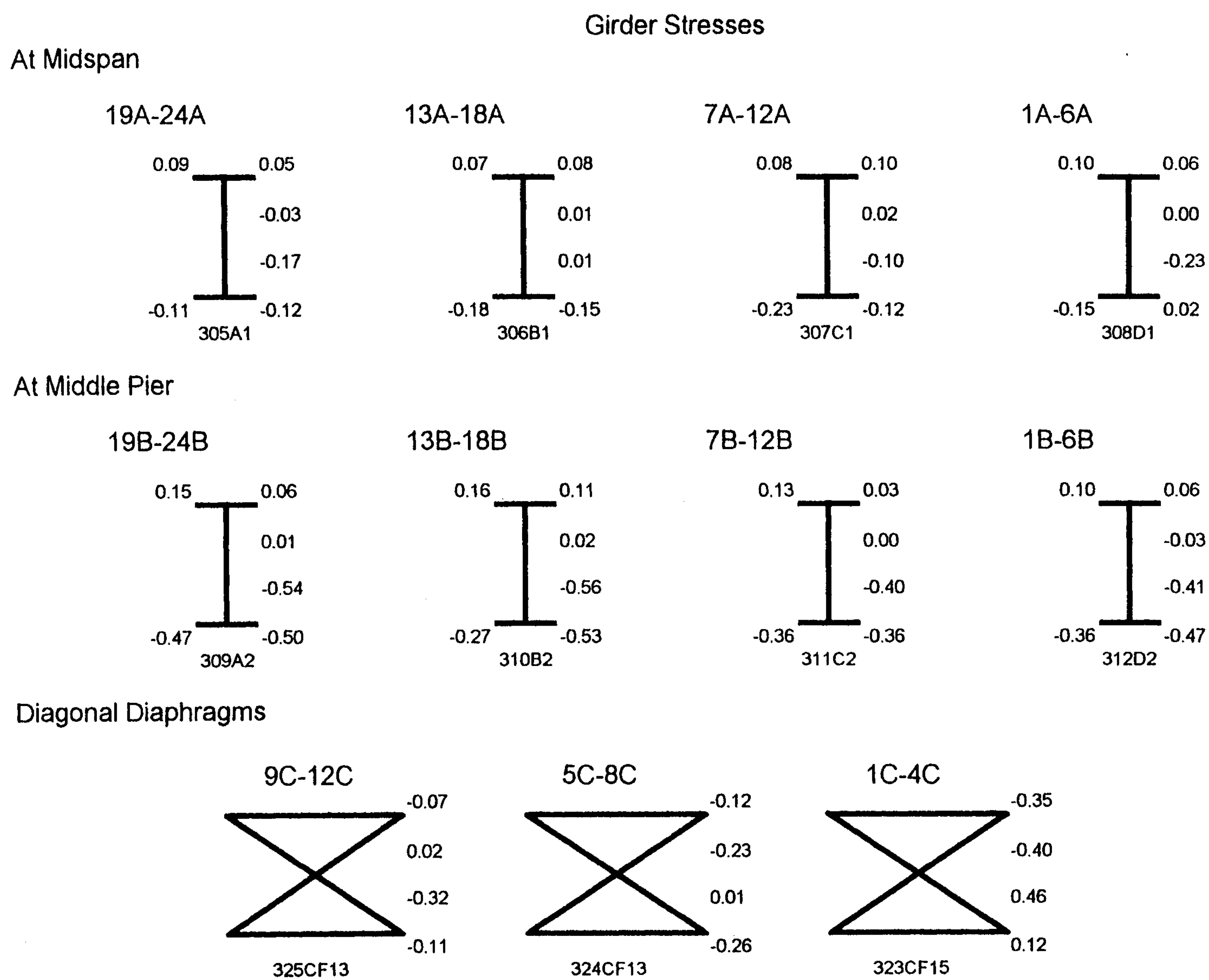

Figure C-37. Change in Stress for Two 50 kip Trucks Placed End to End at the Midspan of Span 2

Date and Time of Reading: October 8, 1995 at 1:10 a.m.

Temperature: 8 °C

Weather: Partly Cloudy

Loading Condition: One 50 kip truck was placed at the midspan of both spans simultaneously.

Objective of Reading: This reading was taken to observe the change in stress due to the loading condition mentioned above

General Observations: At the midspan except for the inside and outside flange tips of girder 4, the top flanges experienced compression, and the bottom flanges experienced tension. These stresses ranged from -0.01 to -0.14 ksi in the top flanges and 0.17 to 0.66 ksi in the bottom flanges. At the middle pier, the top flanges experienced tensile stress, and the bottom flanges experienced compressive stress. These stresses ranged from 0.02 to 0.17 ksi in the top flanges and -0.38 to -0.75 ksi in the bottom flanges. Diaphragm 1 experienced tension in the top two members and compression in the bottom two members. This pattern did not continue in the other two diaphragms. The stress range for the diaphragms was 0.03 to 0.38 ksi and -0.03 to -0.79 ksi.

Notes on Specific Gages: Not Applicable

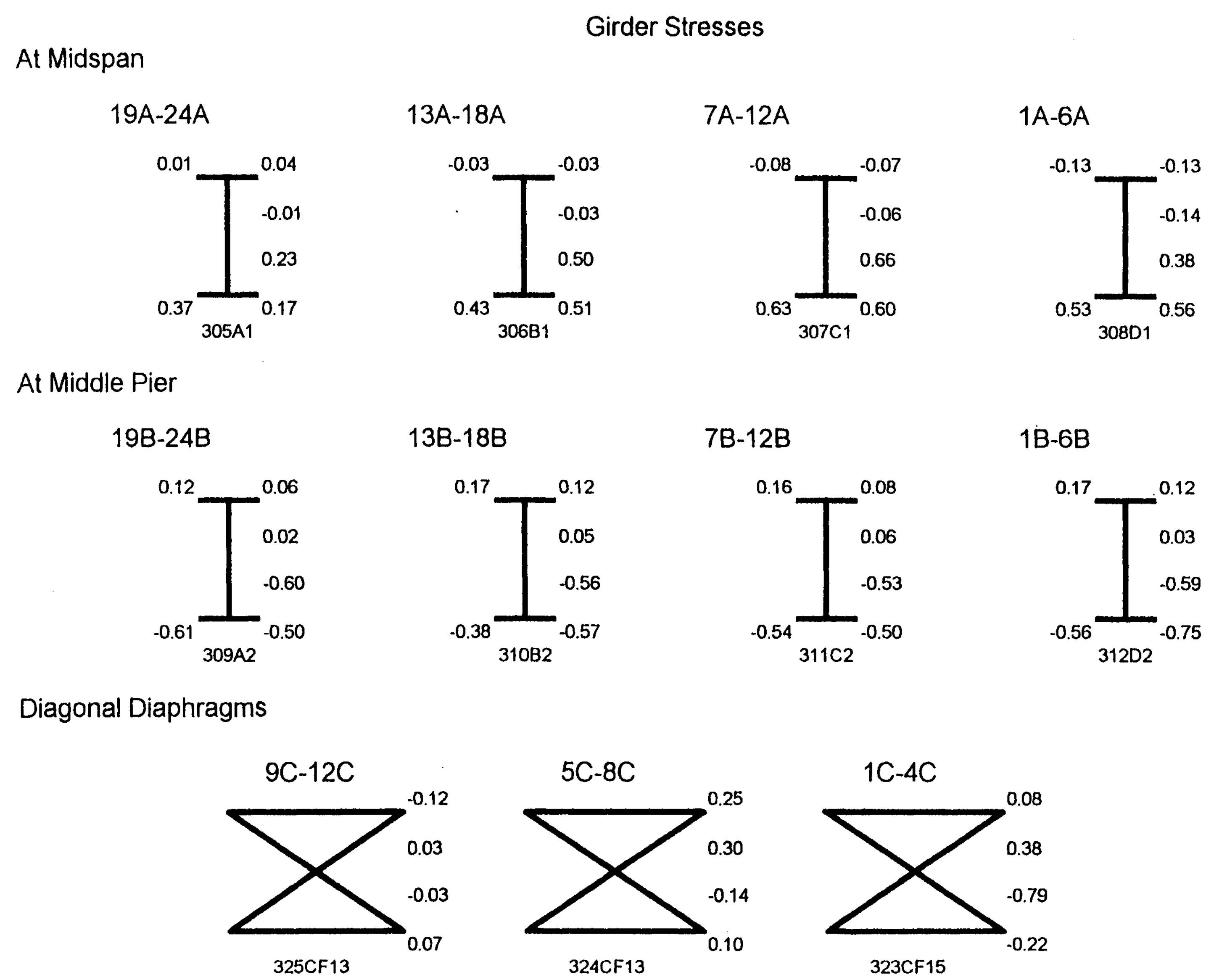

Figure C-38. Change in Stress for Two 50 kip Trucks One Placed at the Midspan of Both Span 1 and 2

APPENDIX D

DETAILED CONSTRUCTION SEQUENCE

APPENDIX D
DETAILED CONSTRUCTION SEQUENCE

Starting from the in-situ steel framing of the superstructure, this appendix describes the construction sequence in four steps. First, assembly of the steel superstructure is introduced, including the method of erection, the equipment used in the erection, and the erection sequence. Placement of formwork plus reinforcing steel is then described, followed by the pouring of the concrete deck. Finally, the construction of parapets and the overlay are outlined. As the construction proceeds, the proof loading under construction will be summarized resulting from the correlation between the field measurement and the structural analysis based on the grillage method.

D.1 STEEL ASSEMBLING

In order to avoid the inconvenience to drivers and to reduce the control volume of the traffic flow, the third-shift hours from 11 p.m. to 7 a.m. were selected by the contractor for the erection of the steel superstructure. A total four nights were spent erecting the steel, including two on the south span and two on the north span.

Three cranes were used on the south span, while two were used on the north span. The erection gear included two crawler cranes with lifting capacity of 100 tons (200 kips) and one 4-wheel crane with a capacity of 50 tons (100 kips) for the south span erection. One crawler crane plus the 4-wheel crane were used for erection of the north span erection, primarily since only one girder segment had to be erected per girder on the north span, versus two on the south span. In addition, a Highlander lifter with a capacity of several tons lifted workers and connection bolts into position, especially when assembling the splices. An air pump driver was employed to tighten the bolts.

One temporary scaffolding-tower, 4 feet by 5 feet in cross-section, was used under each girder line to support the erected girders at mid-span of each span when the girders were being into place and the crossframes being bolted in. These temporary towers were moved from the south span to the north span during the erection of the north span and then totally removed when all of the crossframes and end diaphragms were rattled up.

The prefabricated girders and crossframes for the day were transported separately on the morning of their erection from the fabrication site to the construction site. Preparation for erection, such as setting handrails (for the workers) on the top of the girder, building temporary towers on the ground, building falsework, were done in the afternoon, prior to erection during the early morning hours.

Day 1 on the south span: July 17-18, 1995

1. The girders on this span were erected from the innermost girder to the outermost girder. Girder 305A1 (see Figure 2.4) was first hoisted by both 50 ton crane (50T) using one lifting point on girder's top flange and 100 ton crane (100T) using two lifting points through a 20 foot spreader beam (20-footer).

2. After having moved girder 305A1 to let one end set on the south abutment under one or two workers' guide, two cranes (50T+100T) remained holding girder 305A1. At the same time, another 100 ton crane (100TA) erected girder 306B1 using only two lifting points on girder's top flange, through a 30 foot spreader beam (30-footer), plus a "come-along" (see Figure 3.1). The splice between girders 305A1 and 306B1 was tightened by three workers (group 1) in the lifter.

3. After the bolts for the splice connecting girders 305A1 and 306B1 were tightened, girder 306B1 was aligned on the center pier by two workers (group 2). A temporary scaffolding tower was then added near the midspan of the south span by two workers (group 3) to support the erected girders. The two girders became one continuous girder on three vertical supports and overhung the center pier approximately 38 feet into the north span. Crane 100T with a 20-footer and crane 50T were then released to erect a third girder, while crane 100TA continued holding girder 306B1.

4. The 50T+100T cranes lifted girder 307C1 and moved it to let one end sit on the south abutment. Crane 100T continued holding 307C1, while crane 50T released girder 307C1 and began lifting crossframes.

5. Crane 50T lifted crossframes D1 and D4 (see Figure D.1 for nomenclature). D4 was put into place first by group 2, and one bolt in each corner was tightened snug. Crossframe D1 was then loosely fastened in place.

6. Crane 100TA released 306B1 and lifted 308D1 into place. Group 1 spliced 307C1 and 308D1 while group 2 worked on placing the girder on the center pier.

7. Crossframe D5 was in put into place and group 3 placed a scaffolding tower under girders 307C1 and 308D1 near midspan.

8. The 100T and 100TA cranes were used to lift the remainder of the south span crossframes into place in the following sequence: D2, D9, D3, D6, D7, D8, D10, D11, D12, and D13. These crossframes were originally bolted in with just four bolts, one in each corner of the crossframe. All bolts were tightened up during the daytime of the following day.

Day 2 on the south span: July 18-19, 1995

1. The 50T+100T cranes erected girder 309A2, placing one end on the south abutment. Crane 50T then released girder 309A2 to pick up crossframes, while crane 100T remained holding girder 309A2.

2. Crane 50T lifted crossframes 2a and 5a, and group 2 bolted them into place.

3. Crane 100TA lifted girder 310B2. Group 1 spliced 309A2 and 310B2 while group 2 worked on setting girder 310B2 on the center pier.

4. Crossframes were placed in the following sequence by group 2: 3a, 4a, 9a, 10a, and 11a.

5. Group 3 set a tower under girders 309A2 and 310B2 near the midspan of the south span.

6. Crossframe 2b was erected before girder 311C2 was erected. This type of cantilever erection of a crossframe occurred only once, apparently because of the difficulty of subsequent fitup.

7. The 50T+100T cranes lifted girder 311C2 and held it in place.

8. Crane 100TA lifted girder 312D2. Worker group 1 spliced girders 311C2 and 312D2 while group 2 worked on placing the girder on the center pier.

9. Another sequence of crossframes, including 5b, 3b, and 4b were put into place by group 2, as was the temporary scaffolding tower for girders 311C2 and 312D2, set up by group 3.

10. The rest of the crossframes were put into place in the following approximate sequence: 9b, 10b, 11b, 6a, 7a, 12a, 13a, 8a, 13b, 11b, 6b, 12b, 7b, and 8b. All bolts were tightened fully during the following day.

Generally speaking, the steel assembling on the south span went smoothly, except that the holes in the bottom plate of girders 305A1 and 307C1 at the southern support were too small. Consequently, wood blocks were used for supporting the girders on bearing plates. This problem was fixed later after the south span erection was nearly complete, except that the end diaphragms were still on the ground. To fix this problem, the sole plates were first cut off, the holes were drilled to fit the pintles, and the sole plates were then welded back to the bottom flange and seated in the pintles. It was also found on day 2 that the holes in sole plates to fit the pintles on center pier were drilled too big. The following day, additional sets of bushings were then jammed into the holes to grip the pintles. The end diaphragms were then erected in the order of E1, E2 and E3, thus completing erection of the southern span.

Day 3 on the north span: July 24-25, 1995

1. The girders on this span were erected from the outermost girder to the innermost girder. Girder 313A3 was first raised by the 100 ton crane (100T) using the 30-foot spreader beam and a "come-along". To move girder 313A3 into place, crane 100T had to make a 90 degree turn with the girder due to tight maneuvering room as the girder was wedged between the splice and the north abutment. The splice of girder 313A3 was then tightened by group 1, followed by the girder being placed on the north abutment.

2. Crane 100T released 313A3 and continued to erect girder 314B3, tightening its splice.

3. The 50 ton crane (50T) lifted a sequence of crossframes, put into place by group 2: D20, D19, D18, D14, D15, D17, and D16. All bolts on the crossframes were tightened loosely, and were tightened fully after the north span erection was finished.

4. During the daytime of July 25, the temporary scaffolding towers used in the south span were all moved to support the girders at the midspan of the north span, and the workers began placing the formwork on the south span.

Day 4 on the north span: July 25-26, 1995

1. Crane 100T erected girder 315C3 similarly to how girders 313A3 and 314B3 were done.

2. Crane 50T lifted crossframes 20a and 19a were then erected by crane 50T.

3. Crane 50T was moved to make room for crane 100T, and crane 100T released 315C3 in order to erect 316D3 when one of the scaffolding towers was positioned to support girder 315C3.

4. The last tower was set up to support girder 316D3 once 316D3 was in place.

5. Crane 50T returned to lifting crossframes 20b and 19b.

6. Crane 100T released 316D3 and continued to erect crossframes 14a, 15a, 14b, and 15b.

7. The following few days, all bolts were rattled up.

8. The erection was smooth on the north span.

D.2 FORMWORK PLUS REINFORCING

Wooden formwork decking was set up predominantly from July 28 through August 3, starting at the south abutment. Plywood forms of 3/4" thickness were supported by 2"x10" joists, which connect to the upper part of curved girders by using steel hangers. Overhanging brackets connected to the innermost and the outermost girders were added to support both the overhanging plywood forms and their supporting joists in two directions, including 4"x4" joists in the longitudinal direction supported by 2"x6" joists in the transverse direction. Immediately after the formwork was in place, shear studs were welded to the top flanges of the girders and the end diaphragms, starting from the south abutment to the splice line of the south span and then from the north abutment to the splice line of the north span. Reinforcing bars were then placed on the north span first, from the abutment to center pier, and then extended to the south abutment of the south span. The 50T and 100T cranes were used in this step, alternately. There were, in general, five to ten workers and two air compressors weighing 2,785 lbs each on the bridge. To meet the scheduled date, August 11th, of pouring the concrete, working overtime took place a couple of days before August 10th, and an additional five to ten workers were on the deck during this time. All the preparation work for pouring the concrete was completed by August 10th.

D.3 CONCRETE DECK POURING

The concrete pouring started from the north abutment at 4 a.m. and ended to the south abutment at 8 a.m. on August 11th. A total of 149 cubic yards of concrete were placed on the bridge. The ready mix concrete was delivered by concrete trucks and was then distributed by a concrete mobile hose with an air-pump conveyor. Ten to fourteen people using finishers and vibrators worked on casting, vibrating, finishing, and sloping the casted concrete, but four of them started covering the casted deck when the weather turned to a drizzle, when two thirds of the concrete slab was in place. A small motor to generate power for the vibrators was also on the deck throughout the concrete pouring.

D.4 PARAPETS AND THE OVERLAY

The reinforcement needed for the parapets was placed from August 16-18. The slip former was used here to cast the concrete in the parapets since the parapets of this bridge are uniformly shaped. On August 22, the slip former was used to pour the innermost parapet, and the next day it was used on the outermost parapet. The ready mix concrete was delivered by concrete trucks. Six to eight workers were working with the slip formers. Great care was taking in finishing the concrete surface as the former progressed.

The placement of the two inch thick overlay composed of low slump concrete on the top of concrete was first placed on the east half width of the bridge. The remaining part of the overlay was placed on September 13th, thus completing the construction of the bridge.

NOTES:

1. Girder No.= Length(ft-in)/Weight(kips)
2. G1 - G4 on Day 1
3. G5 - G8 on Day 2
4. G9 - G10 on Day 3
5. G11 - G12 on Day 4

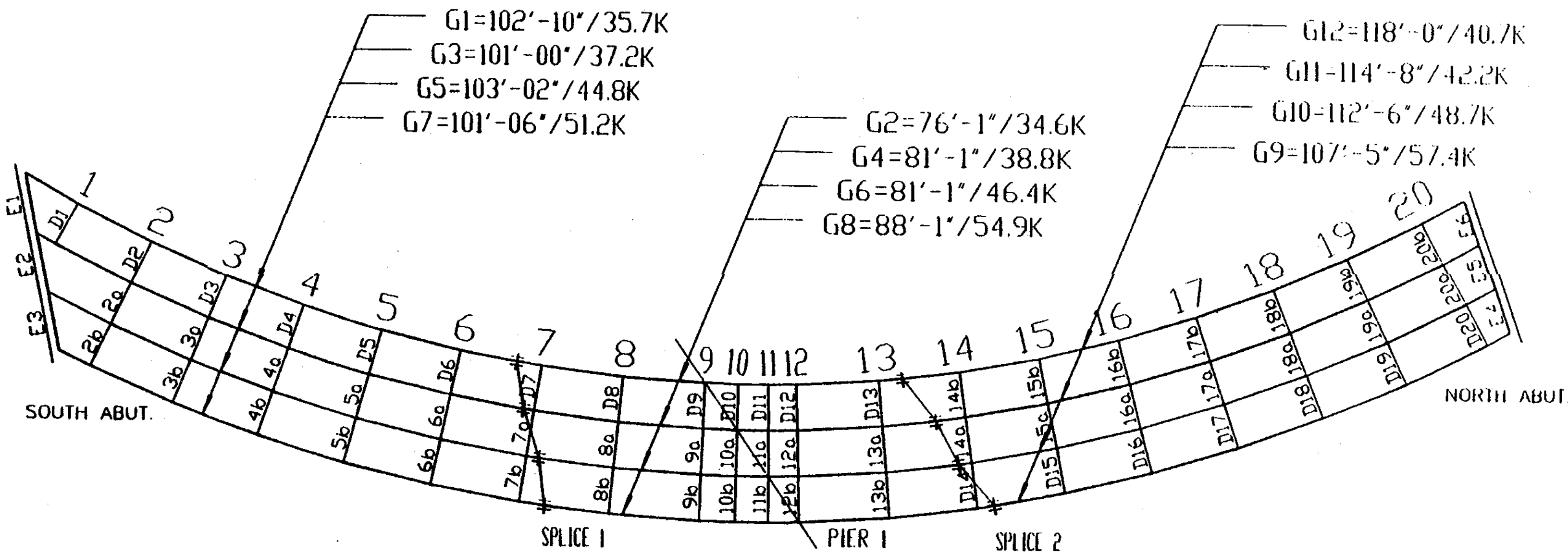

Figure D.1. Designation for erection sequence of the skeleton

APPENDIX E

CALCULATION OF DEAD LOADS FOR ANALYSIS

APPENDIX E

CALCULATION OF DEAD LOADS FOR ANALYSIS

This appendix provides the details of how the dead loads were computed for use in the UM program.

E.1 FORMWORK: 5 PSF

The weight of formwork is estimated as 5 psf based on the information obtained from the construction site of MN/DOT bridge No. 27998. The specific gravity for plywood is assumed 0.55 which turns out to be 35 pcf. It follows that

1. Deck weight: 3/4" thick

   35 x 3/4 x 1/12= 2.19 psf

2. Joist weight: 2x10 joist @ 2'-0" on center

   35 x 2 x 10 x 1/144 x 1/2= 2.43 psf

There is no deduction of the area of beam flanges. This is compensated by the weight of shear studs and that of clamps to connect the beam flanges and the wood joists. Total 4.62 psf is further round off to 5 psf.

E.2 REINFORCEMENT: 10 PSF

A total of 86,985 lbs of reinforcing bar was placed on the plan area of 9940 ft^2.

E.3 PLAIN CONCRETE: 80 PSF

The volume of wet concrete was estimated at 5,520 ft^3 by the following calculation:

$$5{,}698 - (86{,}985/490) = 5{,}520 \text{ ft}^3 = 204 \text{ cubic yards}$$

where the total volume of reinforced concrete is estimated at 5,698 ft^3 and the density of reinforcing bar is estimated to be 490 pcf. The uniform floor load resulting from the concrete slab is then determined by taking 144 pcf as its density.

$$144 \times 5520 / 9940 = 79.97 \text{ psf}$$

APPENDIX F

TRANSFER OF VERTICAL LOADS

APPENDIX F

TRANSFER OF VERTICAL LOADS

This appendix outlines the procedure by which vertical loads applied to the bridge were distributed to the discrete joints of the finite element model.

F.1 RIGOROUS DISTRIBUTION

It is not unusual that the center of applied loads does not coincide with the center of rigidity of the structure in a curved I-girder system with varying depth from girder to girder. As a result, the vertical load transferred to each girder is due not only to the flexural deformation but also to torsional rotation. In order to determine the vertical load distribution factors, it is appropriate to assume that the crossframes provide rigid links to prevent the girders from being deformed differentially. Based on the assumption of no differential deflections, the following equation may be used:

$$\frac{V_i}{I_i} = \alpha = \frac{V}{\Sigma I_i}$$

$$V_i = \frac{I_i}{\Sigma I_i} V \tag{F.1}$$

where V_i is the vertical load taken by I_i, the moment of inertia for each girder. V is the vertical load being transferred and S means summation.

In Figure F.1a, the center of the resultant forces also called the rigidity center is obtained as follows:

$$V_2 d_2 + V_3 d_3 + V_4 d_4 = V \cdot x_0$$

$$x_0 = \frac{I_2 d_2 + I_3 d_3 + I_4 d_4}{I_1 + I_2 + I_3 + I_4} \tag{F.2}$$

where x_0, d_2, d_3, and d_4 are the distance to girder 1 from rigidity center girders 2, 3, and 4 respectively. An additional torque $V \times e_0$ has to be considered when there exists an eccentricity e_0 between the center of external loads and the rigidity center.

Based on the assumption of no differential rotations, the following equation can be written

$$\kappa \frac{T_i}{I_i} = u_i = x_i \bullet \phi$$

$$T_i = \frac{\phi}{\kappa} x_i I_i = \theta \, x_i I_i \qquad \text{(F.3)}$$

where k is a proportional constant, q is a rotation angle, T_i is the shear force taken by each girder, u_i is the vertical deflection on each girder due to rotation, and x_i is the arm length from each girder to the rigidity center as shown in Figure F.1b. Furthermore, f and k are combined into one parameter q.

Setting the sum of T_i equal to zero, one obtains the location of the torsion center which is actually the same point as the rigidity center defined in Eq. F.2. Also making the moment equilibrium yields the following equation

$$\theta = \frac{M_z}{\Sigma x_i^2 I_i} = \frac{V \bullet e_0}{\Sigma x_i^2 I_i} \qquad \text{(F.4)}$$

and substitution of q in Eq. F.3 leads to the following equation.

$$T_i = \frac{x_i I_i e_0}{\Sigma x_i^2 I_i} V \qquad \text{(F.5)}$$

Consequently, the vertical load P_i transferred to each girder is obtained from the combination of Eqs. F.1 and F.5, i.e.,

$$P_i = \left(\frac{I_i}{\Sigma I_i} + \frac{x_i I_i}{\Sigma x_i^2 I_i} e_0\right) V \qquad \text{(F.6)}$$

F.2 EXAMPLES

The following data are used to determine the vertical distribution factors:

1. On an average, the relative moments of inertia are as follows:

   $I_1 = 0.595$, $I_2 = 0.751$, $I_3 = 1.130$, and $I_4 = 1.523$

2. The distance from each girder to girder 1 is denoted as

   $d_1 = 0$, $d_2 = d$, $d_3 = 2d$, and $d_4 = 3d$

3. The distance from rigidity center to girder is computed from Eq. F.2, i.e.,

   $x_0 = 1.895$ d

4. Values of eccentricity varied from case to case are described as follows:

a. For the case of uniform distributed loads

   $e_0 = (1.895-1.5)$ d

b. For the case of parapet loading

   $e_0 = (1.895-1.75)$ d, where the ratio of weight for the inner parapet to the outer one is 2.95/3.85

c. For the case of truck loads

   $e_0 = x_l - 1.895$ d, where x_l is measured along the horizontal distance from truck gravity to girder 1 as shown in Fig. F.2a.

F.3 DISTRIBUTION FACTORS

The distribution factors of vertical loads are listed in Table 6.5 for the cases of 4a and 4b in the previous section, while for case 4c, because of the variation of the truck gravity, a simple method is presented herein. Figure F.2b shows the influenced panel between two crossframes which encloses the truck gravity. Loading transfer in the longitudinal direction is achieved by simple support theory, which is:

$$P_1 = \frac{W(L_s - l_1)}{L_s}; \quad P_2 = \frac{W\, l_1}{L_s}$$

or (F.7)

$$P_i = \eta_i \; W$$

in which W, l_1, and L_s shown in Fig. F.2c are the weight of a truck, the horizontal arc distance from truck gravity to the line of front wheels, and the arc length passing the truck gravity between two crossframes of the influenced panel. It is noted that one of the crossframes is always underneath the line of the front wheels.

Each load P_i is distributed to the panel point j by the method described above in section F.2. The regenerated equation has the following form:

$$F_{ij} = (f_j + t_j)\ P_i \quad \text{or} \quad F_{ij} = \eta_i (f_j + t_j)\ W \tag{F.8}$$

where F_{ij} means the distribution of load P_i to the panel point j; $f_j = I_j/SI_j$ and $t_j = e_0 x_j I_j / S x_j^2 I_j$ are the distribution factors due to flexural and torsional deformations respectively. Therefore the distribution factor is defined as:

$$D_{ij} = \eta_i (f_j + t_j) \tag{F.9}$$

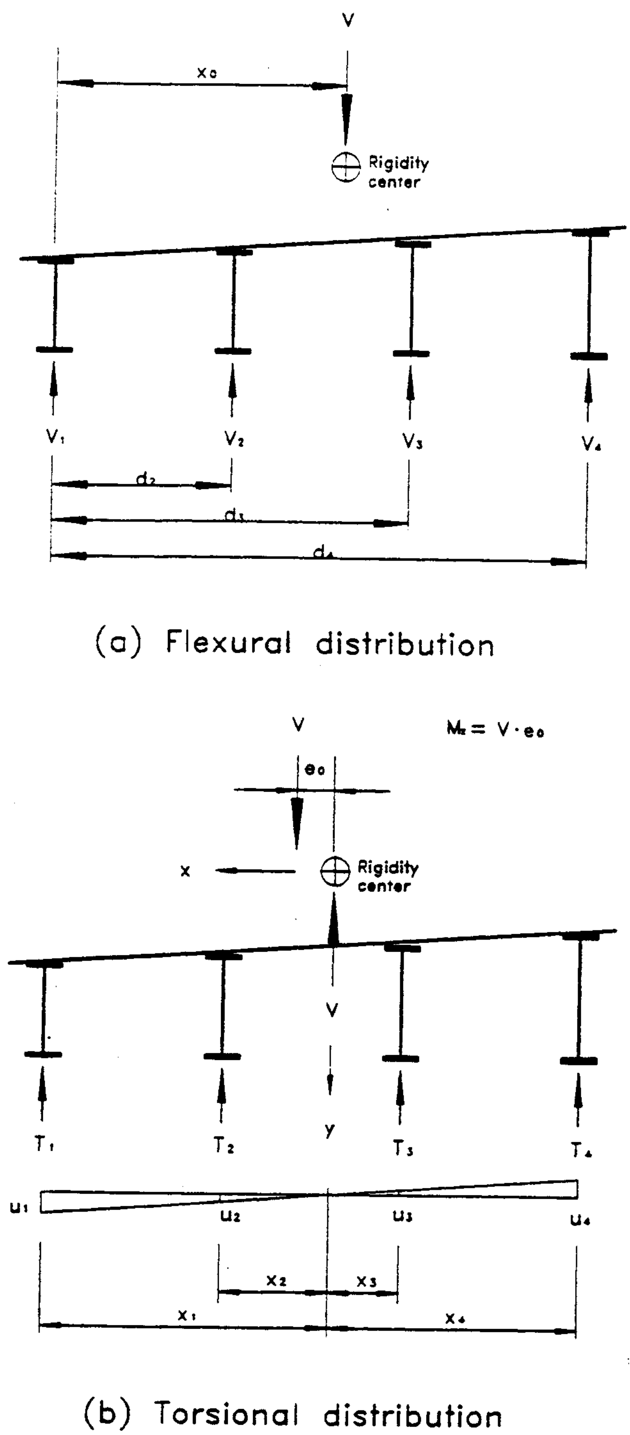

Figure F.1. Distribution of vertical dead loads

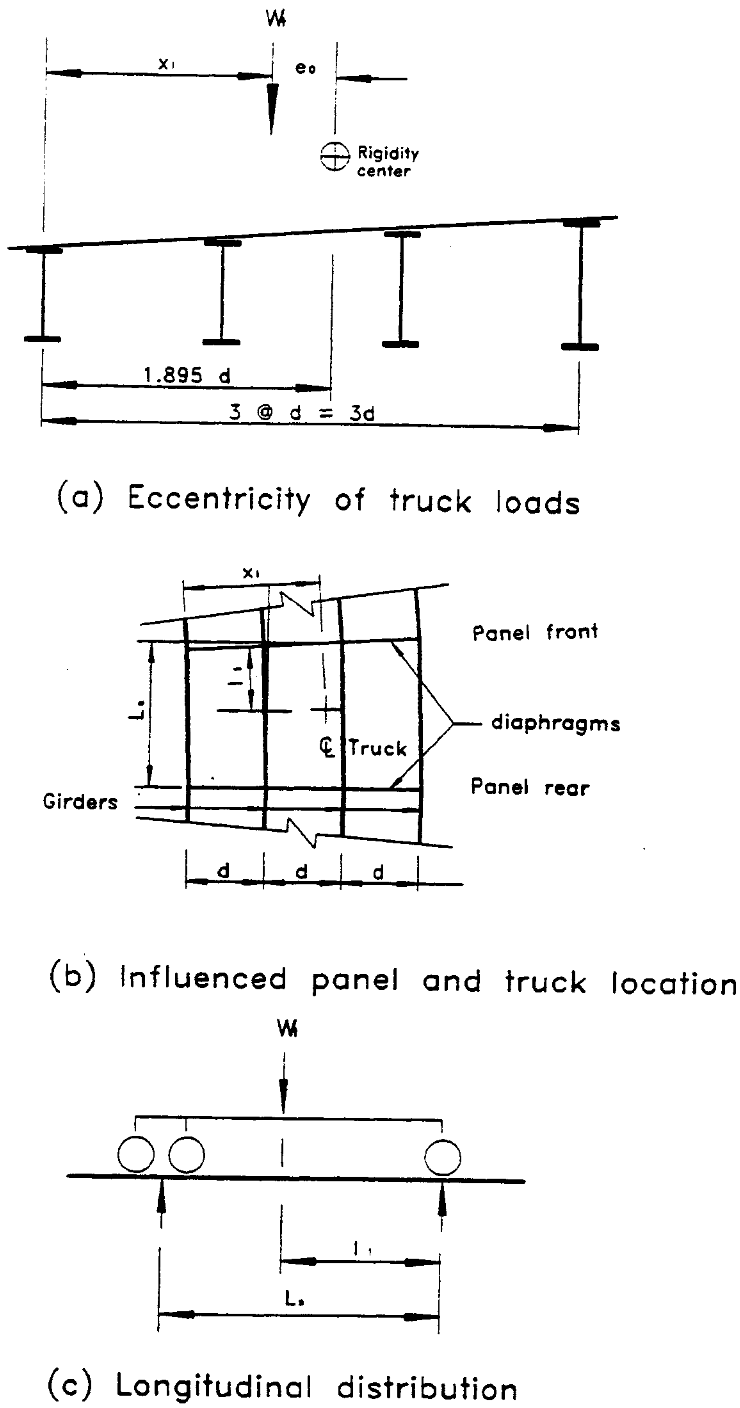

(a) Eccentricity of truck loads

(b) Influenced panel and truck location

(c) Longitudinal distribution

Figure F.2. Distribution of truck loads

APPENDIX G

BACKGROUND ON ANALYSIS OF STEEL CURVED GIRDER BRIDGE SYSTEMS

APPENDIX G

BACKGROUND ON ANALYSIS OF STEEL CURVED GIRDER BRIDGE SYSTEMS

This appendix contains excerpts from a paper by Stegmann and Galambos [6] so as to provide a review of available computer capabilities for use by design agencies.

__Edited Excerpts from STEGMANN AND GALAMBOS [6]__

Additional factors are encountered in the analysis of the curved as opposed to the straight girder in that a load applied perpendicular to the plane of the bridge generates a torque as shown in Figure G.1. This torque then is the cause of three types of stress in addition to the usual normal and shear stress due to the flexural effects, namely St. Venant shear stress, warping shear stress, and warping normal stress. A portion of a girder with these stresses acting on it is shown in Figure G.2. For an open-section girder, the warping normal stresses can be very large (50+%) relative to the bending normal stresses. Thus it is desirable that the structural analysis account for warping normal stresses in a fairly accurate manner.

All analyses cannot and should not do all things. Where very precise and accurate results are required, such as in stress analysis for fatigue strength determinations or for a structure of unusual configuration, a more complex program is warranted. For the first preliminary design of sections in an engineering office, such an involved program would be unnecessary and wasteful. This would then indicate an arbitrary segregation of the methods of analysis into three distinct groups or levels of sophistication.

Level I Analyses are the most sophisticated. They could be of the general finite element analysis type that would take into account the entire girder system and slab (if composite) and would, at any location, give the total stress resultant picture; or they could be general analytical solutions that would take all factors, such as warping, cross-sectional distortion, etc., into account and give dependable, accurate results. This total stress resultant could then be broken down into the normal and shear stresses and the appropriate deformations. Use of such a complex program would obviously be limited. Its main purposes would be in evaluation of research conducted in such areas as box girder distortion effects, diaphragm spacing, precise stress analyses for details with relation to fatigue, effective width studies of composite beams, and so on. The Level I analysis would not be used for the final check analysis of a bridge, but it would serve to calibrate the Level II analysis which would be used in this situation.

The Level II analyses are one step down in complexity from the Level I, but still retain the sophistication necessary to give an accurate final check analysis of a bridge. As opposed to the previous level of analysis, the Level II analysis would not take the entire bridge system into account as a single entity, but would subdivide it into distinct elements such as slab, girder (straight or curved), diaphragms, and braces. This is accomplished through the judicious application of simplifying assumptions and idealizations. Again, the output would consist of the stress resultants at any location of interest to the analyst, and could be broken into the normal and shear stresses. Warping stress values should also be made available because of its relations to the limit state calculations which will be discussed later. Availability of the Level II analysis programs would be much greater in that they should be readily accessible to the state highway departments and consulting design offices that would have need of them. Lastly, the Level II analysis programs are used in calibration of the Level III analyses.

Level III Analyses are the basic tools that the designer would use for the initial formulation of the bridge elements. The objective here is to give quick and approximate values for normal and shear stresses so that member sizes may be selected and organized into a rational configuration. These analyses are usually of the form of a simple design algorithm using stresses obtained from straight girders and modifying these values to account for curvature and bracing spacing.

As of the present (1976) many programs and analyses have been developed. All levels of sophistication are encountered. Following is a summary of some of the available programs.

G.1 THE GRID METHOD

The Grid Method was developed at Syracuse University. The main assumptions are [15]:

1. The structure behaves like a grid, i.e., any force or displacement vector acting at a point has three components, one linear (perpendicular to the plane of the structure) and two angular (about axes in the plane).
2. The principal axes of each member cross-section must lie in the plane of the structure.
3. Uniform torsion is assumed (St. Venant).

The stiffness matrix of a curved member was derived based on these assumptions and a computer program was written utilizing this stiffness matrix to determine the relevant displacements at the selected points. This method gives normal stress distribution in the girders with the same variation as in straight girders; that is, normal stress is a function of the distance from the bending axis, and is constant across the width of the section. Comparison of the stress distributions of this analysis with experimental results and the studies of the influence of the St. Venant torsional constant on the results of the analysis indicate the presence of a significant amount of non-uniform or warping torsion which is not accounted for in this method. Because of this limitation the Grid Method would be of the Level III type analysis, and should be recommended only for use in preliminary design.

G.2 LATERAL FLANGE BENDING METHOD

The Lateral Flange Bending Method was developed at the University of Rhode Island [15]. It is basically an extension of the previously discussed Grid Method, and hence utilizes the same basic assumptions concerning the structure. One additional assumption is that the flange is assumed free to warp at end diaphragms and is considered fixed at intermediate diaphragms. As noted, the major shortcoming of the former analysis is in ignoring the warping stresses produced in the curve member. The Lateral Flange Bending Method overcomes this by the inclusion of two additional angular degrees of freedom, one at each flange about axes that are perpendicular to the plane of the structure as shown in Figure G.3. A stiffness matrix is then derived for the five degrees of freedom at each end of the member. Forces acting on the interface between each flange and the web are ignored and the cross-section is assumed constant along the length of the member. By imposing boundary conditions on the flange degrees of freedom that approximate the end conditions for the flanges of a curved member of a curved girder bridge, the flange degrees of freedom are forced out, and a stiffness matrix in terms of grid degrees of freedom results. Although the flange degrees of freedom are eliminated the effects of flange bending are still present in the stiffness matrix. Warping normal stresses, or rather a normal stress analogous to it, can be computed by assuming the flange to be a beam acted upon by the lateral flange moments producing a linearly varying normal bending stress across the flange which is demonstrated in Figure G.4. These lateral flange moments are obtained through a simple step-by-step algorithm.

Comparisons of this analysis with tests and more sophisticated analyses show that the inclusion of the lateral flange bending mode brings relatively close agreement with the actual states of stress. This, therefore, would indicate that the Lateral Flange Bending Method would be of Level II sophistication, and along with its straightforward input and output format would be a useful tool for the bridge designer.

G.3 THE THREE-DIMENSIONAL METHOD

The Three Dimensional Method of analysis was developed at Syracuse University. This method has been formulated into a computer program and a User's Manual is available [16]. The main assumptions of the analysis are:

1. All members are assumed straight.
2. The girders, slabs, structural diaphragm members and lateral bracing members may act independently satisfying continuity conditions, i.e., fully composite action may be assumed.

3. The principal axes of each member cross-section are assumed to lie in the plane of the structure.
4. Static loading only.
5. Diaphragms and supports can be either radially positioned or skewed.
6. Girders can be arranged concentrically or non-concentrically (i.e., girder spacing may vary).

The bridge is divided into an arbitrary number of individual members and loads are considered to be applied at the joints between these members. The axial forces, shears, bending and twisting moments are then expressed in terms of the six components of deformation that are considered at each joint: three rotations and three displacements as shown in Figure G.5. The geometry of the bridge and applied joint loads are in the input to the program. Deformations are first expressed in terms of a global coordinate system and then components of the deformations with respect to local coordinate system of the member are determined. Next the equilibrium equations for each joint are set up. Using appropriate boundary conditions this system of equations is solved for the unknown joint deformations which are then in turn used to compute the shears and moments of each joint. Thus the output of this analysis program consists of the displacements and rotations of all pre-selected nodes or joints, the axial forces, and the bending and twisting moments. Although the analysis itself does include the effect of warping, the output consisting of forces and moments does not lend itself to a simple computation of the warping stress, which is a drawback in relation to the proposed design criteria. It should be noted that through idealization an order of magnitude type analysis of warping stress could be obtained. The program's sophistication, however, does qualify it as a Level II program which could be used as a final check in the design process.

G.4 THE EQUIVALENT STRAIGHT BEAMS METHOD

The Equivalent Straight Beams method for the analysis of curved girder bridges was developed at the University of Pennsylvania expressly as a simplified approach to be used for preliminary design only [17]. Simply stated the method of analysis used is that an “equivalent” straight beam is chosen to correspond to the curved girder being analyzed. An “equivalent” straight beam is generally one that gives the same magnitude of a certain stress resultant at the same location as in the curved beam. Through utilization of the analogies between curved and "equivalent" straight beams, ψ factors were determined that modify the stress resultants in a straight girder to approximate the stress resultants in a curved girder.

$$\text{Stress Resultant (curved beam)} = \psi \ [\text{ Stress Resultant (straight beam) }]$$

These stress resultants will give a determination of the reactions, bending moments, torsional moments, shears, vertical deflections, and angles of twist. The basic assumptions of this technique are:

1. All the assumptions of the elementary beam theory apply.
2. Only slender beams are considered.
3. Warping torsion is neglected.
4. Only the mid-length radius, R, is considered in computations.
5. All supports are idealized as fixed or pinned.
6. The girder must have a constant, circular curvature.
7. The range of flexural-to-torsional rigidity (EI/GJ) considered is from 1.0 to 100.0, where E, I, G, and J refer to the modulus of elasticity, moment of inertia about the bending axis, shear modulus of elasticity, and St. Venant torsional constant, respectively.
8. Concentrated or distributed loads are allowed.

What is available to the designer are computed charts giving the ψ factors for many various geometric configurations. An equivalent straight beam is then chosen, the ψ factors applied, and the resulting stress and displacement values are determined.

The same limitation applies to the Equivalent Straight Beam Method as to the Grid Method. Warping torsion is ignored which can lead to underestimating the calculation of the flange normal stresses. This would limit the Equivalent Straight Beam Method to being a Level III type analysis, which is what the developers intended for it to be.

G.5 SLOPE-DEFLECTION FOURIER-SERIES METHOD

The Slope Deflection Fourier Series method was developed at the University of Maryland [18]. The basic method of analysis is to establish the general differential equations incorporating the slope deflection equations. The solution to the differential equation for the deflection is assumed as a Fourier Series. The plate forces, girder deflection and girder forces are similarly defined as a Fourier Series. This was first done for a curved orthotropic plate as shown in Figure G.6. This was next extended to a system of curved orthotropic plates continuous over curved girder supports as shown in Figure G.7, evolving into a system of curved plate girders. The method will consider any number of concentrated and/or uniformly distributed loads for a single or two-span continuous case. Also included are the effects of diaphragms and non-uniform torsion.

This method is incorporated into a computer program, COBRA I. The input consists of the bridge configuration, the girder stiffnesses, and the number of Fourier Series terms desired to be used in determining the solution. Output consists of slopes, deflections, shears, bending moments and torsional moments.

As this analysis considers the curved girder as such and does include non-uniform torsion and its effects, it would be relatively sophisticated and could be considered as a Level I analysis for the cases of spans and geometry to which the program is limited.

G.6 DABROWSKI'S ANALYSIS APPROACH

Outside of the CURT program many other methods or techniques have been developed to deal with curved girder systems. One of the most rigorous solutions is that of Dabrowski. The first closed form solution was formulated by Vlasov who derived the differential equations governing the behavior of horizontally curved girders [19]. Dabrowski then took up the problem of torsion and bending of curved thin-walled beams that were asymmetric in cross-section. In 1960 he rederived Vlasov's equations including several terms that had been neglected by Vlasov. Dabrowski then in 1964 derived the governing differential equation for the warping or bimoment of a curved girder of open thin-walled cross-section loaded normal to the plane of curvature. This equation was then solved for deformations and the internal stresses due to the bimoment, the warping shear stress and warping normal stress [20, 21]. The results of Dabrowski's work were four equations which will give at any point along the span the bending moment, St. Venant torque, bimoment, and total torque on the section. The basic assumptions of his method are:

1. No distortion of the cross-section
2. Elastic theory
3. Small deflections only
4. Mild curvature ($a < 0.05$ Radians)
5. Concentrated load and torque may be applied anywhere in the span or a distributed load and distributed torque may be applied.

Although the equations appear involved, all variables, except the position along the girder, are dependent on the cross-section geometry. Once the section properties are determined for the girder the computational effort required to obtain the results is minimal.

Noting the deficiencies of some previously discussed analysis methods, Dabrowski's solution would appear very good in that it takes into account the warping of the cross-section and also gives the designer the ability to determine a value of the warping stress at any point along the span. This method would then be of the Level II or possibly Level I type.

G.7 UNITED STATES STEEL METHODS

Several methods of analysis are given by United States Steel in their "USS Highway Bridge Design Manual" [22]. They are summarized as follows:

G.7.1 Rigorous Analysis

This is a fundamental method of consistent deformation [22]. That is, the various components of the structure must distort in such a way as to maintain geometric compatibility with each other, and at the same time remain in a state of equilibrium. To do this is possible only with a unique set of internal forces. The necessary internal forces can be determined by solving a series of equations which are mathematical statements of equilibrium and geometric compatibility. In the case of a two-girder bridge with intermediate diaphragms (cross-bracing, floor beams, etc.) when the load is applied the girders will deflect and twist which apply torques and vertical shear forces on the floor beams (diaphragms) which will be the redundants. This can be seen in Figure G.8. This will result in "4n" redundants (each end of the floor beam will have two redundants). By considering the equilibrium of the floor beam these can be reduced to "2n" redundants. Then considering the differential deflection and rotation of the panel, two equations may be written for each panel. So, for the entire bridge with N diaphragms or floor beams this results in 2N equations in 2N unknowns. Once the redundants are solved for, the internal shear, torque and moment of each girder can be computed.

G.7.2 Simplified Method

In the Simplified Method the curved girder is straightened out to its full length and the external loads applied [22]. The moment diagram for this condition is then constructed by standard procedures for continuous beams. This is referred to as the Primary Moment Diagram. Next, the Primary Moment Diagram Radius is set equal to the Distributed Torque Diagram. This can be explained as follows: Equivalent axial forces, M/d are computed in the flanges, where M is the bending moment obtained from the Primary Moment Diagram and d is the distance between the flange centroids. Next, consider a free body diagram of a differential element of the flange which is illustrated in Figure G.9. This shows that there must be a radial force, $w = M/Rd$, acting in order to produce static equilibrium. By straightening out the flange and considering it to be laterally supported at each diaphragm line, and applying the radial load as a distributed load on this continuous beam, a lateral bending moment diagram can be obtained. Using the section properties of the flange considered as a beam bending in the horizontal plane, normal stresses caused by this lateral bending can be computed and combined with the normal stresses produced in accordance with the Primary Moment Diagram. Also, the torque at each particular cross-section along the girder can be computed from this lateral force:

$$\text{Torque} = wd = d(M/Rd) = M/R = \text{Distributed Torque}$$

This torque then is transmitted to the cross or floor beams. The shears and moments in return applied to the girders from the floor beams can be easily deduced considering the equilibrium of each member. These shears from the floor beams are then applied to the girder as vertical loads and from this a Secondary Moment Diagram is constructed. The Primary and Secondary Diagrams are then added, and the entire process can be iterated until desired convergence is achieved. From this final moment diagram and the Distributed Torque (which is not altered from its initial state) the girders can then be designed. This is an approximate, Level III type analysis.

G.7.3 Approximate Analysis

The Approximate Analysis is a further simplification of the previously discussed Simplified Method [22]. The same basic procedure is retained in that a Primary Moment Diagram is constructed from the girders straightened to their full developed length and external loads applied, the Distributed Torque Diagram is determined from the lateral forces applied to the flanges, and finally the redundant shears and moments in the floor beams are determined as before. The further simplifications referred to are with respect to distribution of moments and end fixity approximations in the form of empirical factors. As with the Simplified Method this is a very approximate method of obtaining stress resultant values and would be used for preliminary design calculations only.

These previously presented methods are only a few of the many that have been proposed and are currently available in print. McManus et al. [20] include an extensive bibliography and summary of the available analytical tools. From a study of this listing and the individual methods, the most widely available, thorough, and easily employed method would be that of Dabrowski [21]. It is an exact solution of the differential equations of the curved girder arranged in a format that can be easily used, it incorporates warping torsion in the analysis and gives a direct calculation of the bimoment. It is not, however, a computer program, and it does not readily permit the consideration of the composite deck slab. The incorporation of the slab is possible through the sophisticated Level I finite analysis programs (e.g., COBRA) or through the application of simplified equivalent single composite girders in an analysis such as Dabrowski's or any other method which permits the inclusion of unsymmetric curved girders. Considerable research has concentrated on the development of equivalent simple composite sections, especially with reference to their torsional properties [23, 24].

To the designer the most important methods are those which give good Level III results in preliminary design and good Level II performance for the final check analysis. Several of these have been described previously in this appendix. At present, it seems that the relative merits of each must await reporting on the success of their use in the literature. It is not clear as to which method, if any, can be singled out for preferred recommendation.

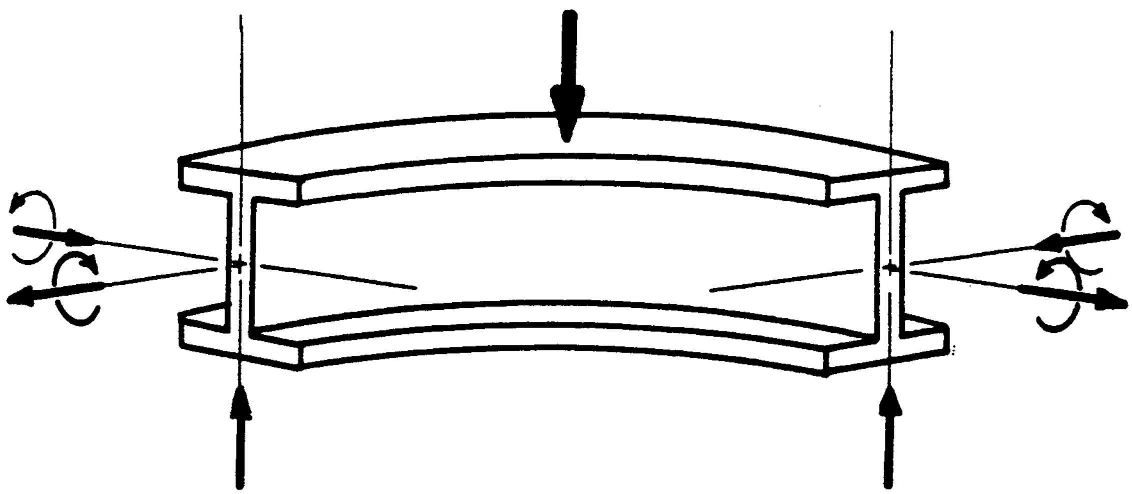

Fig G.1 Loading of curved girder

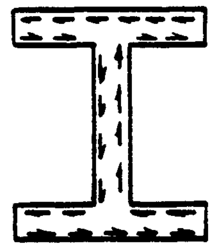

St. Venant Shear Stress

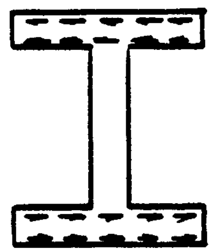

Warping Shear Stress

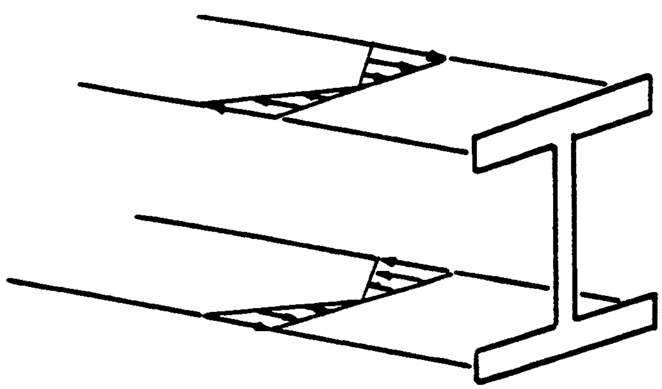

Warping Normal Stress

Fig. G.2 Additional effects due to torsion

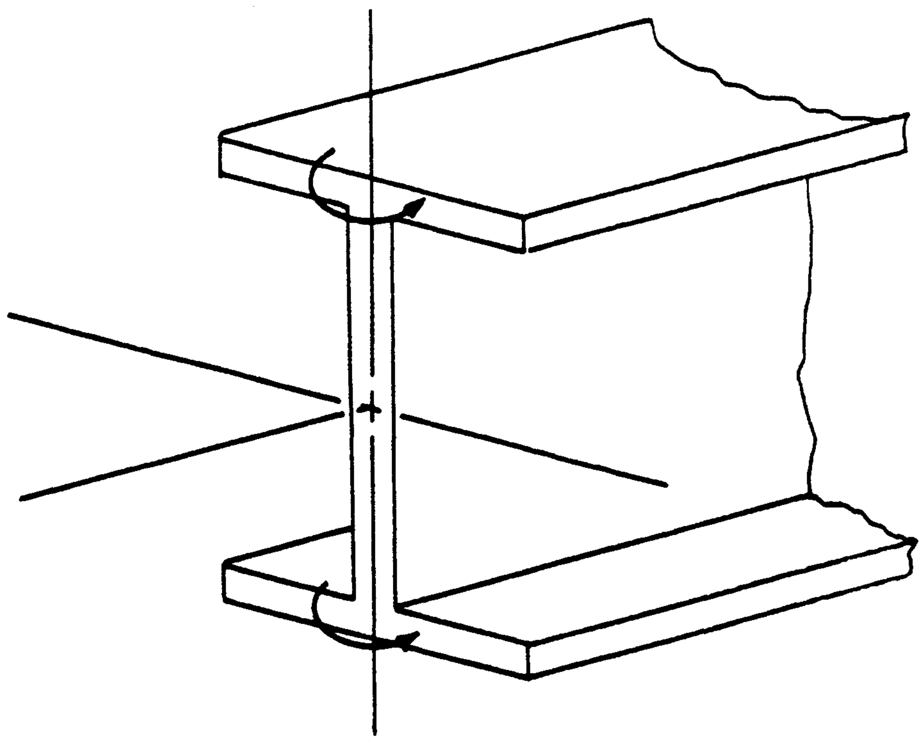

Fig. G.3 Additional flange angular degrees of freedom

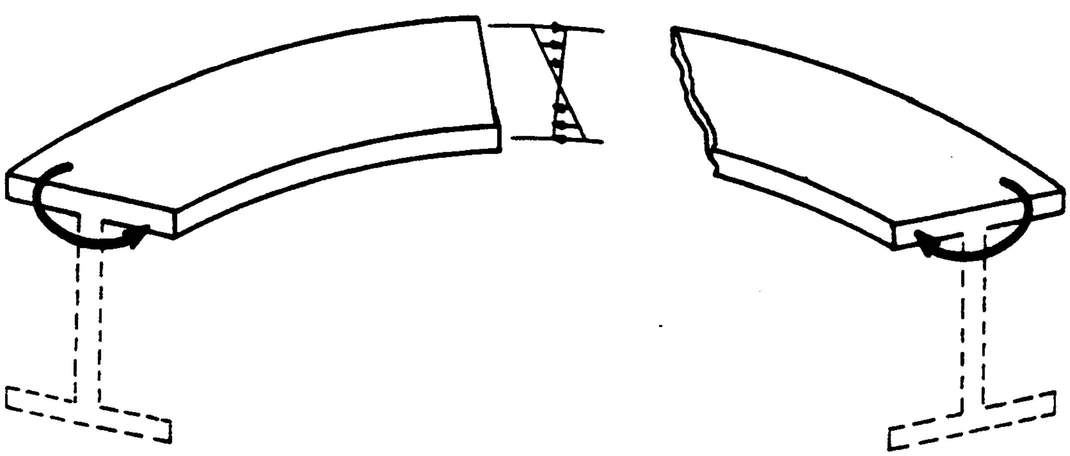

Fig. G.4 Flange acting as laterally loaded beam

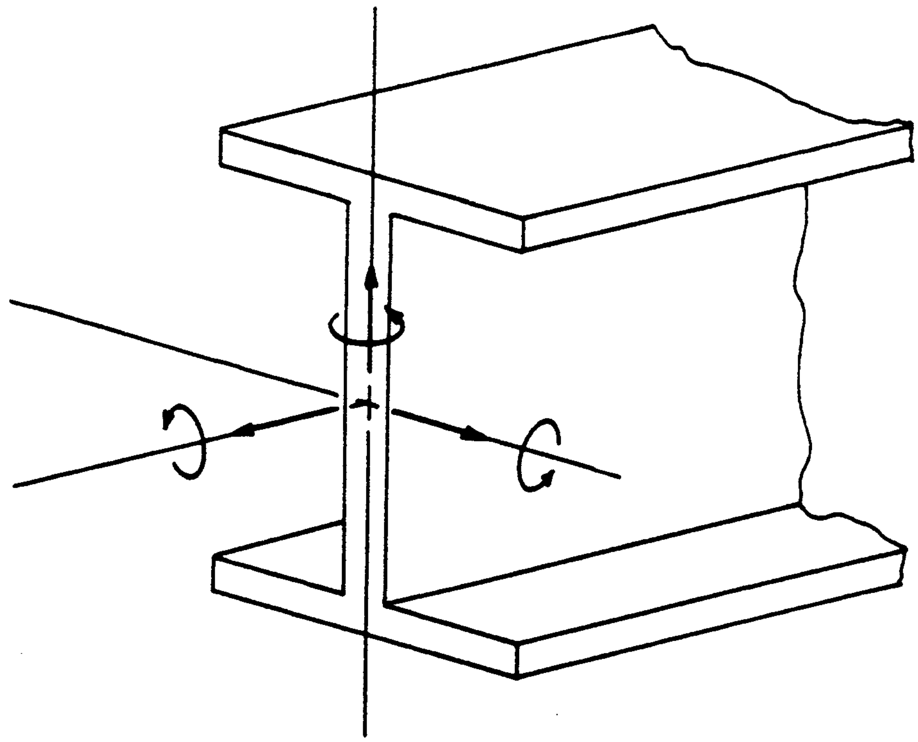

Fig. G.5 Three-dimensional method - six degrees of freedom

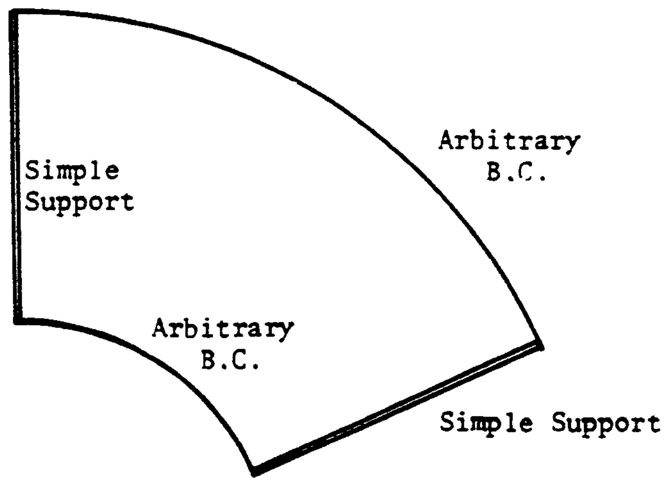

Fig. G.6 Single curved orthotropic plate

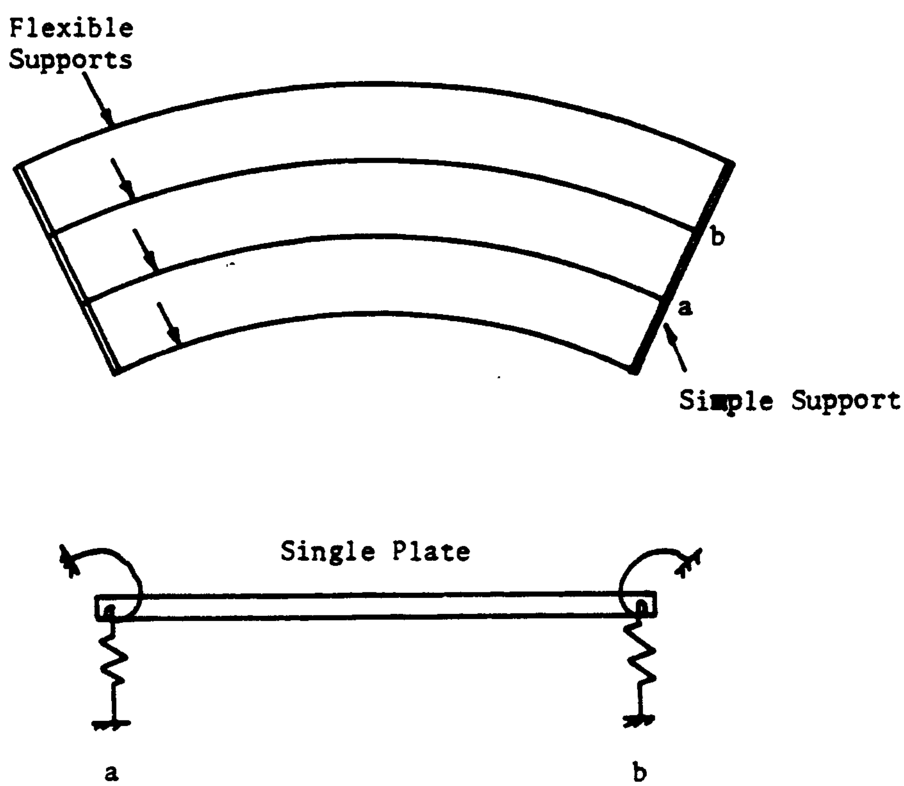

Fig. G.7 System of curved orthotropic plates

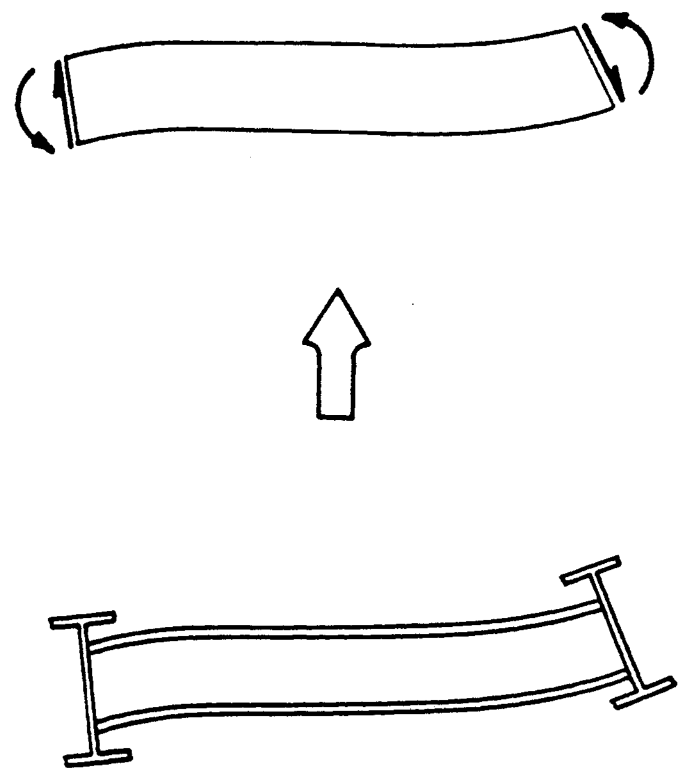

Fig. G.8 Rigorous analysis - distortion of girders and beams

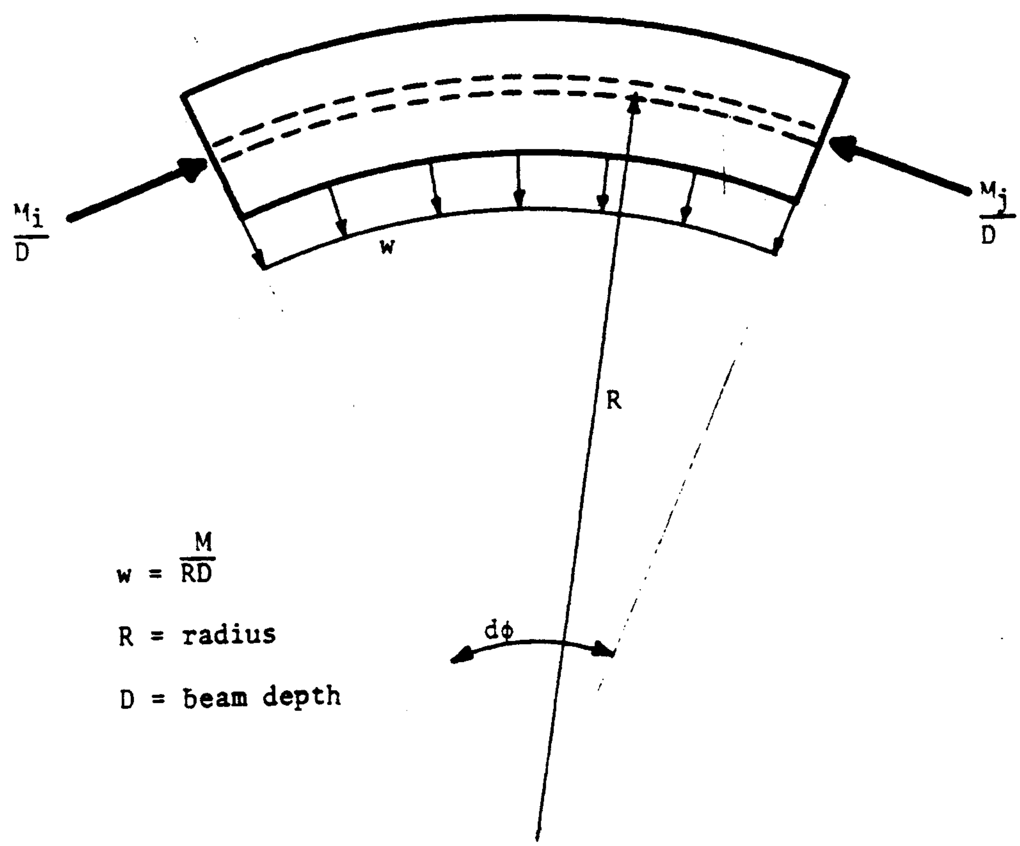

Fig. G.9 Differential element of flange under assumed lateral load

APPENDIX H

SPECIFICATIONS OF THE VIBRATING WIRE STRAIN GAGE

APPENDIX H
SPECIFICATIONS OF THE VIBRATING WIRE STRAIN GAGE

This appendix presents the specifications of the *Geokon* VK-4100 vibrating wire strain gage used for all strain measurements recorded in this research project. The following pages are reproduced from Ref. [12].

geokon
incorporated

GEOTECHNICAL INSTRUMENTATION

SPOT-WELDABLE TYPE
Vibrating Wire Strain Gage

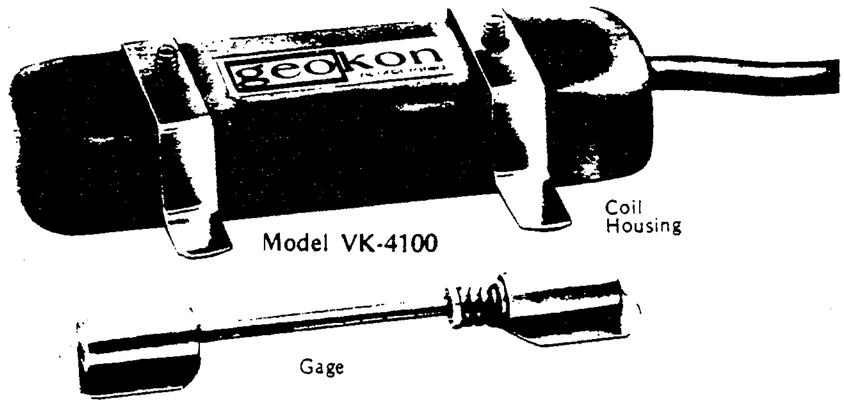

Features
- Spot weldable
- Low profile
- Small size
- Waterproof
- Stainless steel
- Detachable plucking coil
- Adjustable range
- High compliance
- Epoxy bondable

The Model VK-4100 Vibrating Wire Strain Gage is designed to measure strains in steel structures, such as bridges, piles, tunnel linings, buildings etc. It can be installed quickly and easily in the field by means of a spot welder. (Alternatively, the gage may be epoxy-bonded to the surface of either steel or concrete). The VK-4100 has a fully-sealed, all stainless steel construction, making it waterproof and highly resistant to corrosion.

The gage utilizes the vibrating wire principle: a length of steel wire is tensioned between two end blocks which are spot-welded (or epoxy-bonded) to the surface of the steel member. The wire is plucked so that it vibrates at its natural resonant frequency. This frequency depends on the wire tension which will vary as strain in the steel member varies. An electromagnetic coil is used to pluck the wire and to measure the frequency of the vibration so produced. The change in frequency is then displayed as a strain change directly by the readout box. A dual coil auto-resonant circuit and driver is available for low frequency dynamic strain measurements (up to 120Hz).

Advantages of the VK-4100 Vibrating Wire Strain Gage:

•The vibrating wire principle gives maximum accuracy, sensitivity and long-term stability.

•Installation is quick and simple, requiring the use of a portable spot welder only. Surface preparation is minimal. Installation can also be made by epoxy bonding the gage to either steel or concrete.

•The gage is of small size and the wire is in close proximity to the surface to which it is attached.

•The wire is positively gripped in the end blocks by a patented swaging technique.

•True O-ring seals provide complete waterproofing and allow the protective tube to 'float' around the wire. This, coupled with a pretensioning of the wire, makes the gage very compliant, or 'soft', in that strains in the steel or concrete member do not have to stretch the protective tube, as well as the wire, in order to alter wire tension. This places a minimum strain on the weld points and makes epoxy bonding possible.

•An external spring holds the wire at an initial tension which can be set to any desired level by a simple adjustment technique. Thus gages can be set to place the available range mostly in tension or mostly in compression, as required.

•The gage is constructed from carefully selected stainless steel elements so that the corrosion resistance of the gage is maximized.

•Temperature compensation is achieved by matching the coefficient of expansion of the wire to that of the underlying steel. Temperatures can be measured by a thermistor encapsulated in the plucking coil housing.

•The plucking coil housing is separate from the gage element and can be carried around with the readout box so that only the gage element is left behind on the structure. If the gage is inaccessible the coil housing is attached permanently in place around the gage. Also, should the plucking coil or signal cable become damaged in any way they can easily be replaced without disturbing the gage element.

•Lightning protection may be specified for gages in exposed locations.

•Frequency signals can be transmitted over electrical cables many thousands of meters long without loss of accuracy. Cable resistance changes caused by temperature or moisture effects are not a problem with vibrating wire strain gages.

DIMENSIONS

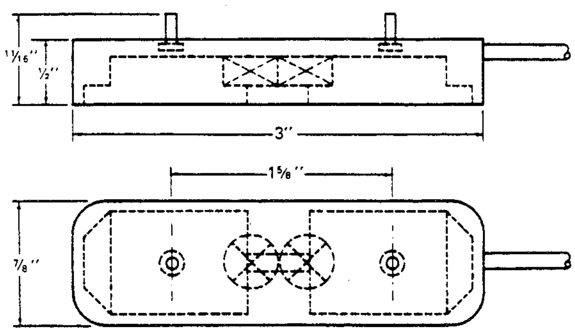

Coil Housing

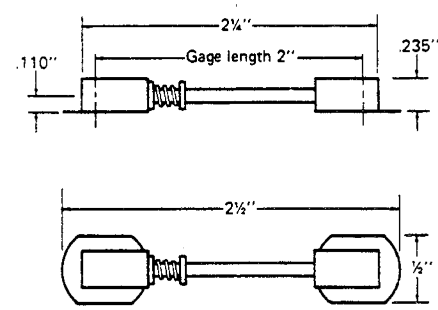

Gage

SPECIFICATIONS – Model VK-4100 Vibrating Wire Strain Gage

Gage Element		
Range	microstrain	2500
Sensitivity	microstrain	0.5 to 1
Active gage length	in (mm)	2 (50.8)
Wire height above surface	in (mm)	.110 (2.79)
Thermal coefficient of expansion	ppm/°F.(/°C)	6.7 (12.0)
Overall dimensions LxWxH	in (mm)	2.5x0.5x0.24"
Temperature range	°F (°C)	–40 to +250 (–40 to +120)
Materials		Stainless steel, buna N
Coil Housing		
Overall dimensions LxWxH	in (mm)	3x.88x.69 (76x22x17)
Temperature range	°F (°C)	–40 to +175 (–40 to +80)
Materials		Waterproof copolymer epoxy
Cable		
Material		4 conductor-shielded 22 gage vinyl jacket
Size	in (mm)	.187 (4.7)

Accessories
Setting tools (test strips, tension adjustment fixture).
Spot welding equipment.
Epoxy kits.
Vibrating Wire Readout Box.
Thermistor Readout Box.
Terminal boxes.

Options
Thermistors.
Lightning protection.
Autoresonant coil assembly.

Ordering Information
Specify: 1.Cable length.
2.Options required.
3.Accessories required.

For further information contact us . . . . .

geokon incorpor
48 SPENCER STREET
LEBANON, NH 03766
TEL: 603/448-1562
FAX: 603/448-3216
TELEX: 4995473GEOK

geokon

Model GK-403

Vibrating Wire Readout

GEOTECHNICAL
INSTRUMENTATION

Features:

- ❑ User friendly.
- ❑ Multi-line LCD.
- ❑ Rugged and reliable.
- ❑ Temperature readout.
- ❑ Rechargeable battery.
- ❑ Cold weather operation.
- ❑ Internal real-time clock.
- ❑ Battery-backed memory.
- ❑ Easy-to-use control panel.
- ❑ RS-232 communications port.
- ❑ Two modes of data acquisition.

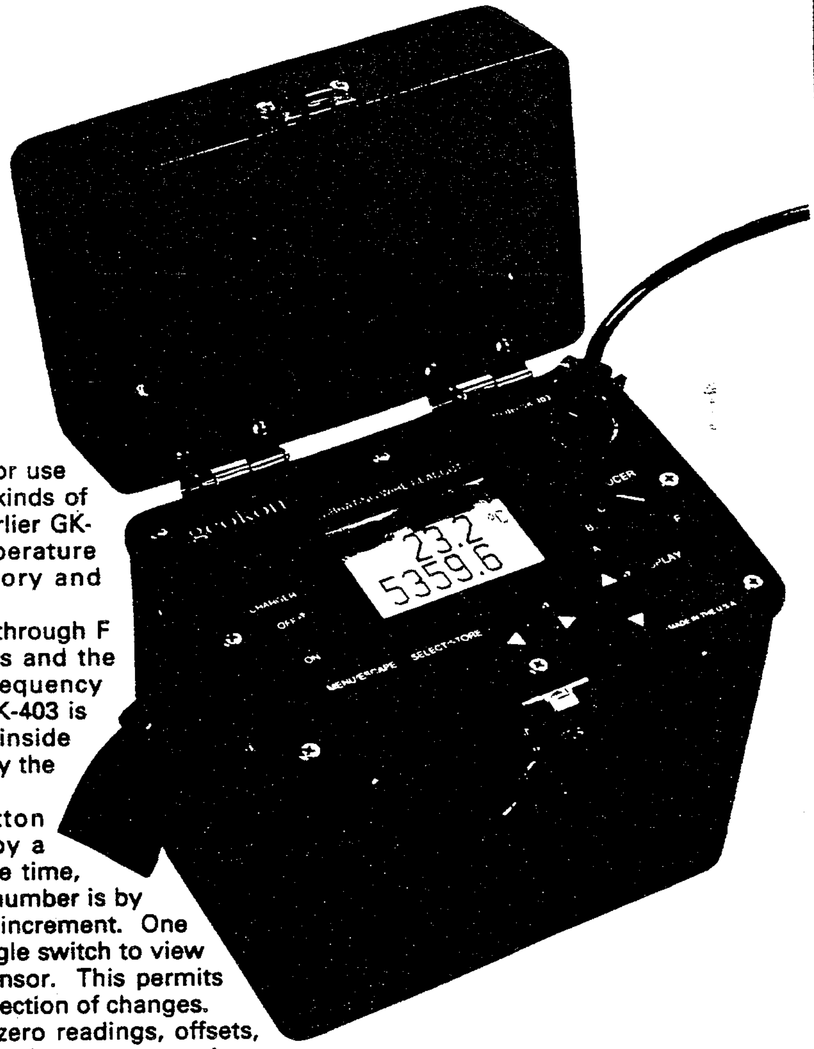

The GK-403 Vibrating Wire Readout is designed for use with all of Geokon's vibrating wire sensors in all kinds of weather. It incorporates all the features of the earlier GK-401 Readout plus it can read and display temperature readings, and can store all readings in memory and transmit the values to a host computer.

There are seven modes of operation. Modes A through F are designed for use with specific Geokon gages and the reading is displayed directly in microstrain, frequency squared or period. A convenient feature of the GK-403 is its ability to read the thermistors encapsulated inside most Geokon vibrating wire sensors, and to display the temperature reading.

Storage of the readings is a simple one-button operation. Each stored reading is identified by a reference number, ranging from 1 to 256, plus the time, date and temperature. Selection of the reference number is by means of a toggle switch or, if preferred, by auto increment. One very useful feature is the ability at the flip of a toggle switch to view the previously stored readings taken from any sensor. This permits on-site evaluation of the readings and the early detection of changes.

Mode G permits programming of gage factors, zero readings, offsets, engineering units and identifiers for up to 256 different gages. A two dimensional storage matrix of rows and columns allows sets of readings from many instruments taken at a particular time (rows) or sequential readings of any particular gage (columns) to be stored. An easy-to-use menu lists options to transmit readings, clear stored readings, set the date and/or time, configure the auto increment of the reference numbers and set gage parameters. Mode G also provides the ability to download a file from an IBM-compatible computer containing gage parameters (zero, gage factor, offset etc.) and the ability to view previously stored data. The comma delineated output format allows easy importing into spreadsheets and database programs such as Lotus 1.2.3, Microsoft Excel etc.

The GK-403 includes a 15x8 column LCD matrix and automatic shutoff to conserve the life of the rechargeable 12-volt lead acid gel-type battery. Waterproof seals are incorporated into the face plate, switches and input connectors.

Included with the readout is a battery charger, a gage patchcord, an RS-232 interface cable, communications software and a manual. See specification overleaf.

48 SPENCER STREET
LEBANON, NH 03766 USA
TEL: 603/448-1562
FAX: 603/448-3216
TELEX: 4995473GEOKON

geokon incorporated
GEOTECHNICAL
INSTRUMENTATION

SPECIFICATIONS
Model GK-403 **Vibrating Wire Readout**

Vibrating Wire Readout:	
Excitation Range:	400Hz to 6000Hz, 5 volt square wave
Measurement resolution:	0.25µs/255
Timebase accuracy:	0.01%
Temperature Readout:	
Sensor type:	Thermistor, Dale #1C3001-B3 (YSI 44005)
Sensor accuracy:	±0.5°C
Measurement range:	-50°C to +150°C
Measurement resolution:	0.1°C
Measurement accuracy:	0.5-1.0% FSR
Memory:	
RAM:	64K Static, 48K used
ROM:	32K EPROM, 16K used
Reading storage:	2000 arrays
Array partition:	256 arrays for Modes A-F, remaining for Mode G
Real-time Clock:	
Features:	Full calendar with automatic leap year correction
Time format:	24 hour (hhmm)
Date storage format:	Julian day
Date display format:	month/day/year (mm/dd/yy)
Oscillator:	32.768kHz
Accuracy:	±1 minute per month
Communications:	
Default parameters:	9600 baud, 8 data bits, 1 stop bit, no parity
Handshake:	XON/XOFF
Transmission format:	Comma-delineated ASCII
Physical:	
Display:	15 column x 8 line backlit LCD
Dimensions:	19.1cm(7.5") x 13.3cm(5.25") x 23.5cm(9.25")
Weight:	3.2kg (7lbs)
Temperature range:	-10°C to +50°C
Battery:	12volt, 2.6aHr (Yuasa NP2.6-12)
Operating time:	Approximately 10 hours

Optional accessories:

- ❑ SPLIT data formatting software.
- ❑ Y-cable (permits simultaneous RS-232 communication and gage measurement).
- ❑ Vibrating wire load cell module.

For further information contact us . . .

geokon incorporated
48 SPENCER STREET
LEBANON, NH 03766 USA
TEL: 603/**448-1562**
FAX: 603/448-3216